THESIS

Evaluation of Spine Biomechanics Through Personalized Lumbar and Thoracolumbar Spine Finite Element Models

Brittany Stott

Department of Mechanical Engineering
McGill University
Montreal, Quebec, Canada

December, 2023

A Thesis submitted to McGill University in fulfillment of the requirements of the Degree of Doctor of Philosophy (Ph.D.) in Mechanical Engineering.

Dedication

This thesis is dedicated to my parents, Brian and Darlene, for your endless support, love, and encouragement in my pursuit of education. Thank you for inspiring dedication and perseverance to pursue what I am passionate about. Also, to my fiancé, Clément, for your unwavering support and belief in me. Thank you for the hours you have spent studying by my side, and the laughter, joy, and time spent together over these years.

Contents

List of Figures

List of Tables

Glossary

ex vivo Experiments conducted outside of the living body.

in silico Experiments conducted on a computer or through simulation.

in vitro Experiments conducted outside the living body, in a controlled environment.

in vivo Experiments conducted in the living body.

2D In 2 dimensions.

3D In 3 dimensions.

ANSYS A 3D design and engineering simulation software.

Cobb angle A measurement of spinal curvature, typically measured in degrees.

Comparator Experimental or published results that are used to ensure modelling outcomes agree with a desired reality.

Context of use The conditions under which the model or device will be used.

Credibility Confidence in the predictive capability of a model.

Finite element analysis A numerical method solving differential equations to simulate the behaviour of an object under given conditions.

Finite element model A model used for finite element analysis composed of discrete finite elements.

Follower load Compressive loads applied tangential to the curve of the spine.

Intersegmental rotation A measure of rotation between segments in the spine.

Intervertebral disc A layer of soft fibrocartilaginous tissue between adjacent vertebrae.

Kyphosis The anterior concave curvature of the thoracic region of the spine.

Lordosis The anterior convex curvature of the cervical and lumbar regions of the spine.

Low back pain Pain in the lumbar region of the spine.

Lumbar spine The five vertebrae, and surrounding tissues, located in the lower region of the spine.

Magnetic resonance imaging A noninvasive medical imaging technique that uses a magnetic field to obtain images of structures inside the body.

Moment The magnitude of a force acting at a distance on an object.

Poisson's ratio The ratio of change in the width per unit width to the change in its length per unit length of a material.

Sagittal plane An anatomical plane that separates the body into left and right.

Thoracolumbar spine The twelve thoracic vertebrae and five lumbar vertebrae, and surrounding soft tissues, in the spine.

Uncertainty quantification The process of quantifying uncertainties associated to the model and reality.

Validation Confirmation that the model is an appropriate representation of a given reality of interest.

Verification Confirmation that the model is implemented correctly and solved accurately.

Young's modulus A measure of the elasticity of a material, or the material's ability to withstand elastic deformation under loads. Representative of the ratio of the stress over strain.

Acronyms

AMSE American Society of Mechanical Engineers.

BMI Body mass index.

BW Body weight.

CAD Computer-aided design.

COU Context of use.

CSA Cross-sectional area.

CT Computed tomography.

D Depth of vertebral body.

FDA Food & Drug Administration.

FE Finite element.

FEA Finite element analysis.

FEM Finite element model.

FL Follower load.

ICC Intraclass correlation coefficient.

IRB Institutional Review Board.

ISR Intersegmental rotation.

IVD Intervertebral disc.

LBP Low back pain.

LSA Lumbosacral angle.

LSJA Lumbosacral joint angle.

M Moment.

M&S Modelling and simulation.

MEF Modèle d'éléments finis.

MRI Magnetic resonance imaging.

PI Pelvic incidence.

PT Pelvic tilt.

SS Sacral slope.

SVA Sagittal vertical alignment.

TLF Thoracolumbar fascia.

UQ Uncertainty quantification.

V&V Verification and validation.

VB Vertebral body.

VVUQ Verification, validation, and uncertainty quantification.

W Width of vertebral body.

Symbols

E Young's modulus [kg/m· s^2] or [kPa].

F Normal force [kg· m/s^2] or [N].

Δ Change or difference between two values.

ε Normal mechanical strain.

ν Poisson's ratio.

π Mathematical constant, 3.14159.

$\propto$ Proportional to.

σ Normal mechanical stress [kg/m·s^2] or [Pa].

θ Angle [°].

g Gravitational acceleration constant, 9.81m/s^2.

n Sample size.

p p-value.

Acknowledgements

First, I would like to express my sincere gratitude and appreciation to my supervisor, Professor Mark Driscoll, who encouraged and supported my interest in biomechanics from my time as an undergraduate student, and for his continuous support and guidance throughout my graduate studies. I consider it an honour to have been given the opportunity to work with Prof. Driscoll. It is, first and foremost, thanks to his dedication, kindness, and belief in my abilities that this work has been completed.

I would like to acknowledge the incredible friends and members of the Musculoskeletal Biomechanics Research Lab, past and present, who continuously provided guidance, encouragement, and support through every step of this thesis. Notably, I would like to acknowledge Dr. Ibrahim El Bojairami for his time, positivity, and willingness to discuss the ins and outs of FEA.

I would like to acknowledge the financial support from the Fonds de Recherche du Québec – Nature et Technologies (FRQNT), the Mechanical Engineering Department at McGill University, and Natural Science and Engineering Research Council of Canada (NSERC).

A warm thanks is extended to all my friends and family, who supported me through hours of studying, writing, and simulation with patience and encouragement. Namely, I would like to thank my parents for their encouragement and continuous belief in my abilities. To my siblings, thank you for your continued interest and support, and the game nights between deadlines and exams. To my grandparents, although we may be far, thank you for always taking an interest in my research, even though it may seem like a different language. To my fiancé, Clément, for providing hugs and support, and for always being my rock, for making me smile, for sharing countless lattes, and for the hikes and adventures between deadlines. Lastly, I consider myself very blessed to have wonderful friends outside of academia, with whom I have shared countless meals, movie nights, book clubs, and walks over the years, and for all the laughs we shared.

Abstract

The spine is a vital musculoskeletal system in the human body. However, a significant portion of the population will experience low back pain (LBP). Computational modelling of biological systems has gained popularity in recent years, allowing researchers and clinicians to study the spine through simulation. If modelling is to be used to advance the knowledge of spine biomechanics, while possibly being used for virtual clinical trials, there is a need for an understanding of how the outcomes may vary patient-to-patient. Thus, the global objective of this thesis was to **develop, validate, and evaluate geometrically personalized finite element models (FEMs) of the spine for analysis of stress distribution within the spinal column**. Specifically, this thesis aimed to study the effects that variation in **geometry**, **biological sex**, and **sagittal alignment** has on spine biomechanics.

Multiple studies have developed FEMs of the spine for biomechanical analysis. Validation is a crucial step to confirm that the modelling results accurately represent what happens in the human body. Several types of comparators are used in literature, including *in silico*, synthetic benchtops, *ex vivo*, and *in vivo* comparators. Studying the use of these comparators to establish model credibility was the first step in understanding the requirements for a credible biomechanical model.

Anatomical and physiological differences are apparent between men and women, however, these changes are seldom considered in spine FEMs. Thus, spine models representing both biological sexes were developed, validated, and compared. Results indicated that the female model was subjected to greater stress distribution throughout the spinal column, demonstrating the importance of considering biological sex for patient-specific modelling and analysis.

A commonly accepted cause of LBP is irregular curvature. To better understand the outcomes of these variations, spine FEMs representing "healthy", kyphotic, and lordotic sagittal profiles were developed, validated, and compared. The spine models with greater curvature exhibited larger stress magnitudes in the discs and vertebrae, while the straighter models showed reduced disc compression. Thus, these findings demonstrated that the stress distribution in the spinal column was impacted by the sagittal alignment.

Lastly, magnetic resonance images of patients with (n = 51) and without LBP (n = 58) were studied to evaluate sagittal alignment. The LBP patients showed reduced lumbar curvature compared to the control subjects, while the female participants had greater curvature than the male participants. Following this analysis, a blind retrospective study was conducted for which patients (n = 12) were randomly selected from the previous subjects, and personalized FEMs were developed from the imaging data. Greater stresses were observed in the female models compared

to the male models, while the models with LBP showed higher stresses in the discs.

In all, the findings demonstrated that geometry, biological sex, and sagittal alignment play an important role in spinal stress distribution. This thesis confirms the importance of developing spine models that accurately represent patient profiles and anatomy to improve the use of modelling and simulation for clinical assessment or targeted treatments.

Résumé

La colonne vertébrale est un système musculosquelettique essentiel du corps humain. Cependant, une grande partie de la population souffrira de lombalgies. La modélisation computationnelle des systèmes biologiques a gagné en popularité au cours des dernières années, permettant aux chercheurs et aux cliniciens d'étudier la colonne vertébrale via la simulation. Si la modélisation est utilisée pour avancer la connaissance de la biomécanique de la colonne vertébrale, tout en étant éventuellement utilisée pour des essais cliniques virtuels, il est nécessaire de comprendre la variation possible des résultats d'un patient à l'autre. Ainsi, l'objectif global de cette thèse était de **développer, valider et évaluer des modèles d'éléments finis (MEFs) géométriquement personnalisés de la colonne vertébrale pour l'analyse de la distribution des contraintes à travers la colonne vertébrale**. Précisément, cette thèse visait à étudier les effets de la variation de la **géométrie**, du **sexe biologique** et de l'**alignement sagittal** sur la biomécanique du rachis.

De nombreuses études ont développé des MEFs de la colonne vertébrale pour l'analyse biomécanique. La validation est une étape cruciale pour confirmer que les résultats de la modélisation représentent fidèlement ce qui se passe dans le corps humain. Plusieurs types de comparateurs sont utilisés dans les écrits, soit des comparateurs *in silico*, synthétiques, *ex vivo* et *in vivo*. L'étude de l'utilisation de ces comparateurs pour établir la crédibilité du modèle a constitué la première étape dans la compréhension des critères d'un modèle biomécanique crédible.

Des différences anatomiques et physiologiques sont apparentes entre les hommes et les femmes, cependant, ces changements sont rarement considérés dans les MEFs de la colonne vertébrale. Des modèles de la colonne vertébrale représentant les deux sexes biologiques ont donc été développés, validés et comparés. Les résultats ont indiqué que le modèle féminin était soumis à une plus grande distribution des contraintes dans la colonne vertébrale, ce qui démontre l'intérêt de prendre en compte le sexe biologique pour la modélisation et l'analyse spécifique du patient.

La courbure irrégulière est une cause fréquemment reconnue de lombalgie. Pour mieux comprendre les résultats de ces variations, des MEFs de colonne vertébrale représentant des profils sagittaux "normaux", cyphotiques et lordosiques ont été développés, validés et comparés. Les modèles à plus grande courbure présentaient des contraintes plus élevées dans les disques et les vertèbres, tandis que les modèles plus étroits présentaient une compression discale réduite. Ces résultats démontrent que le profil sagittal joue un rôle crucial dans la répartition des contraintes dans la colonne vertébrale.

Enfin, les images de résonance magnétique de patients avec (n = 51) et sans lombalgie (n = 58) ont été examinées pour évaluer l'alignement sagittal. Les patients souffrant de lombalgie présentent une courbure lombaire réduite par rapport aux sujets contrôles, tandis que les femmes

ont une courbure plus élevée que les hommes. À la suite de cette analyse, une étude rétrospective en aveugle a été menée pour les patients (n = 12) sélectionnés au hasard à partir des sujets précédents, et des MEFs personnalisés ont été développés à partir des données d'imagerie. Des contraintes plus élevées ont été observées dans les modèles féminins comparés aux modèles masculins, tandis que les modèles avec lombalgie ont montré des contraintes plus élevées dans les disques.

Au total, les résultats ont démontré que la géométrie, le sexe biologique et l'alignement sagittal jouent un rôle important dans la répartition des contraintes sur la colonne vertébrale. Cette thèse confirme l'importance de développer des modèles de colonne vertébrale qui représentent fidèlement les profils et l'anatomie des patients afin d'améliorer l'utilisation de la modélisation et de la simulation pour l'évaluation clinique ou les traitements appropriés.

Author's Contribution

I, Brittany Stott, certify that I am the primary author of all the material included within the manuscripts and chapters of this dissertation. Under the supervision of Professor Mark Driscoll, I designed, modelled, and validated 3-dimensional finite element models of the spine to address the objectives and hypotheses of this thesis. Specifically, I developed 3-dimensional thoracolumbar and lumbar spine finite element models representing male and female anatomy, as well as several models with irregular sagittal profiles, for biomechanical simulations. To add, I was the primary investigator of a retrospective *in vivo* magnetic resonance imaging study evaluating sagittal profiles in both healthy and low back pain patients, for which patient data and images were supplied by Mayo Clinic. Data collected from the magnetic resonance images was leveraged to inform patient-specific lumbar spine finite element models, which were then used to evaluate stress as a biomarker for pain in geometrically personalized spine models. As such, I certify that I devised, implemented, and validated the 3-dimensional finite element models for each objective.

Contribution to Original Knowledge

The research presented in this dissertation contains novel geometric personalization of finite element modelling of the spine. The contributions to knowledge in the field of biomechanics and biomechanical modelling of the spine are the following:

1. Evaluation of existing comparators used to validate spine finite element models, and their effectiveness for validation, in collaboration with the ASME VVUQ40 subcommittee.

2. Scoring metrics to evaluate the ability of comparators to lend credibility to model validation, in collaboration with the ASME VVUQ40 subcommittee.

3. Evaluation of stress distribution between male and female spine models, using developed and validated thoracolumbar spine FEMs. Results demonstrated augmented stresses in the female model.

4. Evaluation of stress distribution in spine models with irregular thoracic curvature, using developed and validated thoracolumbar spine FEMs representing hypokyphotic and hyperkyphotic profiles.

5. Evaluation of stress distribution in spine models with irregular lumbar curvature, using developed and validated thoracolumbar and lumbar spine FEMs representing hypolordotic and hyperlordotic profiles. Results of irregular profile studies demonstrated augmented stresses in the hyper-curvature FEMs and reduced disc compression in the hypo-curved FEMs.

6. A retrospective evaluation of geometrically personalized lumbar spine finite element models based on patient-specific magnetic resonance images and data, following an MRI analysis of the sagittal profile of control subjects and patients with low back pain. Results demonstrated augmented stress magnitudes in the low back pain FEMs.

The above contributions to original knowledge were disseminated through peer-reviewed journal publications and conferences, as listed herein.

Journal publications:

1. B. Stott, P. Afshari, J. Bischoff, J. Clin, A. Francois-Saint-Cyr, M. Goodin, S. Herrmann, X. Liu, M. Driscoll, “A critical comparison of comparators used to demonstrate credibility of physics-based numerical spine models,” *Annals of Biomedical Engineering*, vol. 51, no. 1, pp. 150–162, 2022;

2. B. Stott, M. Driscoll, "Development and evaluation of sex-specific thoracolumbar spine finite element models to study spine biomechanics," *Medical & Biological Engineering & Computing*, (submitted) 2023;

3. B. Stott, M. Driscoll, "Biomechanical evaluation of the thoracolumbar spine comparing healthy and irregular thoracic and lumbar curvatures," *Computers in Biology and Medicine*, vol. 160, 2023;

4. B. Stott, J. C. Benson, C. A. Tiegs-Heiden, M. Driscoll, "Patient-specific lumbar spine modeling of healthy and back pain individuals: a retrospective study," *Journal of Biomechanics*, (submitted) 2023.

Conferences, oral presentations:

1. B. Stott, M. Driscoll, "The effects of variations in lumbar spine curvatures on biomechanical behaviour: a finite element study," 11th Interdisciplinary World Congress on Low Back & Pelvic Girdle Pain, Melbourne, Australia, Nov 1-4, 2023;

2. B. Stott, M. Driscoll, "Is the healthy range of sagittal spinal curvature optimal for biomechanical loading? A finite element study," 4th International Workshop on Spine Loading and Deformation, Berlin, Germany, July 5-7, 2023;

3. B. Stott, M. Driscoll, "Biomechanical analysis of the thoracolumbar fascia based on biological sex: a finite element study," 6th International Fascia Research Congress, Quebec, Canada, Sept 12, 2022.

Conferences, poster presentations:

1. B. Stott, M. Driscoll, "A biomechanical analysis of sex-specific differences between load distribution and intersegmental motion in the thoracolumbar spine: a finite element study," Global Spine Congress 2023, Prague, Czech Republic, May 31-June 3, 2023;

2. B. Stott, P. Afshari, J. Bischoff, J. Clin, A. Francois-Saint-Cyr, M. Goodin, S. Herrmann, X. Liu, M. Driscoll, "An evaluation of the comparators used to establish credibility and validation of spine computational models," 6th International Spine Research Symposium (ORS PSRS), Pennsylvania, USA, Nov 6-10, 2022;

3. B. Stott, M. Driscoll, "Variations in lumbar spine stress distribution based on biological sex: a finite element study," 22nd Annual Conference for the International Society for the Advancement of Spine Surgery, Bahamas, June 1-4, 2022.

1 Introduction

It is known that variations in an individual's spinal anatomy affect the load distribution throughout the spine. Understanding the potential mechanistic causes of back pain is an important step towards comprehending how the spine is loaded during everyday tasks and identifying potential causes of discomfort or pain. Thus, this thesis evaluated how geometric and profile variations may influence the load distributions throughout the spine. A simplified flowchart of how biomechanical loading, morphological changes, spinal alignment adjustments, and back pain may continue to cyclically evolve under day-to-day loading is depicted in Figure 1.0.1.

Although *in vivo* studies will remain the gold standard for studying and understanding the many complexities of the spine, studies involving participants are costly and can present ethical challenges. In comparison, *ex vivo* studies provide the ability to investigate the human body, providing valuable accessibility and insight into measurements that might otherwise not be obtained in living subjects. However, these experiments can present challenges, as they can be costly, lack repeatability, and present difficulties in acquiring a varied sample population, as the available specimens are often skewed towards the elderly population. *In silico* studies permit rapid and repeatable virtual experiments with significant control over the geometry, loading conditions, and material properties. Although biomechanical models are an approximation, they can nevertheless provide useful information regarding biomechanical behaviour. Further, with the evolution of finite element modelling, simulations are beginning to gain traction and acceptance for use in virtual clinical trials, permitting valuable predictive information to be obtained prior to conducting these trials through *in vivo* studies.

Thus, this thesis leveraged *in silico* analyses to gain insight into the loading effects on the spine when geometric properties or alignments are varied.

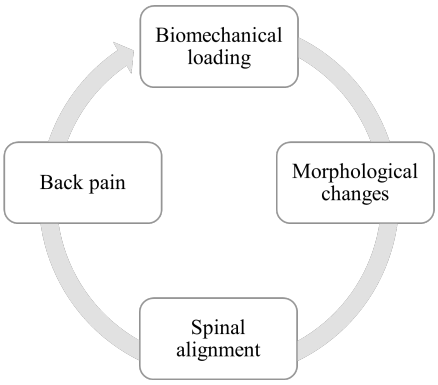

Figure 1.0.1: Simplified cycle of biomechanical loading and low back pain.

2 Literature Review

2.1 Spine Anatomy

The human spine is a complex anatomical structure, resembling a flexible column of bones, known as vertebrae, and the surrounding soft tissues [1]. The spine plays a crucial role in day-to-day activities, such that the primary functions of the spine are to support the body, allow movement of the trunk, and protect the spinal cord and nerve roots [1]–[3].

The spinal column consists of 33 bony elements connected by joints and ligaments [4], [5]. Of these elements, 24 individual vertebrae compose the cervical, thoracic, and lumbar spine, while the remaining fused vertebrae form the sacrum and coccyx [6]. The first seven vertebrae (C1-C7) constitute the cervical spine, providing mobility and support to the neck while maintaining a horizontal line of sight during daily activities [6]. The thoracic spine is formed by 12 vertebrae (T1-T12), which articulate on their lateral anterior bodies with the ribs which form the thoracic cage [7]. The rib cage is reported to play a role in thoracic spine stability and serves to protect the inner organs [8], while the ribs act as attachment points for several trunk muscles [7], [8]. The lower back is formed by five larger lumbar vertebrae (L1-L5), which bear the majority of the support for upper body weight [4], [5]. More specifically, L1 is said to support approximately 45.2% of the body weight, meanwhile, L5 supports 55.6% of the body weight [9]. The tail of the spinal column consists of the sacral vertebrae (S1-S5), which fuse to form a wedge-shaped bone [5] and attach the spine laterally to the hip bones [7]. Lastly, the triangular-shaped coccyx consists of four fused vertebrae (Co_1-Co_4) [5], providing the surface on which pelvic fascia, ligaments, and muscles attach [10]. The sacrum, coccyx, and hip bones form the pelvis, which protects and supports the inferior viscera of the abdominal cavity [7]. Spinal column anatomy for the thoracolumbar spine can be seen in Figure 2.1.1.

The vertebra's anatomical structure can be divided into two main regions: the body and the arch [1], [5]. Both regions are formed by an outer layer of cortical bone and an inner core of cancellous bone [1], as seen in Figure 2.1.2. Cortical bone provides the stiffness and strength needed for organ protection. Unlike cortical bone, cancellous (or trabecular) bone is much more porous, consisting of a framework of interconnecting trabeculae that are surrounded by bone marrow or blood vessels [11]. Consequently, cancellous bone is 20-30% less stiff than cortical bone, though it makes up approximately 80% of the human skeleton [12]. The vertebral body (VB) is cylindrical [5] and acts to support the weight of the human frame [1], [7]. The arch is connected to the body on the posterior face by two horizontal supports known as the pedicles [5]. Together, the body and the arch form the vertebral foramen, an orifice that contains the spinal cord [5], [7]. The arch is

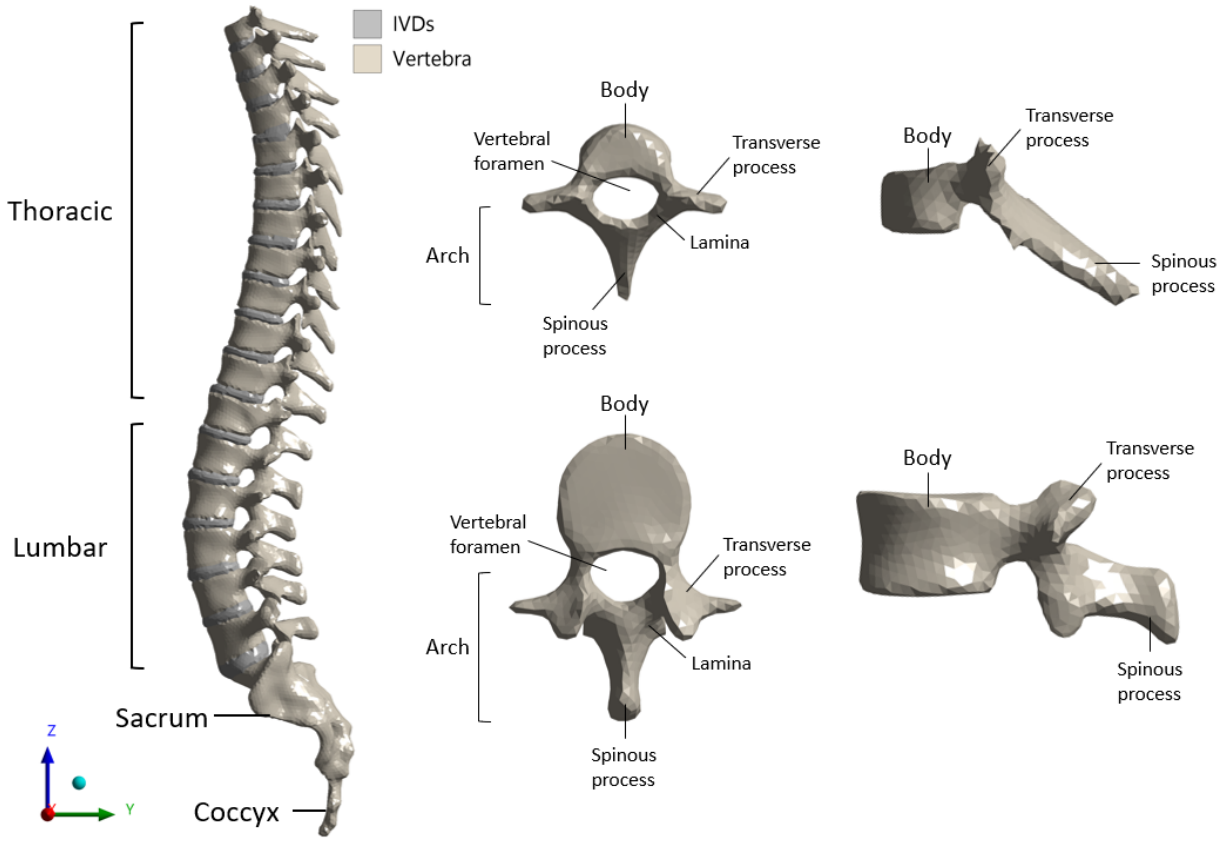

Figure 2.1.1: Anatomy of the spinal column.

composed of two laminae, which join to form the spinous process, the transverse processes, and the superior and inferior articular processes [5]. These processes serve as attachment points for ligaments and muscles [2]. Detailed vertebra anatomy is seen in Figure 2.1.1.

Between each consecutive VB lies a layer of soft, deformable, fibrocartilaginous tissue, known as the intervertebral disc (IVD) [14]. The IVD comprises a peripheral fibrous ring, named the annulus fibrosus, and an inner gelatinous core, termed the nucleus pulposus [2], [7], [14], as seen in Figure 2.1.2. The IVD and adjacent vertebrae are separated by cartilaginous endplates [1], [14] located on the periphery of the superior and inferior faces of the VBs [1]. The discs serve as shock absorbers, transmitting load between vertebrae [7], [14], [15]. Their deformation permits movement around an amphiarthrosis joint in three planes: flexion-extension, inclination, and rotation [14]. The IVDs share this role of passive movement control with other soft tissue.

Ligaments provide stability and protection to the spine by controlling and limiting excess motion and absorbing significant loads [1], [15], [16]. They are bone-to-bone connective tissue made predominately of collagen I fibers [17]. These uniaxial structures portray non-linear viscoelastic, time-dependent characteristics, demonstrating that higher loading rates lead to stiffer

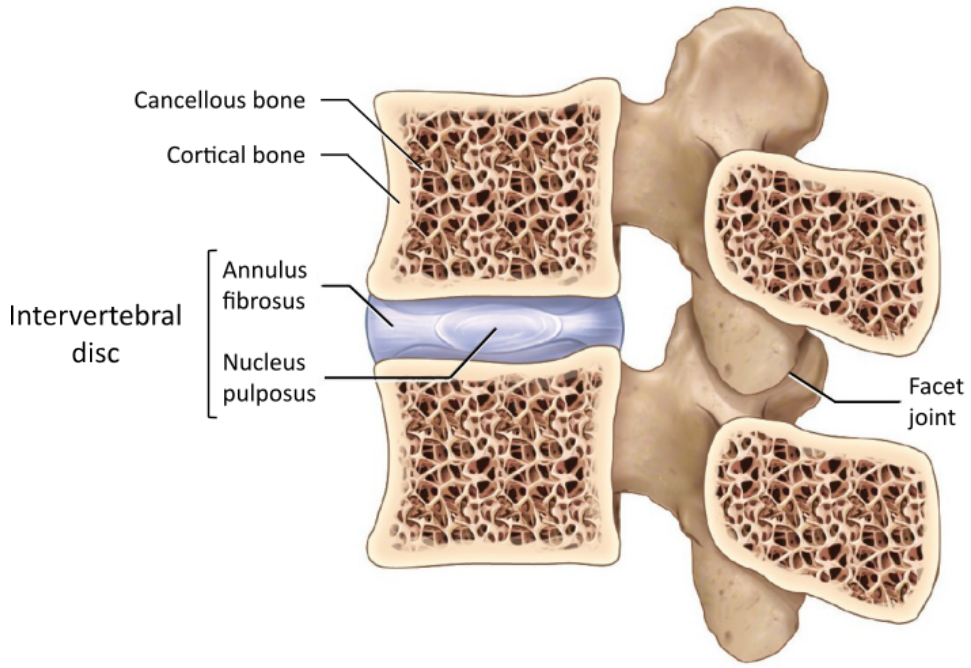

Figure 2.1.2: Cross-sectional sagittal view of the vertebrae and intervertebral disc, consisting of the annulus fibrosus and nucleus pulposus (adapted from www.learnmuscles.com [13], permission from Dr. Joe Muscolino, artwork by Giovanni Rimasti).

load-displacement behaviours [2]. In comparison to ligaments, tendons are mostly muscle-to-bone connective tissue composed of a greater concentration of densely packed collagen I fibers [17]. They provide stability and efficient motion by allowing forces to be transmitted between muscles and bone, behaving in a non-linear viscoelastic manner under applied loads [18].

The ability of the vertebral column to maintain posture and perform spinal movements depends on the spine and trunk muscles [4], [15], [19]. Additionally, the quantity of layered muscles surrounding the spine protects the vertebral column by dispersing applied external loads [19]. Skeletal muscle fibers are made up of several hundred myofibrils [20]. These cylindrical structures are composed of myofilaments which contain the essential proteins for muscular contraction: actin and myosin [20]. Spinal muscles can be categorized by their relative location to the spinal column, i.e., superficial or deep [15], [19]. Several of the important muscles contributing to spinal support described herein are displayed in Figure 2.1.3. The erector spinae muscles make up the largest percentage of superficial back muscle mass, playing a significant role in the maintenance of posture and spinal stability [21]. The erector spinae muscles, composed of the iliocostalis, longissimus, and spinalis muscles [19], [21], extend the length of the spine, filling a groove lateral to the spinous processes [19]. Deep to the erector spinae is the transversopinalis muscle group which functions to connect and stabilise the vertebrae [21]. It consists of several smaller muscles situated obliquely

and longitudinally [15] that attach inferiorly from transverse to spinous processes [19]. The multifidus muscle, a five-band muscle mass, is included in the aforementioned group, contributing to postural stabilisation, VB rotation, and lateral flexion of the spine [19]. More superficial, the latissimus dorsi muscle is a large triangular muscle located in the lower part of the back and often named the "swimmer's muscle" [21]. The latissimus dorsi is the primary extensor muscle of the arm [21], connecting the back to the upper extremities through various functions; one of its roles is to set the thoracolumbar fascia (TLF) under tension.

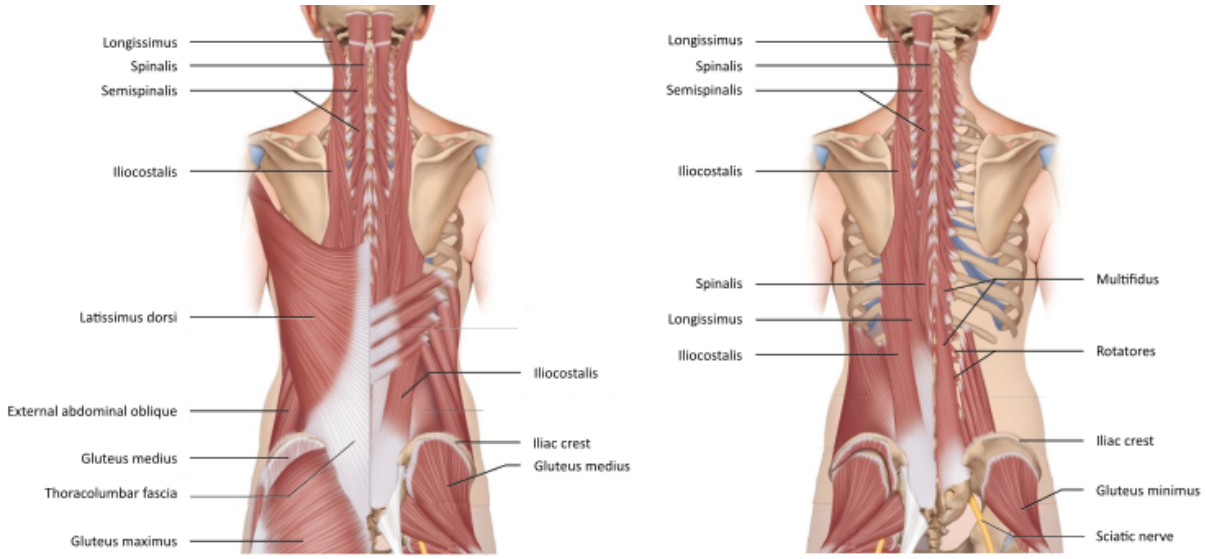

Figure 2.1.3: Select muscles that contribute to spinal support (adapted from www.learnmuscles.com [13], permission from Dr. Joe Muscolino, artwork by Giovanni Rimasti).

The fascia located in the thoracolumbar spine is a multilayer connective tissue consisting of fibrous collagenous tissues that make up a wide tensional force transmission system [22], providing support to the torso. The TLF's ability to provide support and transfer forces is reliant on the many attachment points throughout the spine. Located in proximity to the spinous processes, the TLF has three layers. The thin outer layer is composed of parallel collagen fibers transversely oriented [23]. The thicker middle layer consists of collagen fiber bundles oriented obliquely [23], attaching to the lateral edges of the transverse processes on L2-L4 [24]. This layer forms an aponeurotic attachment between the lumbar vertebrae and the transverse abdominal muscles, thus contributing to tensional force transmission between these components [24]. Lastly, the thin, membranous anterior layer runs between the psoas and quadratus lumborum muscles, attaching to the end of the transverse processes [24]. The fascia plays an important role in transferring forces among trunk muscles and the spine [25], hence reducing spinal loading and providing stability in the lumbar region [26].

2.1.1 Variations in Spine Anatomy: Age and Sex

The anatomy of spinal components has been found to demonstrate notable variations for sex and age. These changes may affect several capabilities, such as strength and range of motion, resulting in a difference in the available physical output between individuals. Studies have found that the cross-sectional area (CSA) of the VBs is reduced by 20-25% in females compared to males [27], [28], although no difference between sexes was observed for VB height [29]. Consequently, females have a lower maximum compressive load (N), although no sex-related difference for maximum compressive stress was observed (i.e., load/CSA) [28]. As the CSA of the vertebrae varies, so does the CSA of the adjacent IVDs. Additionally, the properties of the tissues surrounding the spinal column have been found to vary between sexes. Cooper et al. studied the CSA of various muscles surrounding L4, noting that the CSA for the psoas and the paraspinal muscles were the largest at this vertebral level [30]. These researchers observed a 22% increase in the paraspinal muscle CSA [30], while Watson and colleagues noted a 25% increase in the multifidus CSA [31] in males when compared to females. A summary of several studies analysing sex-specific anatomical variations in the spine has been recorded in Tables 2.1.1-2.1.3, for which "healthy participants" signifies participants absent of spinal disorders or pain. Measures were conducted using computed tomography (CT), x-ray, magnetic resonance imaging (MRI), ultrasound, or manual measurements.

With respect to age, VB CSA was found to increase between 3-30% from a younger population to an older population, with greater changes observed in males [32], [33]. Further, as an individual ages, the bones in the body become weaker and more brittle, resulting in a reduction in the maximum compressive load [28] and the maximum compressive stress [28], [34] as a function of age. An observed reason for the reduced VB load strength is net bone loss, which was found to be reduced in men compared to women since the periosteal bone formation is greater in men [32], [34]. There is a widespread belief that disc height decreases as an individual ages, which is often attributed to disc degeneration. Although findings from several studies support that degenerative changes in the disc are more likely to occur in an older population [35], [36], multiple studies have reported that disc height is positively correlated with age [35], [37]–[40]. Some studies noted that disc height began to decrease after the sixth or seventh decade [37], [38], while others observed that the increase in disc height was primarily in the middle of the disc [39], [40]. Nevertheless, when disc degeneration is present, it generally results in a reduction in IVD height and volume [35].

Table 2.1.1: Summary of anatomical variations in the vertebrae between males and females.

Author [Ref.]	Study type	Participants	Methods	Results and notes
Vertebrae				
Cooper (1992) [30]	*in vivo*	53 male, 39 female LBP patients	CT	• Males have significantly greater bone and muscle CSA than females ($p<0.001$) • L4 VB CSA: males 20% > females
Duan (2001) [32]	*in vivo*	327 male, 686 female Healthy participants	X-ray	• L3 VB CSA: males 24.8% > females in young participants, 32.6% > in older participants
Ebbensen (1999) [28]	*ex vivo*	50 male, 51 female 101 L3 vertebrae	X-ray	• L3 VB CSA: males 20% > females, where $CSA = \frac{volume\ of\ VB}{height\ of\ VB}$ • Maximum compressive loads : males > females, due to larger CSA • Maximum compressive stress: did not vary between sexes
Gilsanz (1994) [27]	*in vivo*	18 male, 25 female Matched for weight, height, and age	CT	• VB CSA: males 25% > females ($p<0.001$) • Mechanical stress in VB: males 30-40% > females for equivalent load • VB height: did not differ between sexes for L1, L2, L3 • Paraspinal CSA: males > females • VB compressive strength: equivalent for both sexes (loading capacity $\propto$ CSA and material) • VB compressive stress during axial compression: males 33% > females ($\propto$ load applied and $\propto$ 1/CSA) • VB compressive stress during bending: male 39% > female
Marras (2001) [41]	*in vivo*	10 male, 20 female Healthy participants T8-S1	MRI	• VB CSA: males > females ($p<0.05$)
Mosekilde (1986) [34]	*ex vivo*	47 male, 43 female Healthy participants 90 L2 vertebrae	Micrometer, material testing	• L2 VB CSA: males 15-20% > females • L2 VB CSA: males 20 years of age 25-30% < males 80 years of age ($p<0.05$) • VB load strength: subjects 20 years of age 60-65% > subjects 80 years of age ($p<0.001$) • VB stress: subjects 20 years of age 65-70% > subjects 80 years of age ($p<0.001$)
Nieves (2005) [29]	*in vivo*	36 male, 36 female Matched for height and weight	X-ray	• VB height: no significant difference between sexes ($p=0.41$) • VB CSA: males > females ($p=0.027$)
Oura (2019) [42]	*in vivo*	490 male, 597 female L4 vertebrae	MRI	• VB CSA: males > females, where $CSA = \pi \times \frac{mean\ width}{2} \times \frac{mean\ depth}{2}$ • Participant height was correlated with VB CSA
Scoles (1988) [43]	*ex vivo*	25 male, 25 female Normal specimens T1, T3, T6, T9, T12, L1, L3	Calipers, protractors, goninometers	• Males had slightly larger vertebral dimensions than females • Vertebral pedicle dimensions and angular relationship to VB are largely unpredictable • Statistical significance not explored

Table 2.1.2: Summary of anatomical variations in the intervertebral discs between males and females.

Author [Ref.]	Study type	Participants	Methods	Results and notes
Demir (2018) [44]	*in vivo*	70 male, 80 female Healthy participants T12 to S1	X-ray	• IVD height: males > females ($p<0.001$) • IVD height increased with age, weight, height, and BMI ($p<0.001$) in both sexes
Kunkel (2011) [45]	*ex vivo*	15 male, 15 female C7 to T12	Calipers, x-ray	• IVD height to VB height ratio: 1:4.1 ($p<0.005$)
Malkoc (2012) [46]	*in vivo*	84 male, 87 female Healthy participants Lumbar IVDs	MRI	• Mean IVD height = $\frac{anterior+posterior}{2}$ • IVD height: not statistically significant between sex or age • IVD depth: changed significantly with age in both sexes ($p<0.05$)
Onishi (2019) [47]	*in vivo*	150 male, 150 female LBP patients L3 to S1	MRI	• Mean IVD height = $\frac{anterior+posterior}{2}$ • Mean disc height: males > females, but not statistically significant ($p>0.05$) • Anterior disc height decreased with age for L3/L4, L4/L5
Pfirrmann (2006) [35]	*in vivo*	37 male, 33 female Healthy participants	MRI	• Increasing age correlated with disc height ($p<0.01$) • No influence of weight, height, or sex on disc height • Disc volume predicts disc degeneration ($p<0.01$), correlated with age ($p<0.01$) and height ($p<0.001$)

Table 2.1.3: Summary of anatomical variations in the muscles between males and females.

Author [Ref.]	Study type	Participants	Methods	Results and notes
Cooper (1992) [30]	*in vivo*	53 male, 39 female LBP patients	CT	• Paraspinal muscle CSA: males 22% > females • Paraspinal and psoas CSA is smaller in patients with chronic LBP compared to healthy participants
Hides (1992) [48]	*in vivo*	21 male, 27 female	Ultrasound	• Multifidus CSA: males 10% > females
Klupp (2018) [49]	*in vivo*	12 male, 9 female	MRI	• Erector spinae CSA: males 32% > females ($p=0.004$)
Marras (2001) [41]	*in vivo*	10 male, 20 female Healthy participants T8 to S1	MRI	• Erector spinae, latissimus dorsi, psoas major, obliques CSA: males > females for most vertebral levels ($p<0.05$) • Variations between right and left sides more apparent in female participants
Watson (2008) [31]	*in vivo*	8 male, 17 female Healthy participants	Ultrasound	• Positive correlation between muscle strength and size • Multifidus CSA: males 25% > females ($p<0.002$)

2.2 Low Back Pain

In 2015, musculoskeletal disorders were identified as the leading global cause of disability [50], with low back pain (LBP) and neck pain representing the single largest cause [50]–[52]. From 2005 to 2015, the global prevalence of LBP persisting for greater than 3 months increased by 18.7% [51] and is likely to continue increasing as the population ages [50]. LBP affects 70-85% of individuals at some point in their lifetime [53]–[57]. In Canada, it is prevalent in more than one-third of individuals suffering from chronic pain [58]. The stages of LBP can be categorized based on the duration of pain as acute (<6 weeks), subacute (6 weeks to 3 months), or chronic (>3 months) [59], [60], where chronic pain can be defined as pain persisting for a duration longer than the expected healing time [61]. LBP is one of the leading causes of consultations of healthcare professionals and work absences [4], [52]. In Canada, annual LBP-related medical costs are

estimated between $6 to $12 billion [62], while in the United States of America, estimations are as high as $100 to $200 billion annually [63].

Despite the heavy burden that LBP places on health and welfare systems, determining the pathomechanism of LBP often eludes clinicians. It is estimated that up to 85% of LBP cases have no specific diagnosis [55]. Identifying the location of injury is complicated by the abundance of muscles, connective tissues, and tendons concentrated over a small vertebral area [15]. Studies suggest that back pain can originate from various spinal structures, including ligaments, musculature, connective tissues, facet joints, annuli fibrosi, or nerve roots [57], [64]. For example, a study by Langevin et al. suggested that abnormal connective tissue structures in the TLF may be caused by injury or changes in physiological movement patterns, consequentially resulting in a potential cause of LBP [65]. Due to the challenge of attributing LBP to a specific cause, some describe LBP more generally, such as symptoms of a disease (tumors, osteoporosis, etc.), tissue trauma (acute injury or excessive loading), or association to various disorders (infectious, metabolic, inflammatory, psychoneurotic, etc.), among others. [4]. Nevertheless, potential risk factors associated with LBP include, but are not limited to, heavy or improper physical labour [4], [15], [56], [66], [67], working environment (awkward posture or whole body vibrations) [66], prolonged postures (sitting or standing) [4], [56], [66], [67], sedentary lifestyle [4], obesity [4], [15], [55], [56], smoking [4], [15], [55], [68], psychological distress [68], or genetic factors [55], [68]. With respect to biological sex, females demonstrate a higher prevalence of LBP than males [68], [69]. It is suggested that possible causes may be due to greater spine compressive loads and lower spine tolerances in females, which may pose a greater risk of low back injuries [70]. Further, the prevalence of LBP has been found to increase with an ageing population [15], [53], [56], [59].

Loss of lumbar lordosis is common among the ageing population, and it is known that age is an important factor in the occurrence of LBP [71]. However, there are conflicting opinions regarding the correlation between changes in spinal lordosis and the development of LBP [71]. In a review conducted by Chun et al., the evaluated studies found that the angle of lordotic curvature was reduced in patients with LBP compared to healthy individuals [71]. Further, results in this review demonstrated that age, disc herniation, and disc degeneration played a role in the correlation of LBP and lumbar lordosis. As disc degeneration becomes more severe, disc height is reduced, and consequently, the lordotic angle may also be reduced [71]. In addition, the spinal column is subjected to various loads during day-to-day activities. Variations in spinal alignment may impact the load distribution throughout the spine, consequently affecting the development or progression of LBP. Thus, the evaluation of spinal loading and alignment may provide crucial insight and understanding while evaluating this common affliction.

2.3 Spinal Loading

The human spine is subjected to a variety of loads and motions during daily activities, including flexion, extension, lateral bending, and axial rotation. The spinal column withstands compressive loads of approximately 2.5 times an individual's body weight during walking [26], and these values are much higher during more strenuous activities. Due to its inferior position in the human torso, the lumbar portion of the spine supports the majority of the weight of the upper body [9] and is consequently subjected to significant mechanical loads. Excessive loading in the spine may play a role in the etiology of back pain and various spinal disorders. Thus, there has been an interest in identifying "normal" loads on the spinal column, as this knowledge may assist healthcare professionals in identifying possible causes of LBP.

The compressive loads on the lumbar spine have been evaluated, taking into account the influence of trunk muscle forces, intra-abdominal pressure, and intradiscal pressure when performing various tasks [9]. It was estimated that the head and each arm accounted for 5% and 4.45% of an individual's body weight, respectively, while 36.1% was allotted to the trunk above L3 [9]. *In vivo* compressive loads in the lumbar spine are estimated to be approximately 1000N when standing and walking, with higher loads reported for heavy lifting tasks [9], [72]. However, *ex vivo* studies have struggled to accurately mimic the magnitude of compressive loads applied on the lumbar spine during daily tasks, instead observing buckling of the spine under compressive loads as low as 80-100N, far below the *in vivo* levels [72]. Patwardhan et al. were able to mimic the observed *in vivo* lumbar loads in an *ex vivo* study by applying a "follower load" through the use of cables attached tangentially to the curve of cadaveric lumbar spine segments [72]. The authors described a follower load as the internal compressive loads passing through the centers of rotation of the lumbar vertebrae, tangential to the curve of the spine, as displayed in Figure 2.3.1. With the implementation of a follower load, which is thought to account for the active contribution of the spinal muscles, *ex vivo* lumbar specimens were successfully loaded up to a maximum of 1200N without buckling [72]. As such, the use of a follower load has been repeated in many *ex vivo* and *in silico* studies to accurately mimic *in vivo* loading scenarios [73]–[78].

The compressive strength of the vertebrae is primarily dependent on bone density and CSA. When subjected to axial compression, the mechanical stress of the vertebra is proportional to the load applied to the bone and inversely proportional to the CSA [27]. In comparison, the compressive strength of the vertebra is proportional to VB CSA and is further dependent on the material properties of bone [27]. Another important parameter to consider when evaluating bone strength is the loading rate, as bone demonstrates higher strength at faster loading rates [2]. While Gilsanz et al. estimated that the VBs in females are under 33% greater compressive stress than in males

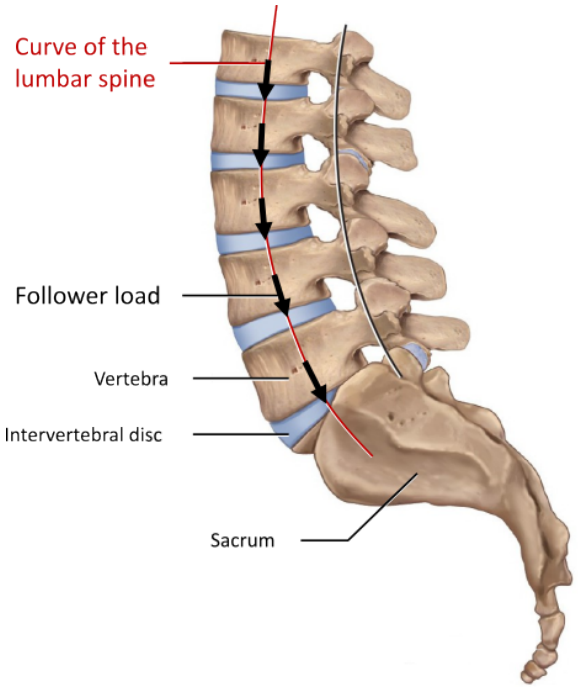

Figure 2.3.1: Follower load in the lumbar spine (adapted from www.learnmuscles.com [13], permission from Dr. Joe Muscolino, artwork by Giovanni Rimasti).

under equivalent loads [27], it has also been found that the compressive strength does not vary between genders [2], [27] or vertebral levels [2], but rather, it is the size of the bone that has an effect. However, changes to the vertebrae, such as osteoporosis, fractures, or other degenerative diseases, will evidently affect the loading capacity of the bone.

Measuring IVD pressure is another useful method for identifying loading in the spinal column. Some of the earliest *in vivo* studies that recorded IVD pressure were conducted by inserting needle-like sensors into the discs of participants to extract the pressures that the discs were subjected to during various tasks [79]–[81]. Several studies measured *in vivo* IVD pressure in the L3/L4 and L4/L5 discs to range between 0.3-0.5 MPa in standing positions [9], [82]–[85]. However, the biomechanical loads felt by the spinal column may be affected by various factors; for example, augmented muscular activity, physical loads, or trunk inclination will increase the loads on the spine [83]. An *in vivo* study by Takahashi et al. observed the mechanical loads on the L4/L5 IVD in an unloaded and in a weighted forward flexion position to be 3.6 times and 4.3 times the loads observed in an upright position, respectively [83]. Values for IVD pressure in the L3/L4 and L4/L5 discs under flexion were found to range between 1-1.6 MPa when measured *in vivo* [9], [82]–[84]. These studies indicated that torso position and external loads affect intradiscal pressures. A summary of previously published literature that measured or computed IVD pressure through *in vivo*, *ex vivo*, or *in silico* studies can be found in Appendix A.1, Tables A.1.1-A.1.3.

Although biological sex was not found to affect the compressive strength of individual vertebrae, age and sex may still play a crucial role in available lumbar motion and strength. A biomechanical rigid body model developed by Jäger et al. evaluated the lumbar load tolerances under lifting tasks and compared them to available literature [86]. The results demonstrated that age and sex affect spinal compressive load tolerances. More specifically, the female model showed an estimated upper limit of the compressive strength in the lumbar spine that was two-thirds of the male model, and a model of a 55-year-old individual exhibited approximately one-half of the compressive strength of a model of a 25-year-old individual [86]. To add, Marras et al. conducted an *in vivo* study in which spinal loading was evaluated with respect to biological sex when participants performed equivalent lifting tasks [70]. Marras and colleagues observed that the compressive loads on the female participants were approximately 47% of their loading tolerance, compared to 38% of the loading tolerance observed in the male participants. These results indicated that older individuals and women are at a higher risk of augmented loading and thus injury when performing physically demanding tasks when compared to younger individuals and men. In addition to age and sex, muscle endurance and range of motion can also affect lumbar tolerances and consequently the onset of LBP [87].

To summarize, muscular forces, external loads, trunk movement, age, and biological sex, among other factors, can affect the load distribution throughout the spine. Thus, the ability of the spine to withstand daily loads is essential to maintaining alignment and ensuring spinal health.

2.4 Spinal Stability and Alignment

The ability of the spine to main a stable behaviour is critical to allow movement, withstand loads, and avoid injury and pain [88]. However, just as the assessment of LBP is a challenge, there is a lack of consensus when defining spinal stability [88]–[91]. Even so, there is a general agreement that a loss of normal patterns of spinal motion may result in pain or neurologic dysfunction [92].

Spinal instability is often classified in terms of mechanical or clinical (functional) instability [89], [92]. Mechanical instability refers to the inability of the spine to carry loads, whereas clinical instability references the consequences of neurological deficit or pain [92]. The concept of spinal instability was first introduced by Barr in 1951 [89], who advocated that a loss in disc height from degenerative discs resulted in increased vertebrae movement, and consequently LBP [89], [93]. Similar to mechanical systems, Pope and Panjabi described an unstable structure as one that "is not in an optimal state of equilibrium," resulting in a loss of stiffness [94]. Stiffness refers to a system's displacement in response to an applied load [94]. White and Panjabi further defined clinical instability as the loss of the spine's ability to maintain its displacement pattern

under physiologic loads, often resulting from trauma, disease, or surgery [91].

Some researchers have chosen to study spinal stability alternatively to instability. The American Academy of Orthopedic Surgeons defined stability as the "capacity of the vertebrae to remain cohesive and to preserve the normal displacements in all physiological body movements" [95], [96]. McGill and Cholewicki analysed spinal stability in terms of potential and elastic energy, defining "sufficient stability" as a requirement to prevent buckling or undesired displacement [90]. Reeves et al. argued that the spine is a dynamic system, and consequently, stability should be defined for both static and dynamic situations [88]. These authors defined a system as stable if, after applying a small perturbation, the new behaviour is approximately equivalent to the previous behaviour [88].

Three subsystems have been described as contributing to the spine's stabilizing system: the spinal (passive) column, the spinal (active) muscles, and the neural control unit [66], [92]. Research has shown that the abdominal cavity may play an important role in the spine's static stability. However, the role of intra-abdominal pressure has remained controversial [97], [98]. It is hypothesized that the co-contraction of the surrounding transverse and oblique abdominal muscles coupled with increased intra-abdominal pressure can unload and stabilize the spine [97], [98]. It is also assumed that an increase in abdominal stiffness may restrict vertebral translation and rotation [99]. Despite the controversy surrounding the definitions of spinal stability and instability, and the uncertainty of the potential causes leading to LBP, there is an unmistakable need for assessment methods that lead to reliable diagnoses.

2.4.1 Quantifying Spine Alignment

The spine is a 3-dimensional (3D) musculoskeletal system; all three planes contribute to spinal alignment and, consequently, may influence the development of various disorders if the spine is misaligned or unstable. The spinal planes can be seen in Figure 2.4.1a). The healthy spine exhibits an S-shaped curve when visualized in the sagittal plane and a straight appearance in the coronal plane [6]. The cervical and lumbar regions typically exhibit lordotic curvature (convex anteriorly), whereas the thoracic spine demonstrates kyphotic curvature (convex posteriorly) [1], [6]. This unique curvature permits an optimal distribution of body weight across the vertebrae [7]. Consequently, "normal" values describing spinal curvature have been identified with the overarching goal of quantifying ideal spinal alignment, disorders, and deformities [100].

The coronal (frontal) plane is primarily utilized to analyse scoliotic deformity [101], which is an abnormal lateral curvature of the spine. One of the earliest methods of evaluating coronal spinal curvatures was proposed by Ferguson [100]. In this method, the apical vertebra and the end vertebrae are connected by straight lines to evaluate the angle of deformity [100], [101]. An alter-

native method of evaluation was proposed by Cobb, who defined the angle between two straight lines tangent to the superior and inferior endplates of the respective end vertebrae [101], [102]. Although the Ferguson and Cobb methods both achieved high correlation for measures of curve severity [103], in 1966, the Scoliosis Research Society adopted the latter as the standard method of scoliosis deformity quantification [101]. Specifically, the Cobb method was preferred for its ease of application and reproducibility, as well as its ability to measure larger angles for more severe spinal curvature [101].

Using the described methods of measurements to assess spinal curvature in the coronal plane, a Cobb angle of up to 10° is referred to as spinal asymmetry [104], meanwhile, a Cobb angle of greater than 10° is defined as scoliosis [104]–[106]. Scoliosis can be present in all stages of life, i.e., childhood, adolescence, or adult life. Although it progresses more rapidly during adolescent growth spurts before skeletal maturity [104], untreated idiopathic scoliosis can continue to increase after skeletal maturity, with an average progression observed of 0.4° per year [107]. Curve progression can also play a role in the advancement of scoliosis, as the loads on a weakened vertebra may cause it to become more wedged and deformed, therefore leading to increased curvature and consequently increased back pain [105].

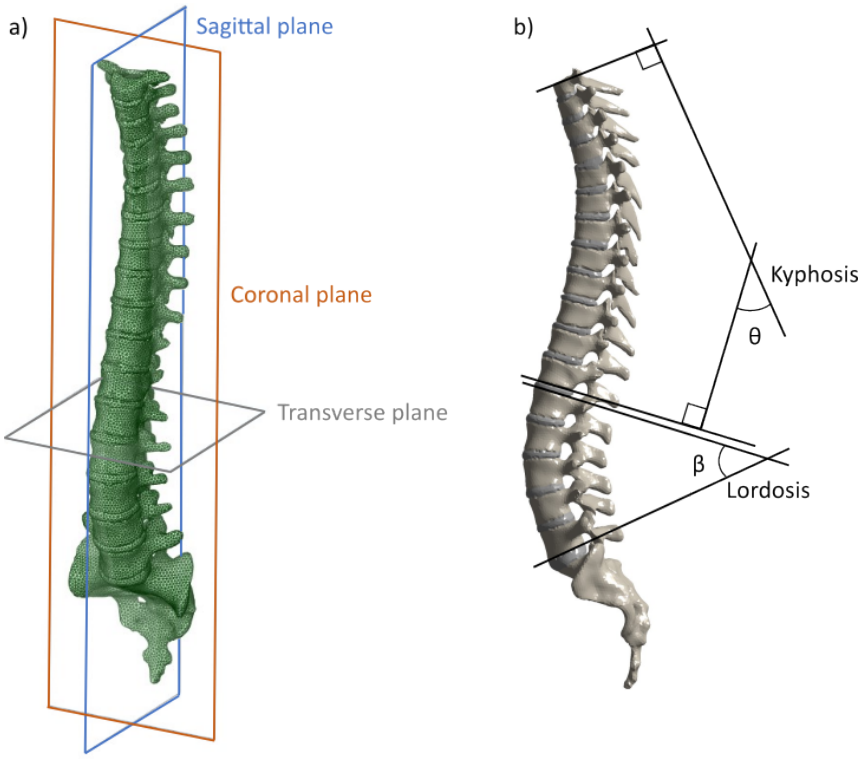

Figure 2.4.1: a) The anatomical planes of the body, and b) the modified Cobb method for measuring thoracic kyphosis and lumbar lordosis in the sagittal plane.

The sagittal (lateral) plane displays measurements of cervical lordosis [101], [108], [109], thoracic kyphosis [101], [110], lumbar lordosis [101], [110], and segmental vertebrae angulation [101]. The "modified Cobb method" was one of the first techniques applied in the sagittal plane [102], in which vertebral endplate lines are drawn on lateral radiographs to measure the sagittal angle of curvature [111]. The corresponding methodology for measuring curvature in the sagittal plane can be seen in Figure 2.4.1b). For asymptomatic adults, cervical lordosis (C2-C7) was reported between -30° to -40° [108], [109], thoracic kyphosis between 10° to 40° [3], [109], [112]–[114], and lumbar lordosis between -40° to -60° [3], [109], [112]–[114]. Values outside of these "normal" ranges are considered exaggerated curvatures, as summarized in Table 2.4.1, and may be correlated to potential spinal disorders and LBP. Specifically, for the thoracic and lumbar regions, curvature values lower than the normal range are considered hypokyphotic and hypolordotic, respectively, whereas curvatures larger than the normal range are considered hyperkyphotic and hyperlordotic, respectively. Despite the common practice of using Cobb's angle to evaluate sagittal spinal curvature, there is no consensus regarding which vertebrae to select for measurements. In previously identified studies, the vertebrae chosen for thoracic kyphosis measurements varied, with researchers selecting superior vertebrae between T1 to T5 while primarily using T12 as the inferior vertebra [3], [109], [110], [113]–[115]. Variations were also observed when measuring lumbar lordosis, selecting T12, L1, or L2 as the superior vertebra and L5 or S1 as the inferior vertebra [113], [116]–[118]. The variations in the selected vertebrae will affect the magnitude of the measured spinal curvatures. A summary of several previously conducted studies with adult participants, and the vertebrae selected for analyses, is included in Table 2.4.2.

Table 2.4.1: Degrees of sagittal curvature for lordosis and kyphosis.

	Kyphosis	Lordosis
Hypo	$<10°$	$<40°$
Normal	10-40°	40-60°
Hyper	$>40°$	$>60°$

Table 2.4.2: Summary of techniques used to measure sagittal spinal curvature.

Author [Ref.]	Upper vertebra	Endplate used	Lower vertebra	Endplate used	Cobb angle	Participant information
Kyphosis						
Alijani (2020) [109]	-	-	-	-	35.2±5.7°	105 healthy volunteers, age: 58.55±7.5 yrs
	-	-	-	-	36.9±7.4°	105 LBP patients, age: 59.96±7.04 yrs
Briggs (2007) [119]	T1	Upper	T12	Lower	55.9±13.3°	31 osteoperotic women, age: 64.3±7.4 yrs, height: 159.8±5 cm, weight: 63.1±10.8 kg
	T4	Upper	T9	Lower	38.9±8.7°	
Gelb (1995) [113]	T1	-	T5	-	14±8°	100 healthy volunteers, age: 57±11 yrs, height: 170.2±10.2 cm weight: 75.5±15.5 kg
	T5	-	T12	-	34±11°	
Jackson (1994) [120]	T1	Upper	T12	Lower	42.1±8.9°	100 healthy volunteers, age: 38.9±9.44 yrs, height: 67.4±3.84 in, weight: 168.5±31.2 lb
					42.6±10.1°	100 LBP patients, age: 3.4±8.95 yrs, height: 67.3±3.65 in, weight: 170.3±40.4 lb
Vialle (2005) [121]	T4	Upper	T12	Lower	40.60±10°	300 healthy volunteers, age: 35.40±12 yrs
Yukawa (2018) [114]	T1	Upper	T12	Lower	37.1±9.9°	305 male volunteers, age: 20-79 yrs, height: 169.1±6.5 cm, weight: 66.7±10.3 kg
	T1	Upper	T12	Lower	35.0±10.5°	321 female volunteers, age: 20-79 yrs, height: 156.2±6.0 cm, weight: 52.9±8.0 kg
Lordosis						
Alijani (2020) [109]	L1	Upper	S1	Upper	53.7±8.7°	105 healthy volunteers, age: 58.55±7.5 yrs
					52.5±9.2°	105 LBP patients, age: 59.96±7.04 yrs
Gelb (1995) [113]	T12	Lower	S1	Upper	64±10°	100 healthy volunteers, age: 57±11 yrs, height: 170.2±10.2 cm, weight: 75.5±15.5 kg
Hansen (2015) [122]	L2	Upper	S1	Upper	52.0±9.5°	38 healthy participants, supine, age: 39±11.9 yrs
					58.0±10.3°	38 healthy participants, standing, age: 39±11.9 yrs
					45.6±12.4°	38 LBP patients, supine, age: 39±11.7 yrs
					52.4±11.4°	38 LBP patients, standing, age: 39±11.7 yrs
Hicks (2006) [118]	L1	Upper	L5	Lower	38.1±12.06°	123 women, age: 70.36±4.74 yrs, BMI: 27.39±4.32 kg/m^2
Jackson (1994) [120]	L1	Upper	S1	Upper	60.9±12.0°	100 healthy volunteers, age: 38.9±9.44 yrs, height: 67.4±3.84 in, weight: 168.5±31.2 lb
					56.3±11.5°	100 LBP patients, age: 3.4±8.95 yrs, height: 67.3±3.65 in, weight: 170.3±40.4 lb
Kalichman (2011) [123]	L1	Upper	S1	Upper	46.8±10.2°	154 healthy participants
Lee (2014) [117]	L1	Upper	S1	Upper	40.16±8.84°	10 healthy men, age: 25.4±2.3 yrs, height: 175.3±3.5 cm, weight: 75.1±8.2 kg
					49.50±13.12°	10 healthy men, age: 66.7±1.7 yrs, height: 168.8±5.3 cm, weight: 73.6±8.5 kg
Mauch (2010) [116]	L2	Upper	S1	Upper	46.3±9.9°	35 healthy athletes, supine, age: 28±6.5 yrs
					52.6±8.9°	35 healthy athletes, standing, age: 28±6.5 yrs
Murrie (2003) [124]	L2	Upper	S1	Upper	48.25°	12 healthy male volunteers
					39.75°	12 male patients with chronic LBP
					51.82°	17 healthy female volunteers
					51.60°	15 female patients with chronic LBP
Vialle (2005) [121]	L1	Upper	L5	Lower	43±11.2°	300 healthy volunteers, age: 35.40±12 yrs
Yukawa (2018) [114]	T12	Lower	S1	Upper	47.8±11.6°	305 male volunteers, age: 20-79 yrs, height: 169.1±6.5 cm, weight: 66.7±10.3 kg
					51.6±11.6°	321 female volunteers, age: 20-79 yrs, height: 156.2±6.0 cm, weight: 52.9±8.0 kg

- unspecified

The orientation in which the patient is placed for imaging may also affect the outcomes of the evaluation. Several studies have identified changes in sagittal curvatures with respect to the adopted posture of the patient. Lee et al. identified a decrease in lumbar lordosis from standing to supine positions of 12.04° ± 11.37° when comparing radiographs of male volunteers [117]. In comparison, a study by Mauch et al. measured a decrease in lumbar lordosis of 6.3° ± 5.6° from standing to supine when measured on MRI images [116]. A similar study was conducted by Hansen et al. who evaluated lumbar lordosis through MRI images in both healthy and LBP patients and found a decrease in curvature from standing to supine of 6.8° ± 6.0° and 6.0° ± 5.3°, respectively [122]. Traditional supine positions for MRI are performed with slight hip or knee flexion, which may contribute to reduced lordosis relative to a standing position [125]. Thus, Andreasen et al. determined that positioning the patient with straightened lower extremities would only result in a median deviation of 3° relative to a standing position [125]. To add, age and biological sex also play a role in spinal alignment. Singer et al. recorded a progressive increase in kyphotic curvature with respect to age in both male and female participants [126]. Lee et al. observed greater lordosis in an older group of healthy individuals compared to a younger group, regardless of body position, although the greatest difference was observed in the supine position [117]. Contrarily, studies by Gelb et al. and Yukawa et al. reported a loss of lumbar lordosis with increasing age [113], [114]. When considering biological sex, studies have observed lower thoracic kyphosis [114], [121] and greater lumbar lordosis in females compared to males [114], [121], [124]. Nevertheless, many patients with LBP, irrespective of age or sex, have demonstrated changes in their sagittal profiles when compared to a healthy population. For example, studies by Kalichman et al. [123] and Jackson and McManus [120] observed that change in lordosis was not correlated to age or biological sex, but the latter study found that patients with LBP demonstrated a mean loss of lordosis of 4.6° [120]. Similarly, Hansen et al. observed a reduction in lumbar curvature of approximately 6° in LBP patients [122].

Another important parameter when considering spinal alignment is the sagittal vertical alignment (SVA). SVA is defined as the horizontal offset from a vertical plumbline dropped from the mid-body of C7 to the posterosuperior corner of the S1 endplate [109], [110], [127]–[129]. A positive value indicates sagittal balance anterior to the front of the sacrum, whereas a negative value denotes sagittal balance behind the sacrum [110]. SVA is observed to increase with age [113], [130], while a larger reading is commonly associated with sagittal deformity [127]. Schwab et al. suggested that global realignment for surgical correction should target SVA$<$50 mm to position the C7 plumb line behind the femoral heads, level the gaze, and achieve a physiologic standing posture [128].

As the pelvis forms the base of the spine, spinopelvic alignment plays a crucial role in the spinal profile [129]. Three parameters are most commonly used to describe the pelvis and spine relationship: pelvic incidence (PI), pelvic tilt (PT), and sacral slope (SS) [127], [131]. PI plays a critical role in sagittal balance [132] and is defined as the angle formed by the middle of the line connecting the center of the bicoxofemoral axis to the perpendicular bisector of the middle of the sacral endplate [133], [134]. PI is constant, but unique, for each individual [132], [133]; it does not change depending on patient age, position, or deformity [129]. The mean PI angle for asymptomatic individuals was reported between 50° to 55° [109], [114], [128], [133]. PT is a dynamic parameter that changes depending on pelvic rotation [129]. It is defined by the angle between the midpoint of the line through the femoral head axis and the vertical [128]. Normal values of PT have been recorded between 10° to 15° [114], [115], [128], [130], [133], with ideal values of PT$<$20° [128]. A backward rotation of the pelvis, or an increase in PT, is often observed as a compensation mechanism to maintain normative spinopelvic alignment as a person ages [128]. SS is the angle between the upper sacral endplate and the horizontal [128], [133]. The geometric relationship for pelvic parameters can be described by the equation PI=PT+SS [128], [133]. From this equation, the range of normative SS is between 35° to 45°. Methodology for measuring PI, PT, and SS can be seen in Figure 2.4.2.

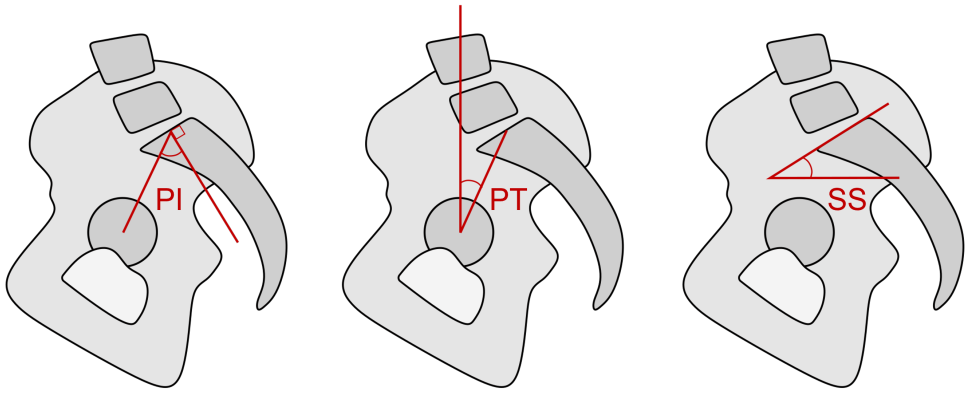

Figure 2.4.2: Pelvic incidence (PI), pelvic tilt (PT), and sacral slope (SS) measurements.

2.4.2 Relationship Between Spine Regions

There are four main regions of the spine: cervical, thoracic, lumbar, and sacrum. These regions are separated by "transition zones," specifically the craniocervical, cervicothoracic, thoracolumbar, and lumbosacropelvic zones, respectively [112]. The interplay between the regions and transition zones may shed light on an individual's spine alignment, health, and biomechanics.

As PI is "fixed," this may set the foundation for an individual's spinal profile. To maintain spinal health, the thoracic and lumbar regions should balance the head over the sacrum [112], thus maintaining a horizontal gaze during daily activities [6]. A C7 plumbline has often been used to evaluate sagittal balance [110], and ideally, should measure within several millimeters of the posterosuperior corner of the S1 endplate [110], [112]. Considering the thoracolumbar transition zone, the Spinal Deformity Study Group identified that the lumbar spine should typically have a 30° greater curvature than the thoracic spine [112].

Several studies have observed correlations between pelvic alignment and sagittal profile. One commonly referenced classification system for sagittal profiles was outlined by Roussouly et al. [135]. These authors observed that the lordotic curvature and apex were influenced by the SS. Specifically, a SS less than 35° and a low PI typically resulted in a reduced lordotic angle, whereas the inverse was observed for a SS greater than 45° and a higher PI. From their findings, Roussouly and colleagues developed a classification system in which they identified four types of lumbar alignment from their findings [135], [136], summarized as:

- **Type 1**: SS <35°, low PI, apex at the middle of L5, minimal lordosis, low inflection point, long thoracolumbar kyphosis, short lumbar lordosis;
- **Type 2**: SS <35°, apex at the base of L4, spine is relatively hypolordotic and hypokyphotic, flat lumbar lordosis;
- **Type 3**: 35° <SS <45°, apex at the middle of L4, spine inflection point at thoracolumbar junction, equal lengths of thoracic kyphosis and lordotic curves;
- **Type 4**: SS >45°, apex at the base of L3 or higher, hyper-curved spine, shorter thoracic kyphosis, longer lumbar lordosis.

A depiction of the classification system can be seen in Figure 2.4.3, which has since been expanded to evaluate the Roussouly classification with the evolution of spines with degenerative diseases [136]. In the coronal plane, the Lenke classification is often used to evaluate patient alignment for scoliosis and corrective surgeries [137].

Despite these findings, many authors have alluded to the high variability in sagittal profiles, regardless of age or sex. Further, the relationship between lumbar curvature and LBP is poorly understood [71]. The variance in an individual's spine curvature makes it difficult to classify patient profiles or predict the onset of various spinal disorders, and as such, clinical evaluations are a crucial step to aid in the diagnosis of potential sources of pain.

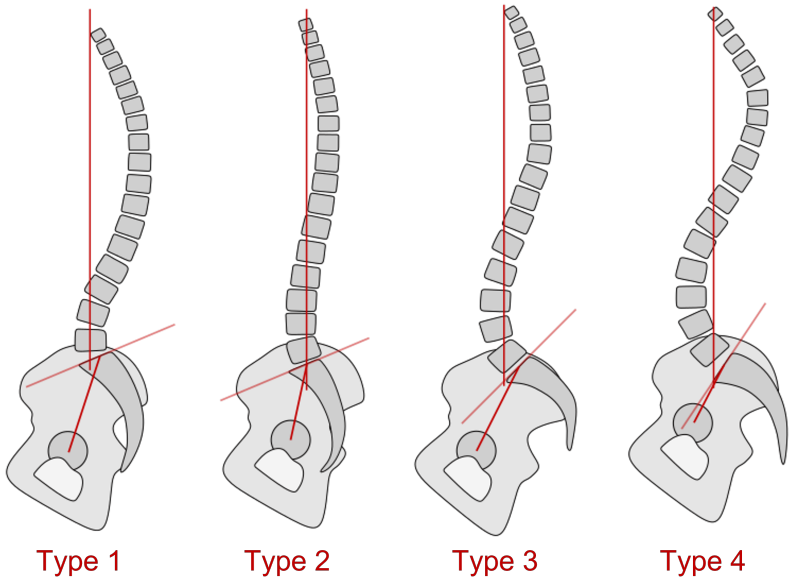

Figure 2.4.3: Roussouly classification of sagittal spine alignment.

2.5 Clinical Evaluation

Details of medical history and physical examination are required for adequate clinical diagnosis of LBP, as no single test is sensitive or specific enough to formulate a definitive diagnosis [57]. Most guidelines for the diagnosis and management of LBP suggest that patients be classified as having: 1) nonspecific mechanical LBP (pain associated with movement or posture), 2) nerve root pain, or 3) possible serious spinal pathology (infection, trauma, inflammation, or neoplasm [60]) [138], [139]. Understanding the history of pain (duration, onset, factors that alleviate or increases symptoms, and associated symptoms) can provide critical information to clinicians and can assist in diagnosis and treatment [56].

A complete spinal examination should be performed when assessing for LBP, including inspection, palpation, range of motion, muscle strength, reflexes, gait, and detailed tests [56]. Musculoskeletal palpation assesses muscle tenderness [56]. Analyzing a patient's range of motion informs clinicians of the function of the IVDs and facet joints and is commonly measured using inclinometers to determine the degree of flexion [140]. Studying lifting capacity provides information on maximum capacity and endurance, however, this test does not isolate individual muscles and is often considered a whole-body activity [140]. Leg length discrepancy is associated with an increased risk of radiculopathy or LBP [56], whereas a patient experiencing fever is an indicator of potential spinal infection [56], [57]. An observed increase or decrease in lumbar lordosis, muscle atrophy, postural asymmetry, or alignment is supportive of diagnosis [56], while atypical postures are often associated with specific musculoskeletal disorders [141]. Patients with

radiculopathy typically have a segmented nerve root lesion within the myotome [142], and often experience numbness and tingling in the lower extremities [56]. Sciatica, a sharp or burning pain radiating down the leg, is usually the first indication of nerve root irritation [57]. After an initial history and physical examination, clinicians often perform a series of tests to better identify potential sources of pain, however, the source of many LBP cases remains idiopathic.

Common treatment plans for LBP often begin with a physical evaluation, although if no clear conclusions may be drawn from these examinations, or if a more serious underlying cause is anticipated, medical imaging may be required. Following examination, physical therapy and targeted core strengthening exercises may be suggested to increase overall spinal strength and stability [143]–[145]. In severe cases where non-invasive treatments, such as physiotherapy or braces, do not alleviate pain, surgical interventions may be required [146].

2.6 Imaging Techniques

Postural alignment and spinal stability are difficult to study as postural assessment is still scientifically inaccurate [147]. Numerous imaging techniques exist that permit clinicians to perform initial or detailed spinal assessments, including photographs, X-rays, CT, and MRI [147].

According to Fortin et al., photographs are one of the most promising techniques to assess sagittal and frontal body angles [148]. This method is rapid, simple, and accessible to clinicians, and is often preferred to taking direct recordings of patient body angles with a goniometer or inclinometer [148]. Goniometers and inclinometers quantify posture characteristics by measuring angle values between 0° to 360° [147]. However, these evaluations can be lengthy and challenging, requiring the patient to remain in a fixed postural position for an extended period of time [148]. Further, photographs do not permit a precise analysis of spinal alignment with respect to the curvatures in the vertebral column.

X-rays are the gold standard for bone evaluation [147]. They produce a conic beam of electrons that penetrate the object under consideration to produce 2D images [147]. Radiographs are commonly used to assess or monitor changes in musculoskeletal disorders and spinal alignment [148]. However, these images are invasive and consequently should not be used for repeated measurements [148]. Today, there is a growing consensus that radiographs are not necessary for all patients due to potentially misleading results and interpretive disagreements [57]. Furthermore, manual measurements are time-consuming and subject to variability [101].

Both CT and MRI provide clear visualization of normal and pathological spine anatomy [1] and are typically sourced when a specific diagnosis or disorder is suspected [31], [149]. CT scans use X-rays that rotate around the body to produce 3D data [147]. This imaging technique is best at visualizing bony structures [5], [115] and is the gold standard for vertebral rotation assessment

[150]. However, CT is costly and exposes the patient to radiation [147], [150], therefore limiting its clinical utility.

In contrast, MRI is better at imaging soft tissues than osseous anatomy [147], [151]. It utilizes an electromagnetic field to align hydrogen atoms, which are present in water and biological tissue fat [147], producing "slices" of images, as depicted in Figure 2.6.1. MRI uses T1-weighted and T2-weighted imaging techniques; T1-weighted is preferable for imaging anatomic details and tissues [1], whereas T2-weighted has lower resolution but better visualization of fluid, edema, and spinal cord pathology [1]. Specifically, T2-weighted images provide insightful visualization of the discs, as disc degeneration and desiccation may be observed through a decreased signal intensity in the IVD [1] and reduced visible distinction between the nucleus and the annulus. Further, MRI technology is advantageous as it is non-invasive and can image various postures [151]. However, while 3D MRI is often described as the gold standard for postural evaluation or disc degeneration assessment, it is costly and not always available in clinics [147].

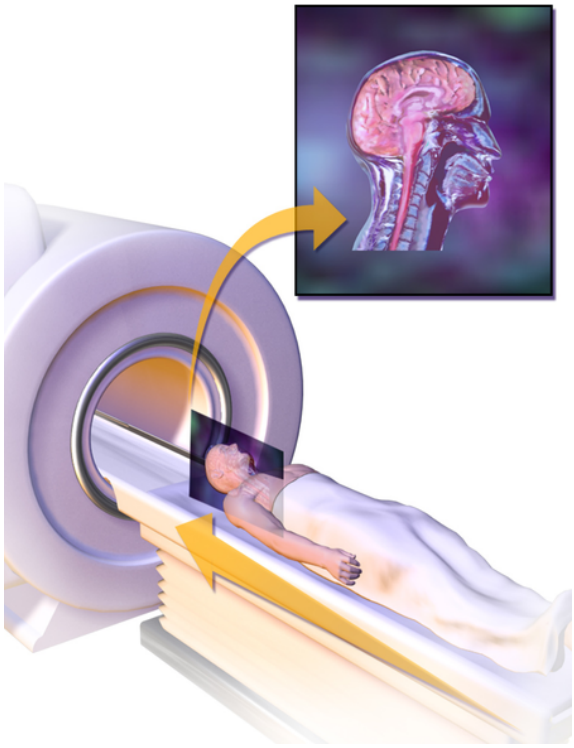

Figure 2.6.1: Magnetic resonance imaging machine, producing an image of the brain and cervical spine (obtained from https://commons.wikimedia.org/wiki/File:MRI_Part_2.png on June 1, 2023).

Though imaging modalities provide valuable information for patient health and spinal assessment, there exist limitations regarding the available information that can be extracted from these images. Thus, leveraging numerical modelling may provide additional insight into spinal

biomechanics, potential pathomechanisms, or the outcomes of various disorders to advance the knowledge of spinal biomechanics, potentially aiding in the diagnosis and treatment of spinal disorders and back pain.

2.7 Finite Element Modelling for Biomechanical Analysis

Although recognized as being established in 1956 [152], [153], the term "finite element method" was first introduced by Clough in 1960 [153], [154]. Finite element analysis (FEA) is a numerical technique, originating as a method of stress analysis for aircraft [155]. Using complex mathematical problems, the finite element (FE) procedure reduces the number of unknowns from an infinite number to a finite number [155]. Since its development, FE modelling has been used in a variety of fields, including structural dynamics, heat transfer, fluid dynamics [155], [156], acoustics, and biomechanics [156]. One of the first evaluations of skeletal parts for biomechanical FEA was introduced by Brekelmans et al. in 1972, who acknowledged the importance of understanding the mechanical behaviour of the skeletal system under physiological loads [157]. Biomechanical modelling encompasses geometry and mechanical characteristics to simulate the exerted forces applied on the model and compute the mechanical response (displacement, local strain, global deformation, or mechanical stress) [158].

FEA has been used to model the biomechanical behaviour of the spine and to support the design of spinal instrumentation [159], [160]. According to Fagan et al., there are four main approaches for assessing the spine through FE modelling: 1) assessment of a healthy spine, 2) assessment of a spine affected by disease, degeneration, trauma, or surgery, 3) assessment of a spine implemented with instrumentation, and 4) design and development of spinal instrumentation [159]. To model the spine in its entirety is an extremely intricate task. Incorporating each segment and its functional units, inclusive of translation and rotation degrees, is computationally costly [161]. As a result, a variety of finite element models (FEMs) have been developed to analyse the spine, ranging from sub-micron scale assessments of bone [162], to vertebrae models, to segments or whole spine models [159], [162]. These models often rely on assumptions and simplifications for successful analysis, such as modelling ligaments, muscles, or discs as springs [159], [163], [164], defining bone tissue as rigid material [159], [165], and excluding surrounding muscles or soft tissues [163], [164]. Despite the knowledge that biological tissues are viscoelastic, many FEM studies have opted to implement simplified material property characteristics for biological modelling, such as linear elastic and isotropic material properties [166]. This linear characterization of the material properties aids in reducing the computational cost of solving the model.

Numerical modelling facilitates the investigation of modifying geometric and material properties [160] between models, thus allowing the exploration of various demographics by adjusting

these parameters and comparing the modelling results. Further, FEA of spine models such as these may permit the investigation of spinal stresses and various loading conditions, as well as the exploration of different treatment options [159], [163]. However, some limitations in the current literature include the lack of sex-specific models, as the majority of available models are constructed from male geometry, or results do not distinguish between biological sexes. To add, there are limited evaluations of the impacts that spinal alignment has on load distribution, as many studies focus on healthy spine anatomy or the effects that device implantation has on the spine. Future developments of patient-specific models are expected to assist with patient analysis and operative planning [159], [163], notably with increased accuracy for geometric personalization.

2.7.1 Previously Developed Finite Element Models

There have been many advancements in FE modelling of the spine in recent decades. One of the first spine models was introduced by Belytschoko et al. in 1974 to study IVD behaviour under axial loading [167]. Later, a vertebra model was developed to study the mechanics of the vertebral column, with computational results that were validated against experimental data from *ex vivo* spine segments [168]. Over the years, published modelling results have expanded from vertebra models with limited elements to functional spine units with nonlinear properties [169], [170], and further to lumbar spine segments to study the biomechanical response under various loading conditions and the influence of muscle activity [171], [172]. In recent years, spine models have become increasingly complex with accurate geometric representation and material properties, allowing a convincing representation of the human musculoskeletal system and physiological loading conditions.

Rohlmann et al. developed a lumbar spine FEM and evaluated different loading modes to achieve model validation against experimental results [164]. The authors determined that the application of a follower load provided a realistic loading scenario when simulating standing [73], [173]. The observed loading conditions from these studies have been applied in several other spine FEAs, including a study by Dreischarf et al. [74]. Dreischarf and colleagues compared the modelling outcomes of 8 lumbar spine FEMs to determine if combining the results of several models improved the strength of the model prediction [74]. In 2020, El Bojairami et al. from McGill University developed a spine FEM representative of male anatomy and inclusive of all major torso elements: vertebrae T1-S1 with adjacent IVDs, spinal muscles (longissimus, multifidus, psoas major, and intertransversarius), thoracolumbar fascia, tendons, and abdominal cavity [174]. This FEM is one of the first full spinal columns including the majority of physiological tissues that contribute to spinal loading [174], resulting in it being one of the most extensive and complex models to date. To add, El Bojairami et al.'s model incorporated pressurized muscles, which provided a

correlation between muscle force and intramuscular pressure in 3D FEMs of muscles, mimicking human muscle contraction [174], [175].

Although age and biological sex are known to impact spinal strength and loading capacity, as previously outlined, these parameters are only occasionally considered in biomechanical modelling. The existence of spine models developed to study ageing specifically is limited. Nevertheless, the effects of disc degeneration, osteoporosis, or vertebral body fractures have often been investigated through modelling studies [176]–[181], and these pathologies are known to have a greater influence with age. When considering biological sex, many models are developed on the basis of male anatomy [75], [174], [182]–[185], do not distinguish between results albeit modelling both sexes [186], [187], or do not specify biological sex [73], [74], [188], despite the fact that there are distinguishable differences between male and female spines and their loading capabilities. Recently, Mills and Sarigul-Klijn developed and validated the first female lumbar spine model specifically to serve as a baseline for modelling a young female spine [163]. These authors highlighted the importance of implementing accurate patient anatomy for realistic modelling results.

Spinal profiles, in both the coronal and sagittal planes, are important indicators of spinal health. Due to its high prevalence, the effects of scoliosis on biomechanical loading, as well as the progression of the disorder as adolescents age, have been evaluated in several FEAs [189]–[192]. Contrarily, changes in sagittal profile are less studied. A study by Naserkhaki et al. evaluated the effects of load-sharing throughout the spine when considering three patient-specific lumbar spine models with varying curvatures: normal, hypolordotic, and hyperlordotic [187]. The authors found that spinal alignment affected the load-sharing, notably in extension. Shirazi-Adl and Parnianpour also studied the effects of changes in lordosis on spine mechanics under lifting scenarios [193]. Their results suggested that slightly straightening the spine may reduce the risk of soft tissue injury in lifting tasks, however, a spine that is too flattened may be at higher risk of injury. With respect to the thoracic spine, Aroeira et al. investigated the biomechanical behaviour of the adolescent spine, with and without kyphotic curvature [194]. Their results indicated that there is a change in spinal load distribution with variations in sagittal curvature, although the study lacked sufficient validation to allow a comparison of results. For the cervical spine, Wei et al. developed a cervical spine model and observed that a straightened spine segment demonstrated reduced range of motion but larger stresses [195]. These studies highlight the importance of including patient-specific profiles in virtual clinical trials. However, despite the current advancements, there is a lack of studies evaluating larger spine portions, as the aforementioned studies have focused specifically on a section of the spine.

The above-mentioned models provide a brief summary of some FEMs that have made notable advancements in biomechanical modelling. However, the summary should not be considered complete, as there are numerous models which provide valuable insight into understanding the biomechanical and physiological aspects of the spinal column.

2.8 Verification and Validation for FEM and Risk-Based Assessment

A significant challenge of computational engineering is to demonstrate that a mathematical model of a given physical reality sufficiently represents that reality, with high enough accuracy to predict and justify engineering decisions [156]. Verification, sensitivity testing, and validation were outlined by Anderson et al. as key elements of computational biomechanics studies [162], [196]. Verification ensures that the input data is correct and that the data errors are within permissible tolerances [156]. This is generally completed by altering mesh resolution and subsequently confirming that the model output produces repeated and accurate results [174]. Sensitivity studies involve altering the input parameters to observe their influence on model predictions [174]. Validation is a "process by which the predictive capabilities of a mathematical model are tested against experimental data" [156]. Direct validation is a comparison to *in vivo* experimental results where model conditions are defined as close as possible to the experiment, whereas indirect validation is a comparison to data from literature or clinical trials where conditions may vary [162]. It is crucial to outline the intended use prior to verification and validation of a model, such as if the model will be used to predict displacement or localized stresses or strains [196].

Verification and validation (V&V) activities can be used to establish model credibility, where credibility refers to "the trust in the predictive capability of a computational model" [197]. The American Society of Mechanical Engineers (ASME) V&V40 Subcommittee developed a risk-based credibility assessment framework to provide guidance on establishing and communicating the credibility requirements for computational models of medical devices [197], [198]. Specifically, ASME's V&V40 principles outline a means to assess a computational model's accuracy in representing a reality of interest. This can be achieved through the comparison of simulation results with theory, carefully designed and controlled experiments, or other sources of relevant information. The steps for the V&V40 standard include: 1) defining the question of interest, 2) defining the content of use (scope and role of the model), 3) assessing the model risk (higher risk may result in patient harm or undesirable outcomes), and 4) establishing credibility factors driven by risk analysis [198].

Identifying the risk associated with the developed biomechanical models is a crucial step in understanding the impact that the model may have on decision consequences, and consequently, on clinical applications and patient safety. The ASME V&V40 risk assessment matrix details the

resulting model risk based on the model influence and decision consequence, depicted in Figure 2.8.1. An incorrect decision resulting from a "low risk" model would not significantly affect patient safety but may result in minor impacts or nuances to the physician, whereas an incorrect decision resulting from a "high risk" model may have severe impacts for the patient, such as grave injury or death. In summary, the greater the model risk, the greater the chances that the patient may experience harm or undesirable outcomes should a wrong decision be taken concerning patient care. Consequently, the intended use, model limitations, and assumptions should be clearly defined prior to using any biomechanical model to guide or influence treatment.

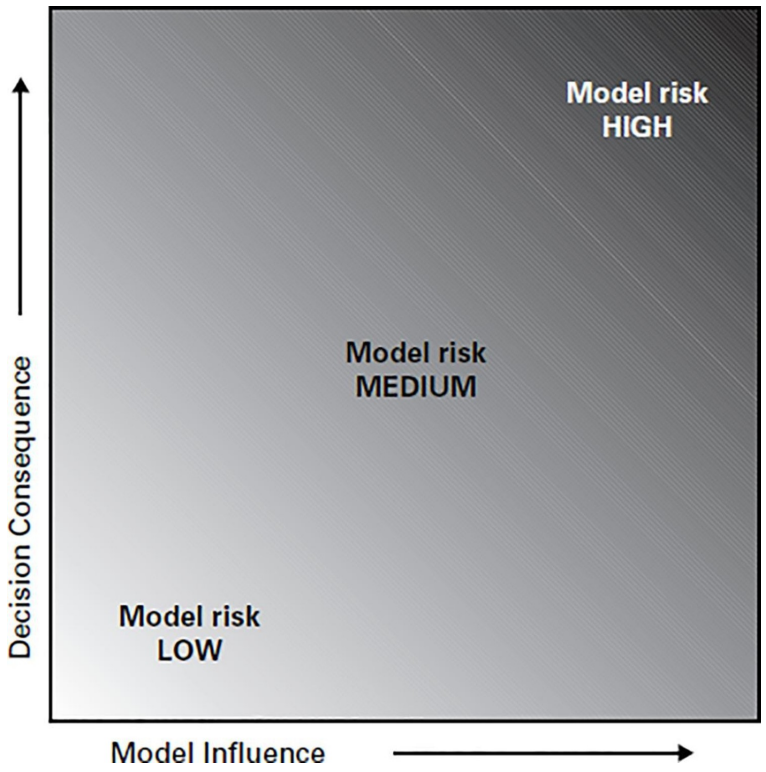

Figure 2.8.1: ASME V&V40 risk assessment matrix (reprinted from ASME V&V40-2018 [197] by permission of The American Society of Mechanical Engineers. All rights reserved.).

2.9 Conclusion

With the global increase in the occurrence of LBP and the immense financial burden and labour shortage this infliction places on society, there is a clear need to leverage technologies that can support and guide the treatment of LBP in an efficient and informative manner. The use of FE modelling for biomechanical analyses of the spine can provide insightful knowledge for studying various spinal pathologies prior to conducting extensive cadaveric or clinical trials, which may help guide these trials or predict expected outcomes. Further, with the growing acceptance of FEMs for virtual clinical trials and regulatory approval, there is a need for biomechanical models

that represent a wide demographic. Although many studies consider patient-specific models, there is a clear gap regarding the effects that geometry, sex, or sagittal profile have on the overall stress distribution throughout the spine. Thus, the studies outlined in the following chapters aim to address geometric personalization of spine FEMs to provide an understanding of how changes in geometry or sagittal profile may impact spinal stress.

3 Research Rationales, Objectives, and Hypotheses

It is widely recognized that each patient is unique, with significant inter-subject variability. However, the existence of FEMs of the spine representative of biological sex or various spinal disorders is minimal. As such, it was the central focus of this thesis to **develop, validate, and analyze geometrically personalized FEMs of the spine**, so that these models may serve as a baseline for future patient-specific FE studies, patient analyses, or medical device development. More specifically, this thesis aimed to study the effects that variations in **geometry**, **biological sex**, or **sagittal profiles** had on the spine's biomechanical behaviour. To successfully realize this global objective, three sub-objectives were identified.

Objective 1: Develop sex-specific thoracolumbar spine FEMs to study spine biomechanics.
Hypothesis 1: The implementation of sex-specific anatomy (geometry and material properties) will yield observable differences in local segmental compressive stresses between sexes.

The prevalence of LBP has been observed to be greater in females when compared to males [199]. Further, it has been shown that the female vertebrae may be subjected to 33% greater compressive stresses relative to male vertebrae when identically loaded [27]. Therefore, the evaluation of sex-specific FEMs may justify these findings. There is substantial anthropometric data comparing male and female anatomy with respect to weight, height, and geometric dimensions, which can be leveraged to create a female model to represent the general population.

Objective 2: Develop thoracolumbar spine FEMs with irregular sagittal curvature in the thoracic and lumbar regions to study spine biomechanics.
Hypothesis 2: Variations in sagittal curvature of 50%, measured by Cobb angle, will impact the local compressive stresses. Evaluating a range of curvatures in the sagittal plane will demonstrate that the healthy profile may be optimal for biomechanical loading in the spinal column.

There exists a range of healthy spinal curvature that identifies optimal spinal alignment. Deviations in this alignment, whether in the sagittal or coronal plane, are considered to be indicative of potential spinal disorders, diseases, and consequently, pain. Although scoliosis, measured in the coronal plane, is widely studied due to its high prevalence, the effects of spinal misalignment in the sagittal plane are less investigated. The development of spine FEMs with variations in sagittal profiles may permit an evaluation of the changes in stress distributions throughout the spinal column when sagittal alignment is not "optimal."

***Objective 3:* Through a retrospective analysis leveraging MRI data, develop patient-specific lumbar spine FEMs to determine the potential for patients to present irregular stresses throughout the spinal column.**

Hypothesis 3: Personalized lumbar spine FEMs can be developed to represent patient geometry and profile within 10%. When comparing models representing healthy and LBP patients, FEA may demonstrate noticeable differences in localized stress distribution throughout the spinal column.

Patient images provide valuable insight regarding spinal balance and various pathologies and can be leveraged to conduct retrospective studies. MRI evaluation has demonstrated variations in sagittal alignment between biological sexes, as well as variations with the onset of LBP. As such, performing a retrospective study to develop and evaluate personalized spinal FEMs of both healthy and LBP patients may provide a comprehensive analysis of load sharing throughout the spine during day-to-day tasks, as well as potential differences in stress distributions related to spinal health, which consequently may lead to back pain.

The expected relationships and overlapping contributions between the aforementioned objectives are illustrated in Figure 3.0.1 below. The corresponding manuscripts are indicated relative to each realized objective and hypothesis.

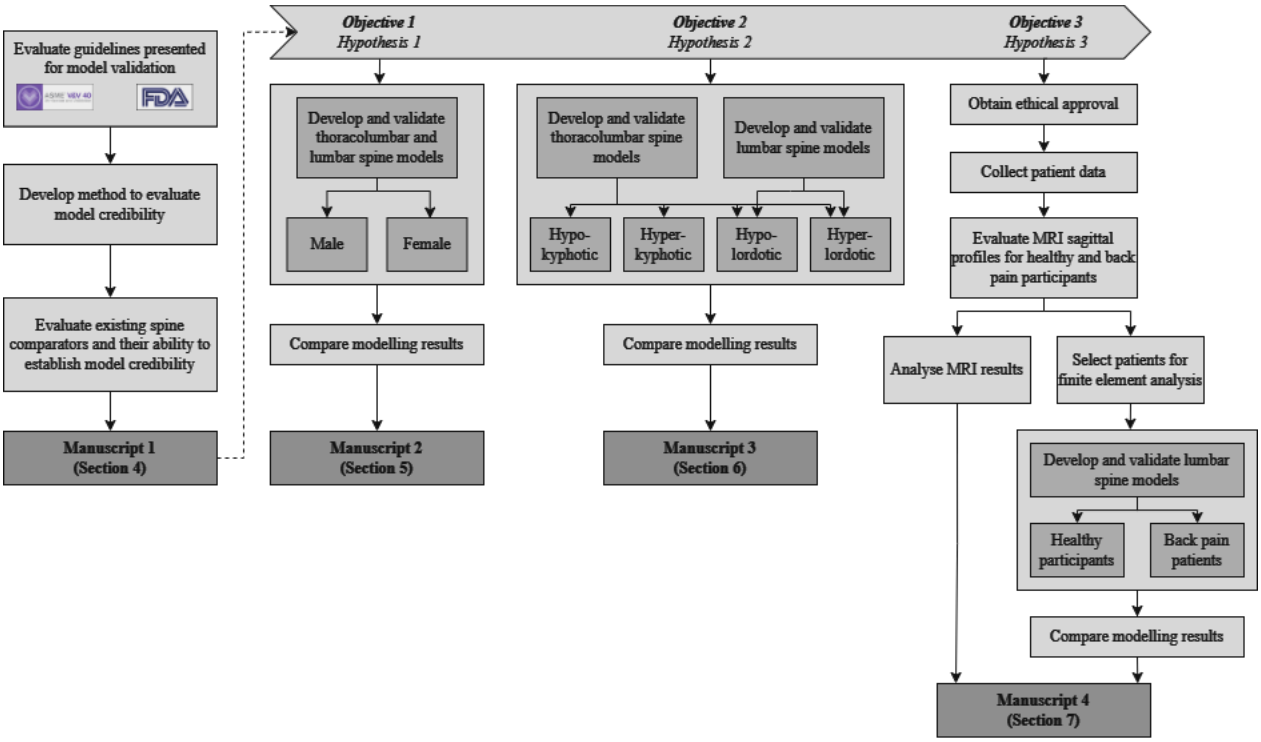

Figure 3.0.1: Flowchart summary for objectives and hypotheses.

4 A critical comparison of comparators used for the validation of spine finite element models

4.1 Framework for Article 1

Biomechanical models are becoming increasingly accepted as useful tools to study loading throughout the body, surgical device development and implementation, patient-specific treatments, and a range of physiological disorders, among other uses. However, it is crucial that the developed models demonstrate accurate representations of the human body prior to confirming their applicability for clinical use. As outlined in Section 2.8, verification, validation, and uncertainty quantification are critical steps to ensure a robust and realistic model. To validate a biomechanical model, it is important to compare the observed modelling results to previously conducted experiments, known as "comparators", which can include data from *in vivo*, *ex vivo*, synthetic benchtop, or *in silico* studies. The selected comparators should reflect the loading conditions applied to the model or the physiological motion the simulation is aiming to mimic, in order to ensure an accurate comparison between modelling and experimental results. Hence, understanding and selecting appropriate comparators is crucial to establish model validation. This review aimed to provide suggested guidelines for the use of comparators in biomechanical modelling, as well as a framework to successfully and robustly validated FEMs, thus ensuring model credibility. As such, this manuscript provided direction for the validation of the models developed for the objectives of this thesis (Sections 5-7).

Thanks are given to the ASME VVUQ40 Subcommittee for their time and valuable discussions regarding the importance of establishing guidelines for robust validation of biomechanical models.

A subset of this work was presented as a poster at the 6th International Spine Research Symposium, hosted by the Philadelphia Spine Research Society (PSRS) and the Orthopaedic Research Society (ORS) from November 6-10, 2022. Further, the following manuscript titled "A critical comparison of comparators used to demonstrate credibility of physics-based numerical spine models" was published in *Annals of Biomedical Engineering* by Springer on September 10, 2022. The contribution of the first author was 60%, which included questionnaire development, data analysis, and manuscript writing. The contribution of the last author was considered to be 15% for research guidance, scoring participation, data analysis, and manuscript review. The final 25% can be attributed to the remaining co-authors for research direction, scoring participation, and manuscript review.

4.2 Article 1: A critical comparison of comparators used to demonstrate credibility of physics-based numerical spine models

Brittany Stott[1,2], Payman Afshari[3], Jeff Bischoff[4], Julien Clin[5], Alexandra Francois-Saint-Cyr[6], Mark Goodin[7], Sven Herrmann[8], Xiangui Liu[9], Mark Driscoll[1,2]

[1]Musculoskeletal Biomechanics Research Lab, Department of Mechanical Engineering, McGill University, Montreal, QC H3A 0C3 Canada

[2]Orthopaedic Research Lab, Research Institute MUHC, Montreal General Hospital, Montreal, QC H3G 1A4 Canada

[3]DePuy Synthes Spine, Johnson and Johnson, Raynham, MA 02767, USA

[4]Zimmer Biomet, Corporate Research, Warsaw, IN 46581-0708, USA

[5]Numalogics, Inc., Montreal, QC H2V 1A2, Canada

[6]Siemens Digital Industries Software, Marlborough, MA 01752, USA

[7]SimuTech Group, Inc., Hudson, OH 44236, USA

[8]CADFEM Medical GmbH, 85567 Grafing bei München, Germany

[9]Stryker Orthopaedics, Mahwah, NJ 07430, USA

Address for notification, correspondence, and reprints:

Mark Driscoll, Ph.D., P.Eng.

Associate Professor, Department of Mechanical Engineering

Canada NSERC Chair Design Eng. for Interdisciplinary Innovation of Medical Technologies

Associate Member, Biomedical Engineering

Associate Member, Department of Surgery

Investigator, Research Institute MUHC, Injury Repair Recovery Program

McGill University, Department of Mechanical Engineering

817 Sherbrooke St. West, Montreal, QC H3A 0C3, Canada

Macdonald Eng. Bldg., office #153

T: +1 (514) 398-6299

F: +1 (514) 398-7365

E-mail: mark.driscoll@mcgill.ca

4.2.1 Abstract

The ability of new medical devices and technology to demonstrate safety and effectiveness, and consequently acquire regulatory approval, has been dependent on benchtop, *in vitro*, and *in vivo* evidence and experimentation. Regulatory agencies have recently begun accepting computational models and simulations as credible evidence for virtual clinical trials and medical device development. However, it is crucial that any computational model undergo rigorous verification and validation activities to attain credibility for its context of use before it can be accepted for regulatory submission. Several recently published numerical models of the human spine were considered for their implementation of various comparators as a means of model validation. The comparators used in each published model were examined and classified as either an engineering or natural comparator. Further, a method of scoring the comparators was developed based on guidelines from ASME V&V40 and the draft guidance from the US FDA, and used to evaluate the pertinence of each comparator in model validation. Thus, this review article aimed to score the various comparators used to validate numerical models of the spine in order to examine the comparator's ability to lend credibility towards computational models of the spine for specific contexts of use.

4.2.2 Introduction

Computational modelling is a valuable tool that can provide information regarding technical performance, efficacy, and safety of medical devices [1]. These *in silico* models can generate data, and reveal associated insights from interpretation of that data, that cannot be obtained through traditional testing methods, such as *in vitro* or *in vivo* experimentation. Of critical importance, a computational model's ability to reliably represent physiological behavior is dependent on the accuracy with which the model can represent the physics of the human body.

Physics-based numerical models and finite element analysis have been used to model the biomechanical behavior of various biological systems, including the human spine. Yet, to model the spine in its entirety is an extremely complex task. According to Fagan et al., there are four central approaches to assessing the spine through finite element modelling: assessment of 1) a healthy spine, 2) a diseased or degenerated spine, 3) a spine implemented with instrumentation, and 4) the development of spinal instrumentation [2]. To date, a variety of spine models have been developed, ranging from sub-micron scale assessments of bone, to vertebral body models, to segments or whole spine models [2], [3]. These models have been used for a range of applications in academia, industry, and clinical settings. As such, spine models have permitted patient specific analyses and evaluation of instrumentation performance and surgical planning, among other applications, thus contributing to informed development of medical instrumentation and safer clinical practices. Given these current applications and the high complexity of this biomechanical system, the spine was selected as the demonstration case to explore. Biomechanical models often rely on assumptions and simplifications for successful analysis, therefore bringing into question the feasibility of using numerical models as accurate representations of the human body.

A significant challenge of biomechanical computational modelling is demonstrating that the model is appropriate for a predefined context of use (COU). Thus, prior to utilizing an *in silico* model to make engineering and clinical decisions, it should first undergo robust analysis to ensure that the results depicted accurately represent the reality of interest, to the extent needed for the COU. Verification, validation, and sensitivity analyses have since been identified as key elements of computational biomechanics [4], [5].

Verification consists of two actions: verification of the code and verification of the calculations [6]. Hence, verification allows the user to ensure that the implemented mathematical model is accurately solved and that the data errors are within permissible tolerances [7]. Validation, on the other hand, consists of evaluating the computational model's appropriateness at representing the desired reality [1]. Furthermore, validation ensures correct implementation of model assumptions, and is generally demonstrated through the use of comparators, such as *ex vivo*, *in vitro*, or

in vivo experimental results. Comparators can be used to evaluate the anatomical or mechanical components in the model or to evaluate the results of the simulation, thus ensuring the model appropriately depicts the COU. Further, it can be expected that the purpose and COU of the simulation will motivate the choice of comparator type, as some comparators will be more relevant than others. For example, models focused on clinical outcomes may require *in vivo* animal or human comparators, whereas synthetic specimens or *ex vivo* mechanical comparators may be beneficial for load distribution studies or implant mechanics. Uncertainty quantification (UQ) is an important part of validation, by which the sensitivities and uncertainties of the model and its respective comparators are quantified, evaluated, and understood. These uncertainties can then be accounted for in the quantitative comparison between the model and the comparator. Sensitivity studies involve altering the input parameters to examine their impact on model predictions [8]. As such, verification, validation, and uncertainty quantification (VVUQ) activities can be used to establish confidence in the predictive capability of the model, known as model credibility [1].

A clear framework for the assessment of the credibility of computational models would help to ensure a consistent approach to VVUQ activities for those models. In 1999, a proposal was created with the aim of forming a specialty committee affiliated with a professional engineering society to develop guidelines for verification and validation (V&V) of computational solid mechanics [9]. As such, the American Society of Mechanical Engineers (ASME) Committee for Verification & Validation of Computational Solid Mechanics was formed, consisting of members from industry, academia, and government [10]. The goal of this committee was to develop standards to evaluate the correctness and credibility in computational solid mechanics models and simulation [9]. Since then, several other ASME committees have been formed, including the ASME VVUQ40 Subcommittee for Verification and Validation in Computational Modelling of Medical Devices, which was founded with the overarching goal of providing standards to guide VVUQ activities to specifically support medical device development and evaluation.

The ASME VVUQ40 Subcommittee has developed a risk-based credibility assessment framework to guide the process of assessing model credibility when utilizing computational models for medical device development. The steps outlined in the V&V40 standard include: 1) defining the question of interest, 2) defining the COU, 3) assessing the model risk, and 4) establishing and achieving credibility factors driven by risk analysis [1]. Recently, the US Food & Drug Administration (FDA) released a guidance draft for the assessment of credibility when using computational models to support medical device regulatory submissions [11]. In this guidance draft, the FDA acknowledges the use of *in silico* models in medical device regulatory submissions, as these numerical models can provide crucial information that is unobtainable from traditional testing methods

or that can act as a substitute for bench testing. The draft further outlines how to establish model credibility and to report V&V activities for computational modelling and simulation (M&S). In the past, obtaining regulatory approval for medical devices required detailed evidence with respect to the efficacy and safety of the proposed device, as demonstrated through controlled benchtop testing, *in vivo* animal studies, and finally extensive *in vivo* patient clinical trials. In recent years, regulatory bodies have begun to acknowledge and accept several other types of comparators for regulatory submissions, notably the use of computational M&S as virtual patients and clinical trials.

Leveraging the use of *in silico* models, whether for academia, industry, or to guide clinical decisions, should be approached with a risk-based credibility assessment model to gauge required VVUQ efforts. Thus, there is a need for critical review and objective assessment of different comparators available to modellers, in order to create a benchmark for VVUQ of biomedical computational models. As such, the objective of this review article is to explore the pertinence and evidence of using various comparators towards establishing the credibility of physics-based numerical models of the human spine for specific COU. This study focused on the applications of VVUQ and the establishment of credibility through comparators in spine biomechanical models, as spine models have been used for a wide range of applications. Further, several published spine models have demonstrated detailed validation techniques, thus presenting a valuable musculoskeletal system for modelling evaluation.

4.2.3 Methods

4.2.3.1 Comparator Classification

There are several types of comparators which have been identified in literature and implemented in biomechanical models. For the purpose of this article, comparators were described by and classified as either engineering or natural comparators.

Engineering Comparators

Synthetic benchtop Synthetic benchtop comparators include sawbones or other synthetic materials representing biological tissues. These synthetic materials permit a superior control over the material properties and testing conditions. For instance, synthetic materials are expected to meet certain requirements [12], and several synthetic bone materials have demonstrated accurate reproduction of biomechanical properties under bending, axial, and torsional loads with low variability [13], [14]. Furthermore, the use of synthetic materials allows for reliable repetition of experiments without requiring ethical approval. However, it should be noted that synthetic materials provide an approximation to the properties of human tissues, therefore generally resulting in lower fidelity as a comparator than biological tissues. Yet, synthetic materials may provide material property data

or insight on the mechanical response of biological systems.

In silico There has been some debate over the use of *in silico* studies as comparators for M&S; as all models are approximations of reality and contain a margin of error, the use specifically of *in silico* models as a comparator for other computational models is not uniformly accepted. Comparing simulation results against previously developed *in silico* models may be considered an assessment of competing implementations, thus evaluating how well the results agree with prior modelling approaches [15]. However, this type of comparator has been used as a means of validation in many published modelling articles. Numerical models allow for the evaluation of complex biological systems through rapid and repetitive studies with significant control over the boundary, initial, and loading conditions [2], [16]. These models also permit control over geometric and material properties [16], thus allowing patient specific models to be developed. Nevertheless, as biomechanical models are an approximation of the human body aiming to represent specific COUs, they consist of ample simplifications and assumptions which must be assessed, thus resulting in a lower fidelity comparator. *In silico* models may provide insight to the mechanical response or load distribution in the modelled biological system, though the accuracy of the reported data may be affected by the simplifications and modelling assumptions. Though these simplifications and assumptions may have been assessed to be acceptable for the original COU of the *in silico* comparator, they may no longer be acceptable for the specific COU of current modeling and simulation effort.

Natural Comparators

Ex vivo The use of *ex vivo* cadaveric specimens, such as animal or human tissues, enables the evaluation of biological tissue samples, therefore providing a realistic comparator. Animal or human cadaver studies fill the void between benchtop and *in vivo* comparators, as they allow studies to be conducted that are otherwise physically or ethically challenging to conduct through *in vivo* studies, while maintaining improved biological, physiological, and anatomical accuracy as compared to synthetic materials. However, limitations of *ex vivo* studies are apparent as the environmental conditions in which these experiments are conducted are not always representative of *in vivo* conditions, such as temperature, humidity, or blood perfusion, as well as the effects of post-mortem degradation [17]. Further, these samples can be costly, and are disproportionally skewed towards samples from the elderly population, therefore affecting the biomechanical properties [13]. Finally, these samples lack the consistency that can be achieved when using engineering materials with known and reproducible material properties, as *ex vivo* material properties cannot be controlled and will reflect biological variability dependent on the sample population. However, *ex vivo* samples are still widely used as comparators in published modelling studies, providing moderate fidelity and accuracy while studying potential mechanical responses or clinical outcomes

under various controlled conditions.

***In vivo* animal** *In vivo* animal experimentation permits the evaluation of the mechanical behavior of tissues, as well as the sampling and collection of data representative of clinical outcomes which are ethically more challenging to obtain from human subjects. Depending on the species of animal selected for the experiment, the material properties and biological outcomes may be similar to those observed in humans [18], [19], thus providing a moderate fidelity comparator for human modelling. Though animal spines have been utilized for various laboratory experimentations, there are notable differences observed between animal and human spines [19]. Despite the similarities between animal and human anatomy and physiology, implementing the findings from these studies in a human computational model is nevertheless an approximation and should be evaluated with care.

***In vivo* human** Clinical studies and *in vivo* evaluations of human subjects provide the highest fidelity regarding the parameters measured in the human body. Measurements, such as material properties, intradiscal or intramuscular pressure, vertebral body rotation, or torso movement, among others, will demonstrate the greatest accuracy when evaluated directly from human subjects. Clinical studies also provide valuable knowledge about the body's reaction and outcomes to medical devices tested through long-term clinical trials. These studies can be classified into two categories: retrospective studies, in which information is gathered regarding a patient's past, or prospective studies, in which subjects are followed over time to evaluate the outcomes, such as disease development. Despite the obvious strengths achieved through the use of human *in vivo* data as a comparator data set, the conditions through which the experiments are conducted, as well as the uncertainties associated with these conditions and the patient characteristics, generally mean that such *in vivo* comparators are difficult to control and measure, and have substantial variability in results.

4.2.3.2 Comparator Scoring

Recent *in silico* spine models were gathered for further interpretation regarding the comparators selected and the rigor by which such comparators enabling VVUQ activities were carried out. The articles were sourced from PubMed and WorldCat, with key words including: 'model' or 'modelling', 'human', 'spine', and 'validation'. Inclusion criteria required publication within the last 8 years, and only studies that developed and detailed validation of the computational model inclusive of the activities outlined by VVUQ were considered. Twelve recently published *in silico* models were selected, whose comparators were then evaluated for their ability to lend credibility towards the developed models. The comparators employed by these models were counted and characterized into two groups: engineering comparators and natural comparators. As described previ-

ously, an engineering comparator utilized synthetic specimens or computational models, whereas a natural comparator utilized biological specimens or *in vivo* samples.

As outlined by the ASME V&V40 standard, the applicability and evidence enabled by such comparators are to be judged by characteristics of the test samples and their test conditions [1], summarized in Table 4.2.1. In comparison, the FDA has outlined several categories to evaluate model credibility evidence [11], summarized in Table 4.2.2.

Table 4.2.1: Summary of ASME V&V40 comparators [1].

ASME V&V40 Comparator Credibility Factors
Comparator test samples (devices tested) - Quantity of test samples (statistics) - Comparator range of sample characteristics - Extent of measurement of test sample, detail, and rigor with which measurements were taken - Uncertainty of test sample (accuracy, reliability)
Comparator test conditions (model set up) - Alternate conditions tested selected (potential redundant validation options) - Range of selected test conditions explored (sensitivity to this condition) - Measures taken from comparator test conditions (type and quantity) - Uncertainty of test conditions or measurement (accuracy, repeatability)

Table 4.2.2: Summary of FDA credibility evidence [11].

FDA Categories for Credibility Evidence
1. Code verification results
2. Model calibration evidence
3. General non-context of use (COU) evidence
4. Evidence generated using bench-top conditions to support the current COU
5. Evidence generated using in vivo conditions to support the current COU
6. Evidence generated using bench-top conditions to support a different COU
7. Evidence generated using in vivo conditions to support a different COU
8. Population-based evidence
9. Emergent model behavior
10. Model plausibility

Inspired by the ASME V&V40 credibility factors in Table 4.2.1 and the FDA credibility evidence categories in Table 4.2.2, a scoring metric was developed to aid in assessing the credibility of the implemented comparators in the respective articles. As such, a scale was created for each metric to identify the strength of the article's model validation, based on how well the

article agreed with the factors identified by the ASME V&V40 standard and the FDA draft. The developed scoring metrics can be seen in the tables below. Per Table 4.2.3, each type of comparator was scored for each article. Then, per Table 4.2.4, each article's selection of comparators was used to evaluate model credibility. Each selected article was scored by 2-3 authors of the present study who are also members of the ASME VVUQ40 subcommittee very familiar with the scoring metrics employed. Authors of the present study were assigned articles that they had not previously collaborated on or co-authored. The results were used to identify the strengths of the pooled articles' comparators for validating the respective computational model. The scores were then awarded a point value (A=1, B=2, C=3, D=4) before being averaged and normalized with respect to the maximum obtainable score for each metric. More specifically, the scores awarded by the reviewers for individual studies were averaged and normalized across each metric. Then, the scores were averaged for all studies across each metric. As an example of normalization, if a metric received an average score of B=2, and the maximum obtainable score for the category was C=3, then the final awarded point value was 0.667. After averaging and normalizing the scores, the methods used to define point value identified the lowest possible score as 0.25, whereas the highest is 1.0. Thus, a value closer to 0.25 is unsatisfactory, whereas a value closer to 1 is highly satisfactory. If a metric was awarded a discrete score (i.e. increments of 1/4=0.25, 1/3=0.333, or 1/2=0.5), it may be indicative of greater agreement between raters and lower score deviations. Descriptive statistics were used to compare the score values and to evaluate the ability of the comparator to lend credibility to the computational model.

Table 4.2.3: Scoring metrics used for each type of comparator (per article), based on the comparator's ability to lend credibility to the model.

TEST SAMPLES				
Quantity of Test Samples	A) A single sample was used	B) Multiple samples were used, but not enough to be statistically relevant	C) A statistically relevant number of samples were used	
Range of Characteristics of Test Samples	A) One or more samples with a single set of test conditions were used	B) Samples representing a range of characteristics near nominal values were used	C) Samples representing the expected extreme values of the parameters were used	D) Samples representing the entire range of parameters were used
Measurements of Test Samples	A) Samples were not measured or characterized	B) Samples representing a range of characteristics near nominal values were used	C) All key characteristics of the samples were measured	
Uncertainty of Test Sample Measurements	A) Samples were not characterized or were characterized with gross observations, and measurement uncertainty was not addressed	B) Uncertainty analysis incorporated instrument accuracy only	C) Uncertainty analysis incorporated instrument accuracy and repeatability	D) Uncertainty analysis incorporated a comprehensive uncertainty quantification, including instrument accuracy, repeatability, or other conditions affecting measurements

Table 4.2.3 continued from previous page

TEST CONDITIONS				
Quantity of Test Conditions	A) A single test condition was examined	B) Multiple (2-4) test conditions were examined	C) More than 4 test conditions were examined	
Range of Test Conditions	A) A single test condition was examined	B) Test conditions representing a range of conditions near nominal were examined	C) Test conditions representing the expected extreme conditions were examined	D) Test conditions representing the entire range of conditions were examined
Measurements of Test Conditions	A) Test conditions were qualitatively measured or characterized	B) One or more key characteristics of the test conditions were measured	C) All key characteristics of the test conditions were measured	
Uncertainty of Test Conditions	A) Test conditions were not characterized or were characterized with gross observations, measurement uncertainty was not addressed	B) Uncertainty analysis incorporated instrument accuracy only	C) Uncertainty analysis incorporated instrument accuracy and repeatability	D) Uncertainty analysis incorporated a comprehensive uncertainty quantification, including instrument accuracy, repeatability, and other conditions affecting measurements

Table 4.2.3 continued from previous page

MODEL FORM				
Model form	A) Influence of model form assumptions was not explored	B) Influence of expected key model form assumptions was explored	C) Comprehensive evaluation of model form assumptions was conducted	
OUTPUT COMPARISON				
Rigor of Output Comparison	A) Visual comparison was performed	B) Comparison was performed by determining the arithmetic difference between computational results and experimental results	C) Uncertainty in the output of the computational model or the comparator was used in the output comparison	D) Uncertainty in the output of the computational model and the comparator were used in the output comparison
Agreement of Output Comparison	A) The level of agreement of the output comparison was not satisfactory for key comparisons	B) The level of agreement of the output comparison was satisfactory for key comparisons, but not all comparisons	C) The level of agreement of the output comparison was satisfactory for all comparisons	

Table 4.2.3 continued from previous page

RELEVANCE TO THE CONTEXT OF USE (COU)				
Relevance of the validation activities to the COU	A) There was no overlap between the ranges of validation points and COU	B) There was partial overlap between the ranges of validation points and COU	C) The COU encompassed some of the validation points	D) The COU encompassed all validation points and the validation points spanned the entire COU space

Comparators were classified as: benchtop (synthetic), *in silico*, *ex vivo*, *in vivo* animal, or *in vivo* human.
The awarded point values were as follows: A=1, B=2, C=3, D=4.

Table 4.2.4: Scoring metrics for the comparators' contribution to model verification, validation, and credibility assessment (per article).

Code verification	A) Code verification was not addressed or evaluated	B) Code verification was confirmed		
Model calibration	A) No evidence of model calibration	B) The model was calibrated with little accuracy	C) The model was calibrated with high accuracy	
Context of use (COU)	A) No COU was evaluated	B) A single COU was evaluated	C) Multiple (2-4) COU were evaluated	D) More than 4 COU were evaluated
Bench-top *ex vivo* evidence	A) No evidence was generated used bench-top conditions to support the COU	B) Evidence from a single bench-top condition was evaluated to support the COU	C) Evidence from multiple bench-top conditions support the COU	
***In vivo* evidence**	A) No evidence was generated using *in vivo* conditions to support the COU	B) Evidence was generated from a single *in vivo* condition to support the COU	C) Evidence was generated from multiple *in vivo* conditions to support the COU	
Population-based evidence	A) The population under consideration was not clearly defined	B) A single population demographic was considered	C) Multiple population demographics were considered, without clear evidence	D) Multiple population demographics were considered and their varying outcomes were described
Model plausibility	A) The model demonstrates weak plausibility through the defined assumptions and input parameters	B) The model demonstrates moderate plausibility through the defined assumptions and input parameters	C) The model demonstrates strong plausibility through the defined assumptions and input parameters	

The awarded point values were as follows: A=1, B=2, C=3, D=4.

4.2.4 Results

Based on the review of current literature, twelve articles were selected and evaluated. The sample size and classification of the comparators used in the respective articles is summarized in Table 4.2.5.

Table 4.2.5: Summary of selected articles, detailing the comparator sample size used per article to validate their respective numerical models.

Study	Spine region	Engineering comparator		Natural comparator		
		Synthetic	*In silico*	*Ex vivo*	*In vivo* animal	*In vivo* human
Dreischarf et al. 2014 [4]	Lumbar (L1-L5)		8	3		4
Bruno et al. 2015 [20]	Thoracolumbar (T1-S1)					7
Raabe and Chaudhari 2016 [21]	Lumbar (L1-L5)		1			8
Xu et al. 2017 [22]	Lumbar (L1-L5)		1	5		4
Amiri et al. 2018 [23]	Lumbar (L1-S1)	1	7	1		
Beaucage-Gauvreau et al. 2019 [24]	Whole spine (C0-L5)					8
Mills and Sarigul-Klijn 2019 [25]	Lumbar (L2-S1)		4	5		
Alizadeh et al. 2020 [26]	Cervical (C0-T1)					1
El Bojairami et al. 2020 [27]	Thoracolumbar (T1-S1)		2	2		
Wang et al. 2020 [28]	Thoracolumbar (T1-S1)		5	8		
Warren et al. 2020 [29]	Lumbar (L1-L5)		1	1		
Newell and Driscoll 2021 [30]	Lumbar (L1-S1)		1			2

A control vs level of fidelity assessment can be found in Figure 4.2.1, which was developed by an ASME VVUQ40 subcommittee. Though a work-in-progress, the figure aims to exemplify the play between control and fidelity for various categories of relevant comparators that may be used for establishing credibility of physics-based *in silico* models.

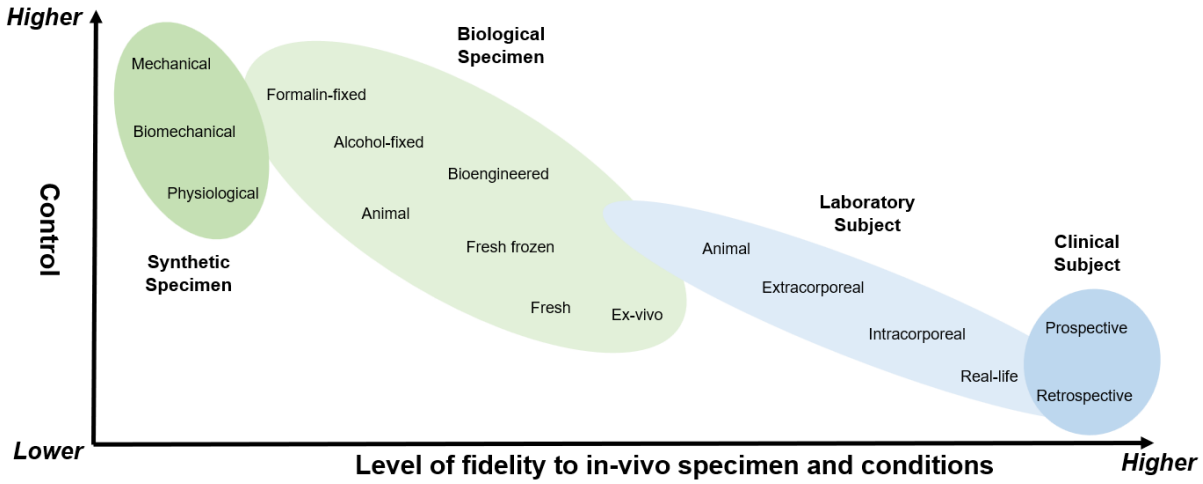

Figure 4.2.1: Control vs level of fidelity assessment for computational modelling comparators. The categories are dark green: synthetic specimen, light green: ex vivo biological specimen, blue: in vivo laboratory and clinical subjects. In silico models are not yet included.

The article reviewers used the scoring metrics in Table 4.2.3 to evaluate the selected articles. Upon interpretation of the scores provided by the article reviewers, the applicability and evidence level of each comparator was evaluated and summarized in Figure 4.2.2.

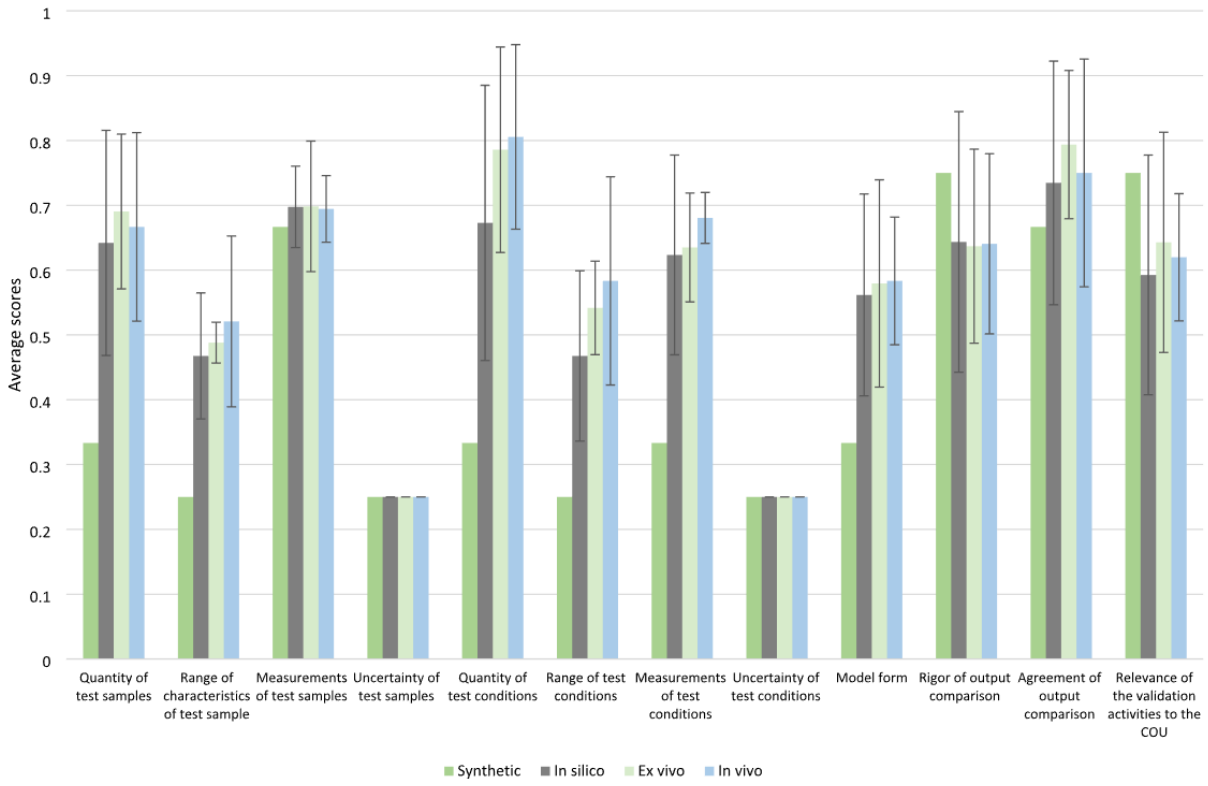

Figure 4.2.2: Average scores for each type of comparators used to validate published models based on the V&V40 scoring metrics. Error bars indicate the standard deviation across articles.

The article reviewers also used the scoring metrics in Table 4.2.4 to evaluate each selected article's model credibility evidence based on the FDA draft. The average normalized scores were evaluated with respect to the sample size and the type of comparators used, and are summarized in Figure 4.2.3 and Figure 4.2.4.

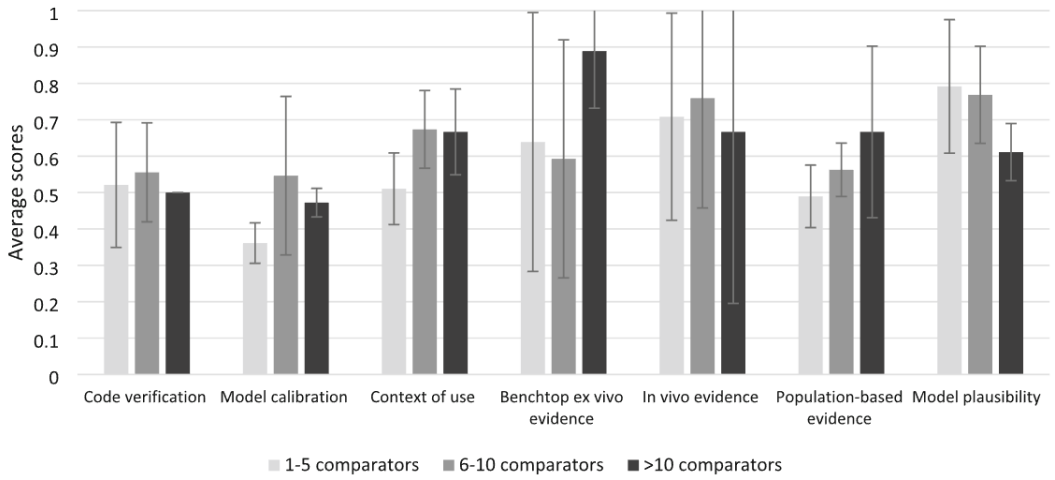

Figure 4.2.3: Average scores according to the FDA categories for credibility evidence, as a function of the comparator sample size used to validate published models per article. Error bars indicate the standard deviation across articles.

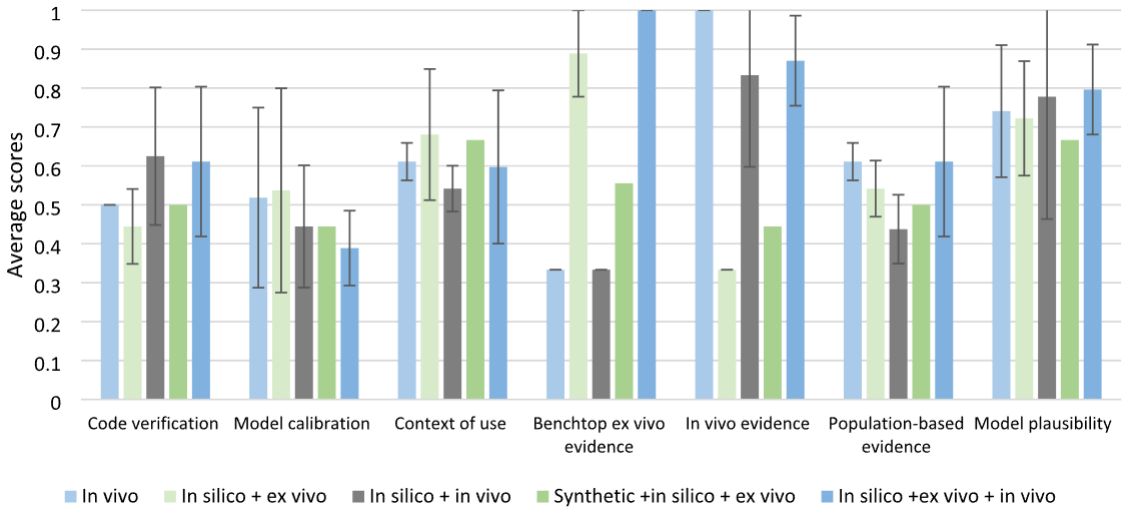

Figure 4.2.4: Average scores according to the FDA categories for credibility evidence, as a function of the type of comparators used to validate published models. Error bars indicate the standard deviation across articles.

The reviewer ratings from the allocated scores demonstrate consistency between the various reviewers. More specifically, for the V&V40 scoring metrics, the mean difference in scores across all articles and metrics was 0.425 (±0.494), with a minimum and maximum difference of 0 and 2, respectively. Similarly, the average difference in scores for the FDA scoring metrics was 0.571 (±0.592), with a minimum and maximum difference of 0 and 2, respectively.

4.2.5 Discussion

In the present review, various articles detailing the use of physics-based numerical models of the human spine have been summarized, compared, and contrasted to evaluate the use of comparators as a means of VVUQ. The selected published models illustrated a range of spine sections, including the cervical, thoracolumbar, and lumbar portions of the spine (Table 4.2.5). The twelve published models evaluated various scenarios of spine loading, thus allowing this review to provide a comprehensive evaluation of comparators across a range of available models. The published models were also developed based on varying patient age groups. However, only a single selected model was developed to specifically represent female anatomy [25]. More specifically, as use of M&S for virtual patients and clinical trials becomes more prominent and accepted as a means of validation for medical device regulatory approval, there is an obvious need to ensure the development of computational models that represent a wider demographic, thus encompassing various age groups, biological sexes, and ethnicities. It should be noted that although each of the explored models aimed to be credible for various contexts of use, including medical device development or testing, they mostly infer to applications related to evaluations of disease conditions prior to intervention towards patient assessment.

Through the assessment of the control vs level of fidelity relationship with respect to *in vivo* specimens and conditions of each comparator seen in Figure 4.2.1, an inverse correlation was observed between the variables considered; the comparators that provide the largest control consequentially result in the lowest fidelity. Hence, the comparators that provide significant control over the samples, testing conditions, or environmental factors, among others, generally provide the lowest resemblance to *in vivo* human conditions. One should note that there is a compromise that must be considered when evaluating which comparators to select as a means to validate computational models.

The majority of explored published models considered several comparators classified as different types of comparators when aiming to provide model credibility (Table 4.2.5), with the most prominent comparator types being *in silico*, *ex vivo*, and *in vivo*. These trends agree with the data reported by Baumann et al., who found that finite element analysis of intervertebral body fusion devices was validated through comparison to bench testing, literature, and finite element analysis of 36%, 26%, and 20%, respectively [31]. The spine is arguably one of the most complex systems in the human body to model from a biomechanical perspective. Due to its complexity, this may encourage the use of multiple comparator adoption for model validation, though the use of these comparator studies does not always allow for the initial and boundary modelling conditions to be known with certainty. To add, a significant challenge of M&S validation is selecting appropriate

comparators. One comparator may only offer a single relevant data set for comparison, such as for mechanical validation or clinical assessment. Hence, this may provide an additional reason for incorporating multiple comparators into validation studies. How multiple comparators are weighed regarding lending model credibility becomes a topic of further discussion.

It was further observed that synthetic materials and *in vivo* animal studies were seldom used as comparators (Table 4.2.5). This was of interest as both comparators provide noteworthy advantages when conducting experimental studies. Synthetic materials allow for considerable control over material properties and testing conditions. Meanwhile, *in vivo* animal studies allow the investigation of pathophysiological changes or events under controlled conditions, while providing insight to human conditions [32]. Nevertheless, there has been evidence of anatomical and physiological differences between animal and human spines [19]. Despite the widespread use of animal subjects in clinical trials for medical device testing and development, the geometric and mechanistic variation between animal and human spines may be an indicator of the lack of application as a comparator in human M&S of the spine.

Moreover, there was overwhelming evidence as to the use of *in silico* models as a comparator (Table 4.2.5), despite the continuing debate concerning the legitimacy of using this type of comparator. If the *in silico* comparator itself is insufficiently validated, this brings into question its appropriateness as a viable benchmark for comparison. Furthermore, care should be taken when validating through comparison to *in silico* models, as these models are generally deemed adequately validated for an intended purpose or a specific loading condition and should thus be used to validate similar scenarios. There is question as to whether comparison against *in silico* comparators is true validation, or whether it is a form of code verification or solution comparison. For example, Dreischarf et al. [4] analyzed and compared the results of eight lumbar spine finite element models as a form of solution comparison, and the results were validated against published *in vivo* data. The authors demonstrated the strength of combining several models to improve model prediction. Another significant challenge with utilizing *in silico* comparators is that their output data is often used for validation, while disregarding the model's geometry origins, which often vary between the comparator and the developed model, hence affecting the results. However, there are also several arguments as to the benefits of *in silico* comparators. These models can be advantageous for validation activities when other data, such as *ex vivo* or *in vivo* values, are limited [4] or unavailable, providing an alternative means to validate the developed computational model. It was also noted that, within the context of this study, none of the selected articles used *in silico* models as their sole comparator, hence, *in silico* comparators were used in conjunction with other comparators, thus corroborating their relevance as comparators.

In addition to *in silico* comparators, *ex vivo* and *in vivo* human comparators demonstrated the highest prevalence as choice of comparators implemented in the published models. Further, ASME V&V40 states that the comparators used for establishing computational model credibility might be from bench testing, animal experimentation, or clinical trials [1]. *Ex vivo* comparators provide valuable data that is challenging to procure through *in vivo* experimentation, and were detected in half of the selected published models. *In vivo* human studies, on the other hand, generally provide the highest fidelity as a comparator, and were identified in eight of the twelve published models. Both comparators demonstrate a means to lend credibility to the models in question. However, significant differences have been found between *ex vivo* and *in vivo* properties, thus highlighting the importance and strength of implementing *in vivo* data for accurate model development [17].

For the V&V40 scoring metrics, consistency was observed between the scores assigned by the reviewers, as the average difference between scores was 0.425. When comparing the assigned scores per comparator type based on the V&V40 metrics (Figure 4.2.2), the quantity, range, and measurement of test conditions were scored highest for the *in vivo* comparators. In comparison, the agreement of output comparison was ranked highest for *ex vivo* comparators, demonstrating the benefits of utilizing comparators that provide additional environmental control. The synthetic specimen was awarded notably lower scores for the quantity and range of test samples and test conditions, the measurements of test conditions, and the model form evaluation. However, only a single published model incorporated a synthetic specimen as a comparator, which is a limitation of this review and should be considered when evaluating the results. Further, it was observed that no comparators received a score of 1.0. This could be attributed to the results being evaluated and averaged across several articles. Since the published articles mostly infer to applications related to patient assessment as opposed to obtaining regulatory approval, it can be expected that models implemented in industry may have higher aspirations. However, the use of computational modelling between academic and non-academic settings often differs. Bandwidth may define the amount of effort that can be contributed to credibility aspirations. Ideally, if open-source models or fully descriptive comparator results, above what is available in literature, were made readily available, this would be beneficial for all involved in M&S.

The metrics derived from the FDA guidance draft were used to assess model credibility through the selected articles' use of comparators. These metrics were further used to demonstrate consistency in the article reviewers' scores, resulting in an average difference in allotted scores of 0.571. As seen in Figure 4.2.3, a clear trend was observed demonstrating an increase in population-based evidence when a greater quantity of comparators was used for model validation. This was

expected as the greater the data set used for validation, the larger the population demographics that may be considered. On the other hand, there was a notable decrease in model plausibility as more comparators were considered. This trend was not anticipated, but demonstrates that it is not the quantity of comparators that will lend to a model's plausibility, but the means with which the comparators are implemented. When evaluating the types of comparators used for model validation (Figure 4.2.4), the population-based evidence did not demonstrate a clear correlation between the type of comparators used and the allotted scores, though the published models' use of *in vivo* comparators received a slightly higher score for model plausibility when compared to the used of *in silico* and *ex vivo* comparators.

Throughout the evaluation of the employed comparators across all selected and recently published articles, several reoccurring shortcomings in the methods of validation were observed. Model form assumptions, calibration, sensitivity analysis, and calculation verification were rarely completed or reported. Calibration may be completed during model development for credibility and error compensation; however, it was rarely reported in the published articles, making model reproducibility and verification a challenge. Statistical analyses were also seldom included to evaluate model results, though at times these assessments could have been relevant and beneficial. Further, even if UQ was completed in the initial comparator's study, on no account was the UQ discussed with respect to the selected comparators in the published articles' model validations, thus receiving the lowest possible score for all published models. The lack of UQ is of significance as this task allows the quantification, evaluation, and understanding of the model's sensitivities and uncertainties, which are an important step in advancing model credibility. Further, the COU was rarely or vaguely described across the recently published articles, despite its importance in identifying the role and scope of the computational model [1]. Instead, some articles detailed the question of interest, although vaguely, for which the model aimed to address a specific question, decision, or concern [1].

Thus, it is the authors' recommendation that, for future model development and validation, the COU be clearly defined, as well as clear descriptions or inclusions of uncertainty quantification and sensitivity analyses. In addition, all model form assumptions and limitations should be explicitly described. Clearly disclosing model calibration details, parameters, and loading conditions will enhance the reproducibility of the model for future studies. Justification for the selection of comparators, as well as a discussion on the agreement of the model and comparator results, should be included. Though uncertainty of model results and comparator data must be accounted for, an acceptable threshold for the agreement of results should be defined and justified, while taking into consideration the accuracy and precision required for this threshold based on the defined

COU. Lastly, a description of possible applications or areas for model implementation should be outlined.

The selected published models provide clear insight to the most prominent types of comparators leveraged for spine M&S. An evaluation of the models' use of comparators provides valuable information regarding the possible directions of validation and credibility assessment, as outlined by ASME V&V40 [1] and the recent guidance from the FDA [11]. The proposed metrics for scoring comparators demonstrated a suitable and reliable scoring method to ensure comparator applicability and credibility evidence of developed spine models. However, limitations to the developed scoring method exist and could be improved for future use. Namely, the developed scoring method does not take into consideration the perceived risk and influence of the model, i.e. a model with larger risk may require a higher score to be deemed credible. In addition, the scoring method was implemented in the present study to evaluate the ability of comparators to lend credibility to the selected published articles as a whole and did not explicitly evaluate an individual study's score. Future evaluations conducted with this scoring method could assess individual published models' scores to gain insight to the strengths and weaknesses of each study. Nevertheless, the assessment reported herein gives an overview of how comparators have been recently employed in spine models and provide valuable information on the strengths and weaknesses of current published models. When developing, evaluating, and validating a numerical model, emphasis should be placed on the importance of credibly conducting VVUQ, with clear communication of the adopted comparators and COU, to ensure accurate representation of the desired reality. While conducting V&V, it is crucial to select comparators that align with the developed virtual patient model, i.e. an appropriate demographic, nationality, and health status, as well as accurate boundary and loading conditions, among other factors.

To conclude, the aim of this review article was to explore the applicability and evidence of using various comparators towards establishing model credibility. From the published articles considered, there is overwhelming evidence that the use of multiple comparator types and an elevated comparator sample size, as opposed to a single comparator, is favoured in literature, thus ensuring the development and validation of a reliable and realistic model. Future model development should strive to ensure a complete, rigorous, and detailed implementation of comparators for model validation, through the employment of several comparators relevant to the model's specific COU.

4.2.6 Funding

Funding was provided by NSERC (Grant No. 172632).

4.2.7 References

[1] American Society of Mechanical Engineers: V&V40 Committee, "Assessing credibility of computational modeling through verification and validation: Application to medical devices," *The American Society of Mechanical Engineers*, 2018.

[2] M. Fagan, S. Julian, and A. Mohsen, "Finite element analysis in spine research," *Proceedings of the institution of mechanical engineers, part h: journal of engineering in medicine*, vol. 216, no. 5, pp. 281–298, 2002.

[3] A. C. Jones and R. K. Wilcox, "Finite element analysis of the spine: Towards a framework of verification, validation and sensitivity analysis," *Medical Engineering & Physics*, vol. 30, no. 10, pp. 1287–1304, 2008.

[4] M. Dreischarf, T. Zander, A. Shirazi-Adl, *et al.*, "Comparison of eight published static finite element models of the intact lumbar spine: Predictive power of models improves when combined together," *Journal of Biomechanics*, vol. 47, no. 8, pp. 1757–1766, 2014.

[5] A. E. Anderson, B. J. Ellis, and J. A. Weiss, "Verification, validation and sensitivity studies in computational biomechanics," *Computer Methods in Biomechanics and Biomedical Engineering*, vol. 10, no. 3, pp. 171–184, 2007.

[6] American Society of Mechanical Engineers: V&V 10 Committee, "Guide for verification and validation in computational solid mechanics," *The American Society of Mechanical Engineers, New York, Technical Report No. V&V*, pp. 10–2006, 2006.

[7] B. A. Szabo and I. Babuska, "Introduction," in *Introduction to finite element analysis: formulation, verification and validation*. John Wiley & Sons, 2011, vol. 35, pp. 1–15.

[8] J. A. Weiss, J. C. Gardiner, B. J. Ellis, T. J. Lujan, and N. S. Phatak, "Three-dimensional finite element modeling of ligaments: Technical aspects," *Medical Engineering & Physics*, vol. 27, no. 10, pp. 845–861, 2005.

[9] L. E. Schwer, "Verification and validation in computational solid mechanics and the asme standards committee," *WIT Transactions on the Built Environment*, vol. 84, 2005.

[10] L. Schwer, "An overview of the asme v&v-10 guide for verification and validation in computational solid mechanics," in *20th International Conference on Structural Mechanics in Reactor Technology*, 2009, pp. 1–10.

[11] US Food and Drug Administration, "Assessing the credibility of computational modeling and simulation in medical device submissions. draft guidance for industry and food and drug administration staff," *Food and Drug Administration: Silver Spring, MD, USA*, 2021.

[12] American Society for Testing and Materials, *Standard specification for rigid polyurethane foam for use as a standard material for testing orthopaedic devices and instruments*. ASTM International, 2008.

[13] J. Elfar, S. Stanbury, R. M. G. Menorca, and J. D. Reed, "Composite bone models in orthopaedic surgery research and education," *The Journal of the American Academy of Orthopaedic Surgeons*, vol. 22, no. 2, p. 111, 2014.

[14] L. Cristofolini and M. Viceconti, "Mechanical validation of whole bone composite tibia models," *Journal of Biomechanics*, vol. 33, no. 3, pp. 279–288, 2000.

[15] A. Erdemir, L. Mulugeta, J. P. Ku, *et al.*, "Credible practice of modeling and simulation in healthcare: Ten rules from a multidisciplinary perspective," *Journal of Translational Medicine*, vol. 18, no. 1, pp. 1–18, 2020.

[16] F. Galbusera and F. Niemeyer, "Mathematical and finite element modeling," in *Biomechanics of the Spine: basic concepts, spinal disorders and treatments*. Elsevier, 2018, pp. 239–255.

[17] N. L. Ramo, S. S. Shetye, F. Streijger, *et al.*, "Comparison of in vivo and ex vivo viscoelastic behavior of the spinal cord," *Acta biomaterialia*, vol. 68, pp. 78–89, 2018.

[18] H.-J. Wilke, S. Krischak, K. Wenger, and L. Claes, "Load-displacement properties of the thoracolumbar calf spine: Experimental results and comparison to known human data," *European Spine Journal*, vol. 6, no. 2, pp. 129–137, 1997.

[19] A. Kettler, L. Liakos, B. Haegele, and H.-J. Wilke, "Are the spines of calf, pig and sheep suitable models for pre-clinical implant tests?" *European Spine Journal*, vol. 16, no. 12, pp. 2186–2192, 2007.

[20] A. G. Bruno, M. L. Bouxsein, and D. E. Anderson, "Development and validation of a musculoskeletal model of the fully articulated thoracolumbar spine and rib cage," *Journal of Biomechanical Engineering*, vol. 137, no. 8, p. 081 003, 2015.

[21] M. E. Raabe and A. M. Chaudhari, "An investigation of jogging biomechanics using the full-body lumbar spine model: Model development and validation," *Journal of Biomechanics*, vol. 49, no. 7, pp. 1238–1243, 2016.

[22] M. Xu, J. Yang, I. H. Lieberman, and R. Haddas, "Lumbar spine finite element model for healthy subjects: Development and validation," *Computer Methods in Biomechanics and Biomedical Engineering*, vol. 20, no. 1, pp. 1–15, 2017.

[23] S. Amiri, S. Naserkhaki, and M. Parnianpour, "Modeling and validation of a detailed fe viscoelastic lumbar spine model for vehicle occupant dummies," *Computers in Biology and Medicine*, vol. 99, pp. 191–200, 2018.

[24] E. Beaucage-Gauvreau, W. S. Robertson, S. C. Brandon, *et al.*, "Validation of an opensim full-body model with detailed lumbar spine for estimating lower lumbar spine loads during symmetric and asymmetric lifting tasks," *Computer Methods in Biomechanics and Biomedical Engineering*, vol. 22, no. 5, pp. 451–464, 2019.

[25] M. J. Mills and N. Sarigul-Klijn, "Validation of an in vivo medical image-based young human lumbar spine finite element model," *Journal of Biomechanical Engineering*, vol. 141, no. 3, p. 031 003, 2019.

[26] M. Alizadeh, A. Aurand, G. G. Knapik, *et al.*, "An electromyography-assisted biomechanical cervical spine model: Model development and validation," *Clinical Biomechanics*, vol. 80, p. 105 169, 2020.

[27] I. El Bojairami, K. El-Monajjed, and M. Driscoll, "Development and validation of a timely and representative finite element human spine model for biomechanical simulations," *Scientific Reports*, vol. 10, no. 1, pp. 1–15, 2020.

[28] W. Wang, D. Wang, F. De Groote, L. Scheys, and I. Jonkers, "Implementation of physiological functional spinal units in a rigid-body model of the thoracolumbar spine," *Journal of Biomechanics*, vol. 98, p. 109 437, 2020.

[29] J. M. Warren, A. P. Mazzoleni, and L. A. Hey, "Development and validation of a computationally efficient finite element model of the human lumbar spine: Application to disc degeneration," *International Journal of Spine Surgery*, vol. 14, no. 4, pp. 502–510, 2020.

[30] E. Newell and M. Driscoll, "The examination of stress shielding in a finite element lumbar spine inclusive of the thoracolumbar fascia," *Medical & Biological Engineering & Computing*, vol. 59, no. 7, pp. 1621–1628, 2021.

[31] A. P. Baumann, T. Graf, J. H. Peck, A. E. Dmitriev, D. Coughlan, and J. C. Lotz, "Assessing the use of finite element analysis for mechanical performance evaluation of intervertebral body fusion devices," *JOR spine*, vol. 4, no. 1, e1137, 2021.

[32] M. Sharif-Alhoseini, M. Khormali, M. Rezaei, *et al.*, "Animal models of spinal cord injury: A systematic review," *Spinal cord*, vol. 55, no. 8, pp. 714–721, 2017.

4.3 Summary

This manuscript was written in collaboration with the ASME VVUQ40 Subcommittee to evaluate the use of comparators to establish credibility for biomechanical model validation. While this manuscript placed an emphasis on existing spine models, the methodology described to establish model credibility can be expanded for the modelling of other musculoskeletal systems, such as the knee, hip, or shoulder.

This study demonstrated the importance of describing the selected comparators and their abilities to validate modelling results. Further, the manuscript summarized the most commonly selected comparator types for spine model validation in recently published FEM studies, namely *in silico*, *ex vivo*, and *in vivo* human comparators. To add, there was a clear preference among previous spine modelling studies to use multiple comparators for validation efforts. After evaluating the strengths and weaknesses of the current validation approaches, several recommendations were provided by the authors for robust model development and validation, which are summarized in Figure 4.3.1.

The comparative analysis provided guidelines and highlighted important aspects of model development, verification, validation, and analyses that were used to guide model validation and establish credibility in the remaining objectives of this thesis (Sections 5-7).

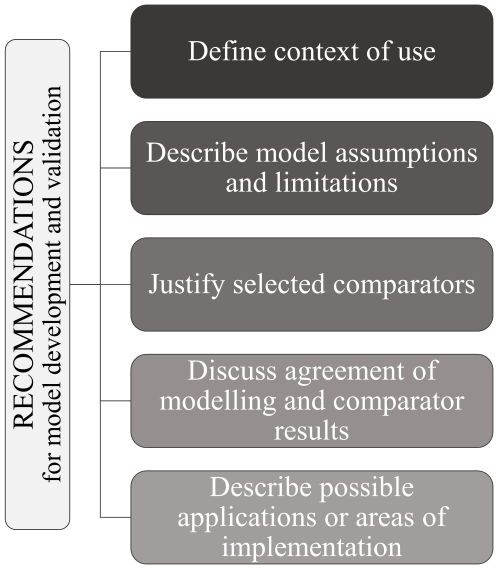

Figure 4.3.1: Summary of recommendations to establish credibility for model development and validation.

5 Development and validation of sex-specific thoracolumbar spine models

5.1 Framework for Article 2

As outlined in Section 2.7.1, there is a lack of sex-specific spine FEMs available in literature. As such, many FE studies rely on male anatomy and models. However, there is clear evidence in literature that male and female anatomy and material properties differ (Section 2.1). Further, females have been found to demonstrate a higher prevalence of LBP compared to their male counterparts (Section 2.2). The anatomical variations between males and females are important as they affect the load distribution throughout the body during daily tasks. Hence, the objective of this study was to develop a FEM of the spine representative of female anatomy and subsequently compare the changes in stress distribution between a male and a female model. The results of this study aim to provide insight into potential variations in spinal stress distributions with the hopes that the observed outcomes may encourage the consideration of sex-specific properties and guide targeted treatments.

The male model was previously developed and validated by Dr. Ibrahim El Bojairami in the Musculoskeletal Biomechanics Research Lab at McGill University [174]. This previously developed model was leveraged as the male model in this study, although modifications were made to the initial model for this thesis. The model consists of the vertebrae, intervertebral discs, tendons, and thoracolumbar fascia, which are modelled as volumetric bodies, and spinal muscles, which are modelled as mixed fluid-shell models incorporating intramuscular pressure [175]. Additional loading scenarios were explored with respect to Dr. El Bojairami's prior work, and consequently, extensive validation of the updated model was completed.

The realization of Objective 1 and the exploration of Hypothesis 1 are detailed in the manuscript below, titled "Development and evaluation of sex-specific thoracolumbar spine finite element models to study spine biomechanics," for which the contribution of the first author is considered to be 85%, including adjustments to the male model, development of the female model, analysis and validation of the modelling results, and manuscript writing. The contribution of the second author is considered to be 15%, as the second author provided valuable support, research guidance, and manuscript review. The manuscript was submitted to *Medical & Biological Engineering & Computing* by Springer on June 22, 2023. An additional study was presented at the 6th International Fascia Research Congress on September 12, 2022. Subsets of the initial study were presented as posters at the 22nd Annual Conference for the International Society for the Advancement of Spine Surgery from June 1-4, 2022, and the Global Spine Congress from May 31-June 3, 2023. Details of additional studies are outlined in Sections 5.3 and 5.4 below.

5.2 Article 2: Development and evaluation of sex-specific thoracolumbar spine finite element models to study spine biomechanics

Brittany Stott[1,2], Mark Driscoll[1,2]

[1]Musculoskeletal Biomechanics Research Lab, Department of Mechanical Engineering, McGill University, Montreal, QC, Canada

[2]Orthopaedic Research Lab, Montreal General Hospital, Montreal, QC, Canada

Address for notification, correspondence, and reprints:

Mark Driscoll, Ph.D., P.Eng.

Associate Professor, Department of Mechanical Engineering

Canada NSERC Chair Design Eng. for Interdisciplinary Innovation of Medical Technologies

Associate Member, Biomedical Engineering

Associate Member, Department of Surgery

Investigator, Research Institute MUHC, Injury Repair Recovery Program

McGill University, Department of Mechanical Engineering

817 Sherbrooke St. West, Montreal, QC H3A 0C3, Canada

Macdonald Eng. Bldg., office #153

T: +1 (514) 398-6299

F: +1 (514) 398-7365

E-mail: mark.driscoll@mcgill.ca

5.2.1 Abstract

Musculoskeletal disorders and low back pain (LBP) are common global afflictions, with a higher prevalence observed in females. However, the cause of many LBP cases continues to elude researchers. Current approaches seldom consider differences in male and female spines. Thus, this study aimed to compare the load distribution between male and female spines through finite element modelling. Two finite element models of the spine, one male and one female, were developed, inclusive of sex-specific geometry and material properties. The models consisted of the vertebrae, intervertebral discs (IVD), tendons, surrounding spinal muscles, and thoracolumbar fascia, and were subjected to loading conditions simulating flexion and extension. Following extensive validation against published literature, intersegmental rotation, IVD stress, and vertebral body stress were evaluated. The female model demonstrated increased magnitudes for rotation and stresses when compared to the male model. Results suggest that the augmented stresses in the female model indicate an increased load distribution throughout the spine compared to the male model. These findings may corroborate the higher prevalence of LBP in females. This study highlights the importance of using patient- and sex-specific models for patient analyses and care.

5.2.2 Introduction

Musculoskeletal disorders are a leading cause of global disability, with neck and low back pain (LBP) ranking as the single largest cause [1]. The high prevalence of musculoskeletal disorders results in increased workplace absences and healthcare professional consultations, placing a significant burden on society. Moreover, the prevalence of LBP has been reported to be considerably higher in females compared to males [2]–[6]. Despite the widespread occurrence of this affliction, it is estimated that up to 85% of LBP cases are idiopathic [7], thus highlighting the need for innovative technological advancements to aid in achieving a more comprehensive understanding of LBP, perhaps improved by sex-specific biomechanical assessments.

The availability of accurate, physiologically-based finite element models (FEMs) of the spine could improve the investigation of spinal alignment and disorders in male and female anatomy. Gaining such insight may lead to a better understanding of the varying load distribution and spinal conditions between sexes and would thus direct researchers and medical professionals towards better in vivo clinical approaches when investigating these conditions. In recent years, finite element modelling has evolved from its initial purpose of stress analysis for aircraft [8] to encompass biomechanical modelling of anatomical geometries. Accurate modelling of complex biological systems, such as the spine, remains a challenge. These FEMs rely on assumptions and simplifications to successfully solve and analyze the model in a timely manner. Thus, model validation is a crucial step to ensure credibility and accurate representation of a biological system. Once validated, there is the potential to use computational modelling to gain insight into biomechanical loading, medical device development, surgical planning, or patient-specific modelling, among others.

To date, a significant number of spine models have been developed, ranging from individual spine components to full spine models. Rohlmann et al. developed a lumbar model subjected to various loading conditions, demonstrating the variability and importance of implementing the correct loading [9]. Among other research groups, Park et al. and Chen et al. each developed FEMs of the lumbar spine based on patient-specific CT scans of male anatomy, namely a young [10] and a middle-aged male subject [11], respectively, meanwhile, Bruno et al. and Wang et al. used a thoracolumbar spine model developed from CT scans of a 25-year-old male [12], [13]. Recently, El Bojairami et al. developed and validated a FEM of the spine, inclusive of the vertebrae, intervertebral discs (IVD), and torso muscles, with an accurate representation of intra-abdominal and intramuscular pressures [14]. Despite the abundance of developed computational spine FEMs, there is a lack of models representing female anatomy. Imai et al. studied the lumbar vertebral strength by modelling the anatomy of elderly women patients [15]. Xu et al. developed five lum-

bar models based on the anatomy of both male and female patients, however, their results did not distinguish between biological sexes [16]. Of late, Mills and Sarigul-Klijn developed the first patient-specific lumbar spine model of a young female patient [17]. These authors highlighted the importance of implementing an accurate representation of patient anatomy and material properties when utilizing computational modelling to improve patient care. Despite the significant advancements in biomechanical modelling, to the authors' knowledge, no full thoracolumbar spine models have been developed and interpreted representing female anatomy.

Thus, this research aimed to develop and validate a female version of a thoracolumbar spine model. In addition, a comparative study was conducted to analyze the changes in load distribution throughout the spine based on biological sex. The successful development and validation of sex-specific FEMs may encourage and support the use of modelling for rapid *in vivo* patient assessment and improve biomechanical knowledge of spinal loading toward a better understanding of potential LBP causes.

5.2.3 Materials and Methods

5.2.3.1 Finite element model development

To perform a comparative analysis of the load distribution throughout the spine based on biological sex, two FEMs were developed: one male and one female. The first model, shown in Figure 5.2.1, represented a male thoracolumbar spine which was leveraged from previously validated work [14], consisting of the vertebrae and adjacent IVDs ranging from T1 to S1. The model contained surrounding soft tissues, namely the tendons, thoracolumbar fascia, and various spinal muscles known to contribute to spinal stability (multifidus, longissimus, intertransversarius, latissimus dorsi, and psoas major). Anatomical structures were acquired from an anatomography database (BodyParts3D) containing volumetric bodies constructed from MRI images of a 22-year-old, healthy male subject [18]. The volumetric bodies were imported into SpaceClaim (ANSYS, Canonsburg, Pennsylvania) to remove any sharp edges and to define the associated mesh, followed by Blender (v.2.93.4, Netherlands) to align the mesh nodes on adjacent contacting bodies, resulting in volumetric bodies with a 3mm tetrahedral mesh. The muscles were constructed as fluid-filled volumetric bodies, consisting of a shell containing pressure elements inside, as previously described by El Bojairami and Driscoll [19]. Lastly, the volumetric bodies were imported into ANSYS for model development and analysis. Bonded contacts were used to avoid slippage or separation between components. The male model was previously found to be validated under loading conditions of forward flexion applied at T1 [14]. The model's material properties have since been updated to reflect available literature, detailed in Table 5.2.1.

The development of the female model took into consideration the anatomical and physio-

logical variations between male and female individuals. Namely, the cross-sectional areas (CSAs) of the vertebral bodies, IVDs, tendons, and muscles were 20-25% reduced in the female FEM to reflect previously published literature [20]–[23]. Further, the material properties in the female model were selected based on available data [20], [22], [24], [25], outlined in Table 5.2.1. Specifically, the Young's modulus of the IVDs was increased by 21% in the female models [25], meanwhile, the modulus of the tendons was reduced by 10% [23]. To add, little to no differences have been reported for vertebral properties, density, or strength depending on sex [21], [26], and consequently, the material properties were kept constant across both models for this component. As material properties of female patients are not readily available, material properties from young healthy patient data were selected, when available, for both models.

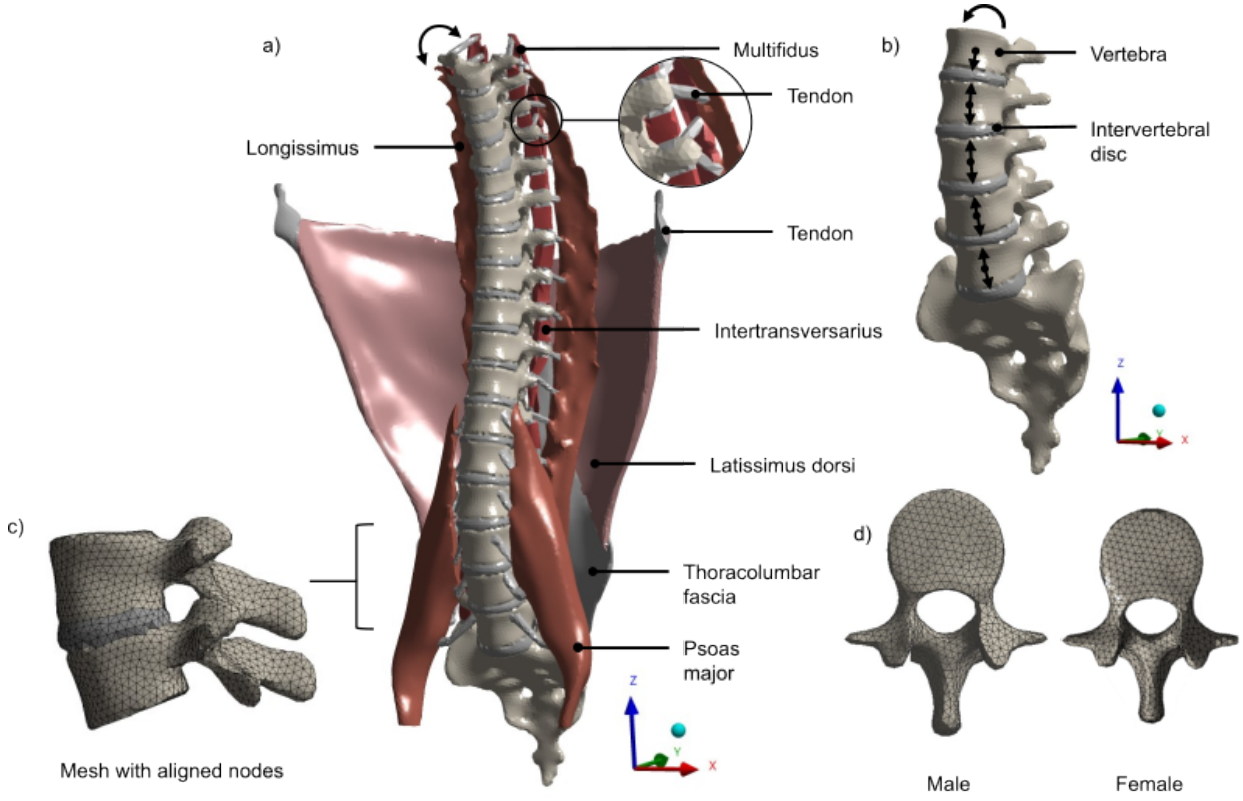

Figure 5.2.1: a) Thoracolumbar and b) lumbar spine models, with c) example of model mesh and aligned nodes. d) Comparison of the vertebral bodies for the male and female FEMs.

5.2.3.2 Boundary and loading conditions

Both FEMs were assessed with ANSYS Static Structural (2020 R1, Canonsburg, Pennsylvania). A fixed support was added at the sacrum and the tendons on the upper extremities of the latissimus dorsi muscles. Three loading scenarios were explored using both male and female models to align with the described loading scenarios in previously published studies. In scenario

Table 5.2.1: Material properties of spinal structures used in the finite element models.

	Young's Modulus			Poisson's Ratio	Reference
	Male FEM	Female FEM	% Difference	Male and Female FEM	
Vertebra	12 GPa	12 GPa	-	0.3	[26], [27]
Intervertebral disc	13.7 MPa	16.6 MPa	21%	0.49	[24]
Tendon	680 MPa	610 MPa	-10%	0.49	[22]
Intertransversarius	36.87 kPa	36.87 kPa	-	0.49	[14]
Multifidus	91.34 kPa	91.34 kPa	-	0.49	[28]
Longissimus	62.85 kPa	62.85 kPa	-	0.49	[28]
Latissimus dorsi	36.87 kPa	36.87 kPa	-	0.49	[14]
Psoas major	55.33 kPa	55.33 kPa	-	0.49	[29]
Thoracolumbar fascia	450 MPa	450 MPa	-	0.49	[30], [31]

1, the lumbar spine was evaluated, consisting solely of the vertebrae and IVDs from L1 to S1. A 1175N follower load was applied with a 7.5Nm moment at L1 to induce forward flexion [9]. In scenario 2, the lumbar model was subjected to pure moments ranging from 10Nm to -10Nm, representing flexion and extension, respectively. In scenario 3, the complete thoracolumbar spine was considered, inclusive of all previously specified surrounding soft tissues. Pure moments were applied at T1, ranging from 7.5Nm to -7.5Nm, to induce flexion and extension, respectively. The applied loading conditions are depicted in Figure 5.2.1.

5.2.3.3 Validation and analysis

To validate the FEMs, for all scenarios, intersegmental rotation (ISR) was measured as described by Dvorák et al. [32] as the relative change in rotation between vertebrae in the sagittal plane. IVD stress was extracted by measuring the maximum normal stress on the surface of the IVD in all scenarios, and the values were compared to published data. To analyze the load distribution throughout the lumbar and thoracolumbar spine models, in scenarios 2 and 3, the average normal stress in the vertebral bodies (VB) was measured. The results for ISR, IVD stress, and VB stress were recorded and compared for both the male and female models to evaluate the change in load distribution based on biological sex.

A sensitivity analysis was performed to confirm model robustness and accuracy of modelling results. Specifically, the mesh size was varied from 3mm to 1mm. In addition, the element type was compared for tetrahedral elements and quadratic hexahedral-dominant elements. For the purpose of this study, the changes were implemented for the IVD volumetric bodies.

5.2.4 Results

5.2.4.1 Lumbar spine model

In scenario 1, ISR was calculated and validated against *in vivo* data of 100 healthy participants presented by Wong et al. [33]. A consistent trend was observed between the FEMs and the *in vivo* comparator, in which vertebral motion decreased for the lower segments, as shown in Figure 5.2.2.

The maximum compressive stress in the IVDs was validated against median lumbar *in silico* results reported by Xu et al. [16] and Dreischarf et al. [34], *in vivo* data from a 25.5-year-old male reported by Takahashi et al. [35], and the maximum reported *ex vivo* data under 2000N compression by Brinckmann and Grootenboer [36], to ensure that the values obtained did not surpass reported literature, depicted in Figure 5.2.3. The male FEM demonstrated IVD stress well within the reported literature ranges. The female FEM portrayed a consistent trend of augmented IVD stress compared to the male FEM, resulting in an average increase of 23%.

In scenario 2, under pure moments applied at L1 to induce flexion and extension, ISR was calculated and compared to *in silico* data from a male lumbar model by Ayturk and Puttlitz [37] and a female lumbar model by Mills and Sarigul-Klijn [17], as well as *ex vivo* data from male cadaveric specimens reported by Panjabi et al. [38], shown in Figure 5.2.4. The FEMs in the current study agreed with the comparators for the superior vertebrae, but underpredicted the rotational magnitudes for the inferior bodies. Compared to the male model, the female model continuously demonstrated an average increased in ISR of 15%.

IVD stress was validated against the abovementioned *in silico* data under a 7.5Nm flexion moment [17], [37], seen in Figure 5.2.5. The presented FEMs demonstrated agreement with the comparators, while the female FEM depicted an average increase of 18% compressive stress in the IVDs compared to the male FEM.

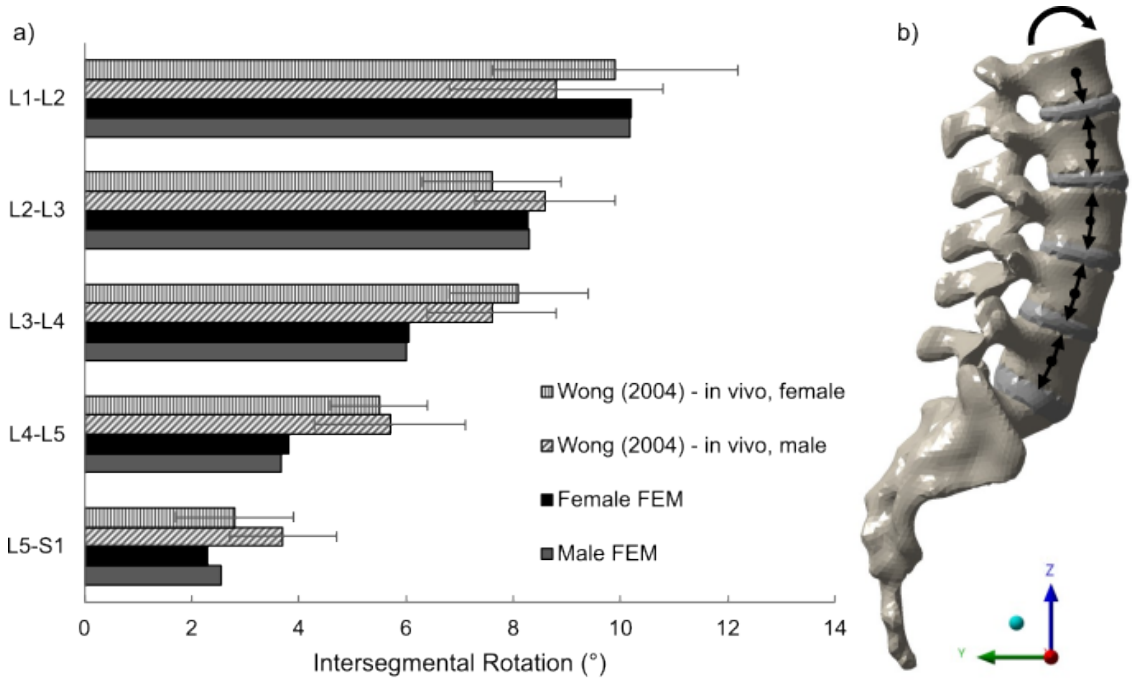

Figure 5.2.2: a) Intersegmental rotation for lumbar vertebra in the male and female FEMs under a 1175N follower load and 7.5Nm moment compared to mean in vivo data from Wong et al. [33]. Error bars indicated standard deviation. b) Loading conditions on the lumbar FEM.

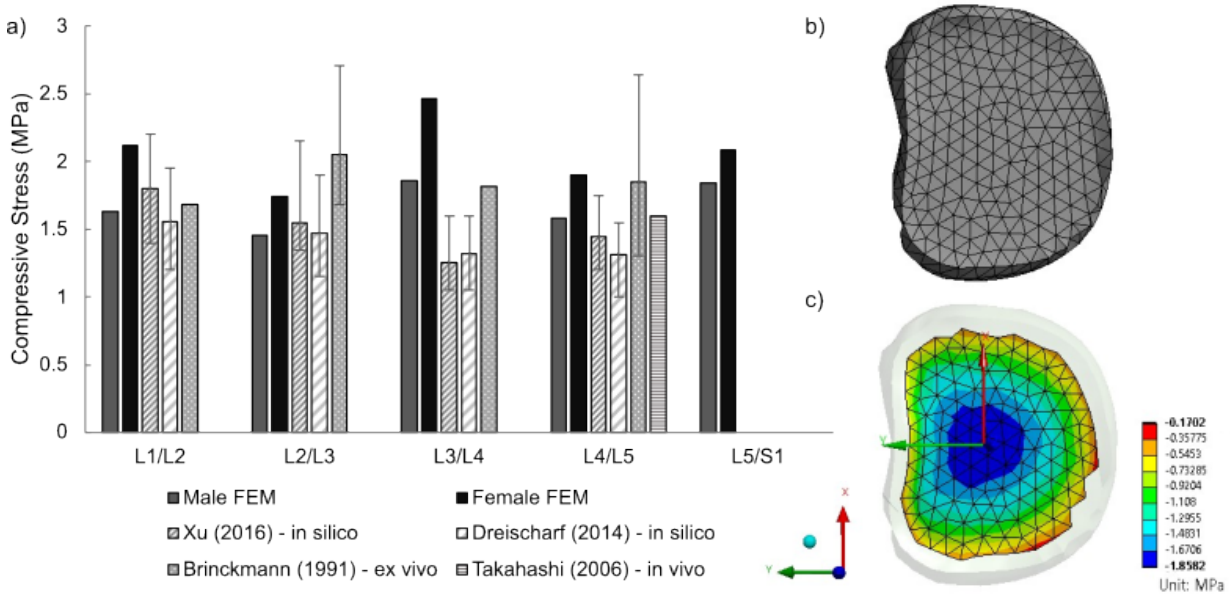

Figure 5.2.3: a) Maximum IVD stress in the male and female FEMs under 1175N follower load and 7.5Nm moment, compared to median in silico data from Xu et al. [16] and Dreischarf et al. [34], ex vivo data from Brinckmann and Grootenboer [36], and in vivo data from Takahashi et al. [35]. Error bars indicate range. b) Example of male L3/L4 IVD, and c) measured IVD stress.

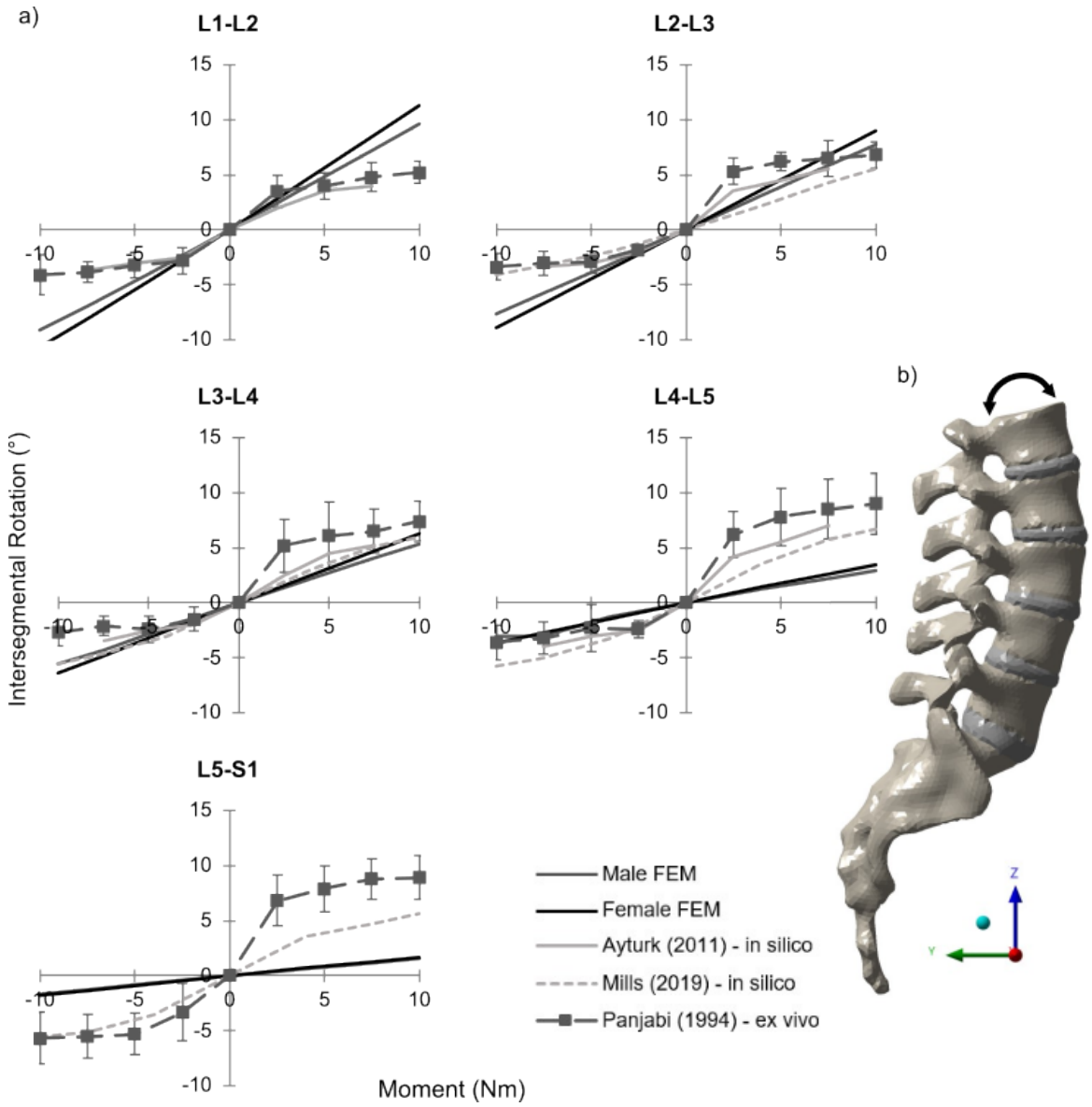

Figure 5.2.4: a) Intersegmental rotation in the male and female FEMs under pure moments, compared to in silico data from Mills and Sarigul-Klijn [17] and Ayturk and Puttlitz [37], and mean ex vivo data from Panjabi et al. [38]. Error bars indicate standard deviation. b) Loading conditions on the lumbar FEM.

5.2.4.2 Thoracolumbar spine model

In scenario 3, the thoracolumbar spine models were subjected to pure moments applied at T1 to induce flexion and extension. ISR was compared to *ex vivo* studies by Sis et al. conducted on a cadaveric thoracic spine under 5Nm flexion-extension [39]. The FEM results are within the standard deviation of the reported literature data for all thoracic spine segments, as shown in Figure 5.2.6. The female model underwent an average increase of 35% rotation at each vertebral level when compared to the male model.

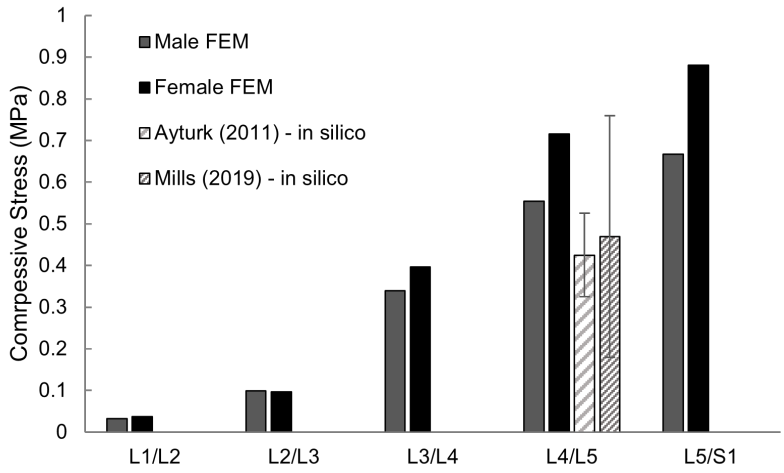

Figure 5.2.5: Maximum IVD stress in the male and female FEMs under pure moments, compared to in silico data from Ayturk and Puttlitz [37] and Mills and Sarigul-Klijn [17]. Error bars indicated standard deviation.

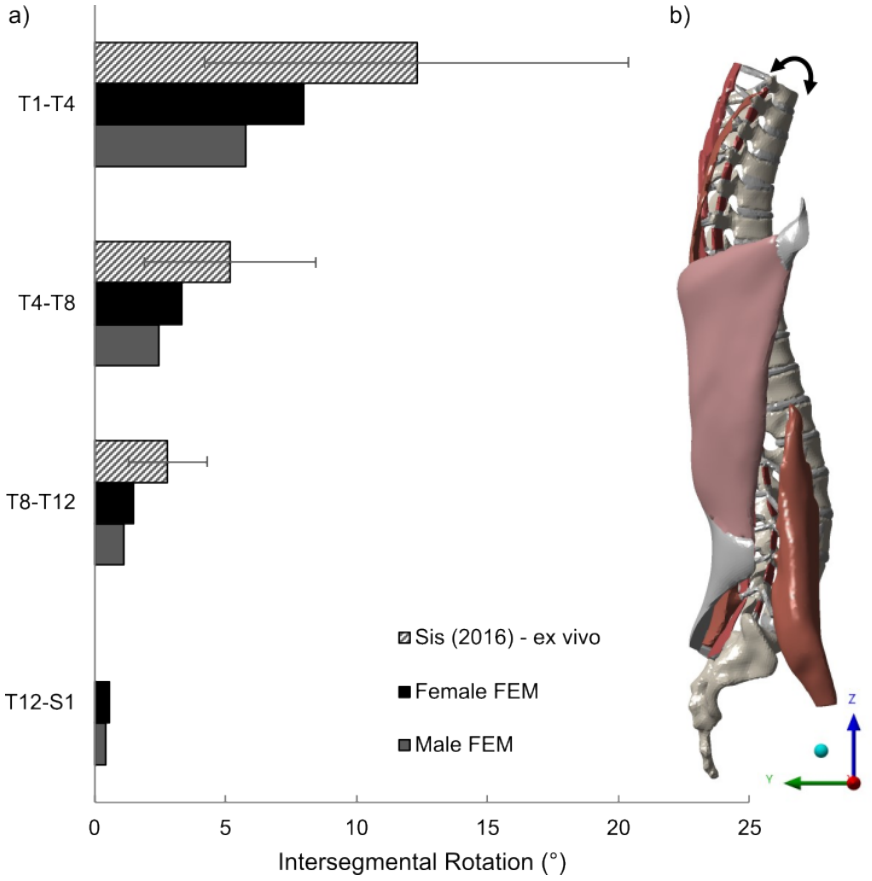

Figure 5.2.6: a) Intersegmental rotation for upper (T1-T4), mid (T4-T8), lower (T8-T12) thoracic and lumbar (T12-S1) spine segments for the male and female FEMs under 5Nm flexion-extension, compared to ex vivo data from Sis et al. [39]. Error bars indicate standard deviation. b) Loading conditions on the thoracolumbar FEM.

IVD stress was evaluated for a range of applied moments. Modelling results were validated against Wilke et al.'s *ex vivo* study on cadaveric thoracic spine units [40] and demonstrated a similar trend in which the IVD pressure increased as the applied moment was amplified, as seen in Figure 5.2.7. IVD stress in the female model was subjected to an average increase of 36% under flexion and 31% extension, relative to the male model.

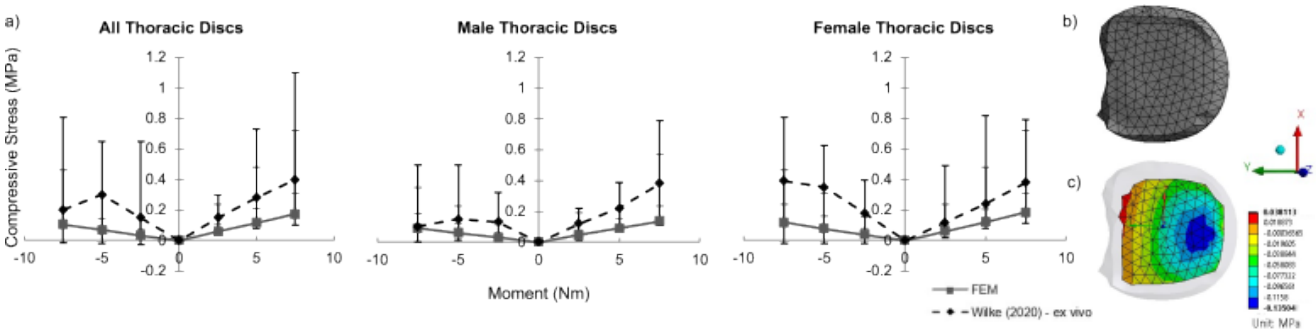

Figure 5.2.7: a) Median maximum IVD stress for the male and female FEMs under pure moments, compared to median ex vivo data from Wilke et al. [40]. Error bars indicate range. b) Example of male T9/T10 IVD, and c) measured IVD stress under 7.5Nm flexion.

5.2.4.3 Vertebral body loading

The load distribution throughout the VBs was analyzed for both the thoracolumbar and lumbar spine models under a 7.5Nm pure flexion moment, shown in Figure 5.2.8. Again, the female FEM demonstrated a consistent trend of augmented stress, resulting in a mean increase of 55% in the thoracolumbar spine model VBs and 51% in the lumbar spine model VBs, respectively, compared to the male FEM.

A summary of the comparative results is outlined in Table 5.2.2. Lastly, the outcomes of the sensitivity analysis confirmed the model robustness and accuracy of results. When subjected to a follower load and moment, changes in mesh size yielded a maximum difference in IVD stress and ISR of 8% and 4%, respectively, while changes in element type yielded a maximum difference of 10% and 6%, respectively. When subjected to pure moments, adjusting the mesh size resulted in a maximum change of 12%, 4%, and 6% for IVD stress, VB stress, and ISR, respectively. For the same variables, changes in element type yielded a maximum change of 13%, 6%, and 7%, respectively.

5.2.5 Discussion

This study aimed to evaluate the changes in load distribution in the thoracolumbar spine through the development and validation of male and female FEMs. The models were validated against available literature to assess their appropriateness in representing biological realities and correct implementation of assumptions [41]. Overall, this study demonstrated evidence that since

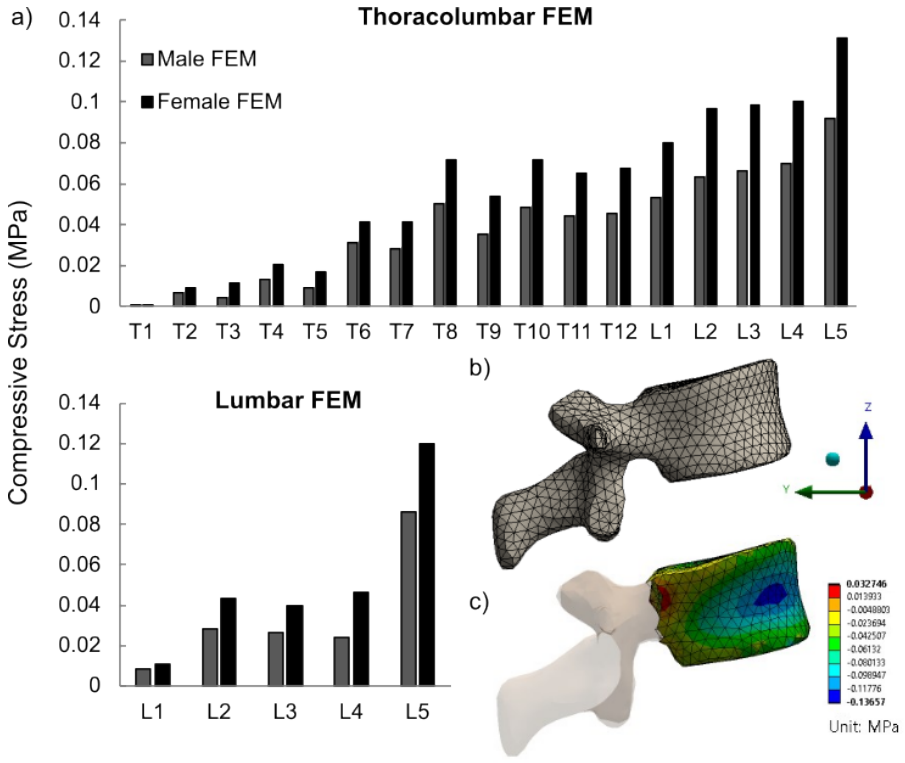

Figure 5.2.8: a) Average normal stress in the vertebral bodies in the thoracolumbar and lumbar FEMs, under 7.5Nm flexion. b) Example of male L1 vertebra, and c) measured VB stress in the thoracolumbar FEM.

male and female anatomy differs, the sex-specific load distribution throughout the spine might also differ. It is assumed that material properties also vary by sex, but such distinction was only integrated regarding the IVDs and tendons. It is possible that additional integration of sex-specific material properties would further add to the divergence of male-female load distributions reported herein.

A follower load is known to stabilize the spine by accounting for the active role of muscles and increasing the spine's load-carrying capacity [42]. ISR in scenario 1 supports this notion, as rotational values and trends were similar across both male and female models, with minimal changes between biological sex. Under both the follower load and pure moment scenarios, the models demonstrated a consistent trend of higher degrees of rotation in the upper spine segments (i.e., T1-T4, L1-L2), and reduced values in the lower segments (i.e., T8-T12, L5-S1). This trend is aligned with reported values from Wong et al. [33] and Sis et al. [39], though the models slightly underestimated the rotational magnitudes in the lower segments. This was further demonstrated in the comparison to data reported by Panjabi et al. [38], in which the L4-L5 and L5-S1 ISRs were well below the *ex vivo* data. The observed FEM results could be influenced by the defined boundary conditions, including the fixed sacrum, which would greatly reduce the range of motion of the

Table 5.2.2: Summary of results demonstrating the percent increase in the physiological parameters in the female model compared to the male model.

	Lumbar FEM		Thoracolumbar FEM		
	1175 N + 7.5 Nm flexion	7.5 Nm flexion	5 Nm flexion-extension	7.5 Nm flexion	7.5 Nm extension
ISR	-1%	15%	35%	-	-
IVD Stress	23%	18%	-	36%	31%
VB Stress	-	51%	-	55%	-

lower vertebrae. Further, the higher concentration of soft tissues near the lower portion of the spine in the FEMs (i.e., psoas major, thoracolumbar fascia) may contribute to reduced motion. Despite this, the validation data lends credibility to the model in which it was explored, demonstrating realistic flexion and extension movement.

The IVD and VB stresses followed similar trends under pure moments, in which the recorded stress increased in the lower anatomical components. This trend was expected as the more inferior human vertebrae are known to withstand higher loads when supporting the human body [43]. Further, the stresses in the female FEM continuously demonstrated trends of augmented stresses compared to the male model. Variations in the stress distribution between the models can in part be attributed to the changes in CSA and material properties; the female FEM had lower CSAs as well as reduced tendon properties and increased IVD properties.

Several literature studies have linked the augmented LBP in females to hormonal changes [44], [45] or pregnancy [6], [44]–[46]. Literature has also reported potential causes for higher LBP as workforce gender segregation, different exposures to the same job, or varying methods of performing the same task [3]. Further studies have considered the influence of women more often holding the role of performing household tasks [3], [6] or providing childcare [5], [6], noting the inadequate static posture as a noticeable risk [3]. Thus, the higher stress in the female FEM may corroborate the increased prevalence of LBP and musculoskeletal disorders observed in female patients from a biomechanical perspective.

As required in the development of any *in silico* human model, several simplifications were made, resulting in limitations. First, the male model was constructed from available geometric bodies of a young, healthy male [18], meanwhile, the female model was constructed through geometric and material adjustments of the male model to align with literature comparing male and female anatomy, resulting in a model representing a young, healthy female. Further, both models were subjected to identical loading scenarios to perform validation with respect to available literature. Although previous *in silico* studies have also taken a similar approach whereby spine

FEMs, whether male or female, were subjected to loading conditions reflective of previous studies (i.e., pure moments or follower loads), it is acknowledged that loading conditions representing realistic body weight may strengthen the results of this study, and as such, this approach is currently being explored in a complimentary study. The modelled spine components were assumed to have linear elastic and isotropic properties, despite human tissues demonstrating anisotropic and viscoelastic qualities, which allowed the models to be solved in an efficient and timely manner. There is limited published research outlining and comparing the material properties of male and female biological components, thus the material properties of the muscles were identical for both FEMs. Future research into female-specific anatomy, material properties, and modelling would benefit this research. Despite these simplifications, the ability to modify the anatomical geometry demonstrates the applicability of this methodology for clinical applications, as rapidly creating realistic patient- and sex-specific models for patient analysis may provide significant advantages to clinical assessments and patient care.

5.2.6 Conclusions

To conclude, the sex-specific models were developed to analyze load distributions throughout the spine and were successfully validated against published literature. Further, the FEM comparisons demonstrated that the female body may be subjected to noticeably higher loading than the male body, thus corroborating the potential for females to be subjected to greater tendencies of LBP and musculoskeletal disorders. These models demonstrate the applicability of modifying model geometries and material properties for patient-specific clinical applications. Though the developed model more accurately represents a younger population, material properties could easily be adjusted to reflect that of an older population, thus demonstrating the applicability of this model in clinical applications.

5.2.7 Acknowledgments

This research was supported by McGill University (MEDA), the Fonds de Recherche du Québec – Nature et Technologies (FRQNT), and the Natural Sciences and Engineering Research Council (NSERC).

5.2.8 References

[1] E. L. Hurwitz, K. Randhawa, H. Yu, P. Côté, and S. Haldeman, "The global spine care initiative: A summary of the global burden of low back and neck pain studies," *European Spine Journal*, vol. 27, no. 6, pp. 796–801, 2018.

[2] A. Bailey, "Risk factors for low back pain in women: Still more questions to be answered," *Menopause*, vol. 16, no. 1, pp. 3–4, 2009.

[3] T. P. F. Bento, C. V. dos Santos Genebra, N. M. Maciel, G. P. Cornelio, S. F. A. P. Simeão, and A. de Vitta, "Low back pain and some associated factors: Is there any difference between genders?" *Brazilian Journal of Physical Therapy*, vol. 24, no. 1, pp. 79–87, 2020.

[4] D. Hoy, C. Bain, G. Williams, *et al.*, "A systematic review of the global prevalence of low back pain," *Arthritis & Rheumatism*, vol. 64, no. 6, pp. 2028–2037, 2012.

[5] A. Bener, E. E. Dafeeah, K. Alnaqbi, *et al.*, "An epidemiologic analysis of low back pain in primary care: A hot humid country and global comparison," *Journal of Primary Care & Community Health*, vol. 4, no. 3, pp. 220–227, 2013.

[6] R. D. Meucci, A. G. Fassa, and N. M. X. Faria, "Prevalence of chronic low back pain: Systematic review," *Revista de saude publica*, vol. 49, p. 73, 2015.

[7] G. I. Polykoff and J. Jackson, "History and physical examination," in *Spine Pain Care*, Springer, 2020, pp. 69–90.

[8] S. Bhavikatti, *Finite element analysis*. New Age International, 2005.

[9] A. Rohlmann, T. Zander, M. Rao, and G. Bergmann, "Realistic loading conditions for upper body bending," *Journal of Biomechanics*, vol. 42, no. 7, pp. 884–890, 2009.

[10] W. M. Park, K. Kim, and Y. H. Kim, "Effects of degenerated intervertebral discs on intersegmental rotations, intradiscal pressures, and facet joint forces of the whole lumbar spine," *Computers in Biology and Medicine*, vol. 43, no. 9, pp. 1234–1240, 2013.

[11] S.-H. Chen, Z.-C. Zhong, C.-S. Chen, W.-J. Chen, and C. Hung, "Biomechanical comparison between lumbar disc arthroplasty and fusion," *Medical Engineering & Physics*, vol. 31, no. 2, pp. 244–253, 2009.

[12] A. G. Bruno, M. L. Bouxsein, and D. E. Anderson, "Development and validation of a musculoskeletal model of the fully articulated thoracolumbar spine and rib cage," *Journal of Biomechanical Engineering*, vol. 137, no. 8, p. 081 003, 2015.

[13] W. Wang, D. Wang, F. De Groote, L. Scheys, and I. Jonkers, "Implementation of physiological functional spinal units in a rigid-body model of the thoracolumbar spine," *Journal of Biomechanics*, vol. 98, p. 109 437, 2020.

[14] I. El Bojairami, K. El-Monajjed, and M. Driscoll, "Development and validation of a timely and representative finite element human spine model for biomechanical simulations," *Scientific Reports*, vol. 10, no. 1, pp. 1–15, 2020.

[15] K. Imai, I. Ohnishi, S. Yamamoto, and K. Nakamura, "In vivo assessment of lumbar vertebral strength in elderly women using computed tomography-based nonlinear finite element model," *Spine*, vol. 33, no. 1, pp. 27–32, 2008.

[16] M. Xu, J. Yang, I. H. Lieberman, and R. Haddas, "Lumbar spine finite element model for healthy subjects: Development and validation," *Computer Methods in Biomechanics and Biomedical Engineering*, vol. 20, no. 1, pp. 1–15, 2017.

[17] M. J. Mills and N. Sarigul-Klijn, "Validation of an in vivo medical image-based young human lumbar spine finite element model," *Journal of Biomechanical Engineering*, vol. 141, no. 3, p. 031 003, 2019.

[18] N. Mitsuhashi, K. Fujieda, T. Tamura, S. Kawamoto, T. Takagi, and K. Okubo, "Bodyparts3d: 3d structure database for anatomical concepts," *Nucleic Acids Research*, vol. 37, no. suppl_1, pp. D782–D785, 2009.

[19] I. El Bojairami and M. Driscoll, "Correlating skeletal muscle output force and intramuscular pressure via a 3-dimensional finite element muscle model," *Journal of Biomechanical Engineering*, 2021.

[20] V. Gilsanz, M. I. Boechat, R. Gilsanz, M. L. Loro, T. F. Roe, and W. G. Goodman, "Gender differences in vertebral sizes in adults: Biomechanical implications," *Radiology*, vol. 190, no. 3, pp. 678–682, 1994.

[21] R. Cooper, S. Holli, and M. Jayson, "Gender variation of human spinal and paraspinal structures," *Clinical Biomechanics*, vol. 7, no. 2, pp. 120–124, 1992.

[22] G. N. Onambélé, K. Burgess, and S. J. Pearson, "Gender-specific in vivo measurement of the structural and mechanical properties of the human patellar tendon," *Journal of Orthopaedic Research*, vol. 25, no. 12, pp. 1635–1642, 2007.

[23] E. N. Ebbesen, J. S. Thomsen, H. Beck-Nielsen, H. J. Nepper-Rasmussen, and L. Mosekilde, "Age-and gender-related differences in vertebral bone mass, density, and strength," *Journal of Bone and Mineral Research*, vol. 14, no. 8, pp. 1394–1403, 1999.

[24] B. D. Stemper, D. Board, N. Yoganandan, and C. E. Wolfla, "Biomechanical properties of human thoracic spine disc segments," *Journal of Craniovertebral Junction and Spine*, vol. 1, no. 1, p. 18, 2010.

[25] T. Keaveny and O. Yeh, "Architecture and trabecular bone-toward an improved understanding of the biomechanical effects of age, sex and osteoporosis," *Journal of Musculoskeletal and Neuronal Interactions*, vol. 2, no. 3, pp. 205–208, 2002.

[26] M. Kurutz, *Finite element modelling of human lumbar spine*. Citeseer, 2010.

[27] D. T. Reilly and A. H. Burstein, "The elastic and ultimate properties of compact bone tissue," *Journal of Biomechanics*, vol. 8, no. 6, pp. 393–405, 1975.

[28] S. R. Ward, A. Tomiya, G. J. Regev, *et al.*, "Passive mechanical properties of the lumbar multifidus muscle support its role as a stabilizer," *Journal of Biomechanics*, vol. 42, no. 10, pp. 1384–1389, 2009.

[29] G. J. Regev, C. W. Kim, A. Tomiya, *et al.*, "Psoas muscle architectural design, in vivo sarcomere length range, and passive tensile properties support its role as a lumbar spine stabilizer," *Spine*, vol. 36, no. 26, E1666–E1674, 2011.

[30] L. Yahia, P. Pigeon, and E. DesRosiers, "Viscoelastic properties of the human lumbodorsal fascia," *Journal of Biomedical Engineering*, vol. 15, no. 5, pp. 425–429, 1993.

[31] K. El-Monajjed and M. Driscoll, "Investigation of reaction forces in the thoracolumbar fascia during different activities: A mechanistic numerical study," *Life*, vol. 11, no. 8, p. 779, 2021.

[32] J. Dvořák, M. Panjabi, D. Chang, R. Theiler, and D. Grob, "Functional radiographic diagnosis of the lumbar spine: Flexion–extension and lateral bending," *Spine*, vol. 16, no. 5, p. 562, 1991.

[33] K. W. Wong, J. C. Leong, M.-k. Chan, K. D. Luk, and W. W. Lu, "The flexion–extension profile of lumbar spine in 100 healthy volunteers," *Spine*, vol. 29, no. 15, pp. 1636–1641, 2004.

[34] M. Dreischarf, T. Zander, A. Shirazi-Adl, *et al.*, "Comparison of eight published static finite element models of the intact lumbar spine: Predictive power of models improves when combined together," *Journal of Biomechanics*, vol. 47, no. 8, pp. 1757–1766, 2014.

[35] I. Takahashi, S.-i. Kikuchi, K. Sato, and N. Sato, "Mechanical load of the lumbar spine during forward bending motion of the trunk–a biomechanical study," *Spine*, vol. 31, no. 1, pp. 18–23, 2006.

[36] P. Brinckmann and H. Grootenboer, "Change of disc height, radial disc bulge, and intradiscal pressure from discectomy an in vitro investigation on human lumbar discs," *Spine*, vol. 16, no. 6, pp. 641–646, 1991.

[37] U. M. Ayturk and C. M. Puttlitz, "Parametric convergence sensitivity and validation of a finite element model of the human lumbar spine," *Computer Methods in Biomechanics and Biomedical Engineering*, vol. 14, no. 8, pp. 695–705, 2011.

[38] M. M. Panjabi, T. Oxland, I. Yamamoto, and J. J. Crisco, "Mechanical behavior of the human lumbar and lumbosacral spine as shown by three-dimensional load-displacement curves," *Journal of Bone and Joint Surgery*, vol. 76, no. 3, pp. 413–424, 1994.

[39] H. L. Sis, E. M. Mannen, B. M. Wong, *et al.*, "Effect of follower load on motion and stiffness of the human thoracic spine with intact rib cage," *Journal of Biomechanics*, vol. 49, no. 14, pp. 3252–3259, 2016.

[40] H.-J. Wilke, A. Herkommer, K. Werner, and C. Liebsch, "In vitro analysis of the intradiscal pressure of the thoracic spine," *Frontiers in Bioengineering and Biotechnology*, vol. 8, p. 614, 2020.

[41] American Society of Mechanical Engineers: V&V40 Committee, "Assessing credibility of computational modeling through verification and validation: Application to medical devices," *The American Society of Mechanical Engineers*, 2018.

[42] A. G. Patwardhan, R. M. Havey, K. P. Meade, B. Lee, and B. Dunlap, "A follower load increases the load-carrying capacity of the lumbar spine in compression," *Spine*, vol. 24, no. 10, pp. 1003–1009, 1999.

[43] A. Nachemson, "The load on lumbar disks in different positions of the body," *Clinical Orthopaedics and Related Research (1976-2007)*, vol. 45, pp. 107–122, 1966.

[44] J. Borg-Stein and S. A. Dugan, "Musculoskeletal disorders of pregnancy, delivery and postpartum," *Physical medicine and rehabilitation clinics of North America*, vol. 18, no. 3, pp. 459–476, 2007.

[45] H.-O. Svensson, G. Andersson, A. Hagstad, and P. Jansson, "The relationship of low-back pain to pregnancy and gynecologic factors," *Spine*, vol. 15, no. 5, pp. 371–375, 1990.

[46] S.-M. Wang, P. Dezinno, I. Maranets, M. R. Berman, A. A. Caldwell-Andrews, and Z. N. Kain, "Low back pain during pregnancy: Prevalence, risk factors, and outcomes," *Obstetrics & Gynecology*, vol. 104, no. 1, pp. 65–70, 2004.

5.3 Additional Study Related to Article 2: Sex-specific body weight loading conditions

Upon completion of the main targets of Objective 1, an additional study was conducted to evaluate the stress distribution when sex-specific loading conditions were applied, as the study in Article 2 (Section 5.2) focused on identical loading conditions for the male and female models. The work detailed below was presented as a poster at the 22nd Annual Conference for the International Society for the Advancement of Spine Surgery (ISASS) from June 1-4, 2022. In addition, these loading conditions were further evaluated in Objective 3 (Section 7).

5.3.1 Methods

The previously developed and validated male and female lumbar spine models were leveraged for this study, consisting of the vertebrae and adjacent intervertebral discs (L1-S1), as described in Section 5.2.3. Both models were fixed at S1. To accurately represent the body weight applied on each vertebra, a 45.2% body weight load was applied on L1 followed by 2.6% on each subsequent vertebra (L2 to L5) [9], detailed in Figure 5.3.1. The loads were then amplified to account for spinal muscle activity [80]. As such, the final loading equation was:

$$F = (15 + 2.1 \times BW) \times g$$

where F is the applied force on each vertebra in N, BW is the selected body weight at each vertebral level in kg, and g is the gravitational acceleration constant in m/s^2. The magnitude of loading selected for each model was reflective of the average body weight of 50% percentile young adults in North America, 20-29 years of age, i.e., 81kg for males and 70kg for females [200]. Lastly, a 7.5 Nm moment was applied at L1 to induce flexion. An FEA was conducted in ANSYS to measure IVD and VB stresses.

The male model, which served as a baseline in this study, was subjected to loading conditions representative of average male body weight. The female model was subjected to two loading scenarios, specifically:

1. Identical loading conditions to the male model;
2. Loading conditions representative of average female body weight.

Lastly, the models underwent validation to confirm the accuracy of the results, as this additional study presented new loading conditions.

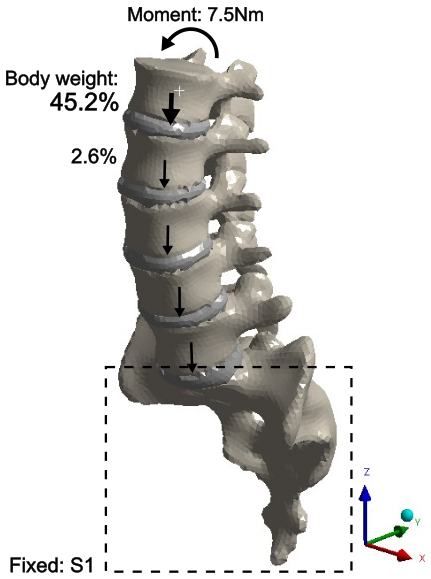

Figure 5.3.1: Loading conditions applied on the lumbar spine model.

5.3.2 Results

IVD stresses for the lumbar spine models were validated and compared against *in silico* data from Dreischarf et al. [74] and Xu et al. [186], and *in vivo* data from Takahashi et al. which evaluated healthy male participants [83], as displayed in Figure 5.3.2. The male model demonstrated agreement with the selected comparators, meanwhile, the female model demonstrated greater IVD stresses than the male model in both loading scenarios, with the exception of L2/L3.

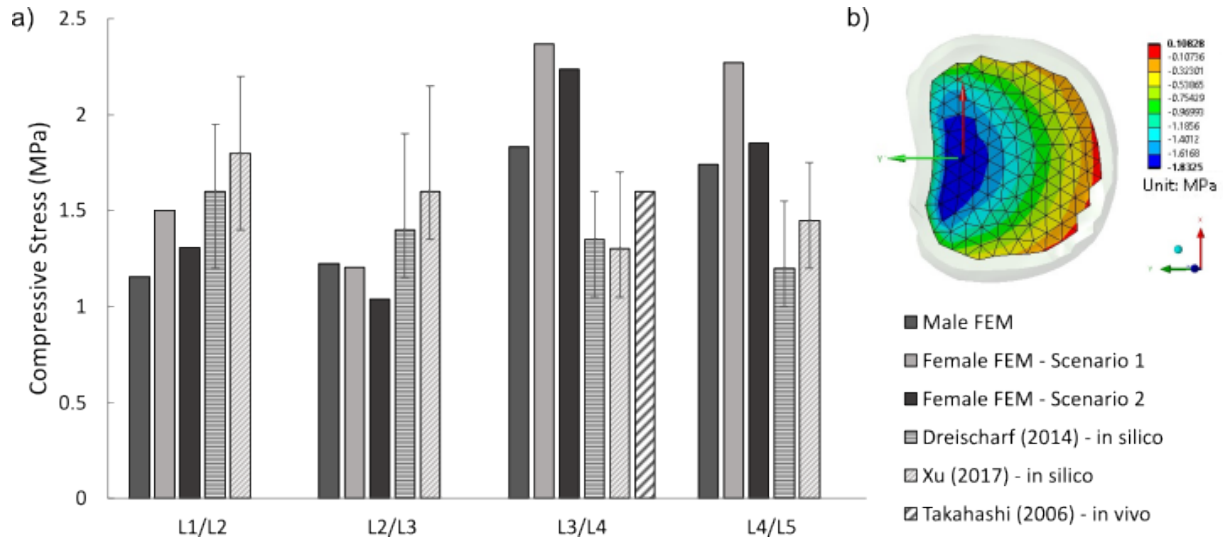

Figure 5.3.2: a) Maximum IVD stress in the lumbar FEMs, compared to median in silico data from Dreischarf et al. [74] and Xu et al. [186], and in vivo data from Takahashi et al. [83]. Error bars represent range. b) Example of L3/L4 IVD stress in the male FEM.

Following initial validation, VB stresses were measured for L1 to L5 for both models. The stresses observed in the female FEM were higher than those in the male FEM for all vertebrae, irrespective of the applied loading condition, as depicted in Figure 5.3.3.

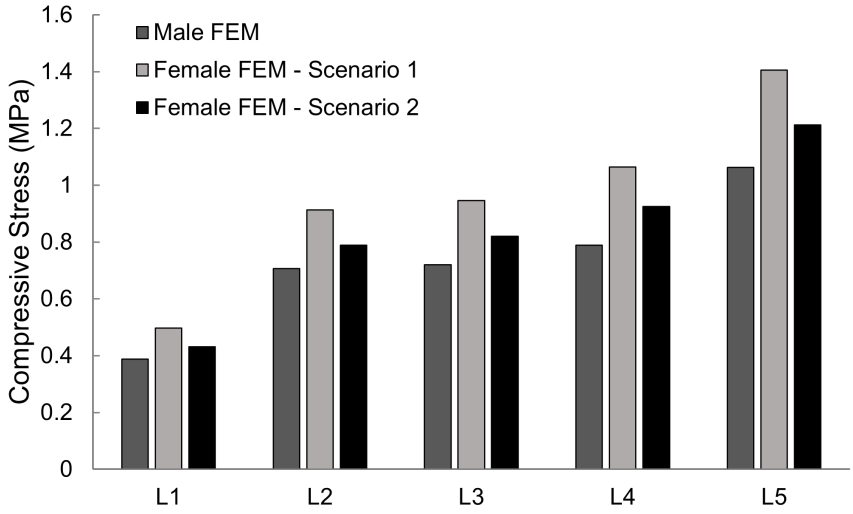

Figure 5.3.3: Average normal stress in the vertebral bodies in the lumbar FEMs.

5.3.3 Discussion and Conclusions

This study aimed to evaluate the stresses observed in the sex-specific models when subjected to loading conditions representative of realistic average body weights for males and females in North America.

When subjected to identical loading conditions, the female model demonstrated an increase in IVD stress and VB stress of 22% and 31%, respectively, relative to the male model. These results are in agreement with a study by Gilsanz et al., who calculated that female VBs would be subjected to approximately 33% greater stresses than male VBs when equivalently loaded [27].

In comparison, when subjected to loading conditions representative of average female body weight, the female model continued to demonstrate augmented stresses in the IVDs and VBs compared to the male model, although by 7% and 14%, respectively. Therefore, the observed stresses remained noticeably higher in the female FEM compared to the male FEM when loaded with respect to body weight.

The results of this additional study indicated that the female model exhibited higher IVD and VB stresses than the male model, irrespective of the applied loading conditions. Further, studies have noted that there is a higher prevalence of LBP cases among female patients compared to males [68], [69]. Therefore, the findings presented herein indicated that females may be routinely subjected to augmented stresses during daily activities, which may contribute to the

greater occurrence of LBP cases. To conclude, this additional study highlights the importance of sex-specific modelling and realistic loading conditions. Implementing loading conditions representative of patient-specific body weights may provide information on spine biomechanics and musculoskeletal pain and may further contribute to knowledge for targeted treatments or surgical planning.

5.4 Additional Study Related to Article 2: Finite element analysis of the thoracolumbar fascia

Once the additional study outlined in Section 5.3 was completed, an extension of this study was conducted to evaluate the changes in tensional stress distribution in the TLF based on biological sex. The work detailed below was presented at the 6th International Fascia Research Congress on September 12, 2022.

5.4.1 Summary of the Thoracolumbar Fascia

As described in Section 2.1, the TLF is a multilayer connective tissue that connects the latissimus dorsi and gluteal muscles [23], [201], wrapping around the lumbar extensor muscles in the spine [202]. The middle layer of the TLF provides a strong attachment to the transverse abdominal muscles and the processes on the lumbar vertebrae, therefore contributing to force transmission and lumbar stability [24]. There has been much debate about the function of the TLF in the human body. Studies have found that this connective tissue plays a part in transferring forces between the trunk muscles and the spine [25], reducing spinal loads and enhancing lumbar stability [26]. However, the role that the TLF plays in LBP is poorly understood [65], [203]. As such, the objective of this additional study was to leverage the previously developed FEMs to evaluate the changes in fascial tissue stress based on biological sex.

5.4.2 Methods

The male and female thoracolumbar spine models described in Section 5.2.3 were leveraged for this study. The models were evaluated under upright standing conditions. Fixed supports were applied to the model at S1, as well as the extremities of the tendons on the latissimus dorsi muscles. The models were subjected to similar loading scenarios as specified in Section 5.3.1: a 14% body weight load was applied on T1 followed by 2.6% on each subsequent vertebra (T2 to L5) [9], detailed in Figure 5.4.1. The loads were then amplified to account for spinal muscle activity [80]. Again, the loading conditions selected for each model were reflective of 50% percentile young adults in North America, 20-29 years of age [200]. Following the application of the boundary and loading conditions, the average normal stress in the TLF was measured in the z-direction in ANSYS. The modelling results were exported to MATLAB (R2021a, MathWorks, Inc., Natick, Massachusetts) for average tensile stress calculations.

The models were evaluated under three cases, whereby each case was subjected to the loading conditions described above:

1. Vertebrae and IVDs (T1-S1);
2. Vertebrae and IVDs (T1-S1), including the TLF;
3. Vertebrae and IVDs (T1-S1), include all previously described tissues.

Lastly, the models underwent validation to ensure accurate representations of previously published studies.

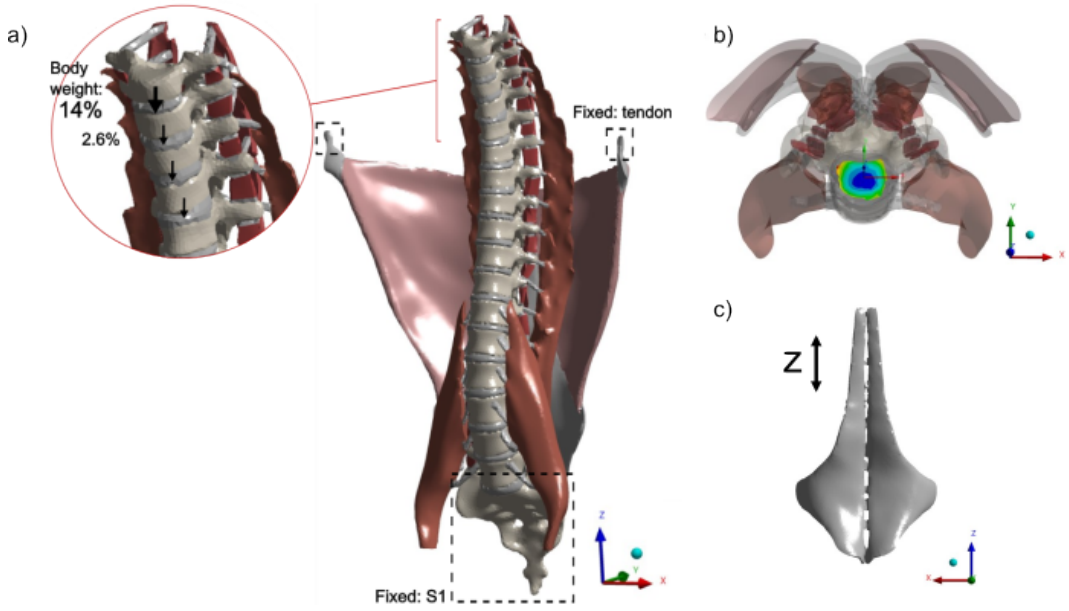

Figure 5.4.1: a) Loading conditions applied on the thoracolumbar spine, b) measured IVD stresses, and c) direction of tensional normal stress evaluation (z) in the thoracolumbar fascia.

5.4.3 Results

IVD stresses were validated and compared against previously published studies, namely, *in silico* data from Dreischarf et al. [74], Wang et al. [182], and Xu et al. [186], and *ex vivo* data measured from cadaveric specimens conducted by Brinckmann and Grootenboer [204]. The comparator studies evaluated IVDs subjected to 1000N compression, providing a suitable comparison with the cumulative load at the lumbar levels in the models. Validation results are depicted in Figure 5.4.2, demonstrating good agreement between the male model and the selected comparators. On average, the IVD stresses in the female model were higher than in the male model, with the exception of L2/L3.

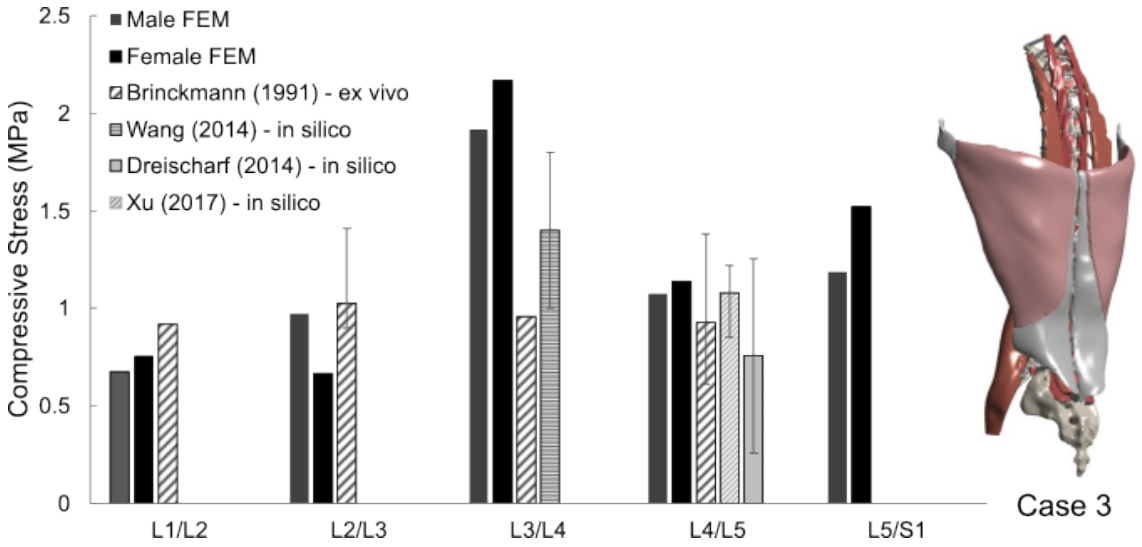

Figure 5.4.2: a) Maximum IVD stress in the lumbar region of the FEMs, compared to median ex vivo data from Brinckmann and Grootenboer [204] and in silico data from Dreischarf et al. [74], Wang et al. [182], and Xu et al. [186]. Error bars represent range.

Following validation, IVD stresses in each case were evaluated and compared. When comparing Case 3 (all soft tissues) to Case 2 (TLF only), the observed IVD stresses were slightly reduced when all tissues were included, however, negligible differences were observed and the magnitudes remained within the validated range. However, when comparing these results against Case 1 (vertebrae and IVDs only), there is a substantial increase in the observed IVD stresses, notably in the lower lumbar discs, as seen in Figure 5.4.3.

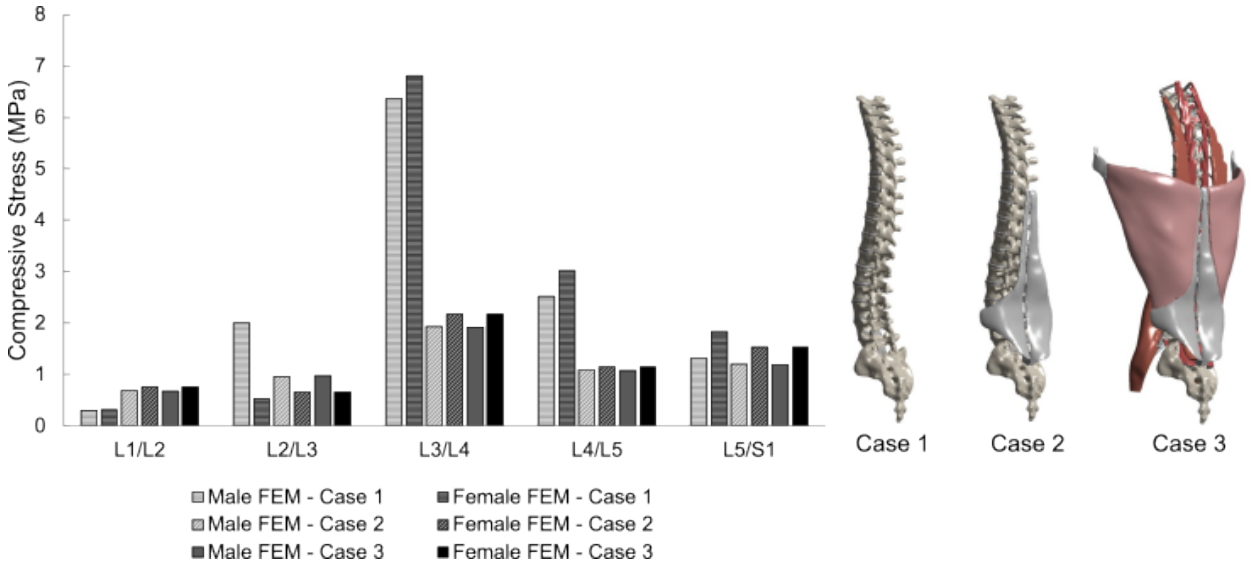

Figure 5.4.3: Comparison of the maximum IVD stresses in the lumbar region of the FEMs for all cases.

The average tensional stress in the TLF was measured in both the male and female models for Case 2 and Case 3, as seen in Figure 5.4.4. There was a substantial increase (7%) in the fascia stress observed in the female model relative to the male model. However, when comparing Case 2 to Case 3, the TLF stress in the male model showed negligible change (-0.5%). Similar trends were observed in the female model (-0.8%).

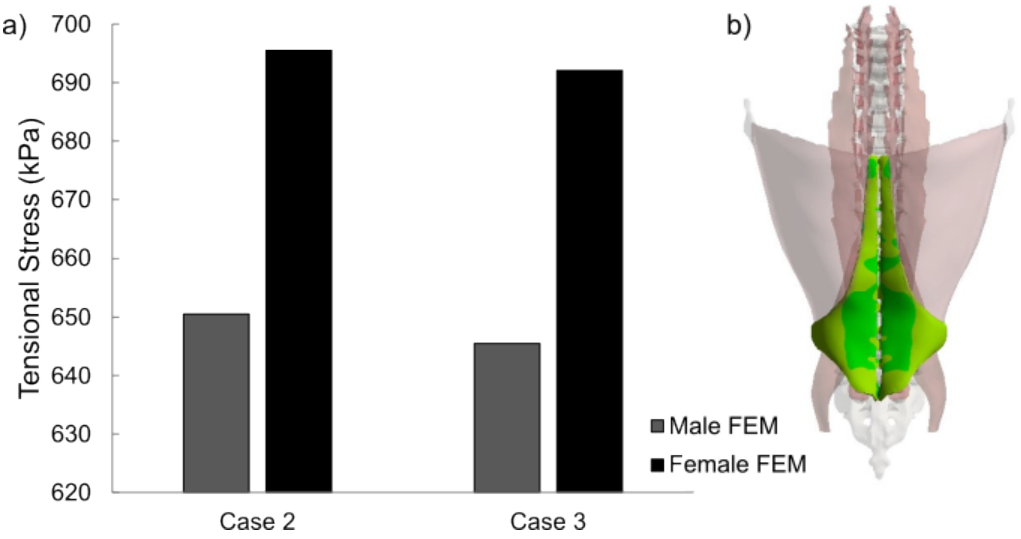

Figure 5.4.4: a) Comparison of the average tensional stress in the thoracolumbar fascia in Case 2 and Case 3 for the male and female FEMs. b) Example of the stress in the thoracolumbar fascia in the male FEM.

5.4.4 Discussion and Conclusions

Overall, this study highlights the critical role that the TLF may play in providing spinal support. When considering Case 1, in which only the vertebrae and IVDs were included in the model, the spine was observed to perform unnatural and exaggerated motions when loaded, and the discs were subjected to substantial stresses. With the addition of the TLF in Case 2, there was a notable reduction in the measured lumbar disc stresses, indicating that the TLF reduced the load distributed throughout the spine, hence providing stability to the model. Lastly, when all tissues were included in Case 3, negligible change was observed in the measured fascial and disc stresses when compared to the previous case. These results suggested that the fascia may provide a large amount of support to the spine, potentially even contributing to a greater portion of spinal support than the passive contribution of the muscles.

In summary, this additional study corroborates the importance of including soft tissues in biomechanical modelling, as the addition of the TLF had substantial impacts on the modelling outputs. This study also confirms the ability to expand body weight loading conditions to the full thoracolumbar spine. The modelling results followed similar trends as observed in Sections 5.2 and

5.3 whereby the female model exhibited greater spinal stresses than the male model, demonstrated in the IVDs, VBs, and TLF. From a mechanical perspective, the observed increase in stresses in the female model discs and fascia may be potential indicators of more prominent LBP cases and tissue injuries in female patients.

5.5 Summary

This chapter offers the contribution of a full thoracolumbar spine model representative of female anatomy with respect to geometry and material properties. Although female spine models have previously been developed, the models generally only considered a section of the spine and often lacked the inclusion of soft tissues. Further, some previously developed FEMs considered both male and female geometry but did not differentiate or compare the results with respect to sex, instead opting to present the mean of the modelling results. This study provided a detailed comparison of male and female spine models under various loading conditions; the main study considered identical loading conditions, while the additional studies considered loading conditions representative of male and female body weights.

The prevalence of LBP is greater in female patients than in male patients [68], [69]. Further, the spinal load tolerances are reduced in females [70], supporting the notion that women are at a higher risk of injury. It was hypothesized that differences in stress magnitudes would be observable when implementing sex-specific differences (i.e., geometry and material properties) in spine models for FEA. The results of the main objective and additional studies support this hypothesis, as the female model exhibited greater stress magnitudes measured in the IVDs, VBs, and TLF under several loading conditions. The observed differences in stress magnitudes in the male and female models may support the greater occurrence of LBP cases in women.

The findings of Objective 1 provide insight into potential biological differences and loading capabilities between sexes. The evident differences in stress distribution between male and female spines, as observed through FEA, may inspire targeted treatments, variations in surgical implant designs, or a broader understanding of sex differences in LBP.

6 Development and validation of thoracolumbar spine models with exaggerated sagittal curvature

6.1 Framework for Article 3

An individual's sagittal spinal profile is unique. As described in Section 2.4, a range of curvatures for both the thoracic and lumbar regions have been identified that are considered normal and healthy. If an individual's sagittal curvature falls outside of this range, their curvature is considered exaggerated or irregular and has often been linked to the development of various spinal disorders and back pain. However, optimal biomechanical loading of the spine is not fully understood. Some individuals have irregular sagittal profiles but may perform day-to-day tasks with sufficient spinal balance and live absent of pain.

Computational modelling allows the opportunity to evaluate both healthy and disordered spinal conditions. Although the evaluation of surgical instrumentation has been investigated in multiple FE studies of the spine [189], [205]–[207], fewer studies have investigated spine models with irregular sagittal curvature. As described in Section 2.7.1, FE modelling has been used to evaluate the adolescent thoracic spine when absent of kyphosis [194]. With respect to the lumbar spine, biomechanical studies were conducted to evaluate variations in sagittal profile under flexion-extension and lifting tasks [187], [193]. These studies focused on a segment of the spine, though the latter study lacked sufficient validation. Therefore, the purpose of the second objective was to analyse changes in stress distribution and range of motion of the full thoracolumbar spine when alterations in sagittal alignment were considered. Further, this study aimed to evaluate if the normal, "healthy" curvature ranges provided a biomechanical advantage.

The outcomes of Objective 2 and the evaluation of Hypothesis 2 are discussed in the manuscript below, titled "Biomechanical evaluation of the thoracolumbar spine comparing healthy and irregular thoracic and lumbar curvatures." The contribution of the first author is considered to be 85% for model development, analysis and validation of modelling results, and manuscript writing, meanwhile, the contribution of the second author is considered to be 15% for research guidance and manuscript review. The manuscript was published in *Computers in Biology and Medicine* by Elsevier on April 28, 2023. A subset of this work was presented at the 4th International Workshop on Spine Loading and Deformation, July 5-7, 2023.

6.2 Article 3: Biomechanical evaluation of the thoracolumbar spine comparing healthy and irregular thoracic and lumbar curvatures

Brittany Stott[1,2], Mark Driscoll[1,2]

[1]Musculoskeletal Biomechanics Research Lab, Department of Mechanical Engineering, McGill University, Montreal, QC, Canada

[2]Orthopaedic Research Lab, Montreal General Hospital, Montreal, QC, Canada

Address for notification, correspondence, and reprints:

Mark Driscoll, Ph.D., P.Eng.

Associate Professor, Department of Mechanical Engineering

Canada NSERC Chair Design Eng. for Interdisciplinary Innovation of Medical Technologies

Associate Member, Biomedical Engineering

Associate Member, Department of Surgery

Investigator, Research Institute MUHC, Injury Repair Recovery Program

McGill University, Department of Mechanical Engineering

817 Sherbrooke St. West, Montreal, QC H3A 0C3, Canada

Macdonald Eng. Bldg., office #153

T: +1 (514) 398-6299

F: +1 (514) 398-7365

E-mail: mark.driscoll@mcgill.ca

6.2.1 Abstract

Background: The geometric alignment of the spine plays an integral role in stability, biomechanical loading, and consequently, pain, and a range of healthy sagittal curvatures has been identified. Spinal biomechanics when sagittal curvature is outside the optimal range remains a debate and may provide insight into the load distribution throughout the spinal column.

Methods: A thoracolumbar spine model (Healthy) was developed. Thoracic and lumbar curvatures were adjusted by 50% to create models with varying sagittal profiles: hypolordotic (HypoL), hyperlordotic (HyperL), hypokyphotic (HypoK), and hyperkyphotic (HyperK). In addition, lumbar spine models were constructed for the former three profiles. The models were subjected to loading conditions simulating flexion and extension. Following validation, intervertebral disc stresses, vertebral body stresses, disc heights, and intersegmental rotations were compared across all models.

Results: Overall trends demonstrated that HyperL and HyperK models had a noticeable reduction in disc height and greater vertebral body stresses compared to the Healthy model. In comparison, the HypoL and HypoK models displayed opposite trends. Considering the lumbar models, the HypoL model had reduced disc stresses and flexibility, while the contrary was observed in the HyperL model. Results indicate that the models with excessive curvature may be subjected to greater stress magnitudes, while the straighter spine models may reduce these stresses.

Conclusions: Finite element modeling of spine biomechanics demonstrated that variations in sagittal profiles influence the load distribution and range of motion of the spine. Considering patient-specific sagittal profiles in finite element modeling may provide valuable insight for biomechanical analyses and targeted treatments.

6.2.2 Introduction

The spine is a vital musculoskeletal system, providing support to the body during day-to-day tasks, allowing trunk movement, and protecting the spinal cord [1], [2]. The spine has an s-shaped curve when visualized in the sagittal plane [3], and this natural curvature permits flexibility and movement. The interplay between the cervical, thoracic, and lumbar curves allows for the human body to efficiently absorb and withstand loads applied to the spine, which is further supported by the spinal musculature [4].

An individual's spinal anatomy is unique, demonstrating variations in their measured curvatures and their body's ability to maintain suitable alignment for optimal biomechanical loading. Despite variations in an individual's spine, there exists a range of acceptable "normal" or "healthy" values for spinal curvature. However, the biomechanics of a healthy spine are not fully understood.

In recent years, there has been increasing interest in the relationship between the curves in the lumbar and thoracic spine segments, as this alignment is critical for sagittal stability. The thoracic spine exhibits kyphotic curvature, with healthy ranges of thoracic kyphosis falling between 10°-40° [5]. The lumbar spine bears the largest relative portion of an individual's upper body weight [6] and exhibits lordotic curvature, which is essential for maintaining biomechanical stability [7]. Healthy ranges of lumbar lordosis are between 40°-60° [5]. Values outside of these ranges are considered "exaggerated" curvatures and are either labeled as "hypo", corresponding to a decrease in the measured curvature, or "hyper", corresponding to an increase in the measured curvature, relative to what is considered normal.

In recent decades, finite element modeling has been used to successfully develop and analyze biomechanical models. Many studies have made important contributions to knowledge regarding the mechanical behavior of the spine [8]–[11]. Geometrically personalized finite element models of the lumbar spine with varying sagittal profiles have demonstrated changes in spinal load-sharing, notably under extension [12]. When considering lifting tasks, lumbar spine models have been used to demonstrate that a slightly straighter spine may reduce the risk of soft tissue injury [13]. In addition, a finite element model of the adolescent thoracic spine has indicated variations in load distribution between kyphotic and hypokyphotic spines [14]. However, there is a gap in the literature regarding the loading effects on the spine when considering the whole spinal column and the impacts of exaggerated spinal curvature.

As such, this study aimed to develop geometrically personalized finite element models of the thoracolumbar spine with respect to sagittal spinal curvature through the comparison of five finite element models. Subsequently, the objective of this study was to evaluate the biomechanical effects that varying spinal curvature have on the load distribution throughout the spine.

6.2.3 Methods

6.2.3.1 Development of finite element models

A previously developed and validated thoracolumbar spine finite element model was leveraged for this study [8]. The spine model consists of the vertebrae and adjacent intervertebral discs (IVDs) from T1 to S1. The model also contains several soft tissues, namely the tendons, thoracolumbar fascia, and various spinal muscles that play a role in stabilizing the spine (multifidus, longissimus, intertransversarius, latissimus dorsi, and psoas major), as seen in Figure 6.2.1. The anatomical bodies that make up the model were acquired from an anatomography database consisting of 3D structures constructed from MRI images of a healthy male volunteer (age: 22 yrs, height: 172.8 cm, weight: 65 kg) [15], [16]. Thus, the model represents healthy male anatomy with normal spinal curvature. The vertebrae, IVDs, tendons, and TLF were modeled from 3mm tetrahedral volumetric elements, while the muscles were fluid-filled volumetric bodies modeled as a shell with 3mm triangular elements [8]. Bonded contacts were used to limit separation and sliding between bodies, and the final model consisted of 371425 elements and 533771 nodes. The material properties of the model are outlined in Table 6.2.1. Cobb's method was used to measure the sagittal curvatures of the initial model, recorded in Table 6.2.2.

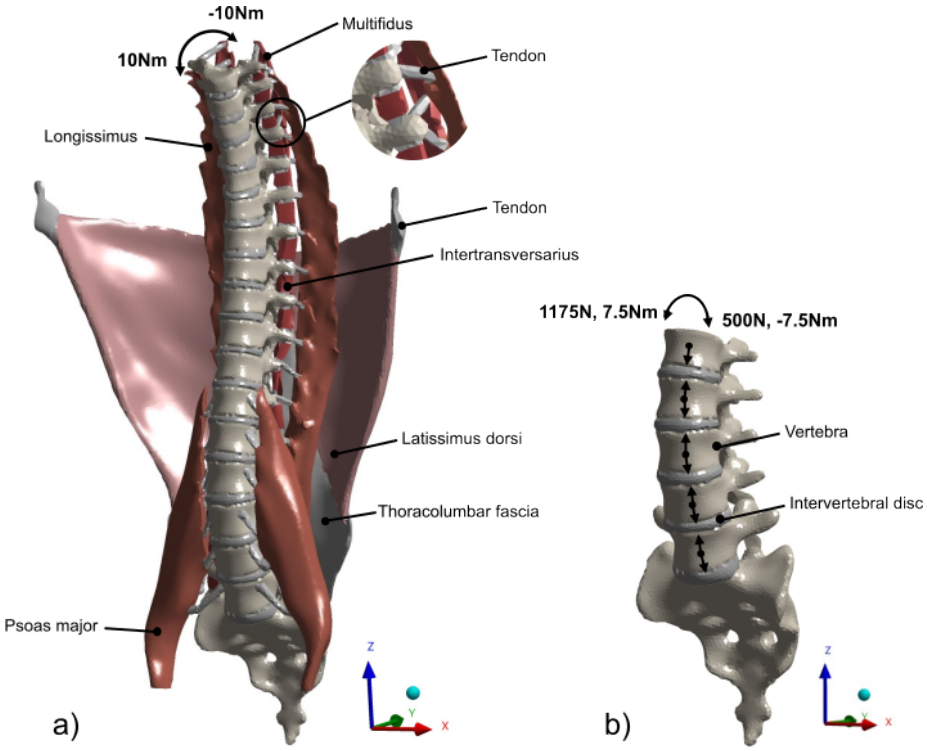

Figure 6.2.1: a) Thoracolumbar and b) lumbar spine models with loading conditions simulating flexion and extension.

Table 6.2.1: Material properties of the spinal structures in the finite element models.

Component	Young's Modulus	Poisson's Ratio
Vertebra	12 GPa [17], [18]	0.3 [17]
Intervertebral disc	13.7 MPa [19]	0.49
Tendon	680 MPa [20]	0.49
Intertransversarius	36.87 kPa [8]	0.49
Multifidus	91.34 kPa [21]	0.49
Longissimus	62.85 kPa [21]	0.49
Latissimus dorsi	36.87 kPa [8]	0.49
Psoas major	55.33 kPa [22]	0.49
Thoracolumbar fascia	450 MPa [23], [24]	0.49

The initial model served as a baseline "Healthy" model for the comparative evaluation in this study, with values for kyphosis and lordosis within the normal ranges as specified in literature. Using ANSYS (2021 R1, Canonsburg, Pennsylvania), the vertebrae were subjected to Structural Displacements to obtain a targeted change in spinal curvature of 50% ±5% with respect to the Healthy model. This technique allows the user to apply a magnitude of displacement vectors to the spine in any direction (x, y, z), displacing the geometric bodies in terms of position and orientation while preserving vertebral anatomy. It also allows the surrounding soft tissues to adapt to the displacement of the vertebrae while maintaining their contacts with the spinal column, thus facilitating the creation of geometrically personalized models. These changes in sagittal profile resulted in four additional models: hypolordotic (HypoL), hyperlordotic (HyperL), hypokyphotic (HypoK), and hyperkyphotic (HyperK). Cobb's method was used to measure the thoracic (T5-T12) and lumbar (L1-S1) angles. Once the targeted curvatures were obtained for each previously described profile, the models were assessed to ensure no abnormal IVD or soft tissue geometry was present. Then, the model solution was imported into a new Static Structural block in ANSYS Workbench, thus creating a model with the desired spinal alignment and absent of residual stresses, as seen in Table 6.2.2. The previously described soft tissues were also included in all thoracolumbar spine models. Following model development, lumbar models consisting of the vertebrae and IVDs from L1 to S1 were created for the Healthy, HypoL, and HyperL models for an additional comparison.

6.2.3.2 Boundary and loading conditions

Each model was assessed through ANSYS Static Structural and was subjected to identical boundary and loading conditions. The models were fixed at the sacrum and the extremities of the tendons attaching to the latissimus dorsi muscles. The lumbar spine models were subjected to a 1175N follower load and 7.5Nm moment to induce flexion, and a 500N follower load and -7.5Nm moment to induce extension [25], [26]. As shown in Figure 6.2.1, the follower load was applied at

Table 6.2.2: Degrees of sagittal curvature in the finite element models, measured using Cobb angle.

	Healthy	**HypoL**	**HyperL**	**HypoK**	**HyperK**
Kyphosis	**23.69**°	22.32°*	27.09°*	11.57°	34.98°
Lordosis	**44.24**°	23.46°	64.29°	40.93°*	49.75°*
Thoracolumbar model**	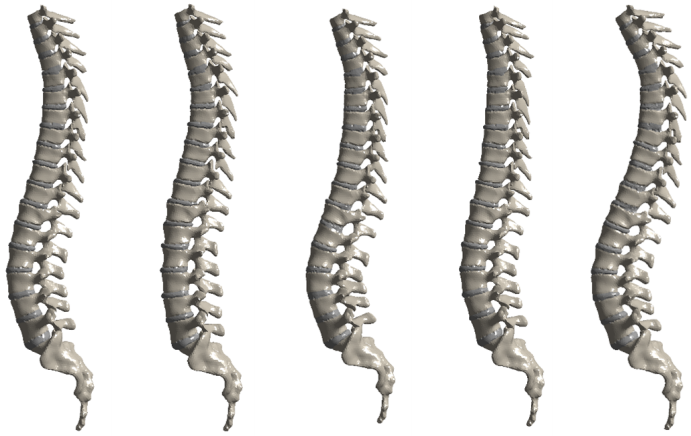				
Lumbar model	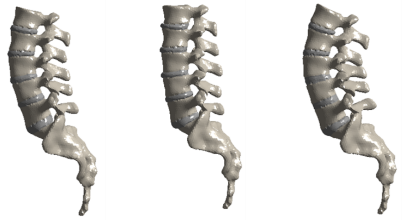			-	-

*Curvature values were kept within 15% of Healthy model values

**Thoracolumbar spine models contain soft tissues. Osseous structures displayed for sagittal curvature visualization.

the center of each vertebral body, while the moment was applied at L1. A follower load accounts for the active contribution of the spinal muscles by acting tangential to the curvature of the spine [7] and has been successfully used in previous studies to demonstrate realistic loading conditions [25], [26]. The thoracolumbar spine models were subject to pure moments at T1 applied in the sagittal plane ranging from 10Nm to -10Nm inducing flexion and extension, respectively, as depicted in Figure 6.2.1.

6.2.3.3 Validation and analysis

To validate and analyze the modeling results, IVD stresses and intersegmental rotations (ISR) were compared to *in vivo*, *ex vivo*, and *in silico* results from previously published literature. The maximum IVD stresses were measured normal to the surface of the disc. ISR were calculated as described by Dvorák et al. [27], by evaluating the relative change in angle of rotation between vertebrae. Following validation, results for IVD stress, change in disc height, vertebral body (VB) stress, and ISR were recorded and compared for each model. Average change in disc height was calculated from the locations of adjacent endplates and VB stresses were determined by the average normal stresses in the body.

A sensitivity analysis was conducted to evaluate the model robustness and accuracy of the presented results. In the first analysis, the mesh size was varied from 3mm to 1mm. In the second analysis, the element type was changed from tetrahedral elements to quadratic hexahedral-dominant elements. For the purpose of comparing the modeling results, the mesh was adjusted in the Healthy lumbar spine model IVDs and was compared to the original model.

6.2.4 Results

6.2.4.1 Lumbar spine models

The Healthy, HypoL, and HyperL lumbar spine models were subjected to a follower load and moment to induce flexion and extension and then IVD stresses were validated against previously published studies for both motions, as seen in Figure 6.2.2. These comparators include an *in silico* study by Dreischarf et al. that compared lumbar spine models [25], an *ex vivo* study by Brinckmann and Grootenboer in which IVDs were subjected to a compressive load (compared 2000N for flexion, 1000N for extension) [28], and lastly, an *in vivo* study conducted by Sato et al. with healthy participants [29]. In flexion, the HypoL model had similar or slightly lower IVD stresses compared to the Healthy model, with the exception of L1/L2, whereas in extension, L1/L2 and L4/L5 had noticeably higher stresses while L5/S1 had lower stresses than the Healthy model. In comparison, the HyperL model had higher IVD stresses than the Healthy model with the exception of L5/S1 in flexion, while the opposite trends were observed in extension.

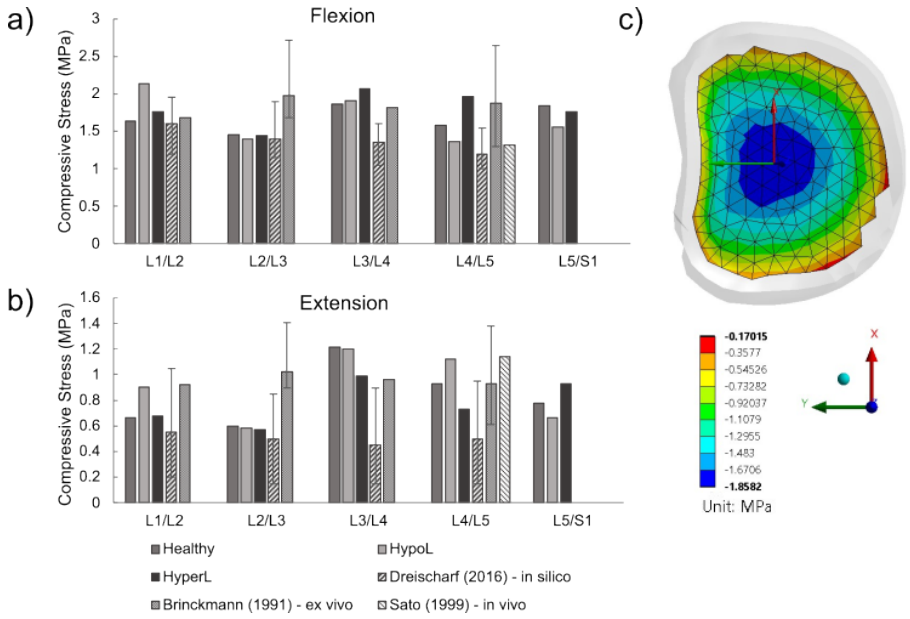

Figure 6.2.2: IVD stress in the lumbar spine models in a) flexion and b) extension compared to median in silico data from Dreischarf et al. [25], ex vivo data from Brinckmann and Grootenboer [28], and in vivo data from Sato et al. [29]. Error bars indicate range. c) L3/L4 IVD stress in the Healthy model under flexion.

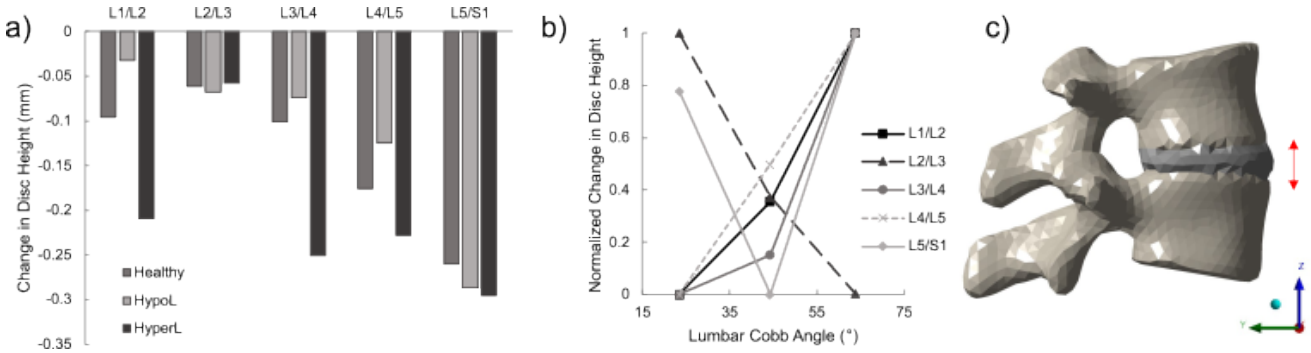

Figure 6.2.3: a) Average change in disc height in the lumbar spine models under flexion. b) Normalized change in disc height with respect to Cobb Angle. c) Change in disc height in the models.

The average change in disc height was evaluated for the lumbar spine models under flexion, as seen in Figure 6.2.3. The HypoL model showed a cumulative reduction in disc height (-50%) with the greatest change observed L3/L4 (-11%), compared to the Healthy model. In comparison, the HypoL model demonstrated a cumulative increase in disc height (16%), with the largest change observed in L1/L2 (31%). In each model, the anterior portion of the disc underwent the greatest change in height.

ISR were evaluated and compared across each lumbar spine model. Although the models slightly underestimated the ISR in the inferior lumbar vertebrae in flexion when validated against the comparator, the trends align with the results presented in the *in vivo* study conducted by Wong et al. on healthy volunteers [30], in which the magnitude of rotation decreased in the lower spinal segments, as seen in Figure 6.2.4. Results demonstrated that the HypoL model was stiffer than the Healthy model in both flexion and extension, demonstrated by reduced ISR. In comparison, the HyperL model was more flexible in flexion, with greater ISR, but stiffer in extension.

VB stress was measured to evaluate the load distribution throughout the spinal column. In flexion, the HypoL model exhibited similar but reduced overall VB stresses compared to the Healthy model, with the greatest reduction observed in L1 (-12%), and the sole increase in VB stress observed in L5 (17%). In extension, this model again displayed reduced VB stresses relative to the Healthy model, as shown in Figure 6.2.5. In comparison, the HyperL model had higher VB stress in both flexion and extension, with the greatest change in VB stress observed in L5 (19% and 14%, respectively), compared to the Healthy model. These results are further supported by the normalized data which indicated that a larger Cobb angle resulted in greater VB stresses, while the inverse was observed for a smaller Cobb angle.

The sensitivity analyses in the lumbar spine model further explored the modeling assumptions and confirmed the accuracy of the results for both flexion and extension. Variations in mesh size results in a maximum deviation in results of 7.4%, 1.7%, and 3.6% for IVD stress, VB stress,

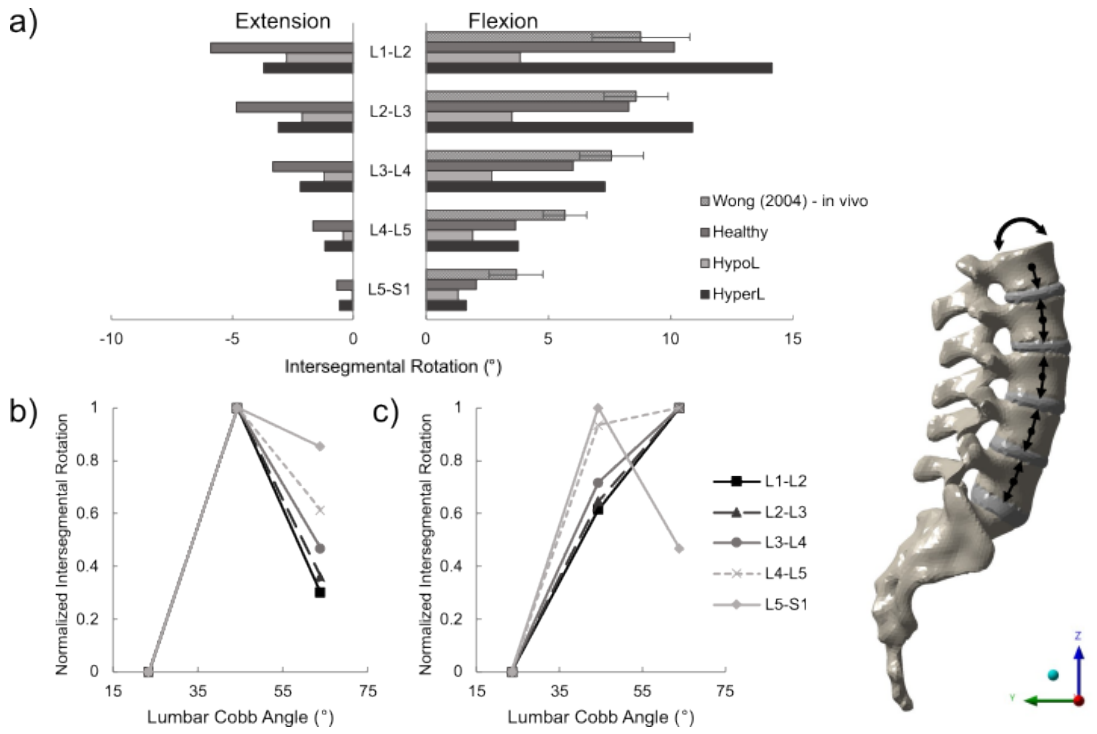

Figure 6.2.4: a) Intersegmental rotation of the lumbar spine models in flexion and extension compared to mean in vivo data by Wong et al. [30]. Error bars indicate standard deviation. Normalized intersegmental rotation with respect to Cobb Angle in b) extension and c) flexion. d) Loading conditions on the lumbar spine models.

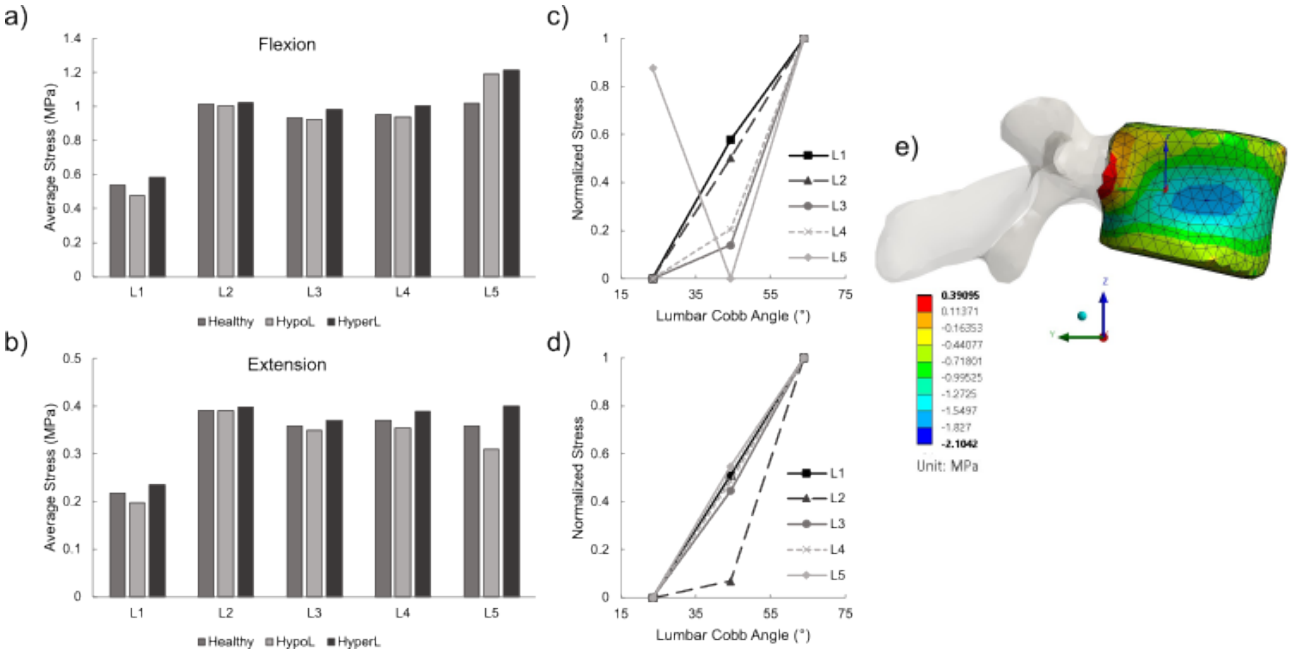

Figure 6.2.5: Average compressive vertebral body stress in the lumbar spine models in a) flexion and b) extension. Normalized compressive stress with respect to Cobb angle in c) flexion and d) extension. e) L3 vertebral body stress in the Healthy model under flexion.

and ISR, respectively. Variations in element type yielded a maximum difference of 10.9%, 2.1%, and 3.0% for IVD stress, VB stress, and ISR, respectively.

6.2.4.2 Thoracolumbar spine models

The thoracolumbar spine models were subjected to moments at T1 simulating flexion and extension. IVD stress in the thoracic region was compared against median *ex vivo* data presented by Wilke et al. [31], which confirmed that the modeling results were within the range of measured values, as shown in Figure 6.2.6. The HyperK model demonstrated reduced IVD stresses compared to the Healthy model in both flexion and extension. This reduction in stress was only observed in extension in the HypoK model, while flexion resulted in similar magnitudes to the Healthy model. Although not presented on the graph, the median thoracic IVD stresses in the HypoL and HyperL models also exhibited similar magnitudes.

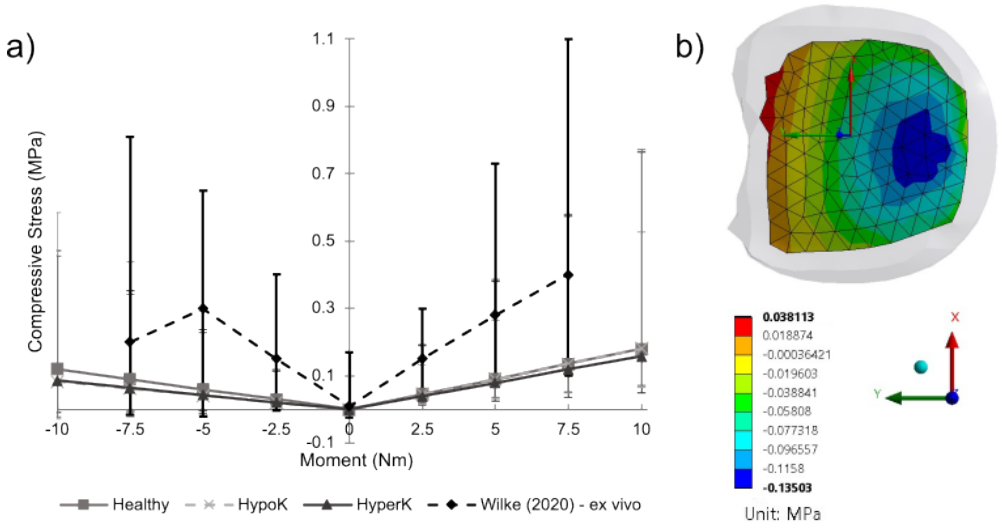

Figure 6.2.6: a) Median IVD stress in the thoracic spine for the Healthy, HypoK, and HyperK thoracolumbar spine models compared to ex vivo data by Wilke et al. [31]. Error bars indicate range. b) T9/T10 IVD stress in the Healthy model under 7.5Nm flexion.

The change in disc height did not show a clear trend in the thoracic region when compared across the five thoracolumbar spine models. However, there was a notable decrease in disc height in the more curved spines (cumulative change in HyperL: -36%, HyperK: -39%) in the lumbar region, as seen in Figure 6.2.7, relative to the Healthy model when evaluated under 7.5Nm flexion. In comparison, increased disc height was observed in the straighter spine models (cumulative change in HypoL: 49%, HypoK: 26%) under 7.5Nm flexion. Similar trends were observed when the models were subjected to a range of moments inducing flexion. Further, it was noted that the anterior disc height demonstrated the largest change, as was observed in the lumbar models.

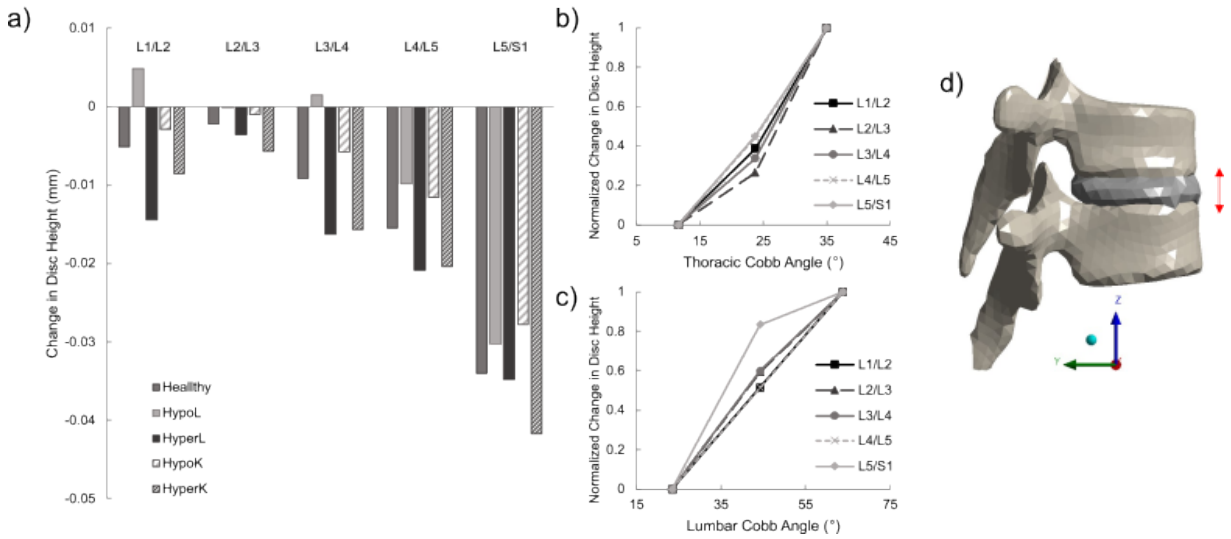

Figure 6.2.7: a) Change in disc height from L1/L2 to L5/S1 in the thoracolumbar spine models under 7.5Nm flexion. Normalized change in disc height with respect to the cobb angle in the b) thoracic and c) lumbar regions. d) Change in disc height in the models.

ISR was evaluated for all models and compared to *ex vivo* data recorded from thoracic cadaveric specimens by Sis et al. [32], as seen in Figure 6.2.8. Results demonstrated that the HypoL, HyperL, and HypoK models had markedly reduced ISR in the upper thoracic segments, whereas the HyperK model had reduced ISR in the lower segments. Further, the normalized data demonstrated that the Healthy model has the highest range of motion when considering variations in both the thoracic and lumbar curvatures.

The trends for VB stress were compared to the Healthy model when considering the upper (T1-T4), mid (T5-T8), lower (T9-T12) thoracic regions and the lumbar (L1-L5) region. The HypoL model showed slightly greater cumulative VB stresses in the mid-thoracic region (4%) but reduced VB stresses in the lower thoracic (-1%) and lumbar regions (-1%). The HypoK model had augmented stress magnitudes in the mid (5%) and lower thoracic regions (6%), but reduced magnitudes in the lumbar region (-2%). In comparison, the HyperL model yielded greater VB stresses in the mid thoracic (58%), lower thoracic (2%) and lumbar regions (6%). Lastly, the HyperK model had reduced stresses in the lower thoracic region (-3%), but notable increases in magnitude in the mid thoracic (30%) and lumbar regions (13%). Overall, the straighter spine models had comparable cumulative VB stresses relative to the Healthy model (HypoL: -1%, HypoK: 2%), while the cumulative VB stresses in the more curved spines was augmented (HyperL: 15%, HyperK: 13%). The results, seen in Figure 6.2.9, represent the measured stress under 7.5Nm flexion, however, similar trends were observed when the models were subjected to a range of moments applied at T1.

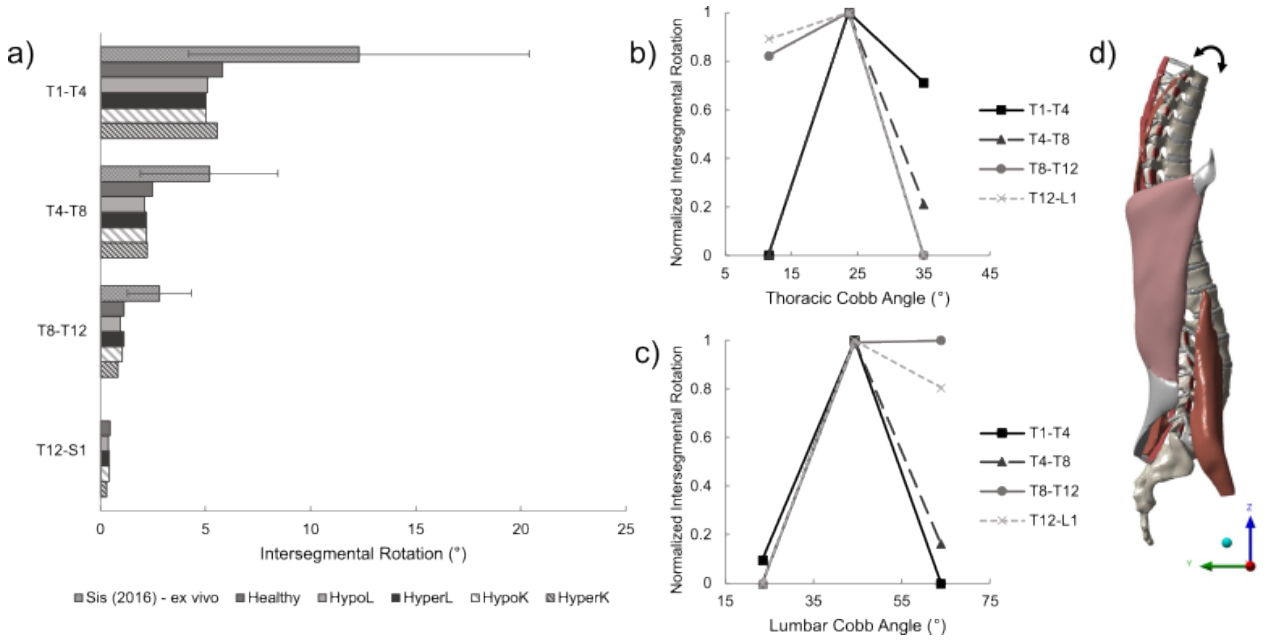

Figure 6.2.8: a) Intersegmental rotation of the thoracolumbar spine models under 5Nm flexion-extension compared to mean in vivo data by Sis et al. [32]. Error bars indicate standard deviation. Normalized intersegmental rotation with respect to Cobb angle in the b) thoracic and c) lumbar regions. d) Loading conditions on the thoracolumbar spine models.

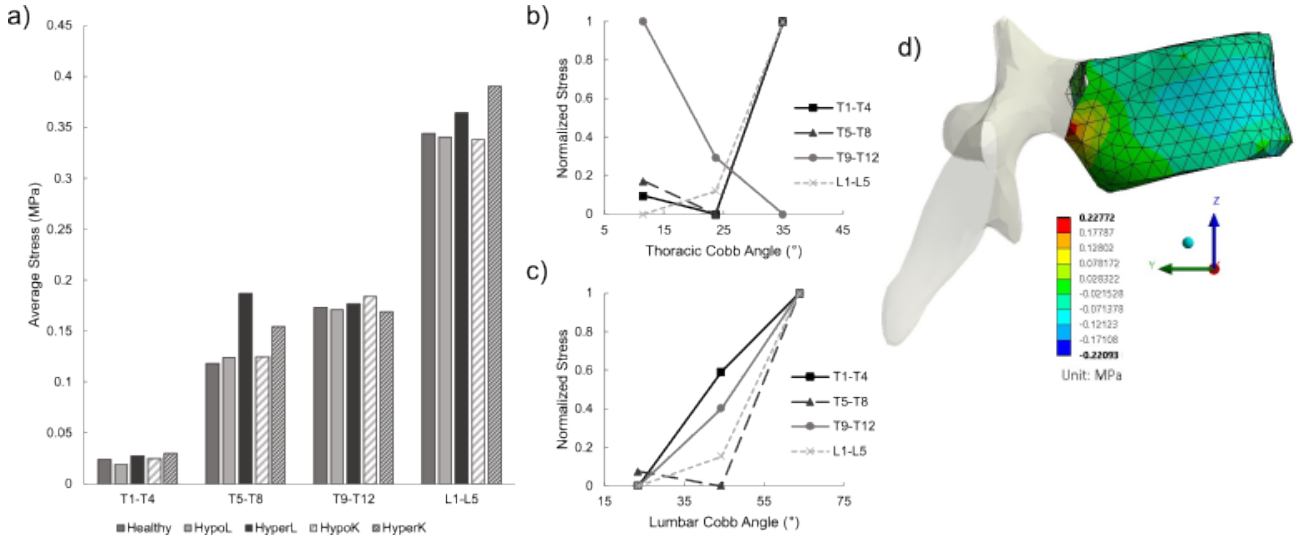

Figure 6.2.9: a) Vertebral body stress in the thoracolumbar spine models under 7.5Nm flexion, in the upper (T1-T4), mid (T5-T8), and lower (T9-T12) thoracic and lumbar (L1-L5) regions. Normalized vertebral body stress with respect to Cobb angle in the b) thoracic and c) lumbar regions. d) T9 vertebral body stress in the Healthy model under flexion.

6.2.5 Discussion

Understanding the effects that spinal curvature has on an individual's ability to maintain optimal posture is challenging. Several factors may affect an individual's spinal alignment, such as weight, height, personalized material properties, growth, age, and the development or progression of various spinal disorders, among others. This study focused on the effects that geometric spinal alignment may have on the overall stress distribution throughout the spine. Both the lumbar and thoracolumbar spine models revealed differences in load distribution throughout the spine as sagittal curvature was varied.

The lumbar models demonstrated that a decrease in lordosis primarily resulted in reduced stresses when compared to "normal" lordotic curvature, while the opposite was observed for an increase in lordosis. The trends for IVD stress were aligned with those presented in Naserkhaki et al.'s study [12]. The HypoL model resulted in lower disc stresses in flexion, while the majority of the discs exhibited higher stresses in extension, compared to the Healthy model. Further, this model demonstrated a reduced range of motion under both loading scenarios. In comparison, the HyperL model demonstrated higher IVD stresses in flexion but reduced magnitudes in extension, compared to the Healthy model, and the same trends were observed for the range of motion. To add, similar observations were recorded for the lumbar models when evaluating VB stress. These results indicate that the straighter spine may work to enforce spinal stability and reduce stress throughout the spinal column, as the IVDs were found to undergo minimal disc compression.

In the thoracolumbar models, variations in sagittal alignment once again affected the range of motion and stress distribution throughout the spine. ISR results demonstrated that the range of motion was greatest for healthy curvatures. Although the observed increase in disc height in the HypoL model was unexpected, the global trends demonstrated that there is a smaller decrease in disc height when the spines have reduced curvatures, similar to the trends observed in the lumbar models. Further, the measured VB stresses corroborate this point, as the greatest stresses were observed in the spines with increased curvature (HyperL and HyperK), indicating that the straighter spines may function to protect the spinal column and ensure stability with greater effectiveness than the more curved models. Nonetheless, the overall trends for VB stresses demonstrated that the exaggerated curvature models generally had greater VB stresses in the thoracic regions, whereas only the hyper-curved models showed this increase in magnitude in the lumbar region, relative to the Healthy model. Further studies with additional loading conditions, such as gravitational loads and muscular forces, may provide added insight for the thoracolumbar spine models.

While variations in curvature have been found to be a potential cause of back pain and various spinal disorders, there is a lack of consensus regarding the influence that spinal alignment

has on back pain. Some authors suggest that a decrease in the lordotic angle provides a more optimal position for biomechanical loading, thus reducing the risk of back pain, whereas an increase augments this risk [33]. In comparison, other authors suggest that a loss of lordosis may cause a shift in the sagittal spinal alignment, thus leading to degenerative changes and back pain [34]. This finite element study found that the straighter spine models had greater disc heights and lower lumbar VB stresses, conversely, the more curved spines demonstrated inverse trends, with reduced disc heights and larger VB stresses. This indicates that the latter may be subjected to greater stresses, causing the discs to undergo amplified compression, which may be indicative of disc degeneration if a patient is subjected to continuous disc compression over a period of time.

However, the question remains if the normal Cobb angles identified in literature provide optimal support and stability to the spine. The sagittal alignment of the spine influences load distribution, but the range of kyphosis and lordosis in any given individual is considerable, therefore making it challenging to define what is "normal" [35]. This study highlighted some important findings regarding the spinal load distribution outcomes under varying sagittal profiles. Considering the thoracolumbar spine model, the VB stresses were minimal and the ISR were maximal in the Healthy model. However, in both the thoracolumbar and lumbar spine models, the change in disc height was lessened in the straighter spines. Thus, the findings in this study suggest that while an individual's sagittal profile in the normal range may be ideal for biomechanical loading and day-to-day tasks, a straighter spine may protect the spine through reduced disc compression, therefore lessening pain caused by compressed IVDs and nerves. However, although possibly alleviating mechanistically imposed back pain, the straighter spine produced a trade-off of limiting the range of motion under both flexion and extension.

There are several limitations that should be considered for this study. The modeled spine components were assumed to have linear elastic and isotropic material properties. Although human tissues are anisotropic and viscoelastic, the implementation of less complex properties allowed for the models to be solved rapidly while still providing accurate and validated results. Additional studies could consider nonlinear material properties for the tissues or biphasic properties for the discs. To add, the models are representative of the anatomy of a young, healthy male. Further, the targeted sagittal curvatures were identified based on the range of ideal Cobb angles specified in literature. Future studies may investigate if age or biological sex influences spinal alignment and biomechanical loading, and may consider implementing patient-specific curvature values to corroborate the presented results. In addition to age and sex, torso position (supine vs standing), weight, and height may impact these results, and should be considered in future studies as these parameters are known to influence sagittal profiles. Despite these simplifications and assumptions,

the comparison between models with different curvatures provides valuable insight into trends that may occur in patients with varying sagittal profiles.

To conclude, to the authors' knowledge, this is the first study to evaluate the changes in stress distribution in finite element models with varying sagittal curvatures when considering the full thoracolumbar spine. This study offers an adaptive technique for modeling, allowing a baseline "healthy" model to be easily adjusted to represent patient-specific sagittal profiles. Further, the results highlight the importance of implementing accurate curvature when using modeling to guide patient-specific treatments, as variations in sagittal alignment may provide insight into areas of greatest stress concentrations.

6.2.6 Funding

This research was supported by McGill University (MEDA), the Fonds de Recherche du Québec – Nature et Technologies (FRQNT), and the Natural Sciences and Engineering Research Council (NSERC).

6.2.7 References

[1] G. D. Cramer, "Chapter 2 - general characteristics of the spine," in *Clinical anatomy of the spine, spinal cord, and ANS*. Elsevier Health Sciences, 2014, pp. 15–64.

[2] T. R. Oxland, "Fundamental biomechanics of the spine—what we have learned in the past 25 years and future directions," *Journal of Biomechanics*, vol. 49, no. 6, pp. 817–832, 2016.

[3] F. Galbusera, "The spine: Its evolution, function, and shape," in *Biomechanics of the Spine: basic concepts, spinal disorders and treatments*. Elsevier, 2018, pp. 3–9.

[4] R. Vialle, N. Levassor, L. Rillardon, A. Templier, W. Skalli, and P. Guigui, "Radiographic analysis of the sagittal alignment and balance of the spine in asymptomatic subjects," *Journal of Bone and Joint Surgery*, vol. 87, no. 2, pp. 260–267, 2005.

[5] P. R. Loughenbury, A. I. Tsirikos, and N. W. Gummerson, "Spinal biomechanics–biomechanical considerations of spinal stability in the context of spinal injury," *Orthopaedics and Trauma*, vol. 30, no. 5, pp. 369–377, 2016.

[6] H. Singh, G. C. Chang Chien, and R. Bolash, "Anatomy of the spine," in *Treatment of Chronic Pain Conditions: A Comprehensive Handbook*. Springer, 2017, pp. 11–20.

[7] A. G. Patwardhan, R. M. Havey, K. P. Meade, B. Lee, and B. Dunlap, "A follower load increases the load-carrying capacity of the lumbar spine in compression," *Spine*, vol. 24, no. 10, pp. 1003–1009, 1999.

[8] I. El Bojairami, K. El-Monajjed, and M. Driscoll, "Development and validation of a timely and representative finite element human spine model for biomechanical simulations," *Scientific Reports*, vol. 10, no. 1, pp. 1–15, 2020.

[9] A. Rohlmann, T. Zander, M. Rao, and G. Bergmann, "Applying a follower load delivers realistic results for simulating standing," *Journal of Biomechanics*, vol. 42, no. 10, pp. 1520–1526, 2009.

[10] A. C. Jones and R. K. Wilcox, "Finite element analysis of the spine: Towards a framework of verification, validation and sensitivity analysis," *Medical Engineering & Physics*, vol. 30, no. 10, pp. 1287–1304, 2008.

[11] M. Fagan, S. Julian, and A. Mohsen, "Finite element analysis in spine research," *Proceedings of the institution of mechanical engineers, part h: journal of engineering in medicine*, vol. 216, no. 5, pp. 281–298, 2002.

[12] S. Naserkhaki, J. L. Jaremko, and M. El-Rich, "Effects of inter-individual lumbar spine geometry variation on load-sharing: Geometrically personalized finite element study," *Journal of Biomechanics*, vol. 49, no. 13, pp. 2909–2917, 2016.

[13] A. Shirazi-Adl and M. Parnianpour, "Effect of changes in lordosis on mechanics of the lumbar spine-lumbar curvature in lifting," *Clinical Spine Surgery*, vol. 12, no. 5, pp. 436–447, 1999.

[14] R. M. C. Aroeira, A. E. M. Pertence, D. T. Kemmoku, and M. Greco, "The effect of hypokyphosis on the biomechanical behavior of the adolescent thoracic spine," *Journal of the Brazilian Society of Mechanical Sciences and Engineering*, vol. 40, no. 3, pp. 1–10, 2018.

[15] N. Mitsuhashi, K. Fujieda, T. Tamura, S. Kawamoto, T. Takagi, and K. Okubo, "Bodyparts3d: 3d structure database for anatomical concepts," *Nucleic Acids Research*, vol. 37, no. suppl_1, pp. D782–D785, 2009.

[16] T. Nagaoka, S. Watanabe, K. Sakurai, *et al.*, "Development of realistic high-resolution whole-body voxel models of japanese adult males and females of average height and weight, and application of models to radio-frequency electromagnetic-field dosimetry," *Physics in Medicine & Biology*, vol. 49, no. 1, p. 1, 2003.

[17] M. Kurutz, *Finite element modelling of human lumbar spine*. Citeseer, 2010.

[18] D. T. Reilly and A. H. Burstein, "The elastic and ultimate properties of compact bone tissue," *Journal of Biomechanics*, vol. 8, no. 6, pp. 393–405, 1975.

[19] B. D. Stemper, D. Board, N. Yoganandan, and C. E. Wolfla, "Biomechanical properties of human thoracic spine disc segments," *Journal of Craniovertebral Junction and Spine*, vol. 1, no. 1, p. 18, 2010.

[20] G. N. Onambélé, K. Burgess, and S. J. Pearson, "Gender-specific in vivo measurement of the structural and mechanical properties of the human patellar tendon," *Journal of Orthopaedic Research*, vol. 25, no. 12, pp. 1635–1642, 2007.

[21] S. R. Ward, A. Tomiya, G. J. Regev, *et al.*, "Passive mechanical properties of the lumbar multifidus muscle support its role as a stabilizer," *Journal of Biomechanics*, vol. 42, no. 10, pp. 1384–1389, 2009.

[22] G. J. Regev, C. W. Kim, A. Tomiya, *et al.*, "Psoas muscle architectural design, in vivo sarcomere length range, and passive tensile properties support its role as a lumbar spine stabilizer," *Spine*, vol. 36, no. 26, E1666–E1674, 2011.

[23] K. El-Monajjed and M. Driscoll, "Investigation of reaction forces in the thoracolumbar fascia during different activities: A mechanistic numerical study," *Life*, vol. 11, no. 8, p. 779, 2021.

[24] L. Yahia, P. Pigeon, and E. DesRosiers, "Viscoelastic properties of the human lumbodorsal fascia," *Journal of Biomedical Engineering*, vol. 15, no. 5, pp. 425–429, 1993.

[25] M. Dreischarf, T. Zander, A. Shirazi-Adl, *et al.*, "Comparison of eight published static finite element models of the intact lumbar spine: Predictive power of models improves when combined together," *Journal of Biomechanics*, vol. 47, no. 8, pp. 1757–1766, 2014.

[26] A. Rohlmann, T. Zander, M. Rao, and G. Bergmann, "Realistic loading conditions for upper body bending," *Journal of Biomechanics*, vol. 42, no. 7, pp. 884–890, 2009.

[27] J. Dvořák, M. Panjabi, D. Chang, R. Theiler, and D. Grob, "Functional radiographic diagnosis of the lumbar spine: Flexion–extension and lateral bending," *Spine*, vol. 16, no. 5, p. 562, 1991.

[28] P. Brinckmann and H. Grootenboer, "Change of disc height, radial disc bulge, and intradiscal pressure from discectomy an in vitro investigation on human lumbar discs," *Spine*, vol. 16, no. 6, pp. 641–646, 1991.

[29] K. Sato, S. Kikuchi, and T. Yonezawa, "In vivo intradiscal pressure measurement in healthy individuals and in patients with ongoing back problems," *Spine*, vol. 24, no. 23, p. 2468, 1999.

[30] K. W. Wong, J. C. Leong, M.-k. Chan, K. D. Luk, and W. W. Lu, "The flexion–extension profile of lumbar spine in 100 healthy volunteers," *Spine*, vol. 29, no. 15, pp. 1636–1641, 2004.

[31] H.-J. Wilke, A. Herkommer, K. Werner, and C. Liebsch, "In vitro analysis of the intradiscal pressure of the thoracic spine," *Frontiers in Bioengineering and Biotechnology*, vol. 8, p. 614, 2020.

[32] H. L. Sis, E. M. Mannen, B. M. Wong, *et al.*, "Effect of follower load on motion and stiffness of the human thoracic spine with intact rib cage," *Journal of Biomechanics*, vol. 49, no. 14, pp. 3252–3259, 2016.

[33] M. Caglayan, O. Tacar, A. Demirant, *et al.*, "Effects of lumbosacral angles on development of low back pain," *Journal of Musculoskeletal Pain*, vol. 22, no. 3, pp. 251–255, 2014.

[34] P. Roussouly, S. Gollogly, E. Berthonnaud, and J. Dimnet, "Classification of the normal variation in the sagittal alignment of the human lumbar spine and pelvis in the standing position," *Spine*, vol. 30, no. 3, pp. 346–353, 2005.

[35] P. Stagnara, J. C. De Mauroy, G. Dran, *et al.*, "Reciprocal angulation of vertebral bodies in a sagittal plane: Approach to references for the evaluation of kyphosis and lordosis," *Spine*, vol. 7, no. 4, pp. 335–342, 1982.

6.3 Summary

Sagittal alignment plays an important role in the development and progression of back pain. Magnitudes of sagittal curvature outside of the "normal" range may lead to various spinal disorders and pain. As such, studying the biomechanical effects of variations in profile may provide valuable insight, from a mechanistic view. This chapter used FEA to successfully develop and assess several thoracolumbar spine models with irregular spinal alignment. Further, a method of adjusting geometric spinal alignment was described, which may facilitate the customization of an existing model to accurately represent patient-specific profiles.

It was hypothesized that differences in sagittal curvature would affect the stress distributions throughout the spinal column. The results of this objective indicated that there is a notable difference in the spinal stress distribution when sagittal curvature is varied. More specifically, the spine models with hyper-curved segments resulted in the largest stress magnitudes and greatest disc compression relative to the model with "healthy" curvature. Meanwhile, the straighter spine models also demonstrated augmented VB stresses relative to the "healthy" model, although this increase was minimal, while additionally reducing disc compression. The "healthy" spine model had the largest range of motion and lowest overall stress magnitudes, indicating that this alignment may indeed be ideal for avoiding the development of spinal disorders and pain.

Despite the individual findings concerning varying sagittal curvatures, this study highlights the importance of incorporating accurate spinal profiles in biomechanical models, as the modelling results may point to areas of augmented stress in individual patients. To add, the techniques outlined in this chapter may permit customized models to be created to evaluate an individual's optimal alignment, which may assist in guiding targeted treatments. However, this FE study used a single spine model for which the sagittal profiles were adjusted. As described in Section 2.1, there is notable variation in spinal anatomy between patients. The findings provided from FEAs may further be strengthened when considering additional variables for patient-specific biomechanical analyses, such as geometry and weight.

7 Retrospective study of magnetic resonance images for patient-specific finite element analysis

7.1 Framework for Article 4

The assessment of spinal curvature, in both the coronal and sagittal planes, is an important part of patient evaluation for LBP. Utilizing both physical assessments and imaging technologies allows clinicians to determine the health status of patients or to identify various diseases and disorders. When considering spinal evaluations, MRI is an important and useful imaging modality that permits physicians to evaluate a patient's spinal column. As outlined in Section 2.6, MRI provides the ability to visualize and gain an understanding of IVD health and various spinal abnormalities, such as endplate changes, vertebral body fractures, or tumors, among others. This technology can also be used to assess spinal alignment, as irregular curvature has been identified as a potential indicator of back pain. As such, the information obtained from MRI can provide valuable insight into a patient's spinal health.

This objective aimed to combine the approaches and findings of Objective 1 (Section 5) and Objective 2 (Section 6) while developing and analysing patient-specific spine FEMs. The models were developed using patient MRI data for VB geometry and sagittal profile. Each model represented the lumbar spine, consisting of the vertebrae, IVDs, tendons, multifidus, longissimus, and TLF, which were modelled as volumetric bodies.

Thanks are given to Dr. John C. Benson and Dr. Christin A. Tiegs-Heiden from Mayo Clinic for supplying the MRI data for this study and for providing a clinical perspective when analysing the results. A special thank you is extended to Emilie Davignon for her assistance in collecting the MRI measurements. Lastly, thanks are given to the Biostatistics Consulting Unit at the Montreal General Hospital for their assistance with the statistical analysis.

The findings of Objective 3 and Hypothesis 3 are detailed in the manuscript below, titled "Patient-specific lumbar spine modeling of healthy and back pain individuals: a retrospective study." The contribution of the first author is considered to be 75% for data collection and processing, modelling, and manuscript writing. The contribution of the last author is considered to be 15% for research guidance and manuscript review. The remaining co-authors are considered to have contributed 10% for supplying the patient data and manuscript review. The manuscript was submitted to *Journal of Biomechanics* by Elsevier on August 30, 2023.

7.2 Article 4: Patient-specific lumbar spine modeling of healthy and back pain individuals: a retrospective study

Brittany Stott[1,2], John C. Benson[3], Christin A. Tiegs-Heiden[4], Mark Driscoll[1,2]

[1]Musculoskeletal Biomechanics Research Lab, Department of Mechanical Engineering, McGill University, Montreal, QC, Canada

[2]Orthopaedic Research Lab, Montreal General Hospital, Montreal, QC, Canada

[3]Neuroradiology, Department of Radiology, Mayo Clinic, Rochester, Minnesota, USA

[4]Musculoskeletal Radiology, Department of Radiology, Mayo Clinic, Rochester, Minnesota, USA

Address for notification, correspondence, and reprints:

Mark Driscoll, Ph.D., P.Eng.

Associate Professor, Department of Mechanical Engineering

Canada NSERC Chair Design Eng. for Interdisciplinary Innovation of Medical Technologies

Associate Member, Biomedical Engineering

Associate Member, Department of Surgery

Investigator, Research Institute MUHC, Injury Repair Recovery Program

McGill University, Department of Mechanical Engineering

817 Sherbrooke St. West, Montreal, QC H3A 0C3, Canada

Macdonald Eng. Bldg., office #153

T: +1 (514) 398-6299

F: +1 (514) 398-7365

E-mail: mark.driscoll@mcgill.ca

7.2.1 Abstract

Background: Low back pain (LBP) is a common affliction that remains a challenge to diagnose. Consequently, imaging technologies are used to visualize spinal alignment and disorders. With the growing acceptance of finite element models (FEMs) for clinical insight, leveraging patient images for biomechanical modeling may provide valuable information for virtual clinical trials. This study aimed to assess the sagittal profile of healthy and LBP patients through magnetic resonance imaging (MRI) and to use these images to guide biomechanical analysis through patient-specific modeling.

Methods: MRI was used to evaluate the sagittal profile of 109 participants (58 healthy, 51 LBP patients). From these images, twelve patients were randomly selected for a blind retrospective study for patient-specific modeling of the lumbar spine. The models consisted of the vertebrae, intervertebral discs (IVDs), and surrounding muscles from L1-S1 and were subjected to body weight loading conditions simulating flexion. Stresses in the IVDs and vertebral bodies, as well as intersegmental rotation, were compared across models.

Results: MRI results demonstrated that the LBP cohort had reduced sagittal curvatures compared to the control group. From the biomechanical analysis, the LBP models had greater IVD stresses compared to the healthy models, while the female models were subjected to greater stresses compared to the male models.

Conclusion: This study demonstrates the potential of using MRI images to guide retrospective analysis of spine biomechanics using FEMs. Further, the results highlight the role that spine geometry and alignment play in stress distribution and the need to leverage patient-specific data in biomechanical studies.

7.2.2 Introduction

Low back pain (LBP) is a leading cause of disability worldwide. Between 1990 and 2015, years lived with disability caused by LBP increased by 54%, which can primarily be attributed to the global growth and aging of the population [1]. In particular, individuals with abnormal spinal alignment may have higher rates of LBP. Several studies have observed that LBP patients display attenuated lordotic curvature compared to healthy individuals [2], [3]. However, there are contradicting views on if reduced lordosis is a cause of LBP, or if these patients maintain a straighter spine as a coping mechanism to alleviate pain [3], [4]. There is need for continued study of the significance of sagittal alignment.

With the growing use and acceptance of *in silico* studies for virtual clinical trials and regulatory approval [5], there is a need for finite element models (FEMs) to illustrate a variety of patient demographics. Finite element analysis is a numerical technique that can be used to model the biomechanical behavior of biological systems. Studies have used FEMs to evaluate lumbar spines with hypolordotic, hyperlordotic, and normal curvatures and have found variations in stress distribution with changing profiles [6], [7]. When assessing lifting tasks, lumbar spine models demonstrated that adopting a slightly straighter spine during lifting may reduce the risk of soft tissue injury, however, higher risks may occur if too flattened [8]. Although these models have provided valuable insight into loading scenarios for a general population, retrospective studies may provide additional patient-specific knowledge. Despite the availability of patient data for retrospective analyses, this approach has seldom been used for spine modeling [9]. To the authors' knowledge, a study evaluating the biomechanics in the lumbar spine considering the sagittal profiles for healthy and LBP patients has not been conducted.

As such, the objectives of this study were two-fold. First, magnetic resonance imaging (MRI) of healthy and LBP patients was used to assess variations in lumbar sagittal alignment. Second, a blind, retrospective study was conducted using the MRI data to develop patient-specific FEMs to evaluate biomechanical variations between cohorts.

7.2.3 Methods

7.2.3.1 Magnetic Resonance Images

Anonymized patient data, MRIs, and ethical approval were provided by Mayo Clinic (IRB no. 20-010796). The selection initially consisted of 205 patients, with a minimum age requirement of 30 years at the time of imaging. Exclusion criteria included surgical intervention, scoliosis greater than 10° measured in the coronal plane, disc degeneration of grade 4 or 5 on the Pfirrmann grading scheme [10], and spinal abnormalities, such as tumors or severe vertebral body (VB) fractures, resulting in 109 subjects (age: 52.92±14.3 years, range: 31-86 years; weight: 71.96±16.17

Table 7.2.1: Summary of participant data, presented as mean ± standard deviation.

	Male Participants			Female Participants			All Participants		
	Control	LBP	Total	Control	LBP	Total	Control	LBP	Total
Patients, *n*	32	25	57	26	26	52	58	51	109
Age (years)	56.72±14.21	49.56±16.20	53.57±15.53	56.27±13.81	48.12±10.01	52.19±12.73	56.51±14.16	48.82±13.56	52.92±14.35
Weight (kg)	83.62±10.41	82.38±10.26	83.08±10.36	61.27±14.95	58.25±7.41	59.76±11.89	73.60±16.98	70.08±15.15	71.96±16.17
Height (m)	1.79±0.07	1.77±0.05	1.78±0.06	1.64±0.07	1.66±0.07	1.65±0.07	1.72±0.10	1.71±0.09	1.72±0.09

kg; height: 1.72±0.09 m). Control subjects were identified as individuals who did not currently have LBP, while LBP subjects were identified as patients suffering from chronic LBP. Descriptive participant information is outlined in Table 7.2.1. Using T2-weighted images, L4 VB cross-sectional area (CSA) was evaluated on axial images using the formula $CSA = \pi \times \frac{width}{2} \times \frac{depth}{2}$ [11]. Mid-sagittal images were selected to measure sagittal profile and L4 VB height, calculated as the mean of the anterior and posterior heights [12]. Two raters performed Cobb angle measurements for lumbar lordosis (L1-L5, L1-S1), as well as measurements for lumbosacral angle (LSA) and lumbosacral joint angle (LSJA). The methodology for MRI measurements is detailed in Figure 7.2.1.

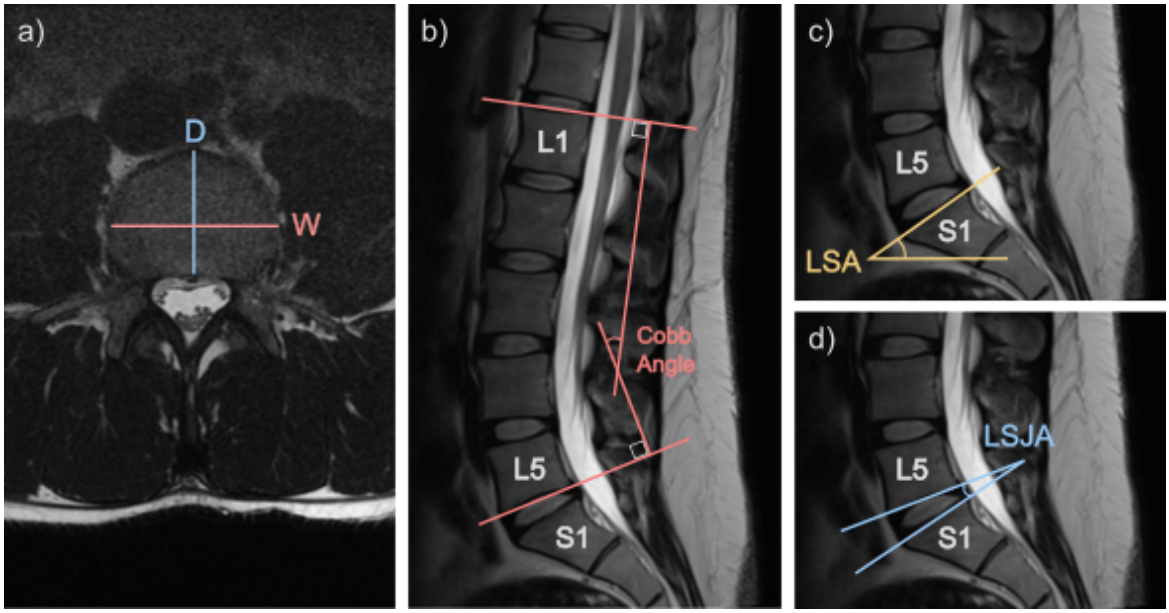

Figure 7.2.1: Magnetic resonance image measurements for a) vertebral body width (W) and depth (D), b) Cobb angle (L1-L5), c) lumbosacral angle (LSA), and d) lumbosacral joint angle (LSJA).

Statistical analyses of the MRI measurements were conducted using SAS Studio (v3.8, SAS Institute, Cary, North Carolina). A non-parametric Mann-Whitney U test was completed, where $p<0.05$ was deemed statistically significant and $p<0.1$ was considered approaching significance. The data was disaggregated based on sex and cohort (control versus LBP). Interrater reliability

was evaluated by calculating the intraclass correlation coefficient (ICC) for each sagittal profile measurement in Python (v3.11.3, Python Software Foundation, Beaverton, Oregon).

7.2.3.2 Finite Element Modeling

A previously developed lumbar spine FEM was leveraged for this study [7], [13]. The model consisted of the vertebrae and intervertebral discs (IVDs) from L1-S1. Passive tissues including the thoracolumbar fascia, multifidus, and longissimus muscles were connected to the model with tendons, shown in Figure 7.2.2a). All components were modeled as volumetric bodies with 3 mm tetrahedral elements, connected by bonded contacts to dissuade separation or slippage between bodies. Material properties are outlined in Table 7.2.2. The model development, validation, and analysis were conducted using ANSYS (2022 R2, Canonsburg, Pennsylvania).

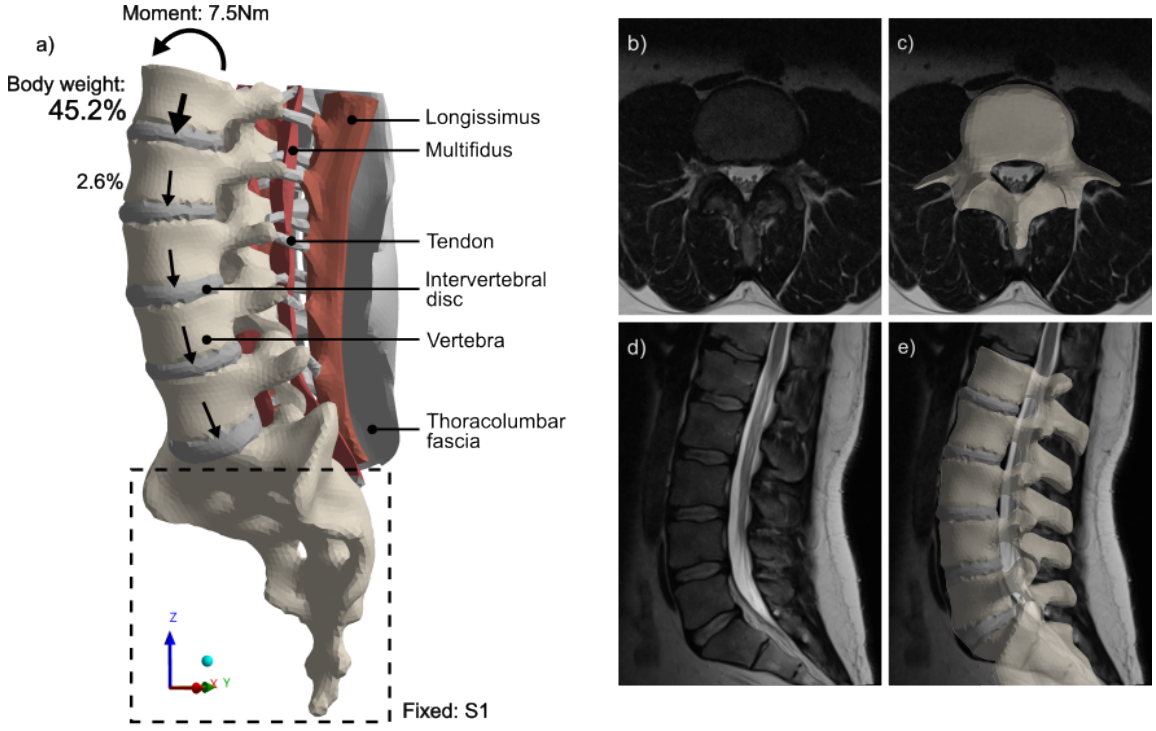

Figure 7.2.2: a) Finite element model of the lumbar spine (L1-S1) with boundary and loading conditions. Comparison of the patient MRI and FEM in b)-c) the axial plane for the L4 vertebra, and d)-e) the sagittal plane for L1-S1.

A blind, retrospective study was conducted by anonymously assigning numbers to each patient using a random number generator and sorting the patients based on assigned values. The first twelve patients were selected for biomechanical analysis: six patients per cohort and equally distributed for each sex. The dimensions for VB CSA and height were used to scale the initial model in order to develop patient-specific FEMs in SpaceClaim (2022 R2, ANSYS) and Blender (v.3.1.2,

Table 7.2.2: Material properties for the lumbar spine models, with male (M) and female (F) properties where available.

Component	Young's Modulus	Poisson's Ratio
Vertebra	12 GPa [14], [15]	0.3 [14]
Intervertebral disc	M: 13.7 MPa [16] F: 16.6 MPa	0.49
Tendon	M: 680 MPa [17] F: 610 MPa	0.49
Thoracolumbar fascia	450 MPa [18], [19]	0.49
Multifidus	91.34 kPa [20]	0.49
Longissimus	62.85 kPa [20]	0.49

Amsterdam, Netherlands) with variations in L4 model geometry not exceeding 1.4% of the MRI measurements for each patient. Sagittal curvature was adjusted to agree with the MRI measurements for Cobb angles, LSA, and LSJA. To obtain the desired curvature, Structural Displacements were applied to the vertebrae in ANSYS. This permitted controlled application of displacement vectors to realign the spine while preserving vertebra anatomy. Further, it allowed the surrounding soft tissues to adapt to the vertebrae displacements while maintaining their orientation and contact. Once the desired sagittal profile was obtained, the model solution was imported into a new Static Structural component in ANSYS Workbench, creating a geometrically personalized model absent of residual stresses. The models' sagittal profile measurements were within 3° of the measured MRI data for each patient. An example of one of the personalized lumbar spine FEMs compared to the patient magnetic resonance images can be seen in Figure 7.2.2.

The models were fixed at S1 and were subjected to a follower load and moment to induce flexion, shown in Figure 7.2.2. A follower load acts tangential to the curvature of the spine and accounts for the active contribution of the muscles [21]. The magnitudes for the applied loading conditions considered weight distribution as was done in previous studies [22], [23]. Specifically, loading conditions were reflective of the patient's body weight (i.e., 45.2% body weight applied at L1, with an additional 2.6% body weight applied on each inferior vertebra) [24] and amplified to account for active muscle contribution [25]. Lastly, a 7.5 Nm moment was applied at L1 to induce forward flexion. As such, similar loading conditions were applied to each model with varying follower load magnitudes depending on patient-specific body weight, however, the loading conditions did not impose identical displacements across the models. As the predictive power of FEM results is strengthened when considering several models [26], the combined modeling results were used for validation against previously published literature for intersegmental rotation (ISR), measured by the change in angular position between adjacent vertebrae described by Dvorák et

al. [27], and IVD stress, determined by the maximum normal stress on the disc surface. The previously developed model compared the normal IVD stress to internal disc pressure in biphasic discs, demonstrating a maximum discrepancy between methods of 4% [13]. As such, the IVDs were modeled as uniform discs to reduce computational costs. Following validation, the models were compared for ISR and IVD stress, as well as VB stress, measured by the average normal stress. Lastly, using Python, Spearman's correlation was calculated to determine the relationship between FEM results and patient data, while a Mann-Whitney U test was used to evaluate the correlation of FEM results between groups.

Sensitivity analyses were performed to confirm model robustness and accuracy of results by adjusting IVD parameters in the initial model. First, the mesh size was varied from 3 mm to 1 mm. Second, the element type was adjusted from tetrahedral to quadratic hexahedral-dominant. Lastly, the male and female IVD material properties were tested for comparison.

7.2.4 Results

7.2.4.1 Magnetic Resonance Images

Sagittal profile measurements were evaluated on MRIs for participants with and without LBP, detailed in Table 7.2.3. Results indicated that the LBP cohorts had reduced lumbar lordosis when compared to the control groups, regardless of which inferior vertebra was selected for Cobb angle evaluation (i.e., bottom of L5 or top of S1). Larger variations were observed for the female participants (ΔL1-L5: 5.28°; ΔL1-S1: 4.43°) than the male participants (ΔL1-L5: 3.13°; ΔL1-S1: 2.61°). To add, the female participants had greater curvature than the male participants. LSA was larger in the control groups compared to the LBP groups, while LSJA did not differ noticeably between cohorts. Although statistical significance was not achieved, the results for Cobb angle approached significance when the male and female data were combined ($p<0.1$). Interrater reliability was considered excellent (ICC>0.9) for all sagittal measurements [28].

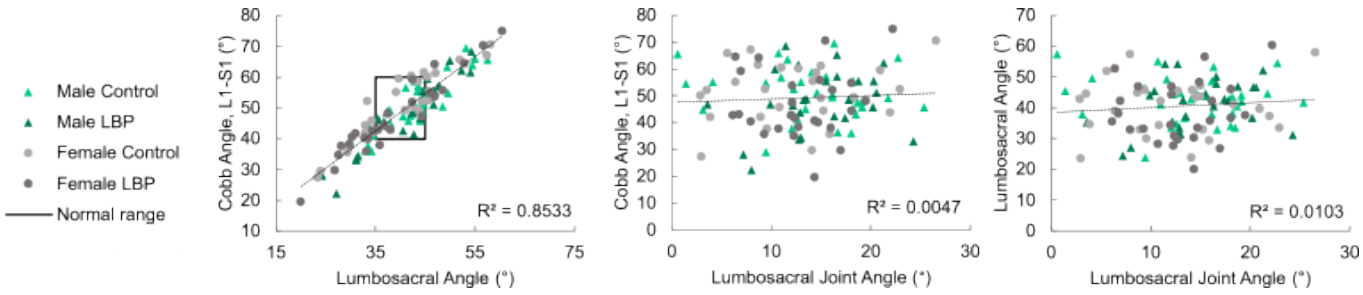

Figure 7.2.3: Correlation between Cobb angle (L1-S1), lumbosacral angle (LSA), and lumbosacral joint angle (LSJA).

Table 7.2.3: Sagittal profile measurements for the control and low back pain (LBP) cohorts, presented as mean ± standard deviation, with the intraclass correlation coefficient (ICC) for each measurement.

	Male Participants			Female Participants			All Participants			ICC
	Control	LBP	p	Control	LBP	p	Control	LBP	p	
L1-L5 (°)	36.71 ±12.03	33.58 ±11.48	0.3852	39.16 ±11.7	33.88 ±13.08	0.1288	37.81 ±11.93	33.73 ±12.20	0.0961*	0.995
L1-S1 (°)	50.73 ±9.46	48.12 ±11.67	0.4594	51.18 ±11.22	46.75 ±12.77	0.1155	50.93 ±10.20	47.42 ±12.14	0.0782*	0.991
LSA (°)	42.58 ±7.31	40.99 ±8.29	0.5735	40.18 ±8.87	38.37 ±9.80	0.4530	41.50 ±8.06	39.66 ±9.10	0.2934	0.989
LSJA (°)	14.08 ±5.91	14.61 ±4.90	0.8849	12.20 ±6.43	12.91 ±4.30	0.5218	13.24 ±6.17	13.74 ±4.64	0.7800	0.960

*p <0.1

Healthy values for lumbar lordosis have been identified between 40-60° [29], while normal values for LSA, also called sacral slope, typically fall between 35-45° [30]. Mean values for L1-S1 and LSA were within the "normal" ranges for both cohorts, recorded as 50.93° and 41.50° for the control cohort, and 47.42° and 39.66° for the LBP cohort, for L1-S1 and LSA, respectively. A strong relationship was observed between these variables, shown in Figure 7.2.3, as sagittal curvature was correlated with LSA. This relationship was not observed when considering Cobb angle versus LSJA, nor LSA versus LSJA.

L4 CSA and VB height were evaluated and detailed in Table 7.2.4. Mean CSA was 24.0% smaller in the female participants compared to the male participants. In comparison, mean VB height yielded a 4.9% reduction in the female participants relative to the male participants.

Table 7.2.4: L4 vertebral body (VB) cross-sectional area (CSA) and height compared for the male and female participants, presented as mean ± standard deviation.

	Male Participants	Female Participants	p
VB CSA (cm^2)	14.70±2.81	11.17±1.46	<0.0001
VB Height (cm)	2.73±0.16	2.60±0.14	<0.0001

7.2.4.2 Finite Element Modeling

Twelve patients were randomly selected from the MRI patient dataset for the construction of geometrically personalized FEMs (age: 49.92±15.68 years, range: 32-81 years; weight: 73.23±20.46 kg; height: 1.72±0.10 m). The sagittal profile measurements for the control subjects in this subset were 35.39±12.95° for L1-L5, 47.70±10.03° for L1-S1, 37.46±6.40° for LSA, and

12.19±4.02° for LSJA. In comparison, measurements for the LBP patients were 30.55±11.91° for L1-L5, 43.75±7.41° for L1-S1, 38.50±6.21° for LSA, and 13.42±6.93° for LSJA. These MRI measurements were aligned with the observed trends in which the pain cohort showed reduced Cobb angle magnitudes. Following model development, the FEMs were loaded with respect to body weight, and the modeling results were compared.

IVD stress was validated against previously published comparators, namely an *in silico* study by Dreischarf et al. [26], an *ex vivo* study by Brinckmann and Grootenboer evaluating IVDs under 1000N compression [31], and an *in vivo* study by Sato et al. with healthy participants [32], depicted in Figure 7.2.4. Results demonstrated that the female models were subjected to significantly greater IVD stresses than the male models (50%) when compared relative to body weight. The LBP models also demonstrated an increase in IVD stress compared to the control FEMs. IVD stress per kg was correlated with VB area ($p<0.002$) and VB height ($p<0.02$) for all discs. For mid-lumbar discs, the maximum stress was generally located near the center of the IVD for the straighter FEMs and was located posteriorly for the "normal" profiles FEMs.

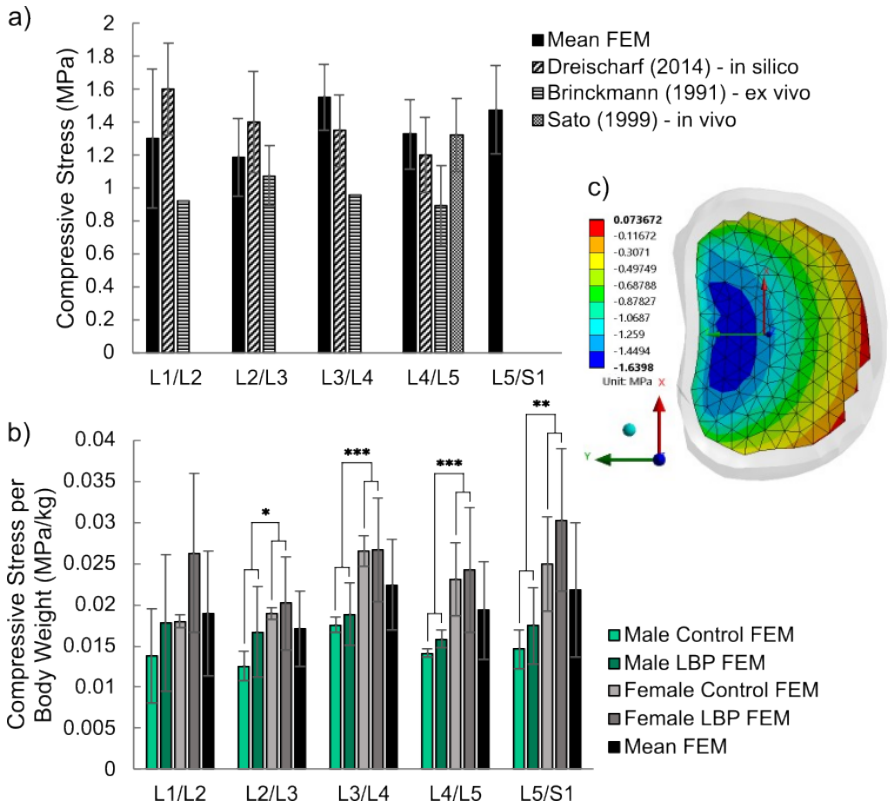

*Figure 7.2.4: a) Maximum IVD stress for the combined lumbar FEMs validated against in silico, ex vivo, and in vivo comparators, and b) per kg of body weight for each cohort of patient-specific FEMs. Results are presented as mean ± standard deviation, *p<0.1, **p<0.01, ***p<0.005. c) Example of IVD stress measured in FEMs.*

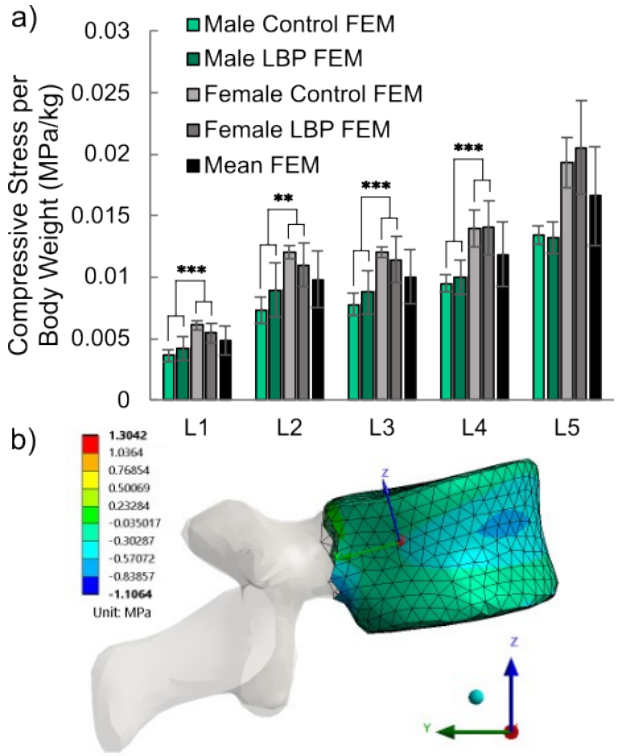

*Figure 7.2.5: a) Average vertebral body compressive stress per kg of body weight for each cohort of patient-specific FEMs. Results are presented as mean ± standard deviation, **p<0.01, ***p<0.005. b) Example of vertebral body stress measured in the FEMs.*

When considering VB stress with respect to body weight, shown in Figure 7.2.5, similar trends were observed as to IVD stress. The female FEMs demonstrated statistically significant difference in compressive stress per body weight when compared to the male FEMs (45%). The male LBP models showed greater VB stresses than the male control models for all vertebrae, apart from L5. Inverse trends were observed for the female models. VB stress magnitudes were correlated with body weight ($p<0.03$) for the inferior vertebrae, while VB stress per kg was correlated with VB area ($p<0.002$) and VB height ($p<0.03$) for all bodies.

ISR was validated against *in vivo* data presented by Wong et al. for healthy participants aged 41-50 years [33] to reflect the average age of the patients selected for biomechanical analysis, shown in Figure 7.2.6. When comparing ISR relative to body weight, the female models showed greater flexibility than the male models, indicated by an increase in ISR (51%). Additionally, the LBP FEMs showed reduced flexibility than the control models, apart from L5-S1 for the male FEMs.

Sensitivity analyses were conducted to confirm model robustness and result accuracy. When mesh size was varied, the modeling results yielded a maximum difference of 4% for IVD stress, 2% for VB stress, and 0.4% for ISR. Changes in element type resulted in maximum differences of

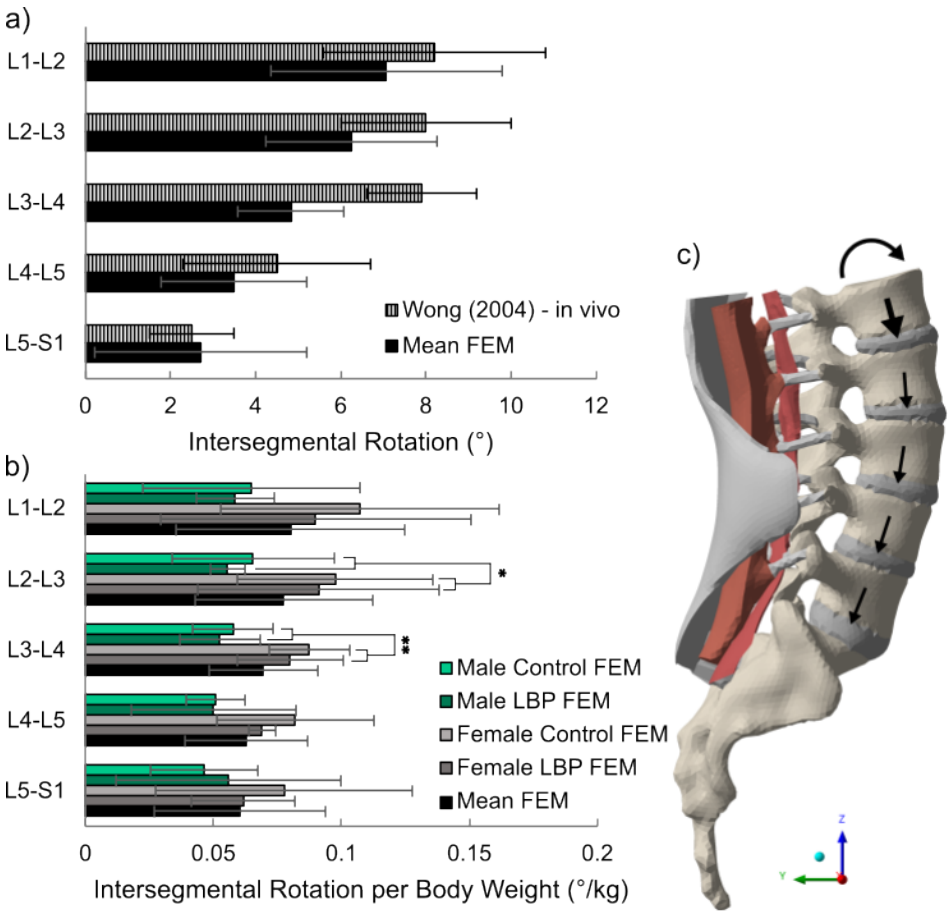

*Figure 7.2.6: a) Intersegmental rotation for the combined lumbar FEMs validated against an in vivo comparator, and b) per kg of body weight for each cohort of patient-specific FEMs. Results are presented as mean ± standard deviation, *p<0.1, **p<0.02. c) Flexion motion and loading conditions for lumbar spine FEMs.*

12%, 2%, and 0.8% for IVD stress, VB stress, and ISR, respectively. Lastly, altering IVD material properties demonstrated maximum differences of 6%, 0.5%, and 12% for IVD stress, VB stress, and ISR, respectively.

7.2.5 Discussion

This study evaluated MRIs for healthy and LBP participants to assess changes in sagittal profile. Using these findings, a high-level *in silico* analysis of personalized FEMs was conducted. Overall, this study aimed to evaluate possible mechanistic sources of stress distribution throughout the spinal column by adjusting patient-specific variables, namely geometry, sagittal profile, and loading conditions, while exploring differences between healthy and LBP spines.

Although this study focused on several biomechanical variables that may influence spinal loading, there exist many factors which impact the development or progression of back pain, such as age, genetics, obesity, lifestyle, and hormonal or protein changes, among others. Both biome-

chanical and psychosocial variables are important risk factors for pain development, affecting work absences and recovery [34]. However, increasing evidence has shown that treating biomechanical factors was critical to lower back pain incidences, which consequently lead to a reduction in psychosocial issues. Thus, understanding these biomechanical factors may provide valuable insight for targeted patient treatments.

From the imaging analysis, the female patients had greater lumbar lordosis than the male patients, which is aligned with previous work [35]. The MRI results also demonstrated that patients with LBP had attenuated lordosis, which agrees with previously conducted studies [3], [4]. It has been suggested that a straighter spine may be a clinical sign of back problems; the lower lumbar curvature may be a coping mechanism to alleviate LBP [4] as this reduction in lordosis may provide a better biomechanical loading position [36]. In addition, LSA was slightly lower in the pain groups relative to the control groups, which may be related to the straighter spinal profile observed in LBP patients. Although statistical significance was not achieved, the MRI results demonstrate clinical relevance through notable changes in sagittal profile between groups. Moreover, the present study further highlights the need for female- and male-specific interpretations of sagittal profiles.

Considering the finite element analysis, IVD stresses per body weight were larger in the LBP FEMs compared to the control FEMs. In addition, the female models exhibited greater stresses than the male models. These outcomes corroborate previous findings, as the female participants demonstrated smaller VB dimensions and VB mechanical stress is inversely proportional to CSA [37]. Although the reduced VB stress in the female LBP FEMs compared to the female control FEMs was not expected, the former patients had the lowest body weights which may contribute to the lower magnitudes. In addition, statistically significant correlations were observed between stresses in the FEMs and patient weight and VB dimensions.

The findings highlighted that geometry and body weight significantly affected spinal stress distribution. Bone geometry or volume will directly affect maximum compressive stress; an individual with smaller VBs may experience greater stresses in their spine when performing day-to-day tasks. Body weight will also influence this outcome, represented herein through the applied loading conditions. Further, variations in patient curvature were found to influence range of motion. These mechanistic variables have been shown to play a critical role in the spine's behavior. As such, the use of MRI data for retrospective *in silico* analyses has shown value when considering the outputs of patient-specific FEMs, which are further affected by *in vivo* variables that are difficult to model, such as individual tissue properties, hormonal changes, or muscle strength. Leveraging patient data to develop personalized models may provide significant value for targeted treatments or a general understanding of an individual's available motion, strengths, limits, or perhaps even spine health,

as clinicians may be able to consider the modeling results to make informed decisions regarding patient care.

This study has several limitations. The MRIs were conducted in the supine position, thus free of gravitational loads on the spine, while the FEMs were subjected to loading conditions simulating flexion from standing. The sample size for biomechanical analysis was small; using a larger number of FEMs may improve the strength of the modeling results. Nevertheless, the comparative nature of this study permits valuable insight into stress distribution throughout the spine when patient geometry, profile, and loading conditions are adjusted. Future studies may consider additional loading scenarios, such as axial rotation and lateral bending. Additionally, the material properties were assumed to be linear elastic and isotropic, despite the viscoelastic nature of human tissues presenting variability across subjects. As such, identifying and implementing individualized patient material properties, or modeling the discs as biphasic components, may enhance the results. The simplification of using linear elastic properties allowed the models to be solved rapidly, which may be beneficial if used to inform physicians in a clinical setting. To add, the geometrically personalized models were constructed from an initial model, using L4 as a reference, as opposed to using image segmentation. Despite this, the dimensions of the remaining VBs were compared between MRI and FEM and yielded an average difference of 2.6% and 2.3% for CSA and height, respectively, with a maximum difference of 12%. The IVD heights were also evaluated using Dabbs method, calculated as the mean of the anterior and posterior disc heights [38], and compared between the MRI and FEM, yielding an average difference of 6.5% with a maximum difference of 25.9%. Future studies may consider segmentation and reconstruction from patient images for model development. Additionally, alternative studies may consider disc degeneration as a potentially compounding factor to those currently explored, or the impact of dynamic loading conditions.

To conclude, this study evaluated the use of stress as a mechanical biomarker of pain, among other possible indicators. Results demonstrated that sagittal profile and body weight play an important role in the stresses throughout an individual's spine. As such, subject-specific FEMs should be considered for modeling studies, such as for patient-specific analyses, targeted treatments, or device development.

7.2.6 Acknowledgments

The authors would like to thank the Biostatistics Consulting Unit at the Montreal General Hospital for their expertise and assistance with the statistical analysis. This research was supported by McGill University (MEDA), the Fonds de Recherche du Québec – Nature et Technologies (FRQNT), and the Natural Sciences and Engineering Research Council (NSERC).

7.2.7 References

[1] J. Hartvigsen, M. J. Hancock, A. Kongsted, *et al.*, "What low back pain is and why we need to pay attention," *The Lancet*, vol. 391, no. 10137, pp. 2356–2367, 2018.

[2] B. B. Hansen, T. Bendix, J. Grindsted, *et al.*, "Effect of lumbar disc degeneration and low-back pain on the lumbar lordosis in supine and standing: A cross-sectional mri study," *Spine*, vol. 40, no. 21, pp. 1690–1696, 2015.

[3] S.-W. Chun, C.-Y. Lim, K. Kim, J. Hwang, and S. G. Chung, "The relationships between low back pain and lumbar lordosis: A systematic review and meta-analysis," *The Spine Journal*, vol. 17, no. 8, pp. 1180–1191, 2017.

[4] V. Murrie, A. Dixon, W. Hollingworth, H. Wilson, and T. Doyle, "Lumbar lordosis: Study of patients with and without low back pain," *Clinical Anatomy: The Official Journal of the American Association of Clinical Anatomists and the British Association of Clinical Anatomists*, vol. 16, no. 2, pp. 144–147, 2003.

[5] US Food and Drug Administration, "Assessing the credibility of computational modeling and simulation in medical device submissions. draft guidance for industry and food and drug administration staff," *Food and Drug Administration: Silver Spring, MD, USA*, 2021.

[6] S. Naserkhaki, J. L. Jaremko, and M. El-Rich, "Effects of inter-individual lumbar spine geometry variation on load-sharing: Geometrically personalized finite element study," *Journal of Biomechanics*, vol. 49, no. 13, pp. 2909–2917, 2016.

[7] B. Stott and M. Driscoll, "Biomechanical evaluation of the thoracolumbar spine comparing healthy and irregular thoracic and lumbar curvatures," *Computers in Biology and Medicine*, vol. 160, p. 106 982, 2023.

[8] A. Shirazi-Adl and M. Parnianpour, "Effect of changes in lordosis on mechanics of the lumbar spine-lumbar curvature in lifting," *Clinical Spine Surgery*, vol. 12, no. 5, pp. 436–447, 1999.

[9] B. Stott, P. Afshari, J. Bischoff, *et al.*, "A critical comparison of comparators used to demonstrate credibility of physics-based numerical spine models," *Annals of Biomedical Engineering*, vol. 51, no. 1, pp. 150–162, 2023.

[10] C. W. Pfirrmann, A. Metzdorf, M. Zanetti, J. Hodler, and N. Boos, "Magnetic resonance classification of lumbar intervertebral disc degeneration," *Spine*, vol. 26, no. 17, pp. 1873–1878, 2001.

[11] P. Oura, M. Nurkkala, J. Auvinen, J. Niinimäki, J. Karppinen, and J.-A. Junno, "The association of body size, shape and composition with vertebral size in midlife–the northern finland birth cohort 1966 study," *Scientific Reports*, vol. 9, no. 1, pp. 1–8, 2019.

[12] M. E. Kunkel, A. Herkommer, M. Reinehr, T. M. Böckers, and H.-J. Wilke, "Morphometric analysis of the relationships between intervertebral disc and vertebral body heights: An anatomical and radiographic study of the human thoracic spine," *Journal of Anatomy*, vol. 219, no. 3, pp. 375–387, 2011.

[13] I. El Bojairami, K. El-Monajjed, and M. Driscoll, "Development and validation of a timely and representative finite element human spine model for biomechanical simulations," *Scientific Reports*, vol. 10, no. 1, pp. 1–15, 2020.

[14] M. Kurutz, *Finite element modelling of human lumbar spine*. Citeseer, 2010.

[15] D. T. Reilly and A. H. Burstein, "The elastic and ultimate properties of compact bone tissue," *Journal of Biomechanics*, vol. 8, no. 6, pp. 393–405, 1975.

[16] B. D. Stemper, D. Board, N. Yoganandan, and C. E. Wolfla, "Biomechanical properties of human thoracic spine disc segments," *Journal of Craniovertebral Junction and Spine*, vol. 1, no. 1, p. 18, 2010.

[17] G. N. Onambélé, K. Burgess, and S. J. Pearson, "Gender-specific in vivo measurement of the structural and mechanical properties of the human patellar tendon," *Journal of Orthopaedic Research*, vol. 25, no. 12, pp. 1635–1642, 2007.

[18] K. El-Monajjed and M. Driscoll, "Investigation of reaction forces in the thoracolumbar fascia during different activities: A mechanistic numerical study," *Life*, vol. 11, no. 8, p. 779, 2021.

[19] L. Yahia, P. Pigeon, and E. DesRosiers, "Viscoelastic properties of the human lumbodorsal fascia," *Journal of Biomedical Engineering*, vol. 15, no. 5, pp. 425–429, 1993.

[20] S. R. Ward, A. Tomiya, G. J. Regev, *et al.*, "Passive mechanical properties of the lumbar multifidus muscle support its role as a stabilizer," *Journal of Biomechanics*, vol. 42, no. 10, pp. 1384–1389, 2009.

[21] A. G. Patwardhan, R. M. Havey, K. P. Meade, B. Lee, and B. Dunlap, "A follower load increases the load-carrying capacity of the lumbar spine in compression," *Spine*, vol. 24, no. 10, pp. 1003–1009, 1999.

[22] I. Villemure, C.-É. Aubin, J. Dansereau, and H. Labelle, "Simulation of progressive deformities in adolescent idiopathic scoliosis using a biomechanical model integrating vertebral growth modulation," *Journal of Biomechanical Engineering*, vol. 124, no. 6, pp. 784–790, 2002.

[23] M. Driscoll, C.-É. Aubin, A. Moreau, I. Villemure, and S. Parent, "The role of spinal concave–convex biases in the progression of idiopathic scoliosis," *European Spine Journal*, vol. 18, pp. 180–187, 2009.

[24] A. Schultz, G. Andersson, R. Ortengren, K. Haderspeck, and A. Nachemson, "Loads on the lumbar spine. validation of a biomechanical analysis by measurements of intradiscal pressures and myoelectric signals," *Journal of Bone and Joint Surgery. American Volume*, vol. 64, no. 5, pp. 713–720, 1982.

[25] A. Nachemson, "The load on lumbar disks in different positions of the body," *Clinical Orthopaedics and Related Research (1976-2007)*, vol. 45, pp. 107–122, 1966.

[26] M. Dreischarf, T. Zander, A. Shirazi-Adl, *et al.*, "Comparison of eight published static finite element models of the intact lumbar spine: Predictive power of models improves when combined together," *Journal of Biomechanics*, vol. 47, no. 8, pp. 1757–1766, 2014.

[27] J. Dvořák, M. Panjabi, D. Chang, R. Theiler, and D. Grob, "Functional radiographic diagnosis of the lumbar spine: Flexion–extension and lateral bending," *Spine*, vol. 16, no. 5, p. 562, 1991.

[28] T. K. Koo and M. Y. Li, "A guideline of selecting and reporting intraclass correlation coefficients for reliability research," *Journal of Chiropractic Medicine*, vol. 15, no. 2, pp. 155–163, 2016.

[29] P. R. Loughenbury, A. I. Tsirikos, and N. W. Gummerson, "Spinal biomechanics–biomechanical considerations of spinal stability in the context of spinal injury," *Orthopaedics and Trauma*, vol. 30, no. 5, pp. 369–377, 2016.

[30] P. Roussouly, "The standing position: Its principles and spinopelvic relations," in *Spinal Anatomy*, Springer, 2020, pp. 113–125.

[31] P. Brinckmann and H. Grootenboer, "Change of disc height, radial disc bulge, and intradiscal pressure from discectomy an in vitro investigation on human lumbar discs," *Spine*, vol. 16, no. 6, pp. 641–646, 1991.

[32] K. Sato, S. Kikuchi, and T. Yonezawa, "In vivo intradiscal pressure measurement in healthy individuals and in patients with ongoing back problems," *Spine*, vol. 24, no. 23, p. 2468, 1999.

[33] K. W. Wong, J. C. Leong, M.-k. Chan, K. D. Luk, and W. W. Lu, "The flexion–extension profile of lumbar spine in 100 healthy volunteers," *Spine*, vol. 29, no. 15, pp. 1636–1641, 2004.

[34] S. McGill, "Epidemiological studies and what they really mean," in *Low back disorders: evidence-based prevention and rehabilitation*. Human Kinetics, 2015, pp. 29–48.

[35] Y. Yukawa, F. Kato, K. Suda, M. Yamagata, T. Ueta, and M. Yoshida, "Normative data for parameters of sagittal spinal alignment in healthy subjects: An analysis of gender specific differences and changes with aging in 626 asymptomatic individuals," *European Spine Journal*, vol. 27, no. 2, pp. 426–432, 2018.

[36] M. Caglayan, O. Tacar, A. Demirant, *et al.*, "Effects of lumbosacral angles on development of low back pain," *Journal of Musculoskeletal Pain*, vol. 22, no. 3, pp. 251–255, 2014.

[37] V. Gilsanz, M. I. Boechat, R. Gilsanz, M. L. Loro, T. F. Roe, and W. G. Goodman, "Gender differences in vertebral sizes in adults: Biomechanical implications," *Radiology*, vol. 190, no. 3, pp. 678–682, 1994.

[38] C. W. Pfirrmann, A. Metzdorf, A. Elfering, J. Hodler, and N. Boos, "Effect of aging and degeneration on disc volume and shape: A quantitative study in asymptomatic volunteers," *Journal of Orthopaedic Research*, vol. 24, no. 5, pp. 1086–1094, 2006.

7.3 Supplemental Data from Magnetic Resonance Imaging Analysis

7.3.1 Analysis of Sagittal Profile in the Thoracic and Lumbar Regions

In addition to the lumbar sagittal profile measurements presented in Section 7.2, thoracic measurements were completed on the MRIs. The methodologies for the additional measurements are outlined in Figure 7.3.1, while descriptive patient data for this supplemental study is presented in Table 7.3.1. The thoracic MRI data were not included in the manuscript in Objective 3 (Section 7.2) as the manuscript focused on the lumbar spine. To add, the available images for the thoracic region were primarily localizer images. Localizer images are considered a "scout" scan used to identify relevant anatomical structures in the body. These scans are done rapidly and consequently have low resolution [208]. Lastly, exclusion criteria for the manuscript and subsequent patient-specific FEMs comprised patients with disc degeneration of grade 4 or 5 on the Pfirrmann grading scheme. The data presented for thoracic measurements, recorded in Table 7.3.2, does not exclude patients with disc degeneration. An analysis of lumbar measurements for participants with and without severe disc degeneration (Pfirrmann grade 4 or 5) is displayed in Table 7.3.3.

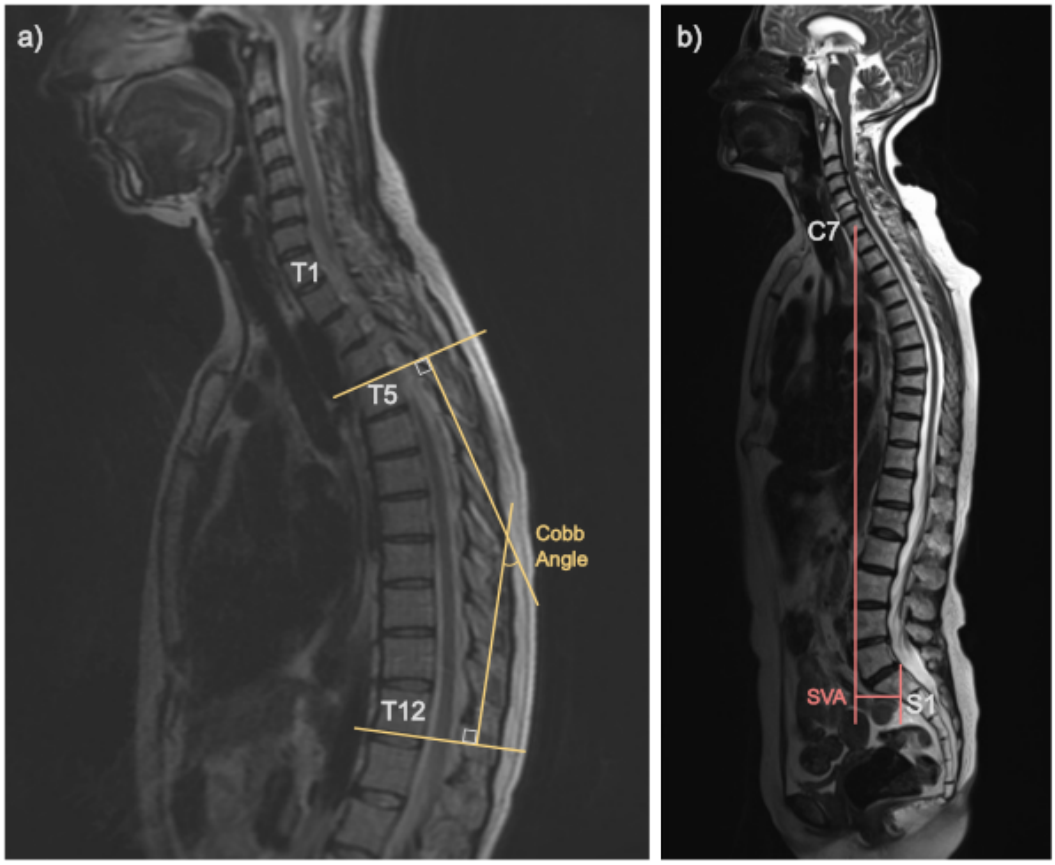

Figure 7.3.1: Magnetic resonance image measurements for a) Cobb angle (T5-T12) and b) sagittal vertical alignment (SVA).

Table 7.3.1: Summary of participant data, presented as mean ± standard deviation.

	Male Participants			Female Participants			All Participants		
	Control	LBP	Total	Control	LBP	Total	Control	LBP	Total
Thoracic Measurements									
Patients, *n*	29	25	54	26	33	59	55	58	113
Age (years)	59.45±13.44	61.00±16.93	60.17±15.18	57.96±13.24	52.45±11.85	54.88±12.78	58.75±13.37	56.14±14.88	57.41±14.22
Weight (kg)	84.69±10.12	86.30±14.15	85.44±12.18	65.35±14.25	60.15±8.00	62.40±11.48	75.50±15.63	71.42±17.04	73.41±16.50
Height (m)	1.79±0.07	1.78±0.06	1.79±0.06	1.65±0.08	1.66±0.09	1.66±0.08	1.73±0.10	1.71±0.09	1.72±0.10
Lumbar Measurements									
Patients, *n*	41	45	86	31	37	68	72	82	154
Age (years)	59.02±13.88	57.18±17.18	58.06±15.72	57.39±13.12	51.49±12.61	54.18±13.18	58.32±13.59	54.61±15.55	56.34±14.78
Weight (kg)	84.50±10.98	85.90±11.87	85.24±11.47	62.23±14.25	60.17±7.76	61.11±11.24	74.92±16.66	74.29±16.38	74.58±16.52
Height (m)	1.80±0.07	1.77±0.06	1.78±0.07	1.65±0.07	1.66±0.08	1.65±0.08	1.73±0.10	1.72±0.09	1.73±0.10

Table 7.3.2: Mean of the average measurements taken by two raters for Cobb angle (T5-T12, T4-T9, T1-T12, T10-L2, T12-S1, L1-L5, L1-S1), sagittal vertical alignment (SVA), lumbosacral angle (LSA), and lumbosacral joint angle (LSJA) for control and low back pain (LBP) participants, presented as mean ± standard deviation.

	Male Participants			Female Participants			All Participants			ICC
	Control	LBP	p	Control	LBP	p	Control	LBP	p	
Thoracic Measurements										
T5-T12 (°)	27.30±8.00	26.34±8.65	0.6937	33.65±12.70	27.89±10.54	0.1258	30.21±10.78	27.17±9.62	0.2020	0.984
T4-T9 (°)	26.47±8.03	26.55±8.64	0.8569	30.23±11.12	27.20±9.98	0.7491	28.20±9.65	26.89±9.27	0.9971	0.981
T1-T12 (°)	45.04±9.99	46.66±11.81	0.8439	44.68±13.12	41.56±12.30	0.3855	44.88±11.39	43.91±12.20	0.4971	0.985
T10-L2 (°)	5.70±3.66	6.63±5.00	0.6012	5.94±2.85	7.48±4.22	0.2014	5.81±3.30	7.12±4.53	0.1940	0.929
SVA (cm)	4.04±1.55	4.09±3.05	0.6902	3.84±1.80	3.25±1.26	0.3855	3.64±2.29	3.95±1.64	0.5412	0.981
Lumbar Measurements										
T12-S1 (°)	53.39±11.51	52.82±10.24	0.9159	51.31±12.26	49.57±13.66	0.2924	52.48±11.80	51.36±11.94	0.4042	0.993
L1-L5 (°)	36.94±13.48	34.07±10.37	0.4978	38.99±12.96	36.04±13.60	0.3399	37.83±13.20	34.96±11.90	0.2149	0.995
L1-S1 (°)	49.41±11.44	48.30±10.64	0.7050	49.89±11.80	48.35±13.30	0.3720	49.62±11.52	48.32±11.84	0.3144	0.992
LSA (°)	40.97±8.35	41.29±8.72	0.8189	39.33±8.82	38.99±10.71	0.5837	40.44±8.76	40.08±9.48	0.6111	0.989
LSJA (°)	12.58±6.49	14.29±4.14	0.3372	11.06±6.84	12.28±4.55	0.3525	11.92±6.64	13.38±4.42	0.2069	0.965

The data summarized in Table 7.3.2 outlines the differences in sagittal profile measurements in healthy and LBP participants for both biological sexes. SVA was measured as the horizontal offset from a vertical plumbline dropped from the mid-body of C7 to the posterosuperior corner of the S1 endplate [110], [127], [128]. Cobb angle was measured for T5-T12, T4-T9, and T1-T12 in the thoracic region, while the same measurements were recorded in the lumbar region as specified in the above manuscript (Section 7.2.3), with the addition of Cobb angle for T12-S1. The decision was made to measure Cobb angles between various vertebrae in the thoracic and lumbar regions as there is no clear consensus in literature regarding the "gold standard" for Cobb angle measurements, as described in Section 2.4, Table 2.4.2.

For the thoracic measurements, the mean Cobb angle magnitudes for T5-T12 and T4-T9 were within the "normal" range (10-40°) for both groups, while T1-T12 resulted in hyperkyphotic curvatures (>40°). The male participants showed negligible differences in Cobb angle (T5-T12, T4-T9, T1-T12) between the control and LBP participants, while SVA was larger in the pain group than in the control group (ΔSVA: 0.35 cm). In comparison, the control female participants had greater Cobb angle measurements than the LBP participants (ΔT5-T12: 4.58°, ΔT1-T12: 1.86°). Similar trends have been observed in previously published studies that compared thoracic curvature of healthy and LBP individuals [109], [120]. Contrarily to the males, the female control group showed slightly augmented SVA magnitudes compared to the female pain group (ΔSVA: 0.45 cm). Overall, the female participants had greater thoracic curvatures than the male participants, with the exception of T1-T12 magnitudes. Yakawa et al. also reported slightly lower T1-T12 values in females compared to males, although recorded values were within the normative range [114].

Considering the lumbar measurements, mean Cobb angle values for T12-S1 and L1-S1 were within the "normal" range (40-60°) for both groups, but values were hypolordotic when measured between L1-L5 (<40°). The control groups had slightly greater Cobb angle measurements (T12-S1, L1-L5, L1-S1) than the pain groups, which is aligned with findings in literature [71], [109], [120], [122], [124]. The female participants showed greater mean Cobb angles for the L1-L5 region than the male participants, although this trend was not observed for T12-S1. LSA values were greater for the male participants than the female participants but showed negligible differences between the pain and control groups. LSJA was larger for the male participants, as well as for the LBP participants, in each comparison. The findings for lumbar measurements in Table 7.3.2 agree with the trends observed in the manuscript (Section 7.2.4). Lastly, interrater reliability was considered excellent (ICC >0.9) for all measurements.

Table 7.3.3: Mean of the average measurements taken by two raters for Cobb angle (T12-S1, L1-L5, L1-S1), lumbosacral angle (LSA), and lumbosacral joint angle (LSJA) for participants with (Y) and without (N) disc degeneration, presented as mean ± standard deviation.

	Male Participants			Female Participants			All Participants		
Disc Degeneration	N	Y	p	N	Y	p	N	Y	p
T12-S1 (°)	53.80±10.20	51.64±11.97	0.2277	50.06±12.52	51.36±14.76	0.8850	52.02±11.47	51.54±12.88	0.5401
L1-L5 (°)	35.34±11.79	35.58±12.48	0.8007	36.52±12.67	40.21±15.25	0.3778	35.90±12.18	37.26±13.56	0.7933
L1-S1 (°)	49.59±10.47	47.26±11.97	0.1664	48.97±12.11	49.32±14.37	0.9079	49.29±11.24	48.01±12.77	0.2642
LSA (°)	41.88±7.73	39.58±9.81	0.1229	39.28±9.30	38.72±11.70	0.4350	40.64±8.57	39.27±10.41	0.1548
LSJA (°)	14.31±5.45	11.80±5.01	0.0330*	12.55±5.43	9.04±5.90	0.0422*	13.47±5.49	10.80±5.45	0.0118*

*p<0.05

Table 7.3.4: Mean L4 vertebral body cross-sectional area (CSA) and height for the control and low back pain (LBP) patients, presented as mean ± standard deviation.

	Male Participants			Female Participants			All Participants		
	Control	LBP	p	Control	LBP	p	Control	LBP	p
CSA (cm^2)	15.31±2.89	14.47±2.71	0.0390*	11.31±1.81	11.47±1.49	0.6268	13.66±3.18	13.10±2.69	0.0563**
Height (cm)	2.74±0.15	2.75±0.16	0.5419	2.65±0.15	2.59±0.15	0.1755	2.70±0.16	2.68±0.18	0.1082

*p<0.05, **p<0.1

Considering the analysis of lumbar profiles affected by severe disc degeneration (Pfirrmann grade 4 or 5) presented in Table 7.3.3, the female participants again showed greater L1-L5 measures than the male participants, while inverse trends were observed for LSA. LSJA was also greater for the male participants. Statistical significance was achieved for LSJA values between participants with and without degeneration ($p<0.05$), indicating that severe disc degeneration in the inferior lumbar IVDs has a significant effect on the orientation of L5 relative to S1. This finding was supported as participants with degenerative changes most often showed damage in the inferior lumbar IVDs, in particular L5/S1.

The data presented above highlights the variability in Cobb angle magnitudes, depending on which vertebrae are selected for analysis. Although statistical significance was solely achieved when considering degenerative changes for LSJA measurements, the MRI results nevertheless provide valuable and clinically relevant comparative information between healthy participants and those experiencing LBP.

7.3.2 Analysis of Vertebral Body Area and Height

To evaluate the anthropometric data of the patients provided for the MRI study, the CSA of the vertebra was calculated using the equation below, as described in Section 7.2.3 and in previous studies [32], [42]:

$$CSA = \pi \times \frac{W}{2} \times \frac{D}{2}$$

where W is the width and D is the depth of the VB, in cm. The dimensions were measured on axial images as depicted in Figure 7.2.1, in which the upper slice of the L4 vertebra was selected for a brief comparative study between the male and female participants. In addition to CSA, VB height was measured on mid-sagittal images and calculated as the mean of the anterior height and posterior height, in cm, as was done in Section 7.2.3 and in previous studies [45]–[47]. The results are recorded in Table 7.3.4. The relationships between L4 VB CSA and VB height with respect to patient age, weight, and height are demonstrated in Figure 7.3.2.

The results in Table 7.2.4 in the manuscript above (Section 7.2.4) and in additional detail in Table 7.3.4 below demonstrated that the female patients had an average of 24.4% reduced CSA compared to the male patients. This data agrees with previously published literature, which found a change of 20-25% in VB CSA between males and females [27], [28], [30]. Further, the results showed a slight change in VB height between the male and female patients. Comparing the control cohort to the LBP cohort, VB CSA was slightly larger in the control group than the LBP group when considering the male participants ($p<0.04$) or when combining the data for both sexes ($p<0.06$). Since mechanical stress in the vertebrae can be approximated as inversely proportional

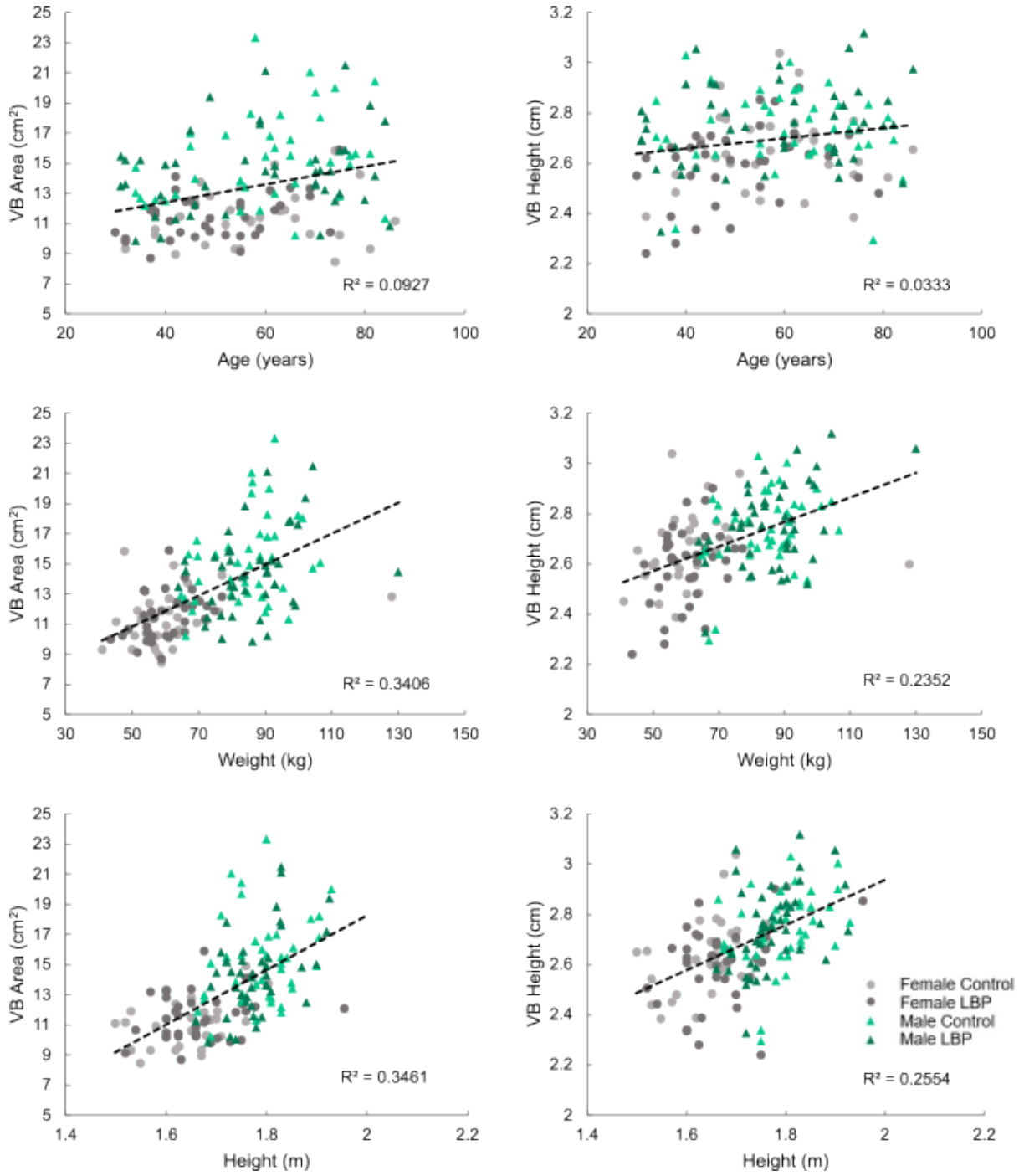

Figure 7.3.2: L4 vertebral body cross-sectional area and height with respect to patient age, weight, and height for the control and low back pain (LBP) patients.

to CSA [27], these findings may provide valuable insight into vertebral strength and the resultant stresses when an individual's spinal column is subjected to day-to-day movements and loads. With respect to VB height, minor variations between groups were observed, indicating that this variable may not be a leading factor in the development of LBP. When evaluating the relationship between

VB geometry and patient age, weight, and height, as shown in Figure 7.3.2, the female patients demonstrated reduced VB CSA and VB height, which was weakly correlated to patient weight and height, as expected. This trend was less clear when comparing VB CSA and VB height with age.

7.4 Summary

The findings of this study are two-fold. First, an *in vivo* MRI study was conducted in which the sagittal profiles of male and female participants, with and without LBP, were evaluated. Second, a blind retrospective study was conducted in which a subset of the patients was randomly selected, and the MRI data was used to inform *in silico* models of the lumbar spine. It was hypothesized that patient geometry and profile for FEA could be adjusted to within 10% of MRI measurements and that there would be observable differences in stress distribution between the modelled healthy and LBP spines.

In the first part of this study, the MRI findings indicated that patients with LBP tended to exhibit reduced lordotic curvature compared to participants without pain, which was in agreement with previous literature. In addition, LSA was correlated with Cobb angle (L1-L5), meaning that as the sacral slope increased, the Cobb angle also increased. The interrater reliability was excellent for all measurements, confirming the consistency and reliability of the MRI measurements. Further correlations were observed between VB CSA and patient weight and height. The MRI results also highlighted the variability in Cobb angle magnitudes depending on which vertebrae were selected for analysis. The supplemental data reported sagittal measures in the thoracic spine and also found that LSJA was correlated with disc degeneration for healthy and LBP participants. Lastly, there was a noticeable difference in VB CSA between healthy and LBP participants, as well as between male and female participants.

In the second part of the study, geometrically personalized FEMs were developed, validated, and used to evaluate the ability to identify patients with potentially augmented stress magnitudes throughout the lumbar spine, while focusing on three controlled parameters: patient size (VB CSA and height), patient weight (affecting loading conditions), and patient sagittal profiles. The developed subject-specific FEMs achieved L4 VB CSA and height to within 1.4% and sagittal profile to within 3° of the MRI measurements, which was below the hypothesis target of 10%. The FEA further confirmed the hypothesis by demonstrating notable differences in modelling results between the control and LBP models. Specifically, the LBP models exhibited higher IVD stresses than the control models, while the opposite trend was observed for range of motion. In addition, the female models were subjected to greater stresses per kg of body weight than the male models, which corroborates the findings in Objective 1 (Section 5).

The retrospective analysis considered patients with healthy and hypolordotic profiles as the

MRI analysis resulted in sagittal profiles that were primarily in the healthy or hypolordotic ranges. Future studies may consider selecting a population with hyperlordotic profiles or evaluating the thoracic spine segment.

In summary, the results of the final objective highlighted the importance of using patient-specific models for accurate biomechanical analyses, as well as the ability to leverage retrospective imaging data to develop these models. Although clear trends were observed from the modelling results, it is important to note that the models cannot be used to diagnose back pain, but rather, were used to demonstrate the variation between cohorts through comparison. To add, many other factors may contribute to the development or progression of LBP which were simplified in this study. Future studies may consider expanding the sample size for FEA or varying additional parameters in the models, such as individualized material properties.

8 General Discussion

Despite being a vital musculoskeletal system in the human body, the spine remains a primary system for which there is a significant occurrence of years lived with disability and reoccurring, long-term disorders [50]–[52]. The challenge in diagnosing many LBP cases revolves around the complexity of the spine. This system consists of an abundance of muscles, connective tissues, tendons, and nerves concentrated over small vertebral areas along the length of the spinal column [15]. Further, each individual has a unique profile, showing variation in their pelvic position, kyphotic and lordotic curvatures, and vertical alignment when visualized in the sagittal and coronal planes. Studies have indicated that many factors contribute to the development and progression of back pain, including biomechanical and psychosocial variables [87]. Due to the high occurrence of spinal afflictions and the significant burden that these musculoskeletal disorders place on society and healthcare systems, further understanding of potential causes may support research findings and clinical treatments.

As such, it was the central objective of this thesis to study spine biomechanics by leveraging FEA. The use of FE modelling for biomechanical systems is becoming increasingly accepted and adopted in research, development, and clinical settings. Computational M&S has permitted the study of musculoskeletal systems for healthy and diseased states, medical device development, and areas of stress concentration in the human body, among other avenues. For example, the stresses throughout the spinal column have been predicted and studied in adolescent scoliosis patients [190], [192]. As a potential solution to aid these patients, FEA has been used to investigate the effectiveness of brace treatments, as well as the application of customized and optimized braces [191], [209], [210]. To understand the physiological motion of the spine and the resulting stresses, techniques for modelling realistic loading conditions throughout the spinal column have been studied by several research groups [73], [77], [164], [165], [211]. Another common modelling direction is the evaluation of spinal instrumentation, such as pedicle screws, rods, and interbody cages [205], [212]–[216]. These studies have provided insight into potential areas of stress concentration, failure modes, biomechanical stability, or suggestions on optimal designs for these devices. Despite the significant advancements that have been made in biomechanical M&S, there exist several gaps in literature which may significantly affect the accuracy of patient-specific models. Consequently, this thesis aimed to study the impact that certain patient-specific variables may have on modelling solutions, with an emphasis on biomechanics.

Although M&S is becoming increasingly accepted as a viable and advantageous method of studying biological systems, a central challenge remains in establishing that the model realis-

tically represents what happens in the human body. V&V have been identified as critical steps in computational modelling studies. Specifically, validation is the process by which the modelling results are compared to experimental data to confirm the model's predictive capabilities and accuracy [156], [197]. Although widely accepted as an important step in model development, and the existence of several guidelines outlining the essential factors to consider when conducting this step [197], [217], there remains wide variability in the adopted methods by researchers for validation efforts. As such, in collaboration with the ASME VVUQ40 Subcommittee, a review of the existing comparators used to establish model credibility was conducted, presented in Section 4. This comparative analysis gathered several recently published spine computational modelling studies to evaluate their use of comparators to establish model credibility. It was observed that it is commonly adopted to use several comparators for model validation, with most of the evaluated studies using between six to ten comparators across several validation assessments. Further, *in silico*, *ex vivo*, and *in vivo* human comparators were the most prevalent categories used in the selected studies. Despite these findings, the ASME VVUQ40 Subcommittee concluded that the comparator implementation held far more significance than the category or quantity of comparators used. Specifically, it is imperative to select comparators that accurately support the model scope and simulation in question. There exists a wide range of available data that could be used as comparators for IVD stress and ISR in future computational studies, but selecting comparators that accurately reflect the physiological motion being simulated is critical. A summary of some of the existing comparators at the time of writing this thesis can be found in Appendix A.1.

Despite the promising findings outlined in the first manuscript (Section 4.2), future work could be done to improve the suggested scoring methods. For example, the manuscript did not evaluate the scored results of individual studies, but instead selected to assess the results of all studies combined. Evaluation of individual studies could provide valuable insight into the strengths and weaknesses of a given model, allowing weaker areas to be identified and improved upon accordingly. Although computational models of the spine were the focus of the manuscript, the authors feel that the developed scoring methods could easily support and be implemented for other biological systems. In addition, spine models evaluating surgical instrumentation were not included in the study. As such, it would be of great interest to repeat the previously conducted investigation with other biological systems or with spine models assessing instrumentation. Nevertheless, the opportunity to work closely with the ASME VVUQ40 Subcommittee was of significant benefit and set the stage for the remaining objectives of this thesis.

Following the extensive research into existing computational models of the spine, several gaps in the literature regarding patient modelling were identified. Specifically, biological sex and

sagittal alignment were seldom considered in the studies evaluated in the first manuscript (Section 4.2). Hence, Objective 1 (Section 5) and Objective 2 (Section 6) hoped to provide insight into the consideration of these variables in computational analyses.

It was observed that many previously published computational studies did not distinguish between nor consider the differences in spinal anatomy and loading between males and females (Sections 2.3, 4.2.5, 5.2.2). However, previous research has highlighted variations in loading capabilities between men and women, as well as biological strength differences [27], [70]. To add, it has been reported that the prevalence of LBP is greater in females compared to their male counterparts [68], [69], [199], [218], [219]. As such, the first objective of this thesis aimed to develop sex-specific FEMs of the spine to evaluate variations in spinal stress distribution.

A healthy spine model representing male anatomy was previously developed in the Musculoskeletal Biomechanics Research Lab by El Bojairami et al. [174], [175] and was leveraged for this thesis. A female model was developed for comparison, taking into consideration the variations in spinal geometry and anatomical material properties (Section 5.2.3). The modelling results indicated a notable increase in stress magnitudes in the female models compared to the male models, when subjected to several loading scenarios, underlining the importance of considering biological sex in FEAs. Specifically, the IVD stresses exhibited increases ranging from 18% to 36%, whereas the VB stresses increased by approximately 50%, depending on the loading conditions. The results also demonstrated an increase in ISR as high as 35% in the female models when subjected to pure moments simulating flexion and extension. However, when a follower load was applied, the rotational values were similar between both male and female FEMs, thus highlighting the ability of a follower load to stabilize the spine. Overall, the observed augmented stresses in the female models may corroborate the higher prevalence of LBP cases and musculoskeletal disorders in female patients from a mechanical perspective.

The decision was made to initially subject the male and female models in Objective 1 to identical loading conditions, despite men and women experiencing different daily loads, such as variations in body weight. This decision was selected to allow comparison to other previously published studies which evaluated spine models under identical loads [27]. Further, although few existing FE spine models considered biological sex, studies that did used loading conditions similar to previously published studies, regardless of model sex [163], [186], [187]. However, acknowledging the differences in daily loading between men and women is necessary, and consequently, an additional study was conducted. This study took into consideration individualized loading on the spine, whereby loads were applied with respect to the percentage of body weight that each vertebra is subjected to, resulting in approximately 50% of the body weight on the lumbar spine

(Sections 5.3, 5.4). As such, the loading conditions for the female model were lower than those for the male model, based on the average body weight of North American individuals [200]. The additional preliminary results highlighted the importance of using sex-specific loading conditions but continued to show similar trends to those observed in Article 2 (Section 5.2). Specifically, the female model continued to display greater VB and IVD stresses compared to the male model, thus corroborating the findings presented in the second manuscript. Analysis of the tensional stresses in the TLF also exhibited similar results. There are anatomical differences between male and female individuals, which were taken into consideration in this objective through changes in CSA and material properties. These morphological differences may have also contributed to the higher stresses since compressive stresses on the vertebrae are proportional to the load applied and inversely proportional to the CSA [27]. As such, the loading conditions explored in the additional studies provided an interesting approach for sex-specific modelling and inspired similar loading conditions in Objective 3 (Section 7.2).

It is widely accepted that variations in spinal alignment, whether in the coronal or sagittal plane, play a role in the prevalence of back pain [71]. Due to its high prevalence and the magnitude by which it affects growth, development, and physical suffering, the impacts of scoliosis have been widely studied through computational modelling [189]–[192]. However, abnormal curvature in the sagittal plane has been studied to a lesser extent. As previously described (Sections 2.7.1, 6.2.2), several modelling studies have evaluated and observed changes in stress distribution or loading capacity when considering variations in sagittal curvature in the thoracic or lumbar regions [187], [193], [194], while focusing on a segment of the spine. The lumbar spine is mechanically linked to the thoracic region, sacrum, and pelvis, and consequently, the sagittal alignment and orientation of these spinal components will affect the overall biomechanical balance of the spine. This gap in the literature inspired the second objective of this thesis.

In Section 6, four FEMs were developed to represent thoracolumbar spines with variations in curvatures in the thoracic and lumbar regions. The computational results from these models were then compared to a "healthy" curvature model, for both the full thoracolumbar spine and the lumbar segment. For this analysis, the FEMs were developed to represent spines with variation in curvature relative to the "normal" kyphotic and lordotic magnitudes identified in literature (i.e., kyphosis: 10-40°, lordosis: 40-60° [3]). This approach was selected since a healthy model with curvatures within the accepted range was previously developed and validated [174] (i.e., T5-T12: 23.69°, L1-S1: 44.24°), and was implemented in the first FE study in this thesis. The methodology adopted in this chapter would also allow an existing base model to be adjusted to accurately, rapidly, and efficiently represent patient-specific profiles in future research studies or virtual clinical trials. The

resultant biomechanics were globally compared across the models.

Findings from the second objective suggest that the straighter spines had similar IVD and VB stresses relative to the Healthy model, but reduced disc compression, i.e., greater disc heights in the final loaded position. In comparison, the hyper-curved spines had augmented stresses in these bodies and larger disc compression, i.e., reduced disc heights in the final loaded position. All exaggerated curvature models demonstrated a generally reduced range of motion, indicated by ISR measurements. As described in Section 2.4, patients with LBP tend to have a straighter spine compared to healthy participants. One explanation is that LBP patients may adopt this profile as a coping mechanism to alleviate pain and support biomechanical loading [220]. Considering this interpretation for the modelling results, the straighter spines may "protect" the discs by reducing disc compression through the stacked vertebral positions. In comparison, the augmented stresses and disc compression in the more curved spine models may be interpreted as potentially leading to back pain if an individual's spine was repeatedly subjected to higher stresses over a period of time, as greater lordosis can be mechanically linked to back pain [221], [222].

There is wide variability in sagittal alignment among individuals. A patient may have thoracic and lumbar curvatures that satisfy definitions for sagittal balance, such as maintaining SVA$<$50 mm [128] or a 30° difference between thoracic and lumbar angles [112], however, they may demonstrate an overly straight or curved spine profile. This complicates the task of defining the "normal" or "healthy" ranges for spinal curvature, as individuals may live absent of pain and maintain sagittal stability without satisfying the ideal curvature measurements. The study in Objective 2 opted to vary the curvatures of the thoracic and lumbar regions individually while maintaining the adjacent curvature values approximately constant. This approach was selected to control uncertainties and to focus on the implications of curvature variations in each segment, without influence from surrounding changes. However, future studies may consider evaluating when multiple segments are adjusted simultaneously, or exploring common profile classifications, such as the Roussouly classification for sagittal profiles [135]. In addition, SS was maintained approximately constant in the second study but was taken into consideration in the final objective.

Objective 1 successfully demonstrated the influences that geometry and material properties play on spinal stress distributions, while Objective 2 confirmed that the sagittal profiles also have an impact. Although the outcomes of the first two objectives provided valuable insight into specific variables that should be considered when modelling the spine, these objectives considered geometry and curvature based on mean values reported in literature. Hence, Objective 3 (Section 7) aimed to combine the modelling approaches and results from Objectives 1 and 2 to focus on model personalization and improve upon the assumptions that represented a general population. In

collaboration with Dr. Tiegs-Heiden and Dr. Benson from Mayo Clinic, the final objective of this thesis used patient-specific data from images to retrospectively evaluate spine biomechanics.

MRI is a useful imaging modality for studying spinal curvature and disc health [1], [147]. The insight gained from evaluating patient images can assist clinicians with diagnoses, pinpoint potential anatomical areas that may cause pain or discomfort, and guide treatment approaches. In Section 7, the sagittal profiles of healthy participants and LBP patients were evaluated through MRI. It was observed that the female participants had greater lumbar curvatures than the male participants. In addition, the patients with LBP had reduced curvature magnitudes compared to the healthy control subjects. Several previously published studies have reported similar results [114], [120], [122], and consequently, the results reported in the final manuscript (Section 7.2.4) and the supplemental data (Section 7.3) corroborate these findings. The MRI measurements provided patient-specific information for the second aim of this study, which was to improve upon the previous objectives by developing geometrically personalized models of the spine while taking into consideration sex, weight, and profile.

Following initial MRI analysis, a blind retrospective study was conducted by selecting a subset of these patients for FEA of the lumbar spine. The randomly selected subset of LBP patients had reduced lumbar lordosis compared to the subset of healthy participants (ΔL1-L5: 4.84°, ΔL1-S1: 3.95°), which agreed with the mean MRI results reported in the manuscript, as well as previously published studies [120], [122]. As each subject-specific model was loaded with respect to individualized body weight conditions, the results for VB stress, IVD stress, and ISR were scaled relative to body weight to obtain normalized results for comparison. The female models demonstrated greater magnitudes for VB stress, IVD stress, and ISR. These results support the findings presented in Objective 1 (Sections 5.2.4, 5.3.2) which also yielded larger stress and rotational magnitudes in the female FEMs relative to the male FEMs. It was also observed that the LBP FEMs demonstrated reduced rotation per body weight relative to the control FEMs, which was aligned with the findings in Objective 2 (Section 7.2.4). However, the LBP FEMs yielded higher IVD and VB stresses compared to the healthy FEMs, which did not fully agree with the previously reported results for the second objective. Specifically, the third manuscript found that the straighter spines had reduced stress magnitudes (Section 6.2.4), meanwhile, in the last manuscript, the LBP FEMs, which had straighter lumbar profiles on average, displayed greater stress magnitudes (Section 7.2.4). The discrepancies in results could be attributed to several possible causes. First, the models in Objective 2 were not developed to represent patients with back pain, but instead represented generalized individuals with adjusted sagittal curvature. In addition, the models in Objective 3, which showed lumbar profiles that were aligned more posteriorly over S1, were

subjected to body weight loading and had adjusted VB dimensions, which were not considered in the second objective. The FEM results in the final objective found a correlation between VB stress and body weight, VB CSA, and VB height, while IVD stress was correlated with the latter two VB parameters. As such, including additional subject-specific parameters was found to impact the outcomes of the FEA. Nevertheless, the results presented in Objective 3 highlighted the potential for retrospective FE studies of personalized spine models for biomechanical analysis.

The study in the final manuscript of this thesis developed subject-specific lumbar spine FEMs using MRI data. To develop the models, the volumetric bodies from the baseline model were scaled, permitting the VB CSA and height to be adjusted to within 1.4% of the MRI measurements. This was deemed to provide sufficient accuracy to represent patient-specific lumbar spines for this study. However, developing subject-specific FEMs through image segmentation would provide additional accuracy concerning patient geometry. Image segmentation was initially tested as a methodology for the final objective, however, this approach would require substantial post-processing to achieve realistic 3D model geometry. Further, the MRI slice thickness did not facilitate a refined and smooth model, causing inter-slice sparsity. Future studies could use image segmentation to improve upon the realism of the models, however, this approach can be time-consuming if done manually. Due to the low contrast between tissues in MRI, the boundaries between anatomical structures can be unclear [223]. Studies that utilize segmentation from MRI typically focus on joints and soft tissues, whereas CT is more commonly used for bone due to the greater contrast between tissues [224]. Therefore, although automated segmentation is improving for both CT and MRI, segmentation of the lumbar spine may be facilitated by selecting CT images for their distinction between anatomical bodies and the smaller slice thicknesses.

The scoring metrics outlined in the first manuscript (Section 4.2) may provide valuable insight into a given biomechanical model's validation approach and the use of comparators to establish model credibility. Although not formally evaluated herein, the aforementioned scoring metrics could be used to determine the level of credibility of the models developed in this thesis (Sections 5.2, 6.2, 7.2). The methodology for the scoring metrics outlined in the first manuscript detailed that no selected articles were evaluated by an individual who had previously developed or collaborated on the given model (Section 4.2.3). As such, it would have been of interest to have another member of the ASME VVUQ40 Subcommittee score the models developed in this thesis. Nevertheless, from a brief evaluation, it was determined that the biomechanical models developed herein would score within the average range of the selected models in the first manuscript. Furthermore, the authors feel that the three presented manuscripts detailing the biomechanical models improved upon some of the recommendations outlined in the first manuscript, namely describing the model

assumptions and limitations, justifying the selected comparators, and describing possible model applications.

Following the ASME V&V40 guidelines, an important consideration of any biomechanical model is risk-based assessment and the potential implications that the modelling results may have on patients. As demonstrated in Figure 2.8.1 (Section 2.8), the evaluation of the model influence and the decision consequence will determine the corresponding model risk. The FEMs outlined in this thesis can be classified as "low risk" models. The models were developed with the purpose of providing insight and knowledge about biomechanical loading and stress distribution throughout the spine, and were not developed to inform approaches for high-risk surgical interventions or patient treatments. Consequently, if an incorrect interpretation of the modelling results were made, the outcomes would not significantly affect the patient's care.

The use of FEMs for virtual clinical trials and regulatory approval of medical devices is becoming increasingly accepted, with several available guidelines outlining expectations and suggested approaches for successful M&S [197], [217]. To ensure a meaningful and prominent impact of biomechanical models in virtual trials, there is a need for diverse and inclusive models that represent a range of individuals, whether that be a general healthy population, commonly observed musculoskeletal disorders and diseases, or patient-specific. As such, this dissertation aimed to evaluate various modelling parameters that could be implemented in spine FEMs, as well as to determine a modelling approach that would allow the adjustment of a base model to include subject-specific parameters. In addition, developing and maintaining a model that could be solved rapidly to facilitate possible patient assessments is an important target to ensure clinical acceptance and to promote the use of modelling in a medical setting. This thesis demonstrated the successful consideration of geometry, sex, weight, and sagittal profile in spine FE modelling, and the effects that these parameters have on stress distribution. In addition, the models allow for future studies to implement individualized parameters, such as osteoporotic or degenerative disc properties or muscle activation, which may permit additional avenues of model assessment to be explored.

This thesis also aimed to provide a preliminary assessment regarding if FEMs could be used as a biomarker for LBP. Although modelling results must be interpreted with caution when considering clinical assessments and the presence of pain, the findings from the presented FEAs outlined potential areas that may indicate pain development, such as augmented stress magnitudes or compressed disc heights. Despite this, identifying areas of pain remain a challenge in biomechanical modelling due to the subjectivity between individuals, such as pain tolerance or sensitivity. Further, at the time of writing this dissertation, the author was not aware of *in vivo* or *ex vivo* studies reporting magnitudes of VB or IVD stress that would indicate the onset of pain. The challenge

in reporting this data remains clear, which is further complicated by the idiopathic nature of various spine pathologies. This gap in knowledge inhibits a confident assessment of pain in FEMs; rather, it allows for interpretations based on the underlying available knowledge regarding pain development.

The baseline "healthy" male model that was described in Objective 1 (Section 5.2) and Objective 2 (Section 6.2) was extensively validated following initial development [174]. However, additional loading scenarios were evaluated in the studies presented in this thesis, and hence, the model was validated for these loading scenarios and the material properties were adjusted. This model was developed using novel meshing techniques to reduce computational cost [174] and also included pressurized muscles [175] which are known to contribute to spinal stability, but which were seldom included in previously published spine models. Considering the complexity of the presented FEM, several assumptions were made when implementing the model in the first two manuscripts. For the purpose of the studies in Sections 5.2 and 6.2, the abdominal cavity, rib cage, and ligaments were excluded, despite the stabilising role that these anatomical components have with respect to the spine [8], [15], [225]. The abdominal cavity is thought to stiffen the spine when intra-abdominal pressure is increased by external forces or muscle contractions [97]. Further, although the rib cage plays a role in thoracic stability [8], it was found to contribute more greatly under dynamic respiration [226]. Ligaments also have a larger impact at high deformations [227]. Due to the static analysis adopted throughout this thesis and the selected, controlled range of motion, the decision to exclude these components can be justified.

Furthermore, the models presented in this dissertation may allow for additional avenues of spine modelling assessment. The FEMs were successfully validated for the specified contexts of use, and thus, additional investigations may require model improvements and further validation. This research restricted the models to specific physiological motions, namely flexion and extension. Additional work could consider motion in the remaining planes, i.e., lateral bending or axial rotation. Further, this thesis considered a static analysis. Studying the spine through FE modelling of dynamic models, time dependency, or viscoelastic properties, for example, could aid in validating the current spine modelling approaches, as well as potentially improving the accuracy of the modelling results. At the time of writing this dissertation, a dynamic thoracolumbar spine model was under development in the Musculoskeletal Biomechanics Research Lab at McGill University. Utilizing a dynamic model could allow the possibility of studying different loading scenarios, such as dynamic lifting or depositing tasks, compared to the static or quasi-static outcomes which have primarily been studied in past spine modelling studies.

To conclude, the objectives achieved in this thesis highlighted the importance of consider-

ing subject-specific parameters in spine biomechanical modelling, as consideration and implementation of parameters including sex, geometry, and sagittal profile were found to considerably affect the model outputs. It further supported the opportunity and ability to use retrospective imaging data to study spinal loading and stress distribution. As such, this thesis aimed to lay the groundwork for future studies considering patient-specific variables and outlined the methodology to adjust existing models to accurately represent individualized spine anatomy.

9 Conclusions and Future Directions

With the global expanding and ageing population, spinal disorders are becoming increasingly prominent, demanding substantial support from healthcare systems. Diagnosing the multitude of potential spine pathologies is further complicated by the intricacies that are the surrounding and highly dense nerves, muscles, and connective tissues over a small vertebral area. The spine is the backbone of the human body, providing the support, stability, and movement required to efficiently perform day-to-day tasks. The presence of spinal pathologies can greatly impact an individual's ability to perform trunk motions. There is a need for a greater, global understanding of spine biomechanics to assist with diagnosing and understanding the complexities of the spinal column.

Leveraging FE methods allows the study of internal loading in the human body in a non-invasive manner. Although biomechanical models remain an approximation of biological systems, accurate validation of modelling results with respect to *in vivo*, *ex vivo*, or *in silico* data can strengthen the model predictions and shed light on outcomes that are otherwise a challenge to obtain *in vivo*. Numerical modelling reduces the dependency on animal trials or cadaveric experiments, which can be costly and can present ethical challenges, while providing realistic predictions and understanding of the physiological performance of the spine. As such, through working with the ASMEVVUQ40 Subcommittee, an evaluation of existing FE spine models and their use of comparators to establish model credibility was realized. Previous studies have favoured the use of multiple comparators for validation efforts, however, it was observed that proper comparator implementation would more effectively support model validation. With the growing acceptance of computational studies for virtual clinical trials, these virtual studies can be conducted prior to running *in vivo* or *ex vivo* trials and may become complementary to clinical studies.

This dissertation aimed to utilize geometrically personalized FEMs of the spine to explore the influence of patient-specific variables on modelling outcomes, with the overarching goal of enhancing and contributing to the knowledge of spine biomechanics. These variables, i.e., geometry, biological sex, and sagittal profile, are natural and unchangeable but are often overlooked when modelling biological systems. However, due to the variability between individuals, the consideration of these commonplace parameters may shed light on distinguishable differences between individual loading capacities or spinal stress distribution. The models adopted and described herein, alongside validation with previously published *in vivo*, *ex vivo*, and *in silico* studies, have led to novel explorations of FEM personalization for accurate biomechanical analyses. The adopted modelling approaches have allowed for an initial model to be modified and adjusted

to accurately represent subject-specific geometry and alignment. Additionally, by customizing the material properties, boundary conditions, and loading conditions, an existing model can be tailored to evaluate patient-specific parameters, loading capacities, or motions, among other outcomes.

The implications of sex-specific models and variations in sagittal profile were first independently explored. The development of a female thoracolumbar spine model for comparison with a validated male model, under several loading scenarios, demonstrated differences in spinal stress distribution and loading capacities between biological sexes. Although this study presented convincing results, there are several gaps in literature which, if filled, would improve the realism of the developed models. For example, sex-specific material properties of spine components, such as the fascia or muscles, are not currently available but would provide valuable additional insight into sex differences for biological systems.

Also of interest is the high variability of spinal alignment between individuals. Although generally accepted that variations in curvature demonstrate clinical significance with respect to the development of spinal pathologies, the biomechanical differences between these spines are less understood. Thus, a comparative study between five FEMs with deviations in sagittal alignment was conducted, demonstrating notable differences in stress distribution. Although omitted from the presented studies, the inclusion of additional components, such as the rib cage or abdominal and thoracic cavities, may contribute to additional spine mechanics and further improve upon the modelling results when considering variations in profile.

Following the independent evaluation of these variables, a retrospective study was conducted using patient MRI to develop lumbar spine models representing both healthy individuals and LBP patients, combining the approaches and findings of the first two objectives. The FEA resulted in differences in stress distribution and range of motion between the modelled cohorts. The final investigation outlined in this thesis supports the retrospective use of available patient images for computational modelling. Expanding upon the current FE study with a larger sample size would further strengthen the modelling results. This approach may encourage additional, similar studies to be conducted to exploit the multitude of available patient images for retrospective analyses.

In summary, the global objective of this thesis was to develop, validate, and evaluate geometrically personalized FEMs of the spine for analysis of stress distribution throughout the spine. This was successfully achieved using several thoracolumbar and lumbar spine models with variations in geometry, alignment, and loading conditions, and comparing the model outcomes to a baseline “healthy” model. Although this research details several avenues for the analysis of spine biomechanics through modelling of subject-specific parameters, studying additional avenues of

interest would support these findings, such as the use of dynamic modelling, image segmentation for model construction, or additional physiological motions. Nevertheless, the comparative studies outlined herein support the notion of variability between individuals and the importance of considering patient parameters for computational M&S.

With a prominent history of back pain in my immediate and extended families, including my younger sister who was diagnosed with degeneration, herniation, and decreased disc space at L4/L5 and L5/S1 at 17, I was inspired to contribute to the expansive knowledge of spine biomechanics and to hopefully assist in furthering targeted treatments for spinal disorders and diseases. It is my hope that the work included in this thesis may guide and inspire the use of personalized computational models for biomechanical analyses. Further, it is my belief that the continued collaboration between clinicians and engineers to advance the knowledge of biological systems is important to fully grasp the mechanisms behind various spine pathologies, shed light on the potential origins of pain, and continue to improve existing treatment approaches.

Despite the advancements presented herein, there exist numerous avenues for additional research and several gaps to be filled in order to fully grasp the impacts of LBP. Thus, the question of the future applications and directions of biomechanical modelling prevails. To continue to remain pertinent for clinical applications, future development of an efficient, user-friendly interface that could rapidly, and with high accuracy, segment patient images to develop FEMs with minimal user interaction would be of interest. If auto-segmentation becomes powerful enough to develop patient-specific models for analysis, while rapidly building models and employing boundary and loading conditions, this could facilitate patient assessment to provide clinical insight. Further, if a database of normative stress magnitudes for healthy and diseased individuals existed, that could be consulted for model validation but also as a reference for expected *in vivo* loads, it may highlight areas of greater concern in subject-specific models. As engineers, we must always keep in mind the clinical recommendations from models, as patient safety should remain at the forefront.

References

[1] G. D. Cramer, "Chapter 2 - general characteristics of the spine," in *Clinical anatomy of the spine, spinal cord, and ANS*. Elsevier Health Sciences, 2014, pp. 15–64.

[2] T. R. Oxland, "Fundamental biomechanics of the spine—what we have learned in the past 25 years and future directions," *Journal of Biomechanics*, vol. 49, no. 6, pp. 817–832, 2016.

[3] P. R. Loughenbury, A. I. Tsirikos, and N. W. Gummerson, "Spinal biomechanics–biomechanical considerations of spinal stability in the context of spinal injury," *Orthopaedics and Trauma*, vol. 30, no. 5, pp. 369–377, 2016.

[4] T. M. Khalil, E. M. Abdel-Moty, R. S. Rosomoff, and H. L. Rosomoff, "Ergonomics in back pain," in *Ergonomics in back pain: a guide to prevention and rehabilitation*. Van Nostrand Reinhold Company, 1993, pp. 8–34.

[5] H. Singh, G. C. Chang Chien, and R. Bolash, "Anatomy of the spine," in *Treatment of Chronic Pain Conditions: A Comprehensive Handbook*. Springer, 2017, pp. 11–20.

[6] F. Galbusera, "The spine: Its evolution, function, and shape," in *Biomechanics of the Spine: basic concepts, spinal disorders and treatments*. Elsevier, 2018, pp. 3–9.

[7] D. Bélanger, "Le système squelettique: Les os," in *Anatomie et physiologie: une approche intégrée*. Chenelière éducation, 2014, pp. 285–350.

[8] C. Liebsch and W. H-J, "Basic biomechanics of the thoracic spine and rib cage," in *Biomechanics of the Spine: basic concepts, spinal disorders and treatments*. Elsevier, 2018, pp. 35–50.

[9] A. Schultz, G. Andersson, R. Ortengren, K. Haderspeck, and A. Nachemson, "Loads on the lumbar spine. validation of a biomechanical analysis by measurements of intradiscal pressures and myoelectric signals," *Journal of Bone and Joint Surgery. American Volume*, vol. 64, no. 5, pp. 713–720, 1982.

[10] J. T. Woon and M. D. Stringer, "Clinical anatomy of the coccyx: A systematic review," *Clinical Anatomy*, vol. 25, no. 2, pp. 158–167, 2012.

[11] C. R. Ethier and C. A. Simmons, *Introductory biomechanics: from cells to organisms*. Cambridge University Press, 2007.

[12] J.-F. Ganghoffer and I. Goda, "6 - micropolar models of trabecular bone," in *Multiscale Biomechanics*. Elsevier, 2018, pp. 362–316.

[13] J. E. Muscolino, *Manual therapy for the low back and pelvis: a clinical orthopedic approach*. Wolters Kluwer Health/Lippincott Williams & Wilkins, 2015.

[14] B. Lavignolle, "The intervertebral disc," in *Spinal Anatomy: Modern Concepts*. Springer, 2020, pp. 207–216.

[15] M. W. Devereaux, "Anatomy and examination of the spine," *Neurologic clinics*, vol. 25, no. 2, pp. 331–351, 2007.

[16] J. M. Vital, "The spinal ligaments," in *Spinal Anatomy: Modern Concepts*. Springer, 2020, pp. 229–242.

[17] J. Buschmann and G. Meier Bürgisser, "1-structure and function of tendon and ligament tissues," in *Biomechanics of tendons and ligaments: tissue reconstruction and regeneration*. Woodhead Publishing, 2017, pp. 3–29.

[18] J. Buschmann and G. Meier Bürgisser, "3-mechanobiology of tendons and ligaments," in *Biomechanics of tendons and ligaments: tissue reconstruction and regeneration*. Woodhead Publishing, 2017, pp. 63–80.

[19] B. W. Bakkum and G. D. Cramer, "Chapter 4 - muslces that influence the spine," in *Clinical anatomy of the spine, spinal cord, and ANS*. Elsevier Health Sciences, 2014, pp. 98–134.

[20] A. Des Serres, "Le tissu musculaire," in *Anatomie et physiologie: une approche intégrée*. Chenelière éducation, 2014, pp. 319–436.

[21] M. Cordeau, "Le système musculaire: Les muscles axiaux et appendiculaires," in *Anatomie et physiologie: une approche intégrée*. Chenelière éducation, 2014, pp. 437–512.

[22] R. Schleip, H. Jäger, and W. Klingler, "What is 'fascia'? a review of different nomenclatures," *Journal of Bodywork and Movement Therapies*, vol. 16, no. 4, pp. 496–502, 2012.

[23] U. Hoheisel, T. Taguchi, and S. Mense, "Nociception: The thoracolumbar fascia as a sensory organ," in *Fascia: The Tensional Network of the Human Body*, Elsevier, 2012, pp. 95–101.

[24] P. J. Barker, D. M. Urquhart, I. H. Story, M. Fahrer, and C. A. Briggs, "The middle layer of lumbar fascia and attachments to lumbar transverse processes: Implications for segmental control and fracture," *European Spine Journal*, vol. 16, no. 12, pp. 2232–2237, 2007.

[25] M. Gatton, M. Pearcy, G. Pettet, and J. Evans, "A three-dimensional mathematical model of the thoracolumbar fascia and an estimate of its biomechanical effect," *Journal of Biomechanics*, vol. 43, no. 14, pp. 2792–2797, 2010.

[26] S. McGill, "Normal and injury mechanics of the lumbar spine," in *Low back disorders: evidence-based prevention and rehabilitation*. Human Kinetics, 2015, pp. 97–152.

[27] V. Gilsanz, M. I. Boechat, R. Gilsanz, M. L. Loro, T. F. Roe, and W. G. Goodman, "Gender differences in vertebral sizes in adults: Biomechanical implications," *Radiology*, vol. 190, no. 3, pp. 678–682, 1994.

[28] E. N. Ebbesen, J. S. Thomsen, H. Beck-Nielsen, H. J. Nepper-Rasmussen, and L. Mosekilde, "Age-and gender-related differences in vertebral bone mass, density, and strength," *Journal of Bone and Mineral Research*, vol. 14, no. 8, pp. 1394–1403, 1999.

[29] J. W. Nieves, C. Formica, J. Ruffing, *et al.*, "Males have larger skeletal size and bone mass than females, despite comparable body size," *Journal of Bone and Mineral Research*, vol. 20, no. 3, pp. 529–535, 2005.

[30] R. Cooper, S. Holli, and M. Jayson, "Gender variation of human spinal and paraspinal structures," *Clinical Biomechanics*, vol. 7, no. 2, pp. 120–124, 1992.

[31] T. Watson, S. McPherson, and K. Starr, "The association of nutritional status and gender with cross-sectional area of the multifidus muscle in establishing normative data," *Journal of Manual & Manipulative Therapy*, vol. 16, no. 4, 93E–98E, 2008.

[32] Y. Duan, C. H. Turner, B.-T. Kim, and E. Seeman, "Sexual dimorphism in vertebral fragility is more the result of gender differences in age-related bone gain than bone loss," *Journal of Bone and Mineral Research*, vol. 16, no. 12, pp. 2267–2275, 2001.

[33] L. Mosekilde, "Sex differences in age-related changes in vertebral body size, density and biomechanical competence in normal individuals," *Bone*, vol. 11, no. 2, pp. 67–73, 1990.

[34] L. Mosekilde and L. Mosekilde, "Normal vertebral body size and compressive strength: Relations to age and to vertebral and iliac trabecular bone compressive strength," *Bone*, vol. 7, no. 3, pp. 207–212, 1986.

[35] C. W. Pfirrmann, A. Metzdorf, A. Elfering, J. Hodler, and N. Boos, "Effect of aging and degeneration on disc volume and shape: A quantitative study in asymptomatic volunteers," *Journal of Orthopaedic Research*, vol. 24, no. 5, pp. 1086–1094, 2006.

[36] J. A. Miller, C. Schmatz, and A. Schultz, "Lumbar disc degeneration: Correlation with age, sex, and spine level in 600 autopsy specimens.," *Spine*, vol. 13, no. 2, pp. 173–178, 1988.

[37] H. S. Amonoo-Kuofi, "Morphometric changes in the heights and anteroposterior diameters of the lumbar intervertebral discs with age.," *Journal of Anatomy*, vol. 175, p. 159, 1991.

[38] Z. Shao, G. Rompe, and M. Schiltenwolf, "Radiographic changes in the lumbar intervertebral discs and lumbar vertebrae with age," *Spine*, vol. 27, no. 3, pp. 263–268, 2002.

[39] K. Bach, J. Ford, R. Foley, *et al.*, "Morphometric analysis of lumbar intervertebral disc height: An imaging study," *World Neurosurgery*, vol. 124, e106–e118, 2019.

[40] L. Twomey and J. Taylor, "Age changes in lumbar intervertebral discs," *Acta orthopaedica scandinavica*, vol. 56, no. 6, pp. 496–499, 1985.

[41] W. Marras, M. Jorgensen, K. Granata, and B. Wiand, "Female and male trunk geometry: Size and prediction of the spine loading trunk muscles derived from mri," *Clinical Biomechanics*, vol. 16, no. 1, pp. 38–46, 2001.

[42] P. Oura, M. Nurkkala, J. Auvinen, J. Niinimäki, J. Karppinen, and J.-A. Junno, "The association of body size, shape and composition with vertebral size in midlife–the northern finland birth cohort 1966 study," *Scientific Reports*, vol. 9, no. 1, pp. 1–8, 2019.

[43] P. V. Scoles, A. E. Linton, B. Latimer, M. E. Levy, and B. F. Digiovanni, "Vertebral body and posterior element morphology: The normal spine in middle life.," *Spine*, vol. 13, no. 10, pp. 1082–1086, 1988.

[44] M. Demir, A. Emre, N. Seringeç, *et al.*, "Intervertebral disc heights and concavity index of the lumbar spine in young healthy adults," *Anatomy*, vol. 12, no. 1, pp. 34–37, 2018.

[45] M. E. Kunkel, A. Herkommer, M. Reinehr, T. M. Böckers, and H.-J. Wilke, "Morphometric analysis of the relationships between intervertebral disc and vertebral body heights: An anatomical and radiographic study of the human thoracic spine," *Journal of Anatomy*, vol. 219, no. 3, pp. 375–387, 2011.

[46] I. Malkoc, S. A. Aydinlioglu, F. Alper, *et al.*, "Age related changes in height and shape of the lumbar intervertebral discus," *European Journal of Basic Medical Sciences*, vol. 2, no. 3, pp. 68–73, 2012.

[47] F. J. Onishi, M. A. de Paiva Neto, S. Cavalheiro, and R. S. Centeno, "Morphometric analysis of 900 lumbar intervertebral discs: Anterior and posterior height analysis and their ratio," *Interdisciplinary Neurosurgery*, vol. 18, p. 100 523, 2019.

[48] J. A. Hides, D. H. Cooper, and M. J. Stokes, "Diagnostic ultrasound imaging for measurement of the lumbar multifidus muscle in normal young adults," *Physiotherapy Theory and Practice*, vol. 8, no. 1, pp. 19–26, 1992.

[49] E. Klupp, B. Cervantes, S. Schlaeger, *et al.*, "Paraspinal muscle dti metrics predict muscle strength," *Journal of Magnetic Resonance Imaging*, vol. 50, no. 3, pp. 816–823, 2019.

[50] E. L. Hurwitz, K. Randhawa, H. Yu, P. Côté, and S. Haldeman, "The global spine care initiative: A summary of the global burden of low back and neck pain studies," *European Spine Journal*, vol. 27, no. 6, pp. 796–801, 2018.

[51] T. Vos, C. Allen, M. Arora, *et al.*, "Global, regional, and national incidence, prevalence, and years lived with disability for 310 diseases and injuries, 1990–2015: A systematic analysis for the global burden of disease study 2015," *The Lancet*, vol. 388, no. 10053, pp. 1545–1602, 2016.

[52] D. G. Patterson, "Overview of chronic pain," in *Treatment of Chronic Pain Conditions: A Comprehensive Handbook*. Springer, 2017, pp. 7–8.

[53] G. B. Andersson, "Epidemiological features of chronic low-back pain," *The Lancet*, vol. 354, no. 9178, pp. 581–585, 1999.

[54] D. P. Gross, R. Ferrari, A. S. Russell, *et al.*, "A population-based survey of back pain beliefs in canada," *Spine*, vol. 31, no. 18, pp. 2142–2145, 2006.

[55] A. Suhaimi, "33 - low back pain," in *Braddom's rehabilitation care: A clinical handbook*. Elsevier Health Sciences, 2017, pp. 228–237.

[56] G. I. Polykoff and J. Jackson, "History and physical examination," in *Spine Pain Care*, Springer, 2020, pp. 69–90.

[57] D. L. Simel and D. Rennie, "Low back pain," in *The rational clinical examination: evidence-based clinical diagnosis*. McGraw Hill Professional, 2008.

[58] D. Schopflocher, P. Taenzer, and R. Jovey, "The prevalence of chronic pain in canada," *Pain Research and Management*, vol. 16, no. 6, pp. 445–450, 2011.

[59] P. Hüllemann, T. Keller, M. Kabelitz, *et al.*, "Clinical manifestation of acute, subacute, and chronic low back pain in different age groups: Low back pain in 35,446 patients," *Pain Practice*, vol. 18, no. 8, pp. 1011–1023, 2018.

[60] P. J. Watson, "Clinical assesment of low back pain," in *Handbook of pain assessment*. Guilford Press, 2011, pp. 294–308.

[61] G. C. Chang Chien, "Chronic pain," in *Treatment of Chronic Pain Conditions: A Comprehensive Handbook*. Springer, 2017, pp. 3–4.

[62] A. E. Bussières, G. Stewart, F. Al-Zoubi, *et al.*, "Spinal manipulative therapy and other conservative treatments for low back pain: A guideline from the canadian chiropractic guideline initiative," *Journal of Manipulative and Physiological Therapeutics*, vol. 41, no. 4, pp. 265–293, 2018.

[63] J. N. Katz, "Lumbar disc disorders and low-back pain: Socioeconomic factors and consequences," *Journal of Bone and Joint Surgery*, vol. 88, no. suppl_2, pp. 21–24, 2006.

[64] R. Deyo and J. Weinstein, "Low back pain. reply," *New England Journal of Medicine*, vol. 344, no. 21, pp. 1644–1645, 2001.

[65] H. M. Langevin, J. R. Fox, C. Koptiuch, *et al.*, "Reduced thoracolumbar fascia shear strain in human chronic low back pain," *BMC Musculoskeletal Disorders*, vol. 12, no. 1, pp. 1–11, 2011.

[66] M. H. Pope, K. L. Goh, and M. L. Magnusson, "Spine ergonomics," *Annual Review of Biomedical Engineering*, vol. 4, no. 1, pp. 49–68, 2002.

[67] E. Ehrlich George, "Low back pain," *Bulletin of the World Health Organization*, vol. 81, pp. 671–676, 2003.

[68] A. Y. Wong, J. Karppinen, and D. Samartzis, "Low back pain in older adults: Risk factors, management options and future directions," *Scoliosis and Spinal Disorders*, vol. 12, no. 1, pp. 1–23, 2017.

[69] D. Hoy, C. Bain, G. Williams, *et al.*, "A systematic review of the global prevalence of low back pain," *Arthritis & Rheumatism*, vol. 64, no. 6, pp. 2028–2037, 2012.

[70] W. S. Marras, K. G. Davis, and M. Jorgensen, "Spine loading as a function of gender," *Spine*, vol. 27, no. 22, pp. 2514–2520, 2002.

[71] S.-W. Chun, C.-Y. Lim, K. Kim, J. Hwang, and S. G. Chung, "The relationships between low back pain and lumbar lordosis: A systematic review and meta-analysis," *The Spine Journal*, vol. 17, no. 8, pp. 1180–1191, 2017.

[72] A. G. Patwardhan, R. M. Havey, K. P. Meade, B. Lee, and B. Dunlap, "A follower load increases the load-carrying capacity of the lumbar spine in compression," *Spine*, vol. 24, no. 10, pp. 1003–1009, 1999.

[73] A. Rohlmann, T. Zander, M. Rao, and G. Bergmann, "Realistic loading conditions for upper body bending," *Journal of Biomechanics*, vol. 42, no. 7, pp. 884–890, 2009.

[74] M. Dreischarf, T. Zander, A. Shirazi-Adl, *et al.*, "Comparison of eight published static finite element models of the intact lumbar spine: Predictive power of models improves when combined together," *Journal of Biomechanics*, vol. 47, no. 8, pp. 1757–1766, 2014.

[75] E. Newell and M. Driscoll, "The examination of stress shielding in a finite element lumbar spine inclusive of the thoracolumbar fascia," *Medical & Biological Engineering & Computing*, vol. 59, no. 7, pp. 1621–1628, 2021.

[76] H. L. Sis, E. M. Mannen, B. M. Wong, *et al.*, "Effect of follower load on motion and stiffness of the human thoracic spine with intact rib cage," *Journal of Biomechanics*, vol. 49, no. 14, pp. 3252–3259, 2016.

[77] S. Naserkhaki and M. El-Rich, "Sensitivity of lumbar spine response to follower load and flexion moment: Finite element study," *Computer Methods in Biomechanics and Biomedical Engineering*, vol. 20, no. 5, pp. 550–557, 2017.

[78] D. E. Anderson, E. M. Mannen, H. L. Sis, *et al.*, "Effects of follower load and rib cage on intervertebral disc pressure and sagittal plane curvature in static tests of cadaveric thoracic spines," *Journal of Biomechanics*, vol. 49, no. 7, pp. 1078–1084, 2016.

[79] A. Nachemson and J. M. Morris, "In vivo measurements of intradiscal pressure: Discometry, a method for the determination of pressure in the lower lumbar discs," *Journal of Bone and Joint Surgery*, vol. 46, no. 5, pp. 1077–1092, 1964.

[80] A. Nachemson, "The load on lumbar disks in different positions of the body," *Clinical Orthopaedics and Related Research (1976-2007)*, vol. 45, pp. 107–122, 1966.

[81] H.-J. Wilke, S. Krischak, K. Wenger, and L. Claes, "Load-displacement properties of the thoracolumbar calf spine: Experimental results and comparison to known human data," *European Spine Journal*, vol. 6, no. 2, pp. 129–137, 1997.

[82] H. Wilke, P. Neef, M. Caimi, T. Hoogland, and L. E. Claes, "New in vivo measurements of pressures in the intervertebral disc in daily life," *Spine*, vol. 24, no. 8, pp. 755–762, 1999.

[83] I. Takahashi, S.-i. Kikuchi, K. Sato, and N. Sato, "Mechanical load of the lumbar spine during forward bending motion of the trunk–a biomechanical study," *Spine*, vol. 31, no. 1, pp. 18–23, 2006.

[84] K. Sato, S. Kikuchi, and T. Yonezawa, "In vivo intradiscal pressure measurement in healthy individuals and in patients with ongoing back problems," *Spine*, vol. 24, no. 23, p. 2468, 1999.

[85] G. Andersson, R. Ortengren, and A. Nachemson, "Intradiskal pressure, intra-abdominal pressure and myoelectric back muscle activity related to posture and loading," *Clinical Orthopaedics and Related Research*, no. 129, pp. 156–164, 1977.

[86] M. Jäger, A. Luttmann, and W. Laurig, "Lumbar load during one-handed bricklaying," *International Journal of Industrial Ergonomics*, vol. 8, no. 3, pp. 261–277, 1991.

[87] S. McGill, "Epidemiological studies and what they really mean," in *Low back disorders: evidence-based prevention and rehabilitation*. Human Kinetics, 2015, pp. 29–48.

[88] N. P. Reeves, K. S. Narendra, and J. Cholewicki, "Spine stability: The six blind men and the elephant," *Clinical Biomechanics*, vol. 22, no. 3, pp. 266–274, 2007.

[89] J. R. Beazell, M. Mullins, and T. L. Grindstaff, "Lumbar instability: An evolving and challenging concept," *Journal of Manual & Manipulative Therapy*, vol. 18, no. 1, pp. 9–14, 2010.

[90] S. M. McGill and J. Cholewicki, "Biomechanical basis for stability: An explanation to enhance clinical utility," *Journal of Orthopaedic & Sports Physical Therapy*, vol. 31, no. 2, pp. 96–100, 2001.

[91] A. White III, "The problem of clinical instability in the human spine: A systematic approach," *Clinical Biomechanics of the Spine*, 1990.

[92] M. M. Panjabi, "Clinical spinal instability and low back pain," *Journal of electromyography and kinesiology*, vol. 13, no. 4, pp. 371–379, 2003.

[93] J. S. Barr, "Low-back and sciatic pain: Results of treatment," *The Journal of Bone & Joint Surgery*, vol. 33, no. 3, pp. 633–649, 1951.

[94] M. H. Pope and M. Panjabi, "Biomechanical definitions of spinal instability," *Spine*, vol. 10, no. 3, pp. 255–256, 1985.

[95] W. Kirkaldy-Willis, "Presidential symposium on instability of the lumbar spine: Introduction," *Spine*, vol. 10, no. 3, p. 254, 1985.

[96] H. Almansour, W. Pepke, and M. Akbar, "Pyogenic spondylodiscitis," *Der Orthopäde*, vol. 49, no. 6, pp. 482–493, 2020.

[97] H. Mokhtarzadeh, F. Farahmand, A. Shirazi-Adl, N. Arjmand, F. Malekipour, and M. Parnianpour, "The effects of intra-abdominal pressure on the stability and unloading of the spine," *Journal of Mechanics in Medicine and Biology*, vol. 12, no. 01, p. 1 250 014, 2012.

[98] N. Arjmand and A. Shirazi-Adl, "Role of intra-abdominal pressure in the unloading and stabilization of the human spine during static lifting tasks," *European Spine Journal*, vol. 15, no. 8, pp. 1265–1275, 2006.

[99] S. McGill and R. W. Norman, "Reassessment of the role of intra-abdominal pressure in spinal compression," *Ergonomics*, vol. 30, no. 11, pp. 1565–1588, 1987.

[100] A. B. Ferguson, "The study and treatment of scoliosis," *Southern Medical Journal*, vol. 23, no. 2, pp. 116–120, 1930.

[101] T. Vrtovec, F. Pernuš, and B. Likar, "A review of methods for quantitative evaluation of spinal curvature," *European Spine Journal*, vol. 18, no. 5, pp. 593–607, 2009.

[102] J. Cobb, "Outlines for the study of scoliosis," *The American Academy of Orthopaedic Surgeons. Instructional Course Lectures*, pp. 261–275, 1948.

[103] I. A. Stokes, D. D. Aronson, P. J. Ronchetti, H. Labelle, and J. Dansereau, "Reexamination of the cobb and ferguson angles: Bigger is not always better," *Journal of Spinal Disorders*, vol. 6, pp. 333–333, 1993.

[104] J. Dunn, N. B. Henrikson, C. C. Morrison, M. Nguyen, P. R. Blasi, and J. S. Lin, "Screening for adolescent idiopathic scoliosis: A systematic evidence review for the us preventive services task force [internet]," 2018.

[105] M. Aebi, "The adult scoliosis," *European Spine Journal*, vol. 14, no. 10, pp. 925–948, 2005.

[106] F. Schwab, A. B. el-Fegoun, L. Gamez, H. Goodman, and J.-P. Farcy, "A lumbar classification of scoliosis in the adult patient: Preliminary approach," *Spine*, vol. 30, no. 14, pp. 1670–1673, 2005.

[107] E. Ascani, P. Bartolozzi, C. Logroscino, *et al.*, "Natural history of untreated idiopathic scoliosis after skeletal maturity.," *Spine*, vol. 11, no. 8, pp. 784–789, 1986.

[108] J. W. Hardacker, R. F. Shuford, P. N. Capicotto, and P. W. Pryor, "Radiographic standing cervical segmental alignment in adult volunteers without neck symptoms," *Spine*, vol. 22, no. 13, pp. 1472–1479, 1997.

[109] B. Alijani and J. Rasoulian, "The sagittal balance of the cervical spine: Radiographic analysis of interdependence between the occipitocervical and spinopelvic alignment," *Asian spine journal*, vol. 14, no. 3, p. 287, 2020.

[110] R. Vedantam, L. G. Lenke, J. A. Keeney, and K. H. Bridwell, "Comparison of standing sagittal spinal alignment in asymptomatic adolescents and adults," *Spine*, vol. 23, no. 2, pp. 211–215, 1998.

[111] D. E. Harrison, R. Cailliet, D. D. Harrison, T. J. Janik, and B. Holland, "Reliability of centroid, cobb, and harrison posterior tangent methods: Which to choose for analysis of thoracic kyphosis," *Spine*, vol. 26, no. 11, e227–e234, 2001.

[112] M. O'Brien, T. Kuklo, K. Blanke, and L. Lenke, *Spinal deformity study group radiographic measurement manual. memphis, tn: Medtronic sofamor danek usa*, 2004.

[113] D. E. Gelb, L. G. Lenke, K. H. Bridwell, K. Blanke, and K. W. McEnery, "An analysis of sagittal spinal alignment in 100 asymptomatic middle and older aged volunteers.," *Spine*, vol. 20, no. 12, pp. 1351–1358, 1995.

[114] Y. Yukawa, F. Kato, K. Suda, M. Yamagata, T. Ueta, and M. Yoshida, "Normative data for parameters of sagittal spinal alignment in healthy subjects: An analysis of gender specific differences and changes with aging in 626 asymptomatic individuals," *European Spine Journal*, vol. 27, no. 2, pp. 426–432, 2018.

[115] J. S. Smith, C. I. Shaffrey, K.-M. G. Fu, *et al.*, "Clinical and radiographic evaluation of the adult spinal deformity patient," *Neurosurgery Clinics*, vol. 24, no. 2, pp. 143–156, 2013.

[116] F. Mauch, C. Jung, J. Huth, and G. Bauer, "Changes in the lumbar spine of athletes from supine to the true-standing position in magnetic resonance imaging," *Spine*, vol. 35, no. 9, pp. 1002–1007, 2010.

[117] E. S. Lee, C. W. Ko, S. W. Suh, S. Kumar, I. K. Kang, and J. H. Yang, "The effect of age on sagittal plane profile of the lumbar spine according to standing, supine, and various sitting positions," *Journal of Orthopaedic Surgery and Research*, vol. 9, no. 1, pp. 1–10, 2014.

[118] G. E. Hicks, S. Z. George, M. A. Nevitt, J. A. Cauley, and M. T. Vogt, "Measurement of lumbar lordosis: Inter-rater reliability, minimum detectable change and longitudinal variation," *Clinical Spine Surgery*, vol. 19, no. 7, pp. 501–506, 2006.

[119] A. Briggs, T. Wrigley, E. Tully, P. Adams, A. Greig, and K. Bennell, "Radiographic measures of thoracic kyphosis in osteoporosis: Cobb and vertebral centroid angles," *Skeletal Radiology*, vol. 36, no. 8, pp. 761–767, 2007.

[120] R. P. Jackson and A. C. McManus, "Radiographic analysis of sagittal plane alignment and balance in standing volunteers and patients with low back pain matched for age, sex, and size. a prospective controlled clinical study.," *Spine*, vol. 19, no. 14, pp. 1611–1618, 1994.

[121] R. Vialle, N. Levassor, L. Rillardon, A. Templier, W. Skalli, and P. Guigui, "Radiographic analysis of the sagittal alignment and balance of the spine in asymptomatic subjects," *Journal of Bone and Joint Surgery*, vol. 87, no. 2, pp. 260–267, 2005.

[122] B. B. Hansen, T. Bendix, J. Grindsted, *et al.*, "Effect of lumbar disc degeneration and low-back pain on the lumbar lordosis in supine and standing: A cross-sectional mri study," *Spine*, vol. 40, no. 21, pp. 1690–1696, 2015.

[123] L. Kalichman, L. Li, D. J. Hunter, and E. Been, "Association between computed tomography–evaluated lumbar lordosis and features of spinal degeneration, evaluated in supine position," *The Spine Journal*, vol. 11, no. 4, pp. 308–315, 2011.

[124] V. Murrie, A. Dixon, W. Hollingworth, H. Wilson, and T. Doyle, "Lumbar lordosis: Study of patients with and without low back pain," *Clinical Anatomy: The Official Journal of the American Association of Clinical Anatomists and the British Association of Clinical Anatomists*, vol. 16, no. 2, pp. 144–147, 2003.

[125] M. L. Andreasen, L. Langhoff, T. S. Jensen, and H. B. Albert, "Reproduction of the lumbar lordosis: A comparison of standing radiographs versus supine magnetic resonance imaging obtained with straightened lower extremities," *Journal of Manipulative and Physiological Therapeutics*, vol. 30, no. 1, pp. 26–30, 2007.

[126] K. Singer, T. Jones, and P. Breidahl, "A comparison of radiographic and computer-assisted measurements of thoracic and thoracolumbar sagittal curvature," *Skeletal Radiology*, vol. 19, no. 1, pp. 21–26, 1990.

[127] F. J. Schwab, B. Blondel, S. Bess, *et al.*, "Radiographical spinopelvic parameters and disability in the setting of adult spinal deformity: A prospective multicenter analysis," *Spine*, vol. 38, no. 13, E803–E812, 2013.

[128] F. Schwab, A. Patel, B. Ungar, J.-P. Farcy, and V. Lafage, "Adult spinal deformity—postoperative standing imbalance: How much can you tolerate? an overview of key parameters in assessing alignment and planning corrective surgery," *Spine*, vol. 35, no. 25, pp. 2224–2231, 2010.

[129] S. Iyer, E. Sheha, M. C. Fu, *et al.*, "Sagittal spinal alignment in adult spinal deformity: An overview of current concepts and a critical analysis review," *JBJS reviews*, vol. 6, no. 5, e2, 2018.

[130] R. R. Pratali, M. A. Nasreddine, B. Diebo, C. E. A. Oliveira, and V. Lafage, "Normal values for sagittal spinal alignment: A study of brazilian subjects," *Clinics*, vol. 73, 2018.

[131] Q. Ma, L. Wang, L. Zhao, *et al.*, "Coronal balance vs. sagittal profile in adolescent idiopathic scoliosis, are they correlated?" *Frontiers in Pediatrics*, vol. 7, p. 523, 2020.

[132] P. Mangione, D. Gomez, and J. Senegas, "Study of the course of the incidence angle during growth," *European Spine Journal*, vol. 6, no. 3, pp. 163–167, 1997.

[133] P. Roussouly, "The standing position: Its principles and spinopelvic relations," in *Spinal Anatomy*, Springer, 2020, pp. 113–125.

[134] C. Marty, B. Boisaubert, H. Descamps, *et al.*, "The sagittal anatomy of the sacrum among young adults, infants, and spondylolisthesis patients," *European Spine Journal*, vol. 11, no. 2, pp. 119–125, 2002.

[135] P. Roussouly, S. Gollogly, E. Berthonnaud, and J. Dimnet, "Classification of the normal variation in the sagittal alignment of the human lumbar spine and pelvis in the standing position," *Spine*, vol. 30, no. 3, pp. 346–353, 2005.

[136] A. Sebaaly, P. Grobost, L. Mallam, and P. Roussouly, "Description of the sagittal alignment of the degenerative human spine," *European Spine Journal*, vol. 27, pp. 489–496, 2018.

[137] L. G. Lenke, R. R. Betz, J. Harms, *et al.*, "Adolescent idiopathic scoliosis: A new classification to determine extent of spinal arthrodesis," *Journal of Bone and Joint Surgery*, vol. 83, no. 8, pp. 1169–1181, 2001.

[138] J. Staal, H. Hlobil, M. Van Tulder, *et al.*, "Occupational health guidelines for the management of low back pain: An international comparison," *Occupational and Environmental Medicine*, vol. 60, no. 9, pp. 618–626, 2003.

[139] O. Airaksinen, J. I. Brox, C. Cedraschi, *et al.*, "European guidelines for the management of chronic nonspecific low back pain," *European Spine Journal*, vol. 15, no. Suppl 2, s192–s300, 2006.

[140] P. B. Polatin, W. E. Worzer, E. Brede, and R. J. Gatchel, "Quantification of function in chronic low back pain," in *Handbook of pain assessment*. Guilford Press, 2011.

[141] K. A. Szucs and E. V. D. Brown, "Rater reliability and construct validity of a mobile application for posture analysis," *Journal of Physical Therapy Science*, vol. 30, no. 1, pp. 31–36, 2018.

[142] D. G. Borenstein, S. W. Wiesel, and S. D. Boden, "Chapter 5 - physical examination," in *Low back and neck pain: comprehensive diagnosis and management.* Saunders, 2004, pp. 103–136.

[143] T. M. Khalil, E. M. Abdel-Moty, R. S. Rosomoff, and H. L. Rosomoff, "Low back pain management and the role of ergonomics," in *Ergonomics in back pain: a guide to prevention and rehabilitation*. Van Nostrand Reinhold Company, 1993, pp. 35–54.

[144] G. Cooper, "Treatment of acute lower back pain," in *Non-Operative Treatment of the Lumbar Spine*. Springer, 2015, pp. 15–18.

[145] G. Cooper, "Exercises for low back pain," in *Non-Operative Treatment of the Lumbar Spine*. Springer, 2015, pp. 85–87.

[146] C. M. Gubbels, P. A. Oakely, J. McAviney, D. E. Harrison, and B. T. Brown, "Reduction of scheuermann's deformity and scoliosis using scolibrace and a scoliosis specific rehabilitation program: A case report," *Journal of Physical Therapy Science*, vol. 31, no. 2, pp. 159–165, 2019.

[147] J. L. P. do Rosário, "Biomechanical assessment of human posture: A literature review," *Journal of Bodywork and Movement Therapies*, vol. 18, no. 3, pp. 368–373, 2014.

[148] C. Fortin, D. Ehrmann Feldman, F. Cheriet, and H. Labelle, "Clinical methods for quantifying body segment posture: A literature review," *Disability and Rehabilitation*, vol. 33, no. 5, pp. 367–383, 2011.

[149] G. Cooper, "When are imaging studies indicated and what do they tell us?" In *Non-Operative Treatment of the Lumbar Spine*. Springer, 2015, pp. 19–20.

[150] S. A. Shah, "Derotation of the spine," *Neurosurgery Clinics of North America*, vol. 18, no. 2, pp. 339–345, 2007.

[151] S. C. Cargill, M. Pearcy, and M. D. Barry, "Three-dimensional lumbar spine postures measured by magnetic resonance imaging reconstruction," *Spine*, vol. 32, no. 11, pp. 1242–1248, 2007.

[152] M. J. Turner, R. W. Clough, H. C. Martin, and L. Topp, "Stiffness and deflection analysis of complex structures," *Journal of the Aeronautical Sciences*, vol. 23, no. 9, pp. 805–823, 1956.

[153] G. E. Barron, "History and development," in *What every engineer should know about finite element analysis*. CRC Press, 1993, pp. 1–6.

[154] R. W. Clough, "The finite element method in plane stress analysis," in *Proceedings of 2nd ASCE Conference on Electronic Computation, Pittsburgh Pa., Sept. 8 and 9, 1960*, 1960.

[155] S. Bhavikatti, "Introduction," in *Finite element analysis*. New Age International, 2005, pp. 1–8.

[156] B. A. Szabo and I. Babuska, "Introduction," in *Introduction to finite element analysis: formulation, verification and validation*. John Wiley & Sons, 2011, vol. 35, pp. 1–15.

[157] W. Brekelmans, H. Poort, and T. Slooff, "A new method to analyse the mechanical behaviour of skeletal parts," *Acta Orthopaedica Scandinavica*, vol. 43, no. 5, pp. 301–317, 1972.

[158] W. Skalli, D. Mitton, P. Rouch, and J. Dubousset, "Biomechanics and spinal modelling," in *Spinal Anatomy: Modern Concepts*. Springer, 2020, pp. 491–503.

[159] M. Fagan, S. Julian, and A. Mohsen, "Finite element analysis in spine research," *Proceedings of the institution of mechanical engineers, part h: journal of engineering in medicine*, vol. 216, no. 5, pp. 281–298, 2002.

[160] F. Galbusera and F. Niemeyer, "Mathematical and finite element modeling," in *Biomechanics of the Spine: basic concepts, spinal disorders and treatments*. Elsevier, 2018, pp. 239–255.

[161] A. Ranavolo, R. Don, F. Draicchio, *et al.*, "Modelling the spine as a deformable body: Feasibility of reconstruction using an optoelectronic system," *Applied Ergonomics*, vol. 44, no. 2, pp. 192–199, 2013.

[162] A. C. Jones and R. K. Wilcox, "Finite element analysis of the spine: Towards a framework of verification, validation and sensitivity analysis," *Medical Engineering & Physics*, vol. 30, no. 10, pp. 1287–1304, 2008.

[163] M. J. Mills and N. Sarigul-Klijn, "Validation of an in vivo medical image-based young human lumbar spine finite element model," *Journal of Biomechanical Engineering*, vol. 141, no. 3, p. 031 003, 2019.

[164] A. Rohlmann, L. Bauer, T. Zander, G. Bergmann, and H.-J. Wilke, "Determination of trunk muscle forces for flexion and extension by using a validated finite element model of the lumbar spine and measured in vivo data," *Journal of Biomechanics*, vol. 39, no. 6, pp. 981–989, 2006.

[165] M. El-Rich and A. Shirazi-Adl, "Effect of load position on muscle forces, internal loads and stability of the human spine in upright postures," *Computer Methods in Biomechanics and Biomedical Engineering*, vol. 8, no. 6, pp. 359–368, 2005.

[166] M. Kurutz, *Finite element modelling of human lumbar spine*. Citeseer, 2010.

[167] T. Belytschko, R. Kulak, A. Schultz, and J. Galante, "Finite element stress analysis of an intervertebral disc," *Journal of Biomechanics*, vol. 7, no. 3, pp. 277–285, 1974.

[168] N. S. Hakim and A. I. King, "A three dimensional finite element dynamic response analysis of a vertebra with experimental verification," *Journal of Biomechanics*, vol. 12, no. 4, pp. 277–292, 1979.

[169] S. A. Shirazi-Adl, S. C. Shrivastava, and A. M. Ahmed, "Stress analysis of the lumbar disc-body unit in compression. a three-dimensional nonlinear finite element study," *Spine*, vol. 9, no. 2, pp. 120–134, 1984.

[170] A. Shirazi-Adl, A. Ahmed, and S. Shrivastava, "A finite element study of a lumbar motion segment subjected to pure sagittal plane moments," *Journal of Biomechanics*, vol. 19, no. 4, pp. 331–350, 1986.

[171] V. K. Goel, W. Kong, J. S. Han, J. N. Weinstein, and L. G. Gilbertson, "A combined finite element and optimization investigation of lumbar spine mechanics with and without muscles," *Spine*, vol. 18, no. 11, pp. 1531–1541, 1993.

[172] W. Z. Kong, V. K. Goel, L. G. Gilbertson, and J. N. Weinstein, "Effects of muscle dysfunction on lumbar spine mechanics: A finite element study based on a two motion segments model," *Spine*, vol. 21, no. 19, pp. 2197–2206, 1996.

[173] A. Rohlmann, T. Zander, M. Rao, and G. Bergmann, "Applying a follower load delivers realistic results for simulating standing," *Journal of Biomechanics*, vol. 42, no. 10, pp. 1520–1526, 2009.

[174] I. El Bojairami, K. El-Monajjed, and M. Driscoll, "Development and validation of a timely and representative finite element human spine model for biomechanical simulations," *Scientific Reports*, vol. 10, no. 1, pp. 1–15, 2020.

[175] I. El Bojairami and M. Driscoll, "Correlating skeletal muscle output force and intramuscular pressure via a 3-dimensional finite element muscle model," *Journal of Biomechanical Engineering*, 2021.

[176] X.-Y. Zhang and Y. Han, "Comparison of the biomechanical effects of lumbar disc degeneration on normal patients and osteoporotic patients: A finite element analysis," *Medical Engineering & Physics*, vol. 112, p. 103 952, 2023.

[177] B. Allaire, D. Lu, F. Johannesdottir, *et al.*, "Prediction of incident vertebral fracture using ct-based finite element analysis," *Osteoporosis International*, vol. 30, pp. 323–331, 2019.

[178] H.-Z. Zeng, L.-D. Zheng, M.-L. Xu, *et al.*, "Biomechanical effect of age-related structural changes on cervical intervertebral disc: A finite element study," *Proceedings of the Institution of Mechanical Engineers, Part H: Journal of Engineering in Medicine*, vol. 236, no. 10, pp. 1541–1551, 2022.

[179] S. Kang, C.-H. Park, H. Jung, *et al.*, "Analysis of the physiological load on lumbar vertebrae in patients with osteoporosis: A finite-element study," *Scientific Reports*, vol. 12, no. 1, p. 11 001, 2022.

[180] M. Bashkuev, S. Reitmaier, and H. Schmidt, "Effect of disc degeneration on the mechanical behavior of the human lumbar spine: A probabilistic finite element study," *The Spine Journal*, vol. 18, no. 10, pp. 1910–1920, 2018.

[181] X.-y. Cai, M.-s. Sun, Y.-p. Huang, *et al.*, "Biomechanical effect of l4–l5 intervertebral disc degeneration on the lower lumbar spine: A finite element study," *Orthopaedic Surgery*, vol. 12, no. 3, pp. 917–930, 2020.

[182] S. Wang, W. M. Park, Y. H. Kim, T. Cha, K. Wood, and G. Li, "In vivo loads in the lumbar l3–4 disc during a weight lifting extension," *Clinical Biomechanics*, vol. 29, no. 2, pp. 155–160, 2014.

[183] W. M. Park, K. Kim, and Y. H. Kim, "Effects of degenerated intervertebral discs on intersegmental rotations, intradiscal pressures, and facet joint forces of the whole lumbar spine," *Computers in Biology and Medicine*, vol. 43, no. 9, pp. 1234–1240, 2013.

[184] S.-H. Chen, Z.-C. Zhong, C.-S. Chen, W.-J. Chen, and C. Hung, "Biomechanical comparison between lumbar disc arthroplasty and fusion," *Medical Engineering & Physics*, vol. 31, no. 2, pp. 244–253, 2009.

[185] A. G. Bruno, M. L. Bouxsein, and D. E. Anderson, "Development and validation of a musculoskeletal model of the fully articulated thoracolumbar spine and rib cage," *Journal of Biomechanical Engineering*, vol. 137, no. 8, p. 081 003, 2015.

[186] M. Xu, J. Yang, I. H. Lieberman, and R. Haddas, "Lumbar spine finite element model for healthy subjects: Development and validation," *Computer Methods in Biomechanics and Biomedical Engineering*, vol. 20, no. 1, pp. 1–15, 2017.

[187] S. Naserkhaki, J. L. Jaremko, and M. El-Rich, "Effects of inter-individual lumbar spine geometry variation on load-sharing: Geometrically personalized finite element study," *Journal of Biomechanics*, vol. 49, no. 13, pp. 2909–2917, 2016.

[188] J. M. Warren, A. P. Mazzoleni, and L. A. Hey, "Development and validation of a computationally efficient finite element model of the human lumbar spine: Application to disc degeneration," *International Journal of Spine Surgery*, vol. 14, no. 4, pp. 502–510, 2020.

[189] M. Driscoll, C.-É. Aubin, A. Moreau, and S. Parent, "Finite element comparison of different growth sparring instrumentation systems for the early treatment of idiopathic scoliosis," in *Research into Spinal Deformities 7*, IOS Press, 2010, pp. 89–94.

[190] I. Villemure, C.-É. Aubin, J. Dansereau, and H. Labelle, "Simulation of progressive deformities in adolescent idiopathic scoliosis using a biomechanical model integrating vertebral growth modulation," *Journal of Biomechanical Engineering*, vol. 124, no. 6, pp. 784–790, 2002.

[191] J. Clin, C.-É. Aubin, A. Sangole, H. Labelle, and S. Parent, "Correlation between immediate in-brace correction and biomechanical effectiveness of brace treatment in adolescent idiopathic scoliosis," *Spine*, vol. 35, no. 18, pp. 1706–1713, 2010.

[192] M. Driscoll, C.-É. Aubin, A. Moreau, I. Villemure, and S. Parent, "The role of spinal concave–convex biases in the progression of idiopathic scoliosis," *European Spine Journal*, vol. 18, pp. 180–187, 2009.

[193] A. Shirazi-Adl and M. Parnianpour, "Effect of changes in lordosis on mechanics of the lumbar spine-lumbar curvature in lifting," *Clinical Spine Surgery*, vol. 12, no. 5, pp. 436–447, 1999.

[194] R. M. C. Aroeira, A. E. M. Pertence, D. T. Kemmoku, and M. Greco, "The effect of hypokyphosis on the biomechanical behavior of the adolescent thoracic spine," *Journal of the Brazilian Society of Mechanical Sciences and Engineering*, vol. 40, no. 3, pp. 1–10, 2018.

[195] W. Wei, S. Liao, S. Shi, J. Fei, Y. Wang, and C. Chen, "Straightened cervical lordosis causes stress concentration: A finite element model study," *Australasian Physical & Engineering Sciences in Medicine*, vol. 36, pp. 27–33, 2013.

[196] A. E. Anderson, B. J. Ellis, and J. A. Weiss, "Verification, validation and sensitivity studies in computational biomechanics," *Computer Methods in Biomechanics and Biomedical Engineering*, vol. 10, no. 3, pp. 171–184, 2007.

[197] American Society of Mechanical Engineers: V&V40 Committee, "Assessing credibility of computational modeling through verification and validation: Application to medical devices," *The American Society of Mechanical Engineers*, 2018.

[198] T. M. Morrison, P. Hariharan, C. M. Funkhouser, P. Afshari, M. Goodin, and M. Horner, "Assessing computational model credibility using a risk-based framework: Application to hemolysis in centrifugal blood pumps," *Asaio Journal*, vol. 65, no. 4, p. 349, 2019.

[199] A. Bailey, "Risk factors for low back pain in women: Still more questions to be answered," *Menopause*, vol. 16, no. 1, pp. 3–4, 2009.

[200] C. D. Fryar, M. D. Carroll, Q. Gu, J. Afful, and C. L. Ogden, "Anthropometric reference data for children and adults: United states, 2015-2018," 2021.

[201] J. Wilke, F. Krause, L. Vogt, and W. Banzer, "What is evidence-based about myofascial chains: A systematic review," *Archives of Physical Medicine and Rehabilitation*, vol. 97, no. 3, pp. 454–461, 2016.

[202] S. McGill, "Functional anatomy of the lumbar spine," in *Low back disorders: evidence-based prevention and rehabilitation*. Human Kinetics, 2015, pp. 49–96.

[203] C. Fan, C. Fede, N. Gaudreault, *et al.*, "Anatomical and functional relationships between external abdominal oblique muscle and posterior layer of thoracolumbar fascia," *Clinical Anatomy*, vol. 31, no. 7, pp. 1092–1098, 2018.

[204] P. Brinckmann and H. Grootenboer, "Change of disc height, radial disc bulge, and intradiscal pressure from discectomy an in vitro investigation on human lumbar discs," *Spine*, vol. 16, no. 6, pp. 641–646, 1991.

[205] A. Rohlmann, H. N. Boustani, G. Bergmann, and T. Zander, "Effect of a pedicle-screw-based motion preservation system on lumbar spine biomechanics: A probabilistic finite element study with subsequent sensitivity analysis," *Journal of Biomechanics*, vol. 43, no. 15, pp. 2963–2969, 2010.

[206] M. Xu, J. Yang, I. Lieberman, and R. Haddas, "Stress distribution in vertebral bone and pedicle screw and screw–bone load transfers among various fixation methods for lumbar spine surgical alignment: A finite element study," *Medical Engineering & Physics*, vol. 63, pp. 26–32, 2019.

[207] Q. H. Zhang and E. C. Teo, "Finite element application in implant research for treatment of lumbar degenerative disc disease," *Medical Engineering & Physics*, vol. 30, no. 10, pp. 1246–1256, 2008.

[208] S. Thaker, R. Botchu, H. Gupta, C. Azzopardi, L. Boyce, and G. Retnasingam, "Magnetic resonance spine localizers – the "forgotten" treasure," *Indian Journal of Musculoskeletal Radiology*, vol. 4, pp. 128–33, 2022.

[209] F. Desbiens-Blais, J. Clin, S. Parent, H. Labelle, and C.-É. Aubin, "New brace design combining cad/cam and biomechanical simulation for the treatment of adolescent idiopathic scoliosis," *Clinical Biomechanics*, vol. 27, no. 10, pp. 999–1005, 2012.

[210] J. Clin, C.-É. Aubin, S. Parent, and H. Labelle, "A biomechanical study of the charleston brace for the treatment of scoliosis," *Spine*, vol. 35, no. 19, E940–E947, 2010.

[211] S. Naserkhaki, J. L. Jaremko, S. Adeeb, and M. El-Rich, "On the load-sharing along the ligamentous lumbosacral spine in flexed and extended postures: Finite element study," *Journal of Biomechanics*, vol. 49, no. 6, pp. 974–982, 2016.

[212] S. Zhang, Z. Liu, C. Lu, *et al.*, "Oblique lateral interbody fusion combined with different internal fixations for the treatment of degenerative lumbar spine disease: A finite element analysis," *BMC Musculoskeletal Disorders*, vol. 23, no. 1, pp. 1–10, 2022.

[213] R. Wang and Z. Wu, "Recent advancement in finite element analysis of spinal interbody cages: A review," *Frontiers in Bioengineering and Biotechnology*, vol. 11, p. 1 041 973, 2023.

[214] X. Liu, J. Ma, P. Park, X. Huang, N. Xie, and X. Ye, "Biomechanical comparison of multi-level lateral interbody fusion with and without supplementary instrumentation: A three-dimensional finite element study," *BMC Musculoskeletal Disorders*, vol. 18, pp. 1–11, 2017.

[215] M. Driscoll, J.-M. Mac-Thiong, H. Labelle, S. Parent, *et al.*, "Development of a detailed volumetric finite element model of the spine to simulate surgical correction of spinal deformities," *BioMed research international*, vol. 2013, 2013.

[216] F. Galbusera, C. M. Bellini, F. Anasetti, C. Ciavarro, A. Lovi, and M. Brayda-Bruno, "Rigid and flexible spinal stabilization devices: A biomechanical comparison," *Medical Engineering & Physics*, vol. 33, no. 4, pp. 490–496, 2011.

[217] US Food and Drug Administration, "Assessing the credibility of computational modeling and simulation in medical device submissions. draft guidance for industry and food and drug administration staff," *Food and Drug Administration: Silver Spring, MD, USA*, 2021.

[218] T. P. F. Bento, C. V. dos Santos Genebra, N. M. Maciel, G. P. Cornelio, S. F. A. P. Simeão, and A. de Vitta, "Low back pain and some associated factors: Is there any difference between genders?" *Brazilian Journal of Physical Therapy*, vol. 24, no. 1, pp. 79–87, 2020.

[219] A. Bener, E. E. Dafeeah, K. Alnaqbi, *et al.*, "An epidemiologic analysis of low back pain in primary care: A hot humid country and global comparison," *Journal of Primary Care & Community Health*, vol. 4, no. 3, pp. 220–227, 2013.

[220] M. Caglayan, O. Tacar, A. Demirant, *et al.*, "Effects of lumbosacral angles on development of low back pain," *Journal of Musculoskeletal Pain*, vol. 22, no. 3, pp. 251–255, 2014.

[221] G. Skundric, V. Vukicevic, and N. Lukic, "Effects of core stability exercises, lumbar lordosis and low-back pain: A systematic review," *Journal of Anthropology of Sport and Physical Education*, vol. 5, no. 1, pp. 17–23, 2021.

[222] F. A. El-Hamalawy, "A newly developed exercise program for treatment of mechanical low back pain associated with accentuated lumbar lordosis," *Journal of American Science*, vol. 7, no. 8, pp. 58–70, 2011.

[223] H. Li, H. Luo, W. Huan, *et al.*, "Automatic lumbar spinal mri image segmentation with a multi-scale attention network," *Neural Computing and Applications*, vol. 33, pp. 11 589–11 602, 2021.

[224] L. Lenchik, L. Heacock, A. A. Weaver, *et al.*, "Automated segmentation of tissues using ct and mri: A systematic review," *Academic Radiology*, vol. 26, no. 12, pp. 1695–1706, 2019.

[225] J.-M. Vital and D. T. Cawley, *Spinal Anatomy: Modern Concepts*. Springer, 2020.

[226] J. M. Morris, D. B. Lucas, and B. Bresler, "Role of the trunk in stability of the spine," *Journal of Bone and Joint Surgery*, vol. 43, no. 3, pp. 327–351, 1961.

[227] M. Sharma, N. A. Langrana, and J. Rodriguez, "Role of ligaments and facets in lumbar spinal stability.," *Spine*, vol. 20, no. 8, pp. 887–900, 1995.

[228] D. J. Polga, B. P. Beaubien, P. M. Kallemeier, *et al.*, "Measurement of in vivo intradiscal pressure in healthy thoracic intervertebral discs," *Spine*, vol. 29, no. 12, pp. 1320–1324, 2004.

[229] H.-J. Wilke, P. Neef, B. Hinz, H. Seidel, and L. Claes, "Intradiscal pressure together with anthropometric data–a data set for the validation of models," *Clinical Biomechanics*, vol. 16, S111–S126, 2001.

[230] F. Heuer, H. Schmidt, L. Claes, and H.-J. Wilke, "Stepwise reduction of functional spinal structures increase vertebral translation and intradiscal pressure," *Journal of Biomechanics*, vol. 40, no. 4, pp. 795–803, 2007.

[231] A. Rohlmann, S. Neller, L. Claes, G. Bergmann, and H.-J. Wilke, "Influence of a follower load on intradiscal pressure and intersegmental rotation of the lumbar spine," *Spine*, vol. 26, no. 24, E557–E561, 2001.

[232] H.-J. Wilke, A. Herkommer, K. Werner, and C. Liebsch, "In vitro analysis of the intradiscal pressure of the thoracic spine," *Frontiers in Bioengineering and Biotechnology*, vol. 8, p. 614, 2020.

[233] U. M. Ayturk and C. M. Puttlitz, "Parametric convergence sensitivity and validation of a finite element model of the human lumbar spine," *Computer Methods in Biomechanics and Biomedical Engineering*, vol. 14, no. 8, pp. 695–705, 2011.

[234] A. Breen, D. De Carvalho, M. Funabashi, *et al.*, "A reference database of standardised continuous lumbar intervertebral motion analysis for conducting patient-specific comparisons," *Frontiers in Bioengineering and Biotechnology*, p. 863, 2021.

[235] J. Dvořák, M. Panjabi, D. Chang, R. Theiler, and D. Grob, "Functional radiographic diagnosis of the lumbar spine: Flexion–extension and lateral bending," *Spine*, vol. 16, no. 5, p. 562, 1991.

[236] R.-M. Lin, C.-Y. Yu, Z.-J. Chang, C.-C. Lee, and F.-C. Su, "Flexion-extension rhythm in the lumbosacral spine.," *Spine*, vol. 19, no. 19, pp. 2204–2209, 1994.

[237] M. Pearcy, I. Portek, and J. Shepherd, "Three-dimensional x-ray analysis of normal movement in the lumbar spine.," *Spine*, vol. 9, no. 3, pp. 294–297, 1984.

[238] M. J. Pearcy, "Stereo radiography of lumbar spine motion," *Acta Orthopaedica Scandinavica*, vol. 56, no. sup212, pp. 1–45, 1985.

[239] A. Plamondon, M. Gagnon, and G. Maurais, "Application of a stereoradiographic method for the study of intervertebral motion," *Spine*, vol. 13, no. 9, pp. 1027–1032, 1988.

[240] K. W. Wong, J. C. Leong, M.-k. Chan, K. D. Luk, and W. W. Lu, "The flexion–extension profile of lumbar spine in 100 healthy volunteers," *Spine*, vol. 29, no. 15, pp. 1636–1641, 2004.

[241] C. P. Ames, M. H. Bozkus, R. H. Chamberlain, *et al.*, "Biomechanics of stabilization after cervicothoracic compression-flexion injury," *Spine*, vol. 30, no. 13, pp. 1505–1512, 2005.

[242] V. Deviren, E. Acaroglu, J. Lee, *et al.*, "Pedicle screw fixation of the thoracic spine: An in vitro biomechanical study on different configurations," *Spine*, vol. 30, no. 22, pp. 2530–2537, 2005.

[243] R. Kothe, M. M. Panjabi, and W. Liu, "Multidirectional instability of the thoracic spine due to iatrogenic pedicle injuries during transpedicular fixation: A biomechanical investigation," *Spine*, vol. 22, no. 16, pp. 1836–1842, 1997.

[244] T. R. Kuklo, A. E. Dmitriev, M. J. Cardoso, R. A. Lehman Jr, M. Erickson, and N. W. Gill, "Biomechanical contribution of transverse connectors to segmental stability following long segment instrumentation with thoracic pedicle screws," *Spine*, vol. 33, no. 15, E482–E487, 2008.

[245] J. Miller, A. Schultz, D. Warwick, and D. Spencer, "Mechanical properties of lumbar spine motion segments under large loads," *Journal of Biomechanics*, vol. 19, no. 1, pp. 79–84, 1986.

[246] W. Morgenstern, S. J. Ferguson, S. Berey, T. E. Orr, and L.-P. Nolte, "Posterior thoracic extrapedicular fixation: A biomechanical study," *Spine*, vol. 28, no. 16, pp. 1829–1835, 2003.

[247] M. M. Panjabi, T. Oxland, I. Yamamoto, and J. J. Crisco, "Mechanical behavior of the human lumbar and lumbosacral spine as shown by three-dimensional load-displacement curves," *Journal of Bone and Joint Surgery*, vol. 76, no. 3, pp. 413–424, 1994.

[248] S. N. Sangiorgio, S. L. Borkowski, R. E. Bowen, A. A. Scaduto, N. L. Frost, and E. Ebramzadeh, "Quantification of increase in three-dimensional spine flexibility following sequential ponte osteotomies in a cadaveric model," *Spine Deformity*, vol. 1, no. 3, pp. 171–178, 2013.

[249] M. M. Sran, K. M. Khan, Q. Zhu, and T. R. Oxland, "Posteroanterior stiffness predicts sagittal plane midthoracic range of motion and three-dimensional flexibility in cadaveric spine segments," *Clinical Biomechanics*, vol. 20, no. 8, pp. 806–812, 2005.

[250] J.-S. Tan, S. Singh, Q.-A. Zhu, M. F. Dvorak, C. G. Fisher, and T. R. Oxland, "The effect of cement augmentation and extension of posterior instrumentation on stabilization and adjacent level effects in the elderly spine," *Spine*, vol. 33, no. 25, pp. 2728–2740, 2008.

[251] R. Watkins IV, R. Watkins III, L. Williams, *et al.*, "Stability provided by the sternum and rib cage in the thoracic spine," *Spine*, vol. 30, no. 11, pp. 1283–1286, 2005.

[252] H.-J. Wilke, A. Herkommer, K. Werner, and C. Liebsch, "In vitro analysis of the segmental flexibility of the thoracic spine," *PLOS ONE*, vol. 12, no. 5, e0177823, 2017.

[253] I. Yamamoto, M. M. Panjabi, T. Crisco, and T. Oxland, "Three-dimensional movements of the whole lumbar spine and lumbosacral joint," *Spine*, vol. 14, no. 11, pp. 1256–1260, 1989.

[254] S. McGill, *Low back disorders: evidence-based prevention and rehabilitation*. Human Kinetics, 2015.

[255] J. Buschmann and G. M. Bürgisser, *Biomechanics of tendons and ligaments: tissue reconstruction and regeneration*. Woodhead Publishing, 2017.

[256] G. Cooper, *Non-Operative Treatment of the Lumbar Spine*. Springer, 2015.

[257] D. C. Turk and R. Melzack, *Handbook of pain assessment*. Guilford Press, 2011.

[258] M. P. McKinley, V. D. O'Loughlin, and T. Stouter, *Anatomie et physiologie: une approche intégrée*. Chenelière éducation, 2014.

[259] F. Galbusera and H.-J. Wilke, *Biomechanics of the Spine: basic concepts, spinal disorders and treatments*. Elsevier, 2018.

[260] T. M. Khalil, *Ergonomics in back pain: a guide to prevention and rehabilitation*. Van Nostrand Reinhold Company, 1993.

[261] G. D. Cramer and S. A. Darby, *Clinical anatomy of the spine, spinal cord, and ANS*. Elsevier Health Sciences, 2014.

[262] J. E. Pope and T. R. Deer, *Treatment of Chronic Pain Conditions: A Comprehensive Handbook*. Springer, 2017.

A Appendix

A.1 Comparator Classification

The following tables provide a brief overview of some available comparators for IVD stress (Tables A.1.1, A.1.2, and A.1.3) and ISR (Tables A.1.4, A.1.5, and A.1.6) existing in literature, at the time of this thesis. The tables serve to provide a reference for available comparators for spine modelling validation and future studies. Values recorded from graphs were measured as accurately as possible but are approximate. The following categories are provided to classify the identified studies:

- **IVD:** The identified intervertebral disc evaluated in the study.
- **Segment:** The identified segment of the spine evaluated in the study.
- **Task or Load:** The task that was performed by the study participant in *in vivo* studies, or the loading conditions that were described in *ex vivo* or *in silico* studies.
- **Pressure:** The measured intervertebral disc pressure.
- **Rotation:** The measured rotational movement of the spinal segment.
- **Subject:** Relevant information pertaining to the study subject or participant, including the number of participants, sex, age, height, and weight, when available.

The following abbreviations are of note:

- **IVD:** Intervertebral disc.
- **FL:** Follower load.
- **M:** Moment.
- **N:** Newton.
- **Nm:** Newton-meter.

Table A.1.1: Reference Summary for Intervertebral Disc Pressure Comparators: in vivo.

Ref.	First Author (year)	IVD	Task or Loads	Pressure (MPa)*	Subject
[85]	Andersson (1977)†‡	L3/L4	Standing	0.331 (0.034 std error)	4 participants, 1 male, 3 females (age: 26-34 yrs,
		L3/L4	Flexion: 30°	0.8	weight: 52-69 kg)
[79]	Nachemson (1964)‡	L3	Standing	0.88	19 patients with back pain
		L3	Sitting	1.24	
		L4	Standing	0.9	
		L4	Sitting	1.12	
[80]	Nachemson (1966)‡	L3	Upright	0.29	1 male (approximate loads, weight: 70 kg)
		L3	Flexion: 20°	0.39	
		L3	Upright	0.59	1 male (approximate loads, weight: 70 kg)
		L3	Flexion: 20°	0.78	Moderately degenerated disc
		L3	Upright	0.29	1 male (approximate loads, weight: 90 kg)
		L3	Flexion: 20°	0.49	
[228]	Polga (2004)†‡	T6/T7, T7/T8	Upright	1.01 ± 0.06 *(0.87-1.15)*	6 participants, 4 males, 2 females (mean age: 28 yrs,
		T9/T10, T10/T11	Upright	0.86 ± 0.06 *(0.59-1.04)*	height: 178 cm, weight: 73 kg)
		T6/T7, T7/T8	Extension: 15°	1.17 ± 0.16 *(0.83-1.77)*	
		T9/T10, T10/T11	Extension: 15°	1.00 ± 0.08 *(0.72-1.34)*	
		T6/T7, T7/T8	Flexion: 30°	0.94 ± 0.09 *(0.79-1.14)*	
		T9/T10, T10/T11	Flexion: 30°	1.09 ± 0.05 *(0.85-1.23)*	
[84]	Sato (1999)	L4/L5	Upright	0.539 ± 0.179	8 healthy individuals (mean age: 25 yrs, height:
		L4/L5	Flexion	1.324 ± 0.222	174 cm, weight: 73 kg)
		L4/L5	Extension	0.600 ± 0.187	
		L4/L5	Sitting: upright	0.623 ± 0.154	
		L4/L5	Sitting: flexion	1.133 ± 0.254	
		L4/L5	Sitting: extension	0.737 ± 0.167	
		L4/L5	Prone (healthy disc)	0.091 ± 0.025	

Table A.1.1 continued from previous page

Ref.	First Author (year)	IVD	Task or Loads	Pressure (MPa)*	Subject
Cont.	Sato (1999)	L4/L5	Prone (mild degeneration)	0.072 ± 0.042	28 back pain patients, 18 males, 10 females (mean
		L4/L5	Prone (moderate degeneration)	0.032 ± 0.045	age: 45 yrs, height: 165 cm, weight: 68 kg)
		L4/L5	Prone (severe degeneration)	0.010 ± 0.020	
[9]	Schultz (1982)†‡	L3	Standing	0.27	4 participants, 1 male, 3 females (age: 19-23 yrs)
		L3	Flexion: 30°	1.04	
[83]	Takahashi (2006)‡	L4/L5	Upright	0.35	3 healthy males (mean age: 25.5 yrs, height: 176 cm,
		L4/L5	Flexion: 30°	1.6	weight: 72 kg)
[82]	Wilke (1999)‡	L4/L5	Standing	0.5	1 male (age: 45 yrs, height: 168 cm, weight: 70 kg)
		L4/L5	Standing, bent forward	1.10	
		L4/L5	Sitting	0.46	
		L4/L5	Sitting, maximum flexion	0.83	
		L4/L5	Lying prone	0.11	
[229]	Wilke (2001)†‡	L4/L5	Flexion: 36°	1.08	1 male (age: 45 yrs, height: 168 cm, weight: 70 kg)
		L4/L5	Extension: 19°	0.6	
		L4/L5	Sitting	0.45 to 0.5	
		L4/L5	Sitting, bending forward 20°	0.63	

*Values are reported as mean ± standard deviation or *median (range)*

†Authors also reported lateral bending and/or axial rotation

‡Authors also reported additional and/or weighted positions

Table A.1.2: Reference Summary for Intervertebral Disc Pressure Comparators: ex vivo.

Ref.	First Author (year)	IVD	Task or Loads	Pressure (MPa)*	Subject
[204]	Brinckmann (1991)	T12/L1	Compression: 300N	0.55 ± 0.06, *0.54 (0.49-0.64)*	15 discs from cadaveric specimens (age: 20-40 yrs)
		T12/L1	Compression: 1000N	1.35 ± 0.14, *1.41 (1.12-1.47)*	
		T12/L1	Compression: 2000N	2.57 ± 0.29, *2.69 (2.08-2.82)*	
		L1/L2	Compression: 300N	0.32	
		L1/L2	Compression: 1000N	0.92	
		L1/L2	Compression: 2000N	1.68	
		L2/L3	Compression: 300N	0.38 ± 0.06, *0.36 (0.31-0.49)*	
		L2/L3	Compression: 1000N	1.08 ± 0.18, *1.03 (0.9-1.41)*	
		L2/L3	Compression: 2000N	2.05 ± 0.36, *1.98 (1.68-2.71)*	
		L3/L4	Compression: 300N	0.34	
		L3/L4	Compression: 1000N	0.96	
		L3/L4	Compression: 2000N	1.82	
		L4/L5	Compression: 300N	0.30 ± 0.08, *0.31 (0.20-0.46)*	
		L4/L5	Compression: 1000N	0.90 ± 0.24, *0.93 (0.61-1.38)*	
		L4/L5	Compression: 2000N	1.85 ± 0.42, *1.88 (1.3-2.64)*	
[230]	Heuer (2007)†	L4/L5	Flexion: 1Nm	*0.05 (0.02-0.15)*	Cadaveric specimens, 4 males, 4 females (mean age:
		L4/L5	Extension: 1Nm	*0.03 (0.01-0.15)*	52 yrs, range: 38-59)
		L4/L5	Flexion: 2.5Nm	*0.1 (0.06-0.18)*	
		L4/L5	Extension: 2.5Nm	*0.85 (0-0.18)*	
		L4/L5	Flexion: 5Nm	*0.2 (0.11-0.22)*	
		L4/L5	Extension: 5Nm	*0.17 (0-0.22)*	
		L4/L5	Flexion: 7.5Nm	*0.24 (0.2-0.35)*	
		L4/L5	Extension: 7.5Nm	*0.18 (0-0.3)*	
		L4/L5	Flexion: 10Nm	*0.37 (0.22-0.4)*	
		L4/L5	Extension: 10Nm	*0.19 (0-0.35)*	
[231]	Rohlmann (2001)†	L4-L5	Flexion: 3.75Nm	0.04	10 cadaveric specimens (mean age: 46 yrs, range: 18-74)

Table A.1.2 continued from previous page

Ref.	First Author (year)	IVD	Task or Loads	Pressure (MPa)*	Subject
Cont.	Rohlmann (2001)†	L4/L5	Extension: 3.75Nm	0.1	
		L4/L5	Flexion: 7.5Nm	0.095	
		L4/L5	Extension: 7.5Nm	0.15	
		L4/L5	Flexion: 280N FL+7.5Nm M	0.22	
		L4/L5	Extension: 280N FL+7.5Nm M	0.28	
[232]	Wilke (2020)†	T1-T12	Flexion: 2.5Nm	*0.15 (0.05-0.3)*	Cadaveric specimens, 11 males, 19 females (mean age:
		T1-T12	Extension: 2.5Nm	*0.15 (-0.025-0.65)*	56 yrs, range: 43-75)
		T1-T12	Flexion: 5Nm	*0.28 (0.08-0.73)*	
		T1-T12	Extension: 5Nm	*0.3 (-0.02-0.65)*	
		T1-T12	Flexion: 7.5Nm	*0.4 (0.1-1.1)*	
		T1-T12	Extension: 7.5Nm	*0.2 (-0.015-0.81)*	
		T1-T5	Flexion: 2.5Nm	*0.22 (0.12-0.4)*	
		T1-T5	Extension: 2.5Nm	*0.16 (-0.02-0.4)*	
		T1-T5	Flexion: 5Nm	*0.52 (0.24-0.79)*	
		T1-T5	Extension: 5Nm	*0.16 (-0.01-0.5)*	
		T1-T5	Flexion: 7.5Nm	*0.8 (0.38-1.22)*	
		T1-T5	Extension: 7.5Nm	*0.1 (-0.005-0.34)*	
		T5-T8	Flexion: 2.5Nm	*0.1 (0.02-0.3)*	
		T5-T8	Extension: 2.5Nm	*0.1 (-0.04-0.4)*	
		T5-T8	Flexion: 5Nm	*0.2 (0.08-0.85)*	
		T5-T8	Extension: 5Nm	*0.1 (-0.03-0.66)*	
		T5-T8	Flexion: 7.5Nm	*0.32 (0.12-1.12)*	
		T5-T8	Extension: 7.5Nm	*0.08 (-0.02-0.81)*	
		T8-T12	Flexion: 2.5Nm	*0.1 (0.06-1.16)*	
		T8-T12	Extension: 2.5Nm	*0.18 (0-0.32)*	
		T8-T12	Flexion: 5Nm	*0.24 (0.16-0.34)*	
		T8-T12	Extension: 5Nm	*0.31 (-0.01-0.57)*	

Table A.1.2 continued from previous page

Ref.	First Author (year)	IVD	Task or Loads	Pressure (MPa)*	Subject
Cont.	Wilke (2020)†	T8-T12	Flexion: 7.5Nm	*0.39 (0.28-0.5)*	
		T8-T12	Extension: 7.5Nm	*0.4 (-0.01-0.76)*	
		T1-T12	Flexion: 2.5Nm	*0.12 (0.01-0.22)*	Male cadaver discs
		T1-T12	Extension: 2.5Nm	*0.13 (0.02-0.32)*	
		T1-T12	Flexion: 5Nm	*0.22 (0.08-0.39)*	
		T1-T12	Extension: 5Nm	*0.15 (0.015-0.5)*	
		T1-T12	Flexion: 7.5Nm	*0.38 (0.11-0.79)*	
		T1-T12	Extension: 7.5Nm	*0.1 (0-0.5)*	
		T1-T12	Flexion: 2.5Nm	*0.12 (0.02-0.49)*	Female cadaver discs
		T1-T12	Extension: 2.5Nm	*0.18 (-0.02-0.4)*	
		T1-T12	Flexion: 5Nm	*0.24 (0.08-0.82)*	
		T1-T12	Extension: 5Nm	*0.35 (-0.02-0.62)*	
		T1-T12	Flexion: 7.5Nm	*0.38 (0.11-0.79)*	
		T1-T12	Extension: 7.5Nm	*0.39 (-0.02-0.81)*	

*Values are reported as mean ± standard deviation or *median (range)*

†Authors also reported lateral bending and/or axial rotation

‡Authors also reported additional and/or weighted positionsor, or with spinal instrumentation

Table A.1.3: Reference Summary for Intervertebral Disc Pressure Comparators: in silico.

Ref.	First Author (year)	IVD	Task or Loads	Pressure (MPa)*	Subject
[233]	Ayturk (2011)†	L2/L3	Flexion: 3Nm	0.22 ± 0.12	1 lumbar spine model (L1-L5)
		L2/L3	Extension: 3Nm	0.12 ± 0.1	
		L3/L4	Flexion: 3Nm	0.155 ± 0.09	
		L3/L4	Extension: 3Nm	0.115 ± 0.07	
		L4/L5	Flexion: 7.5Nm	0.425 ± 0.08	
		L4/L5	Extension: 7.5Nm	0.24 ± 0.1	
[74]	Dreischarf (2014)	L1/L2	Flexion: 1175N FL+7.5Nm M	*1.6 (1.2-1.95)*	8 lumbar spine models (L1-L5)
		L1/L2	Extension: 500N FL+7.5Nm M	*0.55 (0.2-1.05)*	
		L2/L3	Flexion: 1175N FL+7.5Nm M	*1.4 (1.15-1.9)*	
		L2/L3	Extension: 500N FL+7.5Nm M	*0.5 (0.15-0.85)*	
		L3/L4	Flexion: 1175N FL+7.5Nm M	*1.35 (1.05-1.6)*	
		L3/L4	Extension: 500N FL+7.5Nm M	*0.45 (0.15-0.9)*	
		L4/L5	Flexion: 1175N FL+7.5Nm M	*1.2 (1-1.55)*	
		L4/L5	Extension: 500N FL+7.5Nm M	*0.5 (0.15-0.95)*	
		L4/L5	Compression: 300N	*(0.2-0.5)*	
		L4/L5	Compression: 1000N	*(0.255-.255)*	
[163]	Mills (2019)	L2/L3	Moment: 3Nm	0.12 ± 0.1	1 female lumbar spine model (L2-L5, age: 20 yrs)
		L3/L4	Moment: 3Nm	0.18 ± 0.13	
		L4/L5	Moment: 7.5Nm	0.47 ± 0.29	
		L4/L5	Compression: 300N	0.33	
		L4/L5	Compression: 1000N	0.93	
[187]	Naserkhaki (2016)‡	L1/L2	Flexion: 500N FL+12Nm M	1	1 lumbar spine model (L1-S1), normal curvature
		L1/L2	Extension: 500N FL+7.5Nm M	0.5	
		L2/L3	Flexion: 500N FL+12Nm M	0.9	
		L2/L3	Extension: 500N FL+7.5Nm M	0.4	

Table A.1.3 continued from previous page

Ref.	First Author (year)	IVD	Task or Loads	Pressure (MPa)*	Subject
Cont.	Naserkhaki (2016)‡	L3/L4	Flexion: 500N FL+12Nm M	0.85	
		L3/L4	Extension: 500N FL+7.5Nm M	0.45	
		L4/L5	Flexion: 500N FL+12Nm M	0.75	
		L4/L5	Extension: 500N FL+7.5Nm M	0.4	
		L5/S1	Flexion: 500N FL+12Nm M	0.97	
		L5/S1	Extension: 500N FL+7.5Nm M	0.43	
		L1/L2	Flexion: 500N FL+12Nm M	1.05	1 lumbar spine model (L1-S1), hypolordotic curvature
		L1/L2	Extension: 500N FL+7.5Nm M	0.6	
		L2/L3	Flexion: 500N FL+12Nm M	0.85	
		L2/L3	Extension: 500N FL+7.5Nm M	0.42	
		L3/L4	Flexion: 500N FL+12Nm M	0.8	
		L3/L4	Extension: 500N FL+7.5Nm M	0.4	
		L4/L5	Flexion: 500N FL+12Nm M	0.85	
		L4/L5	Extension: 500N FL+7.5Nm M	0.5	
		L5/S1	Flexion: 500N FL+12Nm M	0.83	
		L5/S1	Extension: 500N FL+7.5Nm M	0.47	
		L1/L2	Flexion: 500N FL+12Nm M	1.13	1 lumbar spine model (L1-S1), hyperlordotic curvature
		L1-L2	Extension: 500N FL+7.5Nm M	0.42	
		L2/L3	Flexion: 500N FL+12Nm M	0.96	
		L2/L3	Extension: 500N FL+7.5Nm M	0.45	
		L3/L4	Flexion: 500N FL+12Nm M	0.9	
		L3/L4	Extension: 500N FL+7.5Nm M	0.47	
		L4/L5	Flexion: 500N FL+12Nm M	0.84	
		L4/L5	Extension: 500N FL+7.5Nm M	0.4	
		L5/S1	Flexion: 500N FL+12Nm M	0.8	
		L5/S1	Extension: 500N FL+7.5Nm M	0.31	
[75]	Newell (2021)	L1/L2	Flexion: 1175N FL+7.5Nm M	1.457	1 healthy lumbar spine model (L1-S1)

Table A.1.3 continued from previous page

Ref.	First Author (year)	IVD	Task or Loads	Pressure (MPa)*	Subject
Cont.	Newell (2021)	L2/L3	Flexion: 1175N FL+7.5Nm M	1.364	
		L3/L4	Flexion: 1175N FL+7.5Nm M	1.494	
		L4/L5	Flexion: 1175N FL+7.5Nm M	1.198	
		L5/S1	Flexion: 1175N FL+7.5Nm M	1.079	
		L1/L2	Flexion: 1175N FL+7.5Nm M	1.454	1 LBP lumbar spine model (L1-S1)
		L2/L3	Flexion: 1175N FL+7.5Nm M	1.362	
		L3/L4	Flexion: 1175N FL+7.5Nm M	1.486	
		L4/L5	Flexion: 1175N FL+7.5Nm M	1.188	
		L5/S1	Flexion: 1175N FL+7.5Nm M	1.074	
[73]	Rohlmann (2009)‡	L1/L2	Flexion: 500N FL+7.5Nm M	0.6	1 lumbar spine model (L1-L5)
		L1/L2	Extension: 500N FL+7.5Nm M	0.65	
		L2/L3	Flexion: 500N FL+7.5Nm M	0.55	
		L2/L3	Extension: 500N FL+7.5Nm M	0.55	
		L3/L4	Flexion: 500N FL+7.5Nm M	0.5	
		L3/L4	Extension: 500N FL+7.5Nm M	0.51	
		L4/L5	Flexion: 500N FL+7.5Nm M	0.5	
		L4/L5	Extension: 500N FL+7.5Nm M	0.58	
		L5/S1	Flexion: 500N FL+7.5Nm M	0.52	
		L5/S1	Extension: 500N FL+7.5Nm M	0.6	
[182]	Wang (2014)†	L3/L4	Upright	1.4 *(1.0-1.6)*	3 lumbar spine models (L1-L5) of healthy males (mean age:
		L3/L4	Flexion: 20°	0.6 *(0.4-0.8)*	48.3 yrs, height: 177 cm, weight: 7.4 kg)
		L3/L4	Extension: 20°	0.6 *(0.5-0.7)*	
[188]	Warren (2020)	L4/L5	Compression: 1000N	0.68	1 healthy lumbar spine model (L1-L5)
[186]	Xu (2017)†	L1/L2	Flexion: 1175N FL+7.5Nm M	*1.8 (1.4-2.2)*	5 lumbar spine models (L1-L5), 3 males, 2 females (age:
		L1/L2	Extension: 500N FL+7.5Nm M	*0.8 (0.5-1.3)*	22-49 yrs)
		L2/L3	Flexion: 1175N FL+7.5Nm M	*1.55 (1.35-2.15)*	

Table A.1.3 continued from previous page

Ref.	First Author (year)	IVD	Task or Loads	Pressure (MPa)*	Subject
Cont.	Xu (2017)†	L2/L3	Extension: 500N FL+7.5Nm M	*0.6 (0.3-1)*	
		L3/L4	Flexion: 1175N FL+7.5NM M	*1.25 (1.05-1.6)*	
		L3/L4	Extension: 500N FL+7.5Nm M	*0.65 (0.25-1)*	
		L4/L5	Flexion: 1175N FL+7.5Nm M	*1.45 (1.2-1.75)*	
		L4/L5	Extension: 500N FL+7.5Nm M	*0.68 (0.35-1.15)*	
		L4/L5	Compression: 300N	0.4 ± 0.05	
		L4/L5	Compression: 1000N	1.05 ± 0.17	

*Values are reported as mean ± standard deviation or *median (range)*

†Authors also reported lateral bending and/or axial rotation

‡Authors also reported additional and/or weighted positions, or with spinal instrumentation

Table A.1.4: Reference Summary for Intersegmental Rotation Comparators: in vivo.

Ref.	First Author (year)	Segment	Task or Loads	Rotation (°)*	Subject
[234]	Breen (2021)	L2-L3	Flexion: 60°	9.5 ± 3.87	127 participants, 75 males, 62 females (mean age: 38.6 yrs, height:
		L3-L4	Flexion: 60°	10.6 ± 2.96	1.73 m, weight: 71.6 kg)
		L4-L5	Flexion: 60°	10.4 ± 3.93	
		L5-S1	Flexion: 60°	5.7 ± 5.60	
		L2-L3	Flexion: 60°	10.2 ± 1.4	8 healthy participants, 5 males, 3 females (mean age: 48.1 yrs, height:
		L3-L4	Flexion: 60°	11.5 ± 2.8	1.70 m, weight: 74.5 kg)
		L4-L5	Flexion: 60°	11.9 ± 3.5	
		L5-S1	Flexion: 60°	7.2 ± 3.9	
		L2-L3	Flexion: 60°	8.9 ± 5.2	8 LBP patients, 5 males, 3 females (mean age: 48.8 yrs, height: 1.70 m,
		L3-L4	Flexion: 60°	10.1 ± 2.8	weight: 75.4 kg)
		L4-L5	Flexion: 60°	8.7 ± 1.1	
		L5-S1	Flexion: 60°	3.2 ± 2.9	
[235]	Dvorák (1991)†	L1-L2	Flexion-extension	11.9 ± 2.27 *(8.6-17.9)*	41 healthy participants
		L2-L3	Flexion-extension	14.5 ± 2.29 *(9.5-19.1)*	23 males (mean age: 36 yrs, range 22-45)
		L3-L4	Flexion-extension	15.3 ± 2.04 *(11.9-21.0)*	18 females (mean age: 39 yrs, range: 29-50)
		L4-L5	Flexion-extension	18.2 ± 2.99 *(11.6-25.6)*	
		L5-S1	Flexion-extension	17.0 ± 4.33 *(6.3-23.7)*	
[236]	Lin (1994)	L1-L2	Standing	7.4 ± 2.9	89 healthy volunteers, 50 males, 39 females (mean age: 52 yrs)
		L1-L2	Flexion	1.7 ± 2.3	
		L1-L2	Extension	8.6 ± 2.9	
		L2-L3	Standing	9.6 ± 3.4	
		L2-L3	Flexion	2.0 ± 3.3	
		L2-L3	Extension	10.7 ± 3.6	
		L3-L4	Standing	10.9 ± 3.4	
		L3-L4	Flexion	0.4 ± 2.8	
		L3-L4	Extension	13.0 ± 4.4	

Table A.1.4 continued from previous page

Ref.	First Author (year)	Segment	Task or Loads	Rotation (°)*	Subject
Cont.	Lin (1994)	L4-L5	Standing	12.2 ± 4.4	
		L4-L5	Flexion	-0.4 ± 3.5	
		L4-L5	Extension	14.0 ± 3.8	
		L5-S1	Standing	13.7 ± 5.0	
		L5-S1	Flexion	5.3 ± 3.6	
		L5-S1	Extension	17.1 ± 5.8	
[237]	Pearcy (1984)†	L1-L2	Flexion	8 ± 5	11 healthy male participants (mean age: 29.5 yrs, range: 25-36)
		L1-L2	Extension	5 ± 2	*Note: this data is also reported in [238]*
		L2-L3	Flexion	10 ± 2	
		L2-L3	Extension	3 ± 2	
		L3-L4	Flexion	12 ± 1	
		L3-L4	Extension	1 ± 1	
		L4-L5	Flexion	13 ± 4	
		L4-L5	Extension	2 ± 1	
		L5-S1	Flexion	9 ± 6	
		L5-S1	Extension	5 ± 4	
[238]	Pearcy (1985)†	L1-S1	Flexion-extension	67 ± 11 *(55-83)*	11 healthy male participants (mean age: 29 yrs)
		L1-S1	Flexion	51 ± 9 *(40-62)*	
		L1-S1	Extension	16 ± 6 *(9-21)*	
		L1-L2	Flexion-extension	13 ± 5 *(6-20)*	
		L1-L2	Flexion	8 ± 5	
		L1-L2	Extension	5 ± 2	
		L2-L3	Flexion-extension	14 ± 2 *(10-16)*	
		L2-L3	Flexion	10 ± 2	
		L2-L3	Extension	3 ± 2	
		L3-L4	Flexion-extension	13 ± 2 *(11-18)*	
		L3-L4	Flexion	12 ± 1	

Table A.1.4 continued from previous page

Ref.	First Author (year)	Segment	Task or Loads	Rotation (°)*	Subject
Cont.	Pearcy (1985)†	L3-L4	Extension	1 ± 1	
		L4-L5	Flexion-extension	16 ± 4 *(9-19)*	
		L4-L5	Flexion	13 ± 4	
		L4-L5	Extension	2 ± 1	
		L5-S1	Flexion-extension	14 ± 5 *(3-21)*	
		L5-S1	Flexion	9 ± 6	
		L5-S1	Extension	5 ± 4	
[239]	Plamondon (1988)†	L1	Flexion	5.1 ± 2.1	16 participants, 11 males, 5 females (age: 25±7 yrs, height: 1.72±0.06 m,
		L1	Extension	3.0 ± 3.0	weight: 67.7±8.4 kg)
		L2	Flexion	8.8 ± 0.8	
		L2	Extension	3.9 ± 2.9	
		L3	Flexion	11.6 ± 2.7	
		L3	Extension	2.1 ± 0.9	
		L4	Flexion	13.1 ± 1.7	
		L4	Extension	1.2 ± 1.2	
[240]	Wong (2004)‡	L1-L2	Flexion: 30°	9.4	100 healthy participants, 50 males, 50 females (mean age: 39.2 yrs,
		L2-L3	Flexion: 30°	8.1	range: 20-76)
		L3-L4	Flexion: 30°	7.9	
		L4-L5	Flexion: 30°	5.8	
		L5-S1	Flexion: 30°	3.5	
		L1-L2	Flexion: 30°	7.9 ± 3.3	30 participants (age: 21-30 yrs)
		L2-L3	Flexion: 30°	7.6 ± 2.4	
		L3-L4	Flexion: 30°	6.4 ± 2.4	
		L4-L5	Flexion: 30°	4.3 ± 2.1	
		L5-S1	Flexion: 30°	1.9 ± 2.1	
		L1-L2	Flexion: 30°	8.2 ± 3.0	26 participants (age: 31-40yrs)
		L2-L3	Flexion: 30°	7.4 ± 2.2	

Table A.1.4 continued from previous page

Ref.	First Author (year)	Segment	Task or Loads	Rotation (°)*	Subject
Cont.	Wong (2004)‡	L3-L4	Flexion: 30°	6.0 ± 1.9	
		L4-L5	Flexion: 30°	3.2 ± 2.0	
		L5-S1	Flexion: 30°	2.0 ± 1.0	
		L1-L2	Flexion: 30°	8.2 ± 2.6	21 participants (age: 41-50 yrs)
		L2-L3	Flexion: 30°	8.0 ± 2.0	
		L3-L4	Flexion: 30°	7.9 ± 1.3	
		L4-L5	Flexion: 30°	4.5 ± 2.2	
		L5-S1	Flexion: 30°	2.5 ± 1.0	
		L1-L2	Flexion: 30°	11.8 ± 3.0	23 participants (age: >50 yrs)
		L2-L3	Flexion: 30°	11.7 ± 2.7	
		L3-L4	Flexion: 30°	10.1 ± 2.1	
		L4-L5	Flexion: 30°	6.4 ± 2.0	
		L5-S1	Flexion: 30°	5.5 ± 1.6	
		L1-L2	Flexion: 30°	8.8 ± 2.0	50 male participants
		L2-L3	Flexion: 30°	8.6 ± 1.3	
		L3-L4	Flexion: 30°	7.6 ± 1.2	
		L4-L5	Flexion: 30°	5.7 ± 1.4	
		L5-S1	Flexion: 30°	3.7 ± 1.0	
		L1-L2	Flexion: 30°	9.9 ± 2.3	50 female participants
		L2-L3	Flexion: 30°	7.6 ± 1.3	
		L3-L4	Flexion: 30°	8.1 ± 1.3	
		L4-L5	Flexion: 30°	5.5 ± 0.9	
		L5-S1	Flexion: 30°	2.8 ± 1.1	

*Values are reported as mean ± standard deviation or *median (range)*

†Authors also reported lateral bending and/or axial rotation

‡Authors also reported additional and/or weighted positions

Table A.1.5: Reference Summary for Intersegmental Rotation Comparators: ex vivo.

Ref.	First Author (year)	Segment	Task or Loads	Rotation (°)*	Subject
[241]	Ames (2005)†‡	C6-C7	Flexion: 1.5Nm	4.88 ± 1.45	7 cadaveric specimens, 6 males, 1 female (mean age:
		C6-C7	Extension: 1.5Nm	4.35 ± 1.44	49.3 yrs, range: 21-72)
		C7-T1	Flexion: 1.5Nm	3.29 ± 0.69	
		C7-T1	Extension: 1.5Nm	2.28 ± 0.85	
		T1-T2	Flexion: 1.5Nm	1.92 ± 0.63	
		T1-T2	Extension: 1.5Nm	1.46 ± 0.44	
[242]	Deviren (2005)†‡	T5-T11	Flexion-extension: 4Nm	17.5 ± 2	8 cadaveric specimens (mean age: 63 yrs)
[243]	Kothe (1997)‡	T5-T9, T6-T10	Flexion-extension: 5Nm	6.2 ± 1.4	10 cadaveric specimens, 7 males, 3 females (mean age:
		T8-T12, T9-L1	Flexion-extension: 5Nm	5.7 ± 2.1	48 yrs, range: 19-73)
[244]	Kuklo (2008)†‡	T4-T10	Flexion-extension: 6Nm	14.01 ± 4.90	8 cadaveric specimens
[245]	Miller (1986)†	Lumbar	Flexion: 70Nm	4.9 ± 0.3	9 male cadaveric specimens (T12-L5, mean age: 28.7
		segments	Extension: 70Nm	4.1 ± 1.0	yrs, range: 18-41)
[246]	Morgenstern (2003)†	T5-T8	Flexion-extension: 8Nm	*11.5 (1.5-17.3)*	12 cadaveric specimens, 9 males, 3 females
[247]	Panjabi (1994)†	L1-L2	Flexion: 2.5Nm	3.5 ± 1.5	9 male lumbosacral spine cadaveric specimens (L1 or
		L1-L2	Extension: 2.5Nm	2.8 ± 1.2	L2 to S1, mean age: 51 yrs, range: 35-62)
		L1-L2	Flexion: 5Nm	4 ± 1.2	
		L1-L2	Extension: 5Nm	3.2 ± 1.2	
		L1-L2	Flexion: 7.5Nm	4.8 ± 1.3	
		L1-L2	Extension: 7.5Nm	3.9 ± 1	
		L1-L2	Flexion: 10Nm	5.2 ± 1	
		L1-L2	Extension: 10Nm	4.1 ± 1.8	
		L2-L3	Flexion: 2.5Nm	5.3 ± 1.2	
		L2-L3	Extension: 2.5Nm	1.8 ± 0.4	
		L2-L3	Flexion: 5Nm	6.2 ± 0.8	
		L2-L3	Extension: 5Nm	2.9 ± 1	

Table A.1.5 continued from previous page

Ref.	First Author (year)	Segment	Task or Loads	Rotation (°)*	Subject
Cont.	Panjabi (1994)†	L2-L3	Flexion: 7.5Nm	6.5 ± 1.3	
		L2-L3	Extension: 7.5Nm	3 ± 1.1	
		L2-L3	Flexion: 10Nm	6.8 ± 1.2	
		L2-L3	Extension: 10Nm	3.4 ± 1.2	
		L3-L4	Flexion: 2.5 Nm	5.2 ± 2.4	
		L3-L4	Extension: 2.5Nm	1.5 ± 1.1	
		L3-L4	Flexion: 5Nm	6.1 ± 3	
		L3-L4	Extension: 5Nm	2.4 ± 1.2	
		L3-L4	Flexion: 7.5Nm	6.5 ± 2	
		L3-L4	Extension: 7.5Nm	2.1 ± 0.9	
		L3-L4	Flexion: 10Nm	7.4 ± 1.8	
		L3-L4	Extension: 10Nm	2.7 ± 1.2	
		L4-L5	Flexion: 2.5Nm	6.2 ± 2.1	
		L4-L5	Extension: 2.5Nm	2.4 ± 0.8	
		L4-L5	Flexion: 5Nm	7.8 ± 2.6	
		L4-L5	Extension: 5Nm	2.3 ± 2.1	
		L4-L5	Flexion: 7.5Nm	8.5 ± 2.7	
		L4-L5	Extension: 7.5Nm	3.2 ± 1.5	
		L4-L5	Flexion: 10Nm	9 ± 2.8	
		L4-L5	Extension: 10Nm	3.6 ± 1.6	
		L5-S1	Flexion: 2.5Nm	6.8 ± 2.3	
		L5-S1	Extension: 2.5Nm	3.3 ± 2.7	
		L5-S1	Flexion: 5Nm	7.9 ± 2.1	
		L5-S1	Extension: 5Nm	5.3 ± 1.9	
		L5-S1	Flexion: 7.5 Nm	8.8 ± 1.8	
		L5-S1	Extension: 7.5Nm	5.5 ± 2	
		L5-S1	Flexion: 10Nm	8.9 ± 2	

Table A.1.5 continued from previous page

Ref.	First Author (year)	Segment	Task or Loads	Rotation (°)*	Subject
Cont.	Panjabi (1994)†	L5-S1	Extension: 10Nm	5.7 ± 2.4	
[231]	Rohlmann (2001)†	L1-L5	Flexion-extension: 3.75Nm	*16.5 (16-22)*	5 cadaveric specimens (age: 18-33 yrs)
		L1-L5	Flexion-extension: 7.5Nm	*29 (27-34)*	
		L1-L5	Flexion-extension: 280N FL + 7.5Nm M	*32 (28-35.5)*	
		L1-L5	Flexion-extension: 3.75Nm	*23.5 (16-25)*	5 cadaveric specimens (age: 58-74 yrs)
		L1-L5	Flexion-extension: 7.5Nm	*33 (23-37)*	
		L1-L5	Flexion-extension: 280N FL + 7.5Nm M	*33 (23-37.5)*	
[248]	Sangiorgio (2013)†	T2-T5, T8-T11	Flexion-extension: 6Nm	5.7 ± 4.9 *(1.0-11.0)*	4 cadaveric specimens, 3 males, 1 female (age: 72±10 yrs)
		T2-T5, T8-T11	Flexion: 6Nm	2.7 ± 1.9 *(0.5-5.3)*	
		T2-T5, T8-T11	Extension: 6Nm	3.0 ± 3.1 *(0.5-7.1)*	
[76]	Sis (2016)†‡	T1-T4	Flexion-extension: 5Nm	12.3 ± 8.09	8 cadaveric specimens, 4 males, 4 females (T1-T12, age: 66.9±4.4 yrs)
		T1-T4	Flexion: 5Nm	8.23 ± 5.60	
		T1-T4	Extension: 5Nm	4.08 ± 2.54	
		T4-T8	Flexion-extension: 5Nm	5.17 ± 3.27	
		T4-T8	Flexion: 5Nm	3.70 ± 2.50	
		T4-T8	Extension: 5Nm	1.44 ± 0.81	
		T8-T12	Flexion-extension: 5Nm	2.80 ± 1.51	
		T8-T12	Flexion: 5Nm	5.63 ± 3.28	
		T8-T12	Extension: 5Nm	2.17 ± 1.14	
		T1-T2	Flexion-extension: 5Nm	7.23 ± 5.73	
		T1-T2	Flexion: 5Nm	4.58 ± 3.73	
		T1-T2	Extension: 5Nm	2.79 ± 1.99	
		T4-T5	Flexion-extension: 5Nm	1.53 ± 1.06	
		T4-T5	Flexion: 5Nm	1.10 ± 0.89	
		T4-T5	Extension: 5Nm	0.42 ± 0.21	

Table A.1.5 continued from previous page

Ref.	First Author (year)	Segment	Task or Loads	Rotation (°)*	Subject
Cont.	Sis (2016)†‡	T8-T9	Flexion-extension: 5Nm	1.57 ± 1.00	
		T8-T9	Flexion: 5Nm	1.12 ± 0.76	
		T8-T9	Extension: 5Nm	0.44 ± 0.25	
		T11-T12	Flexion-extension: 5Nm	3.90 ± 2.54	
		T11-T12	Flexion: 5Nm	2.62 ± 1.75	
		T11-T12	Extension: 5Nm	1.23 ± 0.81	
[249]	Sran (2005)†	T5-T6	Flexion: 4Nm	0.65 ± 0.66 *(0.02-2.06)*	8 cadaveric specimens, 3 males, 5 females (mean age:
		T5-T6	Extension: 4Nm	0.80 ± 0.73 *(0.07-1.92)*	81 yrs)
		T6-T7	Flexion: 4Nm	1.25 ± 0.87 *(0.17-2.54)*	
		T6-T7	Extension: 4Nm	1.31 ± 0.81 *(0.15-2.24)*	
		T7-T8	Extension: 4Nm	0.99 ± 0.74 *(0.28-2.52)*	
[250]	Tan (2008)†‡	T10-T12	Flexion-extension: 5Nm	4.3 ± 1.2	10 cadaveric specimens, 3 males, 7 females (mean age:
		T12-L1	Flexion-extension: 5Nm	2.7 ± 1.3	75 yrs, range: 64-84)
[251]	Watkins (2005)†	T1-T12	Flexion-extension: 2Nm	7.93 *(2.64-15.64)*	10 cadaveric specimens (mean age: 72 yrs) + rib cage
		T1-T12	Flexion-extension: 2Nm	13.17 *(3.11-29.29)*	without rib cage
[252]	Wilke (2017)†	T1-T2	Flexion: 7.5Nm	7.1 ± 0.5	29 cadaveric specimens, 13 males, 16 females (mean
		T1-T2	Extension: 7.5Nm	6.7 ± 0.3	age: 57 yrs, range: 40-80)
		T2-T3	Flexion: 7.5Nm	4.1 ± 1.8	Total of 68 thoracic functional spinal units: 6 tested
		T2-T3	Extension: 7.5Nm	4.0 ± 1.7	per thoracic segment
		T3-T4	Flexion: 7.5Nm	3.8 ± 1.0	
		T3-T4	Extension: 7.5Nm	3.8 ± 1.0	
		T4-T5	Flexion: 7.5Nm	3.4 ± 0.7	
		T4-T5	Extension: 7.5Nm	3.3 ± 0.7	
		T5-T6	Flexion: 7.5Nm	3.8 ± 1.3	
		T5-T6	Extension: 7.5Nm	3.8 ± 1.3	
		T6-T7	Flexion: 7.5Nm	3.9 ± 0.9	

Table A.1.5 continued from previous page

Ref.	First Author (year)	Segment	Task or Loads	Rotation (°)*	Subject
Cont.	Wilke (2017)†	T6-T7	Extension: 7.5Nm	3.7 ± 1.0	
		T7-T8	Flexion: 7.5Nm	2.8 ± 0.5	
		T7-T8	Extension: 7.5Nm	2.8 ± 0.5	
		T8-T9	Flexion: 7.5 Nm	3.2 ± 0.7	
		T8-T9	Extension: 7.5Nm	3.2 ± 0.7	
		T9-T10	Flexion: 7.5Nm	3.5 ± 0.8	
		T9-T10	Extension: 7.5Nm	3.5 ± 0.8	
		T10-T11	Flexion: 7.5Nm	3.1 ± 0.9	
		T10-T11	Extension: 7.5Nm	3.1 ± 1.0	
		T11-T12	Flexion: 7.5Nm	3.6 ± 0.7	
		T11-T12	Extension: 7.5Nm	3.5 ± 0.8	
[253]	Yamamoto (1989)†	L1-L2	Flexion: 10Nm	5.8 ± 0.6	10 cadaveric specimens (age: 25-63 yrs)
		L1-L2	Extension: 10Nm	4.3 ± 0.5	
		L2-L3	Flexion: 10Nm	6.5 ± 0.3	
		L2-L3	Extension: 10Nm	4.3 ± 0.3	
		L3-L4	Flexion: 10Nm	7.5 ± 0.8	
		L3-L4	Extension: 10Nm	3.7 ± 0.3	
		L4-L5	Flexion: 10Nm	8.9 ± 0.7	
		L4-L5	Extension: 10Nm	5.8 ± 0.4	
		L5-S1	Flexion: 10Nm	10.0 ± 1.0	
		L5-S1	Extension: 10Nm	7.8 ± 0.7	

*Values are reported as mean ± standard deviation or *median (range)*

†Authors also reported lateral bending and/or axial rotation

‡Authors also reported additional and/or weighted positions, or with spinal instrumentation

Table A.1.6: Reference Summary for Intersegmental Rotation Comparators: in silico.

Ref.	First Author (year)	Segment	Task or Loads	Rotation (°)*	Subject
[233]	Ayturk (2011)†‡	L1-L5	Flexion-extension: 7.5Nm	35.27	1 lumbar spine model (L1-L5)
		L1-L2	Flexion: 7.5Nm	4	
		L1-L2	Extension: 7.5Nm	4	
		L2-L3	Flexion: 7.5Nm	5.5	
		L2-L3	Extension: 7.5Nm	3	
		L3-L4	Flexion: 7.5Nm	5.5	
		L3-L4	Extension: 7.5Nm	2.6	
		L4-L5	Flexion: 7.5Nm	6	
		L4-L5	Extension: 7.5Nm	4	
[184]	Chen (2009)†‡	L1-L5	Flexion: 10Nm M+150N preload	17	1 male lumbar spine model (L1-L5, middle-aged)
		L1-L5	Extension: 10Nm M+150N preload	15	
[74]	Dreischarf (2014)	L1-L5	Flexion-extension: 7.5Nm	*33.5 (24-40.5)*	8 lumbar spine models (L1-L5)
		L1-L2	Flexion: 1175N FL+7.5Nm M	*3.5 (3.8-6)*	
		L1-L2	Extension: 500N FL+7.5Nm M	*3.2 (1.8-4.4)*	
		L2-L3	Flexion: 1175N FL+7.5Nm M	*5.5 (3.5-6)*	
		L2-L3	Extension: 500N FL+7.5Nm M	*2.9 (1.99-3.9)*	
		L3-L4	Flexion: 1175N FL+7.5Nm M	*5.3 (4.2-5.5)*	
		L3-L4	Extension: 500N FL+7.5Nm M	*3 (2-3.8)*	
		L4-L5	Flexion: 1175N FL+7.5Nm M	*6 (4-7)*	
		L4-L5	Extension: 500N FL+7.5Nm M	*3.2 (2.1-4.5)*	
[163]	Mills (2019)†	L2-S1	Flexion-extension: 7.5Nm	38	1 female lumbar spine model (L2-L5, age: 20 yrs)
		L2-L3	Flexion: 10Nm	5	
		L2-L3	Extension: 10Nm	4.5	
		L3-L4	Flexion: 10Nm	6	
		L3-L4	Extension: 10Nm	6	
		L4-L5	Flexion: 10Nm	6.5	

Table A.1.6 continued from previous page

Ref.	First Author (year)	Segment	Task or Loads	Rotation (°)*	Subject
Cont.	Mills (2019)†	L4-L5	Extension: 10Nm	5.5	
		L5-S1	Flexion: 10Nm	5.5	
		L5-S1	Extension: 10Nm	5.8	
[187]	Naserkhaki (2016)	L1-L2	Flexion: 500N FL+12Nm M	4.5	1 lumbar spine model (L1-S1), normal curvature
		L1-L2	Extension: 500N FL+7.5Nm M	3	
		L2-L3	Flexion: 500N FL+12Nm M	5.5	
		L2-L3	Extension: 500N FL+7.5Nm M	2.5	
		L3-L4	Flexion: 500N FL+12Nm M	6	
		L3-L4	Extension: 500N FL+7.5Nm M	3	
		L4-L5	Flexion: 500N FL+12Nm M	7	
		L4-L5	Extension: 500N FL+7.5Nm M	3.5	
		L5-S1	Flexion: 500N FL+12Nm M	7	
		L5-S1	Extension: 500N FL+7.5Nm M	4	
		L1-L2	Flexion: 500N FL+12Nm M	5	1 lumbar spine model (L1-S1), hypolordotic curvature
		L1-L2	Extension: 500N FL+7.5Nm M	4	
		L2-L3	Flexion: 500N FL+12Nm M	5.2	
		L2-L3	Extension: 500N FL+7.5Nm M	3.5	
		L3-L4	Flexion: 500N FL+12Nm M	5.1	
		L3-L4	Extension: 500N FL+7.5Nm M	4	
		L4-L5	Flexion: 500N FL+12Nm M	5	
		L4-L5	Extension: 500N FL+7.5Nm M	4.5	
		L5-S1	Flexion: 500N FL+12Nm M	5.5	
		L5-S1	Extension: 500N FL+7.5Nm M	4.5	
		L1-L2	Flexion: 500N FL+12Nm M	5	1 lumbar spine model (L1-S1), hyperlordotic curvature
		L1-L2	Extension: 500N FL+7.5Nm M	3	
		L2-L3	Flexion: 500N FL+12Nm M	5.5	
		L2-L3	Extension: 500N FL+7.5Nm M	2.5	

Table A.1.6 continued from previous page

Ref.	First Author (year)	Segment	Task or Loads	Rotation (°)*	Subject
Cont.	Naserkhaki (2016)	L3-L4	Flexion: 500N FL+12Nm M	5.2	
		L3-L4	Extension: 500N FL+7.5Nm M	3.6	
		L4-L5	Flexion: 500N FL+12Nm M	6	
		L4-L5	Extension: 500N FL+7.5Nm M	2.5	
		L5-S1	Flexion: 500N FL+12Nm M	5.5	
		L5-S1	Extension: 500N FL+7.5Nm M	1.5	
[75]	Newell (2021)	L1-L2	Flexion: 1175N FL+7.5Nm M	10	1 healthy lumbar spine model (L1-S1)
		L2-L3	Flexion: 1175N FL+7.5Nm M	8.38	
		L3-L4	Flexion: 1175N FL+7.5Nm M	6.7	
		L4-L5	Flexion: 1175N FL+ 7.5Nm M	4.78	
		L5-S1	Flexion: 1175N FL+7.5Nm M	4.2	
		L1-L2	Flexion: 1175N FL+7.5Nm M	10.08	1 LBP lumbar model (L1-L5)
		L2-L3	Flexion: 1175N FL+7.5Nm M	8.46	
		L3-L4	Flexion: 1175N FL+7.5Nm M	6.89	
		L4-L5	Flexion: 1175N FL+7.5Nm M	4.87	
		L5-S1	Flexion: 1175N FL+7.5Nm M	4.26	
[73]	Rohlmann (2009)‡	L1-L2	Flexion: 500N FL+7.5Nm M	5.1	1 lumbar spine model (L1-L5)
		L1-L2	Extension: 500N FL+7.5Nm M	5.1	
		L2-L3	Flexion: 500N FL+7.5Nm M	5.3	
		L2-L3	Extension: 500N FL+7.5Nm M	3.5	
		L3-L4	Flexion: 500N FL+7.5Nm M	5.5	
		L3-L4	Extension: 500N FL+7.5Nm M	3.2	
		L4-L5	Flexion: 500N FL+7.5Nm M	5.6	
		L4-L5	Extension: 500N FL+7.5Nm M	4.1	
		L5-S1	Flexion: 500N FL+7.5Nm M	5	
		L5-S1	Extension: 500N FL+7.5Nm M	3.7	
[188]	Warren (2020)†	L1-L5	Flexion-extension: 7.5Nm	31.0	1 healthy lumbar spine model (L1-L5)

Table A.1.6 continued from previous page

Ref.	First Author (year)	Segment	Task or Loads	Rotation (°)*	Subject
Cont.	Warren (2020)†	L1-L5	Flexion: 7.5Nm	20.3	
		L1-L5	Extension: 7.5Nm	10.7	
		L1-L2	Flexion: 7.5Nm	5	
		L1-L2	Extension: 7.5Nm	2.7	
		L2-L3	Flexion: 7.5Nm	4.9	
		L2-L3	Extension: 7.5Nm	2.5	
		L3-L4	Flexion: 7.5Nm	4.8	
		L3-L4	Extension: 7.5Nm	2.6	
		L4-L5	Flexion: 7.5Nm	5.6	
		L4-L5	Extension: 7.5Nm	2.8	
		L1-L2	Flexion: 7.5Nm	2.95	1 lumbar spine model (L1-L5), L1-L2 degeneration
		L1-L2	Extension: 7.5Nm	2.1	
		L2-L3	Flexion: 7.5Nm	5	
		L2-L3	Extension: 7.5Nm	2.6	
		L3-L4	Flexion: 7.5Nm	4.8	
		L3-L4	Extension: 7.5Nm	2.6	
		L4-L5	Flexion: 7.5Nm	5.5	
		L4-L5	Extension: 7.5Nm	2.8	
		L1-L2	Flexion:7.5Nm	5.1	1 lumbar spine model (L1-L5), L2-L3 degeneration
		L1-L2	Extension: 7.5Nm	2.1	
		L2-L3	Flexion: 7.5Nm	3.7	
		L2-L3	Extension: 7.5Nm	2.6	
		L3-L4	Flexion: 7.5Nm	4.9	
		L3-L4	Extension: 7.5Nm	2.6	
		L4-L5	Flexion: 7.5Nm	5.6	
		L4-L5	Extension: 7.5Nm	2.8	
		L1-L2	Flexion:7.5Nm	5	1 lumbar spine model (L1-L5), L3-L4 degeneration
		L1-L2	Extension: 7.5Nm	2.75	

Table A.1.6 continued from previous page

Ref.	First Author (year)	Segment	Task or Loads	Rotation (°)*	Subject
Cont.	Warren (2020)†	L2-L3	Flexion: 7.5Nm	2.3	
		L2-L3	Extension: 7.5Nm	1.8	
		L3-L4	Flexion: 7.5Nm	4.8	
		L3-L4	Extension: 7.5Nm	2.65	
		L4-L5	Flexion: 7.5Nm	4.7	
		L4-L5	Extension: 7.5Nm	2.8	
		L1-L2	Flexion: 7.5Nm	5	1 lumbar spine model (L1-L5), L4-L5 degeneration
		L1-L2	Extension: 7.5Nm	2.7	
		L2-L3	Flexion: 7.5Nm	4.8	
		L2-L3	Extension: 7.5Nm	2.5	
		L3-L4	Flexion: 7.5Nm	4.9	
		L3-L4	Extension: 7.5Nm	2.6	
		L4-L5	Flexion: 7.5Nm	3.1	
		L4-L5	Extension: 7.5Nm	2.1	
[186]	Xu (2017)†	L1-L2	Flexion: 1175N FL+7.5Nm M	*5.8 (4.9-7.6)*	5 lumbar spine models (L1-L5), 3 males, 2 females
		L1-L2	Extension: 500N FL+7.5Nm M	*4.3 (4-4.7)*	(age: 22-49yrs)
		L2-L3	Flexion: 1175N FL+7.5Nm M	*4.8 (3.9-7.2)*	
		L2-L3	Extension: 500N FL+7.5Nm M	*3.9 (3.6-4.2)*	
		L3-L4	Flexion: 1175N FL+7.5Nm M	*4.3 (4-4.9)*	
		L3-L4	Extension: 500N FL+7.5Nm M	*3.2 (2.5-4.9)*	
		L4-L5	Flexion: 1175N FL+7.5Nm M	*4.8 (4.7-5.1)*	
		L4-L5	Extension: 500N FL+7.5Nm M	*3.9 (2-4)*	

*Values are reported as mean ± standard deviation or *median (range)*

†Authors also reported lateral bending and/or axial rotation

‡Authors also reported additional and/or weighted positions or loading scenarios, or with spinal instrumentation

A.2 International Review Board Ethical Approval

Ethical approval was sought from Mayo Clinic's International Review Board (IRB) for the use of the patient images on 10/27/2020, IRB no. 20-010796. An amendment to the IRB application was approved on 1/24/2023 for the completion of the study outlined in Objective 3 (Section 7). The application for ethical approval was submitted by Dr. Christin Tiegs-Heiden and Dr. John Benson from Mayo Clinic. A copy of the amendment approval is appended in Figure A.2.1.

Principal Investigator Notification:

From: Mayo Clinic IRB

To: Christin Tiegs Heiden

CC: John Benson
Christin Tiegs Heiden

Re: IRB Application #: 20-010796
Title: The Effect of Low Back Pain as a Potential Consequence of Physiological Stress Shielding

IRB Approval Date: 10/27/2020
IRB Expiration Date:

The above referenced application was reviewed by expedited review procedures and is determined to be exempt from the requirement for IRB approval (45 CFR 46.104d, category 4). Continued IRB review of this study is not required as it is currently written. However, requests for modifications to the study design or procedures must be submitted to the IRB to determine whether the study continues to be exempt.

The Reviewer approved waiver of HIPAA authorization in accordance with applicable HIPAA regulations.

AS THE PRINCIPAL INVESTIGATOR OF THIS PROJECT, YOU ARE RESPONSIBLE FOR THE FOLLOWING RELATING TO THIS STUDY.

1) When applicable, use only IRB approved materials which are located under the documents tab of the IRBe workspace. Materials include consent forms, HIPAA, questionnaires, contact letters, advertisements, etc.

2) Submission to the IRB of any modifications to approved research along with any supporting documents for review and approval prior to initiation of the changes.

3) Submission to the IRB of all Unanticipated Problems Involving Risks to Subjects or Others (UPIRTSO) and major protocol violations/deviations within 5 working days of becoming aware of the occurrence.

4) Compliance with applicable regulations for the protection of human subjects and with Mayo Clinic Institutional Policies.

Mayo Clinic Institutional Reviewer

Figure A.2.1: Approval of the amendment to ethical application for use of patient data in the MRI study.